

OXIDATIVE REFORMING OF METHANE: THERMODYNAMIC AND MODELING STUDY

A DISSERTATION

Submitted in the partial fulfillment of the

requirements for the award

of

INTEGRATED DUAL DEGREE

In

CHEMICAL ENGINEERING

(With specialization in Hydrocarbon Engineering)

By

ABHINAV MALHOTRA

Integrated Dual Degree with M.Tech specialization in Hydrocarbon Engineering



**DEPARTMENT OF CHEMICAL ENGINEERING
INDIAN INSTITUTE OF TECHNOLOGY, ROORKEE
ROORKEE-247667**

JUNE, 2013



INDIAN INSTITUTE OF TECHNOLOGY

CANDIDATE'S DECLARATION

I hereby declare that the work being presented in the dissertation titled "Oxidative Reforming of Methane : Thermodynamic and Modeling Study" in partial fulfillment of the requirements for the award of Integrated Dual Degree (With M.Tech Specialization in Hydrocarbon Engineering) and submitted in the department of Chemical Engineering of the Indian Institute of Technology Roorkee, Roorkee is an authentic record of my own work under the supervision of Dr.(Mrs.) Shashi, Associate Professor, Department of Chemical Engineering, Indian Institute of Technology Roorkee, Roorkee, India.

The matter presented in this report has not been submitted by me for the award of any other degree of this or any other institute

Date:

Place: IIT Roorkee

(Abhinav Malhotra)

CERTIFICATE

This is to certify that the above statement made by the candidate is correct to the best of my knowledge and belief.

Date:

(Dr. Shashi)

Associate Professor,
Chemical Engineering Department,
Indian Institute of Technology
Roorkee-247667

ACKNOWLEDGEMENTS

I wish to express my sincere gratitude to my mentor and guide Dr.Shashi, Associate Professor, Department of Chemical Engineering, Indian Institute of Technology Roorkee, Roorkee for providing me an opportunity to work under her illuminating guidance. Her vast knowledge and constant understanding and support at every stage of the present work have proved to be extremely beneficial to me. More than anything her supportive nature not only to me, but to every one of her students makes her a true teacher.

I would also like to thank Dr. Surendra Kumar, Professor, Department of Chemical Engineering for his inspiring words of wisdom.

I would also express my gratitude to my parents,Dr. Suresh Malhotra and Dr. Sita Malhotra, and my brother, Dr. Suhail Malhotra for things that would take pages to fill. I wish to make you prouder.

I would also take a moment to thank all the friends that I made here in Roorkee. I had the best times of my life and thanks to all of you.

Abhinav Malhotra

CONTENTS

DECLARATION	i
ACKNOWLEDGEMENTS	iii
CONTENTS	v
LIST OF FIGURES	vii
LIST OF TABLES	xi
ABSTRACT.....	xiii
CHAPTER 1: INTRODUCTION.....	1
1.1 SYNGAS AND HYDROGEN	2
1.2 APPLICATION OF SYNGAS	3
1.3 REFORMING PROCESSES	5
1.4 FIXED BED REACTOR SYSTEM	10
1.5 OBJECTIVES.....	10
1.6 ORGANIZATION OF THESIS	11
CHAPTER 2: LITERATURE REVIEW.....	13
2.1 THERMODYNAMIC STUDIES	14
2.2 MODELING AND SIMULATION STUDIES	15
2.3 CATALYST STUDIES	18
2.4 CONCLUDING REMARKS.....	21
CHAPTER 3: THERMODYNAMIC ANALYSIS.....	23
3.1 DETERMINATION OF AUTOTHERMAL POINT	23
3.2 THERMODYNAMIC FEASIBILITY OF REACTIONS	32
3.3 GIBB'S ENERGY MINIMIZATION	39
CHAPTER 4: MODEL DEVELOPMENT	41
4.1 KINETICS	41
4.2 REACTOR MODEL	43
4.3 MODEL VALIDATION	45
CHAPTER 5: RESULTS AND DISCUSSION	47
5.1 RESULTS OF THERMODYNAMIC ANALYSIS	47
5.2 MODEL SIMULATION	76
CHAPTER 6: CONCLUSIONS AND RECOMMENDATIONS	97
REFERENCES.....	101

LIST OF FIGURES

Figure No.	Title	Page No.
1.1	FLOW SCHEME FOR FT SYNTHESIS	4
1.2	SYNGAS UTILIZATION ROUTES	5
1.3	INCREASING ENTHALPIES IN DIFFERENT REFORMING PROCESSES WITH OXIDATIVE REFORMING REGION SHOWN	9
2.1	THERMODYNAMIC REPRESENTATION OF METHANE OXIDATION	13
2.2	REACTION MECHANISM FOR PARTIAL OXIDATION OF METHANE ON DIFFERENT CATALYSTS WITH NOBLE METAL	20
3.1	HEAT OF REACTION DURING ATR OF METHANE AT 298K AS A FUNCTION OF OXYGEN-TO-METHANE RATIO	29
3.2	HEAT OF REACTION DURING ATR OF METHANE AT 800K AS A FUNCTION OF OXYGEN-TO-METHANE RATIO	29
3.3	HEAT OF REACTION DURING ATR OF METHANE AT 1000K AS A FUNCTION OF OXYGEN-TO-METHANE RATIO	30
3.4	HEAT OF REACTION DURING ATR OF METHANE AT 1200K AS A FUNCTION OF OXYGEN-TO-METHANE RATIO	30
3.5	VARIATION OF CRITICAL OXYGEN TO FUEL RATIO WITH TEMPERATURE	31
3.6	VARIATION OF STOICHIOMETRIC STEAM TO METHANE REQUIREMENT WITH TEMPERATURE	31
3.7	ENTHALPY AND GIBB'S FREE ENERGY VARIATION FOR R1	34
3.8	ENTHALPY AND GIBB'S FREE ENERGY VARIATION FOR R2	34
3.9	ENTHALPY AND GIBB'S FREE ENERGY VARIATION FOR R3	35
3.10	ENTHALPY AND GIBB'S FREE ENERGY VARIATION FOR R4	35
3.11	EQUILIBRIUM CONSTANT AS A FUNCTION OF TEMPERATURE FOR R1	37
3.12	EQUILIBRIUM CONSTANT AS A FUNCTION OF TEMPERATURE FOR R2	37
3.13	EQUILIBRIUM CONSTANT AS A FUNCTION OF TEMPERATURE FOR R3	38
4.1	REACTOR DIAGRAM	44
5.1	COKE FORMATION AT DIFFERENT STEAM/METHANE RATIOS WITH OXYGEN/METHANE=0.2	50
5.2	HYDROGEN MOLES AT DIFFERENT STEAM/METHANE RATIOS WITH OXYGEN/METHANE=0.2	51
5.3	HYDROGEN/CARBON MONOXIDE RATIO AT DIFFERENT STEAM/METHANE RATIOS WITH OXYGEN/METHANE=0.2	52
5.4	CONVERSION OF METHANE AT DIFFERENT STEAM/METHANE RATIOS WITH OXYGEN/METHANE=0.2	53
5.5	COKE FORMATION AT DIFFERENT STEAM/METHANE RATIOS WITH OXYGEN/METHANE=0.3	54
5.6	HYDROGEN MOLES AT DIFFERENT STEAM/METHANE RATIOS WITH OXYGEN/METHANE=0.3	55
5.7	HYDROGEN/CARBON MONOXIDE RATIO AT DIFFERENT STEAM/METHANE RATIOS WITH OXYGEN/METHANE=0.3	56
5.8	CONVERSION OF METHANE AT DIFFERENT STEAM/METHANE RATIOS WITH OXYGEN/METHANE=0.3	57
5.9	COKE FORMATION AT DIFFERENT STEAM/METHANE RATIOS WITH OXYGEN/METHANE=0.4	58

5.10	HYDROGEN MOLES AT DIFFERENT STEAM/METHANE RATIOS WITH OXYGEN/METHANE=0.4	59
5.11	HYDROGEN/CARBON MONOXIDE RATIO AT DIFFERENT STEAM/METHANE RATIOS WITH OXYGEN/METHANE=0.4	60
5.12	CONVERSION OF METHANE AT DIFFERENT STEAM/METHANE RATIOS WITH OXYGEN/METHANE=0.4	61
5.13	COKE FORMATION AT DIFFERENT STEAM/METHANE RATIOS WITH OXYGEN/METHANE=0.5	62
5.14	HYDROGEN MOLES AT DIFFERENT STEAM/METHANE RATIOS WITH OXYGEN/METHANE=0.5	63
5.15	HYDROGEN/CARBON MONOXIDE RATIO AT DIFFERENT STEAM/METHANE RATIOS WITH OXYGEN/METHANE=0.5	64
5.16	CONVERSION OF METHANE AT DIFFERENT STEAM/METHANE RATIOS WITH OXYGEN/METHANE=0.5	65
5.17	COKE FORMATION AT DIFFERENT STEAM/METHANE RATIOS WITH OXYGEN/METHANE=1.0	66
5.18	HYDROGEN MOLES AT DIFFERENT STEAM/METHANE RATIOS WITH OXYGEN/METHANE=1.0	67
5.19	HYDROGEN/CARBON MONOXIDE RATIO AT DIFFERENT STEAM/METHANE RATIOS WITH OXYGEN/METHANE=1.0	68
5.20	CONVERSION OF METHANE AT DIFFERENT STEAM/METHANE RATIOS WITH OXYGEN/METHANE=1.0	69
5.21	EFFECT OF CHANGING OXYGEN/METHANE RATIO ON COKE FORMATION AT STEAM/METHANE=1.0	70
5.22	EFFECT OF CHANGING OXYGEN/METHANE RATIO ON COKE FORMATION AT STEAM/METHANE=2.0	71
5.23	EFFECT OF CHANGING OXYGEN/METHANE RATIO ON HYDROGEN MOLES AT STEAM/METHANE=1.0	72
5.24	EFFECT OF CHANGING OXYGEN/METHANE RATIO ON HYDROGEN MOLES AT STEAM/METHANE=2.0	73
5.25	EFFECT OF CHANGING OXYGEN/METHANE RATIO ON METHANE CONVERSION AT STEAM/METHANE=1.0	74
5.26	EFFECT OF CHANGING OXYGEN/METHANE RATIO ON METHANE CONVERSION AT STEAM/METHANE=2.0	75
5.27	CONVERSION AT DIFFERENT POSITIONS WITH VARYING OXYGEN CONTENT	77
5.28	HYDROGEN MOLE FRACTION AT DIFFERENT POSITIONS WITH VARYING OXYGEN CONTENT	78
5.29	CO ₂ MOLE FRACTION AT DIFFERENT POSITIONS WITH VARYING OXYGEN CONTENT	79
5.30	CO MOLE FRACTION AT DIFFERENT POSITIONS WITH VARYING OXYGEN CONTENT	80
5.31	HYDROGEN MOLE FRACTION AT DIFFERENT POSITIONS WITH VARYING STEAM CONTENT	81
5.32	HYDROGEN YIELD AT DIFFERENT POSITIONS WITH VARYING STEAM CONTENT	82
5.33	CO MOLE FRACTION AT DIFFERENT POSITIONS WITH VARYING STEAM CONTENT	83
5.34	CO ₂ MOLE FRACTION AT DIFFERENT POSITIONS WITH VARYING STEAM CONTENT	84
5.35	CONVERSION AT DIFFERENT POSITIONS WITH VARYING STEAM CONTENT	85

5.36	CO MOLE FRACTION AT DIFFERENT POSITIONS WITH VARYING TEMPERATURES	86
5.37	HYDROGEN YIELD AT DIFFERENT POSITIONS WITH VARYING TEMPERATURES	87
5.35	CO ₂ MOLE FRACTION AT DIFFERENT POSITIONS WITH VARYING TEMPERATURES	88
5.39	HYDROGEN MOLE FRACTION AT DIFFERENT POSITIONS WITH VARYING TEMPERATURES	89
5.40	CONVERSION AT DIFFERENT POSITIONS WITH VARYING TEMPERATURES	90
5.41	H ₂ /CO RATIOS AT DIFFERENT TEMPERATURES WITH VARYING STEAM CONTENT	91
5.42	H ₂ /CO RATIOS AT DIFFERENT STEAM CONTENT WITH VARYING OXYGEN CONTENT	92

LIST OF TABLES

Table No.	Title	Page No.
1.1	MAJOR REACTIONS IN SMR	6
3.1	STANDARD HEAT OF FORMATION	25
3.2	SHOMATE EQUATION PARAMETERS FOR DIFFERENT COMPONENTS	26
3.3	RESULTS OF CRITICAL OXYGEN-FUEL RATIO AT DIFFERENT TEMPERATURES	27
3.4	STEAM TO FUEL RATIO CORRESPONDING TO THE CALCULATED CRITICAL OXYGEN TO METHANE RATIO (OBTAINED VIA STOICHIOMETRIC BALANCE)	27
3.5	REACTIONS IN OXIDATIVE REFORMING	32
3.6	FEASIBLE TEMPERATURE RANGE FOR THE INVOLVED REACTIONS	36
4.1	ARRHENIUS PARAMETER AND ACTIVATION ENERGIES	43
4.2	VAN'T HOFF ADSORPTION PARAMETERS AND HEATS OF ADSORPTION FOR COMPONENTS	43
4.3	INPUT CONDITIONS OF INDUSTRIAL REACTOR	45
4.4	COMPARISON BETWEEN MODEL PREDICTIONS WITH INDUSTRIAL DATA	46
5.1	INPUT VARIABLES AND THEIR POSSIBLE RANGES	47
5.2	VALUES OBTAINED FOR INPUT PARAMETERS BY ANALYSIS	49
5.3	INITIAL FLOW RATES FOR SIMULATION OF MODEL	76
5.4	REACTOR SPECIFICATIONS FOR SIMULATION OF MODEL	76
5.5	OPERATING CONDITIONS FOR SIMULATION OF MODEL	76

ABSTRACT

Energy is the pivot upon which our modern society is hinged. Everything in this world depends on energy. Traditionally fossil fuels found in the nature have been the relied and trusted sources of energy. All our modern technologies are developed to run on fossil fuels, be it a thermal power generation plant running on coal or the engine of a car, designed to draw power from crude oil derivatives. Now we know that excessive use of fossil fuel has a huge environmental cost attached with it. The rapidly changing climatic scenario, melting of polar ice caps and rise in sea levels are offshoots of global warming. Our over dependence on fossil fuel adds to it.

Hydrogen has been touted as the fuel of the future owing to its large calorific value and harmless by products of its combustion. Reforming of natural gas is a process by which industrial scale production of hydrogen can be carried out. Syngas is another fuel of a similar origin. It is a majorly a mixture of hydrogen and carbon monoxide in varying proportions. It finds its applications in Gas to liquid (GTL) fuel production. Syngas is an important feedstock for a large number of industrial products including ammonia, methanol, urea etc.

Oxidative reforming involves addition of steam and oxygen to methane (natural gas) at a sufficiently high temperature in presence of a catalyst to produce hydrogen and carbon monoxide along with other side products. It comprises of both endothermic reforming reactions and exothermic combustion reaction. In a perfect autothermal system, the amount of added oxygen is fixed in such a way that the net $\Delta H = 0$ for the system. This point acts as the lower bound for the amount of oxygen considered in this study. For an estimate on the temperature range over which the considered reactions occur, the region where $\Delta G < 0$ is evaluated, which comes out to 900-1100 K. Based on these values as a pointer, a thermodynamic analysis by minimizing the Gibb's free energies is conducted to find out the equilibrium moles of each species including carbon. The results of thermodynamic analysis act as a starting point for the simulation study. It is found that at temperatures exceeding 1000K the theoretical conversion is sufficiently high and coke deposited is in miniscule amount. A large range of steam to methane ratio was evaluated and ultimately a range of 0.5-3.0 was selected for simulation study on the basis of conversion, coke formation and H_2/CO ratio. The large values of H_2/CO ratio were not considered relevant since

the primary motive was to study the syngas production. At those high ratios, it is beneficial to go for pure hydrogen production. O_2/CH_4 ratio was upper bounded by considering the fact that the number of hydrogen moles produced drops off with an increase in oxygen supplied.

The steady state one-dimensional, non-isothermal model was developed. Nickel based catalyst was selected and a fixed tubular reactor system was considered. The kinetic model was based on the experimental works of Xu and Froment (on steam reforming reactions), and Trimm and Lam (on methane combustion). The industrial data of De Groote and Froment was used for validation. On the basis of simulation of model for a low pressure operation, it was concluded that a temperature of 1000K- 1100K with an O_2/CH_4 ratio of 0.8 is suitable for syngas production, with varying H_2/CO ratios. The minimum H_2/CO for this configuration was found to be 2.7 when the steam to methane ratio was taken as 0.5 and a peak value of $H_2/CO=9.1$ was found with steam to methane ratio=3.0. This ratio can be further altered as desired by using another separation unit. It is further stated that this operation requires low pressure and reasonable temperature. Thus, it is preferable to be used in practice.

CHAPTER 1

INTRODUCTION

Today, we live in a modern 21st century society where everything is growing at a rapid pace. Scientific development has ushered in an era of technological growth and economic prosperity. We as humans have access to comforts and amenities. However, all of our modern society-its growth, prosperity and progress is hinged upon one crucial requirement- the need for energy.

The energy requirement of the world has been increasing over the past few years at an average annual rate of 2.5%. The most widely used sources of energy are the fossil fuels including natural gas, coal, crude oil and crude oil based products. For the year 2011 the consumption of oil increased marginally at a rate of 0.6 million barrels per day to attain a value of 88 million barrels per day. Natural Gas consumption of the world increased by 2.2 % to reach a high of 3222 billion cubic metres and production by 3% for a value of 2954.8 billion cubic metres. Coal consumption for the same year jumped by a hefty 5.4% [1]. From the statistics available, it is evident that the demand for energy and hence our limited fuel sources is constantly increasing. We are dependent on fossil fuels for a majority of our energy requirement.

The use of fossil fuels entails with it an environmental cost especially in the form of greenhouse emissions. Climatic variations are one of the biggest risks created by the modern human growth. Greenhouse effect is leading to an overall increase in the temperature of the Earth. The greenhouse emissions contribute to the global warming of Earth by trapping the heat of the Sun. Carbon dioxide is largely produced in the combustion of all fossil fuels. Before the Industrial Revolution, the carbon dioxide levels in our atmosphere were about 280 parts per million by volume (ppmv), and current levels are greater than 380 ppmv. The major reason of concern is the fact that these levels have been increasing at a rate of 1.9 ppm yr⁻¹ since 2000 [2]. The global concentration of CO₂ in our atmosphere today far exceeds the natural range over the last 650,000 years of 180 to 300 ppmv. These increasing temperatures lead to a rising sea levels, impacting the lives of millions of people living on coastal lands and islands.

Hence, the burgeoning demand makes not only the economics of the energy supply an important issue, the question of sustainability of the energy source has become a big topic for debate nowadays. The issue of sustainability makes the case for hydrogen as an energy source. Hydrogen is clean burning fuel as it produces water as a by-product in place of harmful greenhouse gases. Another option is the development of syngas as a source to produce fuels via Fischer-Tropsch synthesis. As the fuels by the second route do not contain sulfur and other heteroatoms, they are a cleaner option to be used especially in internal combustion engines. Using these fuels there is a lesser production of harmful contaminants in the air [3].

1.1 SYNGAS AND HYDROGEN

Hydrogen is the simplest element consisting of just one proton in its nucleus. It is found in trace amount as gas in our atmosphere but is found in abundance in a combined form with oxygen (i.e. as water) on Earth. Hydrogen is rich in energy. Its heat of combustion is 141.8 MJ/kg, while for natural gas it depends on the source and quality but taking the higher heating value for its main constituent methane we can take a value of approximately 55.4 MJ/kg [4]. The value for coal and liquid fuels is even lower. This shows that a plethora of energy is available in hydrogen fuel.

The two major sources of hydrogen are the petrochemical sector and the electrolysis of water. Production of hydrogen from other hydrocarbons like naphtha, coal, heavy oil etc. has achieved a certain degree of importance in the last few years. The major driving force in this regard has been the rising demand for hydrogen in refineries and petrochemical complexes. Processes like hydrotreating, hydrocracking used for fuel upgradation utilize hydrogen. In the petrochemical industry hydrogen finds wide applications in production of important chemicals like ammonia, methanol etc. and also in hydrocarbon synthesis via Fischer Tropsch processes. Another method to produce hydrogen is via electrolysis of water. This method is energy intensive and a large amount of current has to be passed before water molecule is split. For the utilization of hydrogen fuel cells have been suggested as a good alternative. The principle behind the fuel cells was discovered by Swiss scientist Christian Schönbein. In a fuel cell hydrogen is combusted to release electricity.

Synthesis Gas is a mixture of carbon monoxide and hydrogen in varying ratios. Synthesis gas or Syngas, as it is most commonly called, is the name that is attributed to a gas mixture of Carbon monoxide and Hydrogen in varying proportions. This important factor, more easily named as the hydrogen-to-carbon monoxide ratio is a determining factor of the usability and property of the available synthesis gas. The heating value, density and other important properties are determined by this ratio. For example the Fischer Tropsch Process requires an optimum value of this ratio to be less than 3.5 [5]. This ratio can be varied by changing temperatures, steam content in the steam reforming process among others.

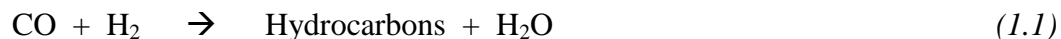
The name synthesis gas is given because it is widely used as an intermediate to create or synthesize synthetic fuels and for producing ammonia or methanol. Syngas is also used as intermediate in producing synthetic petroleum for use as a fuel or lubricant via the Fischer–Tropsch process. Syngas consists primarily of hydrogen, carbon monoxide, and very often some carbon dioxide, and has lesser energy density than that of natural gas. Syngas is combustible and often used as a fuel in internal combustion engines or as an intermediate for the production of other chemicals. The heating value of syngas depends on the proportion of carbon monoxide and hydrogen in the gas.

Out of all the production methods reforming of natural gas is the one that is widely implemented in the industry. Natural gas (which primarily contains methane) is the major feed for production of hydrogen and syngas owing to its large availability. Coal is also widely available but investment in a coal based syngas production unit is three times larger than that of a natural-gas dependent plant [6]. Thus it is an issue of a large capital investment v/s a higher operating costs. Economic analysis can determine which type of feed based plant should be setup. Since it is a gaseous fuel, natural gas has a large transportation and storage cost as compared to fuels like petroleum, which adds to the production cost of hydrogen and syngas. Liquid fuels have a higher energy density and thus the cost per unit energy produced is lower in the case of liquid fuels.

1.2 APPLICATION OF SYNGAS

Methane which is the primary constituent of natural gas is an important feedstock for manufacturing a large number of industrial chemicals as well as used in Gas-to-Liquid (GTL)

process. The major GTL process that has become ubiquitous is the Fischer-Tropsch (FT) synthesis. Methane is converted to syngas majorly via the reforming process and the syngas is used in FT synthesis to produce a wide array of liquid hydrocarbons. Group VIII transition metals are used as catalysts for the conversion process.



Another route is by first converting syngas to methanol using Cu/ZnO as a catalyst and then in a series conversion over a Zeolite ZSM-5 catalyst.

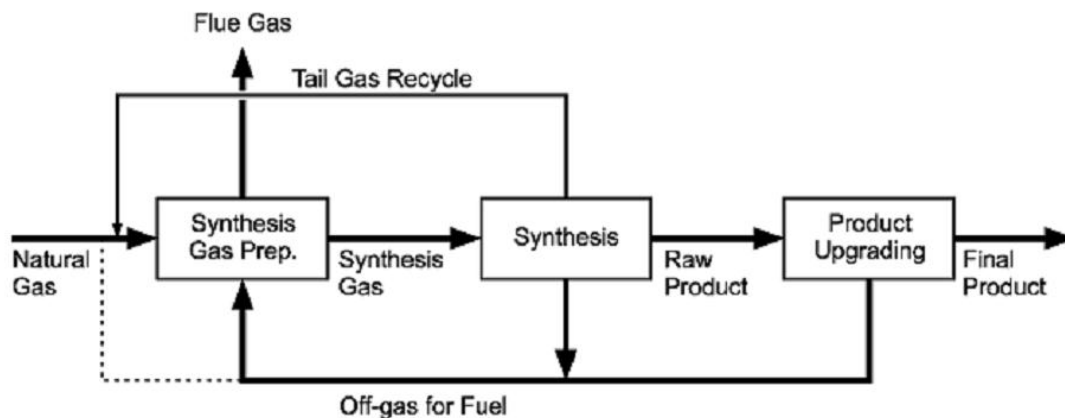


Figure 1.1: Flow Scheme for FT synthesis^[3]

Technologies required for the conversion and utilization of natural gas by converting it to syngas are well established. Syngas is then used as a feedstock for important chemicals. Ammonia synthesis is another large consumer of syngas. The world production of ammonia in the calendar year '08 was 133 MT with an average growth rate of 2.4% over the previous 5 years. Similarly another important chemical is methanol whose annual production in 2010 was 45 MT. The total natural gas required for producing these two chemicals amounts to 100 billion Nm³ annually [7]. Thus the areas where syngas is used are:

- Urea manufacture
- Gasoline blends

- Ammonia synthesis
- Methanol synthesis

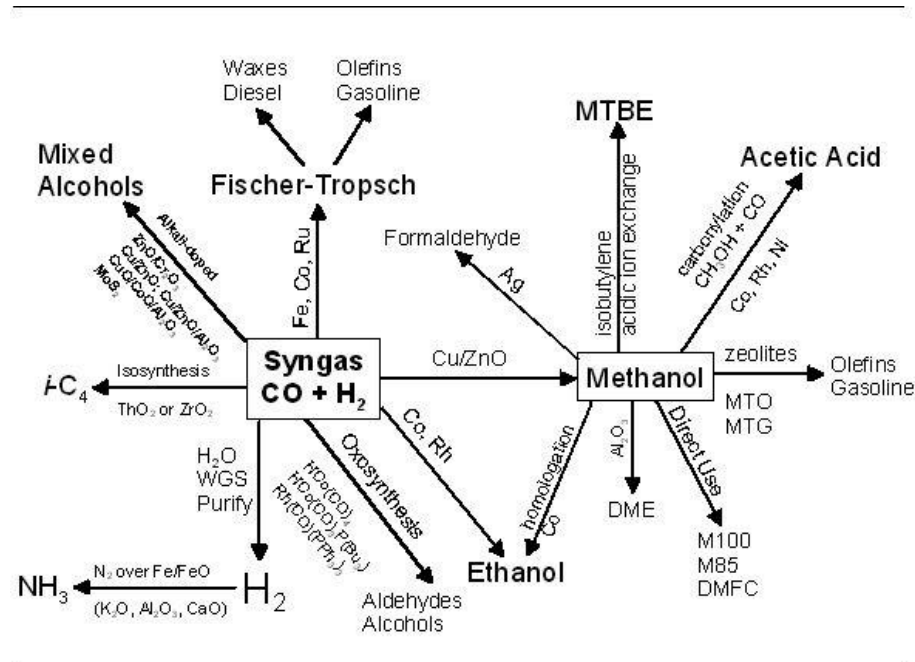


Figure 1.2: Syngas Utilization Routes ^[8]

1.3 REFORMING PROCESSES

Theoretically, syngas can be produced from any feedstock with carbon and hydrogen. It may be coal, biomass, naphtha, natural gas, and even petroleum coke. However considering the economics and availability, natural gas is the feedstock of interest. There are a number of factors at play. Upgrading a low value feedstock is a factor to be considered. But at the same time it is important to consider the costs of gasification based systems that will be required for low value feeds like coal or coke. Although coal or coke based syngas will be cheaper in terms of operating costs, the capital cost entailed is much higher [6]. The target feedstock in this regard has been natural gas, especially low-value natural gas which is found in remote reservoirs or found associated with oil reservoirs.

Reforming has been the cornerstone of natural gas conversion to syngas. The first step towards reforming was Steam Methane Reforming (SMR). It was developed in 1885 but

implemented at a large scale by BASF. There are a large number of reforming processes which can be classified on the basis of the use of air/oxygen and steam. In this work we will be focusing more on the oxidative reforming. However to gain a perspective of what oxidative reforming comprises of, and the differences between oxidative reforming and other reforming processes, it is essential to have a brief overview about them.

1.3.1 Steam Methane Reforming (SMR)

Steam Methane Reforming is the oldest and widely used process for industrial reforming. As the name entails steam is added in this type of reforming process. Owing to the stability of the methane molecule, somewhat severe conditions are requisite for the reforming process. The major reactions involved in the steam reforming are:

Table 1.1: Major Reactions in SMR

Reaction name	Reaction	ΔH_{298K}° (kJ/mol)
Partial Steam Reforming	$CH_4 + H_2O \leftrightarrow CO + 3H_2$	206.2
Water Gas Shift	$CO + H_2O \leftrightarrow CO_2 + H_2$	-41.1

The overall SMR is an endothermic reaction and hence a higher temperature pushes the reaction forward. Primarily a Ni/Al₂O₃ catalyst is used for conversion [9]. External heat needs to be supplied for optimum conversion which adds to the cost [10] as it is clearly evident that it is a highly endothermic process. For a complete GTL system based on natural gas as a feedstock, the SMR unit alone accounts for a major fraction of the total cost. The benefit lies in the fact that no oxygen is needed thus savings can be achieved on reducing the equipment necessary for the same. Further the temperature needed in SRM is lowest when compared to all other reforming processes. Thus, it helps save cost by savings on the material of construction and the insulation cost. The H₂/CO ratio in this case is higher than those required for FT synthesis and is applicable for hydrogen production.

1.3.2 Dry Reforming of Methane (DRM)

Dry reforming of methane, as the name suggests does not require steam to be provided as a reactant. The water in the steam reforming reactions is replaced by carbon dioxide.



The dry reforming of methane utilizes the greenhouse gas carbon dioxide and hence is a topic which receives a great deal of attention. It consumes one of the greenhouse gases to yield hydrogen. However, the H_2/CO ratio in this process is low (~ 1) which makes it suitable for applications other than hydrogen production like downstream conversion in FT synthesis.

The aforesaid reforming methods do not require oxygen for the reforming process. In the next section we will be covering the reforming methods that require air/oxygen as a feed and briefly analyze the advantages and disadvantages of the reforming processes. However, the industrial applicability of this method has been limited till now [11]. Developing this method holds huge potential for environmental sustainability by converting two undesirable greenhouse gases into an eco-friendly fuel in terms of emissions in the form of hydrogen.

1.3.3 Oxidative Reforming

When oxygen is supplied in conjunction with natural gas to achieve the reforming reactions, it is termed as the oxidative reforming process. The supplied oxygen can be in the form of pure oxygen or as air. The former requires equipment to produce pure oxygen which is most commonly achieved by liquefaction of air. This method is cost intensive. However, using pure oxygen gives better selectivity and gets rid of the wasted volume of inert gases like nitrogen which make up almost three-fourth of atmosphere. The drawback is additional equipment and capital cost along with cooling costs if liquefaction of air is employed as the method of choice for the production of pure oxygen.

1.3.3.1 Partial Oxidation of Methane (POX)

Partial Oxidation of Methane can be carried out via two basic routes- one without the use of catalyst wherein it is named as a direct oxidation process and second with the use of catalyst, with the title of catalytic partial oxidation. The two methods differ in the use of catalysts-the former employs no catalyst and relies on the direct combustion of methane, while the latter employs a catalyst bed to tilt the balance in the favour of reactions that are favourable and reducing the coke deposited. A simplified view of the reactions can be presented as:



This is a very simplified view of the highly exothermic incomplete combustion reaction. In reality the reaction products of combustion will also include water in its vapour state i.e. as steam. In the presence of water/steam the endothermic steam reforming reaction will also play its part; especially, if the catalyst is also being used, like the case in catalytic partial oxidation reforming.



The first commercial POX technologies were developed by Shell and Texaco and use a burner. This technology is also used in Shell's GTL-plant in Malaysia. The disadvantages of this technology are the very high reactor outlet temperature (± 1600 K), the high required O_2/CH_4 ratio (~ 0.7) with the accompanying moderate syngas selectivity ($< 90\%$) [12]. Some points in favour of POX include a H_2/CO ratio of around 2 which is suitable for FT synthesis. Also the equipment required to produce oxygen increases the cost. It can work without the need of external heat due to the intrinsic exothermicity of the combustion reactions. Unlike the autothermal reformer, for the control of heat, tube wall heating/cooling is employed in a partial oxidation reactor. Insulation may be used to ensure near adiabatic conditions. POX is able to sustain without external heating due to combustion reaction and without cooling due to endothermic steam reforming reaction.

1.3.3.2 Autothermal Reforming of Methane (ATR)

An ideal autothermal reforming reaction, as the name suggests does not require any external control of temperature. This happens because the endothermic steam reforming reactions are coupled with the exothermic methane combustion reaction. The ratio of steam to fuel and oxygen to fuel is set in such a way that the overall enthalpy of the reaction system is zero. The H_2/CO ratio obtained in this process is favourable for the GTL need. The controlled coupling of the endothermic reactions with the exothermic ones ensures that the temperature is lower than POX where steam is not supplied in feed. The energy requirement is lower because of the opposing contributions to enthalpy of the two sets of reactions. The gas space velocity is also higher in comparison to a traditional steam reformer [13]. However, autothermal reforming has a limited industrial application. There are limited tried catalysts for the same. Also, need for pure oxygen adds to the cost of operation.

Thus, in oxidative reforming we can see that oxygen is supplied in the feed which ensures the fact that the exothermic methane combustion will take place. Water may or may not be supplied with the feed. Not supplying water does not imply that the endothermic steam reforming reactions will not occur. The combustion product will include water which will ensure some endothermicity in the reacting mixture even in the absence of feed steam. A perfect ATR adjusts the supplied oxygen and steam values in such a way that the overall enthalpy of the reacting system is zero. It is also possible to supply steam in the feed in a proportion that the overall reaction is exothermic. Thus on that basis we can draw the following schematic for a system with oxidative reforming. The POX lies between total combustion and ATR conditions. The region for oxidative reforming can be defined as the one from Steam reforming to Total combustion, excluding both the limiting points.

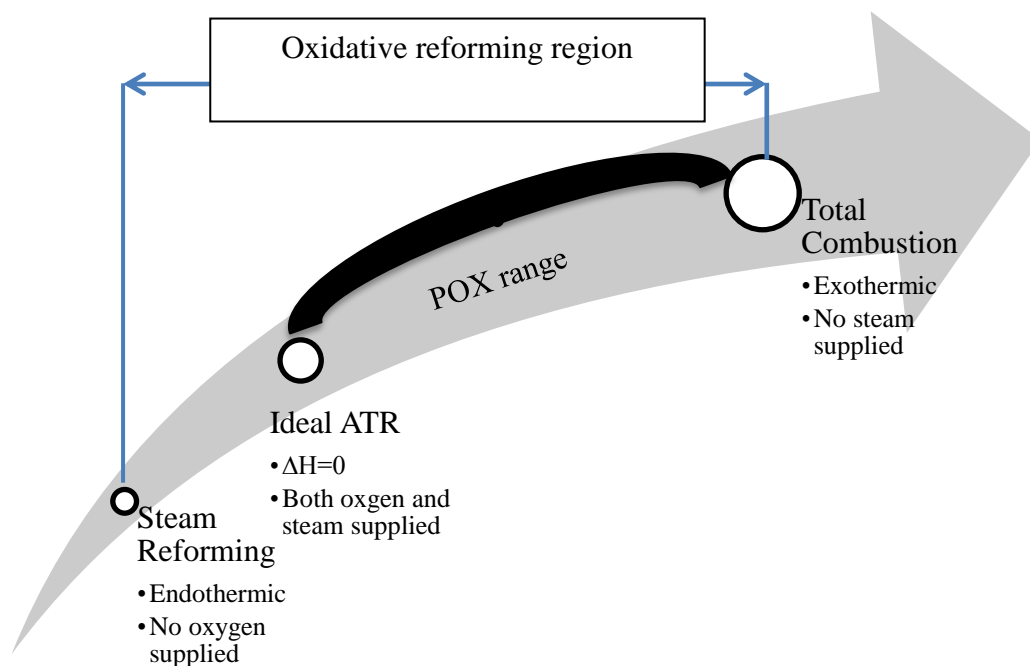


Figure 1.3: Increasing enthalpies in different reforming processes with oxidative reforming region shown

1.4 FIXED BED REACTOR SYSTEM

A fixed bed reactor in its most common form consists of a cylindrical column with a bed of catalyst particles in place. The catalyst bed is stagnant and the flow rates of the reacting streams are kept sufficiently low to prevent the bed from having an increased voidage, and become fluidized. It is a continuous reactor with the feed constantly entering and after conversion leaving. At steady state operation, the accumulation term in the mass and energy balances is neglected and no change in conversion is assumed with time. Steady state assumption makes the modeling of a fixed bed reactor easier. Most of the industrial and experimental reformers are fixed bed type owing to stability and ease of operation. Also a quicker startup if the catalyst bed needs to be changed can be initiated. For continuous operation two parallel fixed bed reactors are operated so that one of them can be taken out of operation for catalyst removal and/or regeneration and the other reactor ensures continuity of operation with minimum down time. Thus, the ease of operation, wide acceptance and easy availability are some of the reasons that have made a fixed bed reactor the basic reactor for all chemical industries.

1.5 OBJECTIVES

The objectives that were formulated for this work are as follows:

- Evaluation of oxygen-to-fuel ratio to obtain theoretical autothermal point for oxidative reforming region.
- A thermodynamic analysis of the reactions under consideration to find the feasibility range of different reactions.
- Thermodynamic analysis by Gibb's energy minimization for the determination of optimum operating parameters for the reactor using optimization tools in MATLAB.
- Collating kinetic data for different reactions under consideration using previously published research works.
- Formulating a one dimensional, steady state, non-isothermal mathematical model for a tubular reformer where oxidative reforming is being carried out.
- Solving the formulated equations using differential equation solver in MATLAB.
- Validating the model using an experimental/industrial data set.

- Using the operating parameters determined by thermodynamic analysis, simulate the mathematical model around that range of parameters to find the effect of varying the operating conditions on output parameters (e.g. methane conversion, hydrogen-to-carbon monoxide ratio etc.)

1.6 ORGANIZATION OF THESIS

Chapter 1 includes a brief introduction on the need for reforming natural gas to hydrogen and syngas. It also enumerates the different reforming routes and the objectives of this work. Chapter 2 contains a brief literature review. Chapter 3 pertains to the thermodynamic analysis of oxidative reforming of methane. Chapter 4 contains the mathematical model and validation of the model of oxidative reforming. Chapter 5 contains the results and discussions of the thermodynamic analysis and the simulation of the model prepared in the previous chapter. Chapter 6 concludes the work and makes recommendations for future work.

This chapter deals with the crucial research works done in the past in the area of modeling and simulation studies of the oxidative reforming as well as thermodynamic analysis of the reactions involved in the oxidative reforming. For the sake of avoiding superfluous information, the literature review has been focused on the objectives of this thesis.

The chapter is divided into three sections on the basis of the content that each section covers. The first section deals with the works of past on the thermodynamic analysis of reactions, mostly pertaining to reforming reactions. In some cases, however, the papers cited do not cover oxidative reforming. Their study is crucial to understand the methodology of thermodynamic analysis and using it as a tool to further its use in the scope of the current thesis. The second section deals with the important works on modeling and simulation of oxidative reforming. The final section is smaller and comprises of research work done on the catalysts for oxidative reforming processes.

2.1 THERMODYNAMIC STUDIES

Thermodynamic analysis is an important tool in the study of any reaction or a system of reactions. Thermodynamic analysis puts the theoretical limits to maximum achievable yields and conversions.

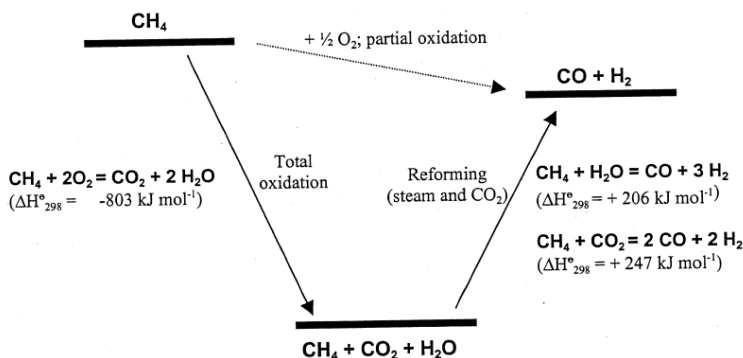


Figure 2.1: Thermodynamic representation of methane oxidation

Lutz et al. (2004) [14] conducted the thermodynamic analysis for producing hydrogen via partial oxidation route. In their analysis the authors have considered a global balance on the reactions which assists in giving the upper limits in theory to the steam-carbon and oxygen-carbon ratios. The equilibrium analysis provides a closer to reality estimate to product compositions and the efficiency of the process. The equilibrium calculations were cross checked with experimental data of a diesel fuel based reformer and as expected, it was found that the reformer efficiency was lower than that predicted by the equilibrium analysis. This goes on to show that thermodynamic analysis provides the theoretical maximum limits to our process.

Amin et al. (2007) [15] studied the combined reforming of methane with carbon dioxide and oxygen. The authors relied on an equilibrium analysis using Gibb's free energy minimization technique using Lagrange's multiplier method. It was found that at the equilibrium, the product compositions were highly dependent on the amount of methane, carbon dioxide and oxygen provided in the feed. Initial temperature was another determining factor. The analysis pointed out that the oxidation reaction was dominant at lower temperatures while carbon dioxide reforming was highly dependent on the oxygen to fuel ratio. The work eventually concluded with the optimum proportions of methane-carbon dioxide-oxygen which were found to be in the range of 1:0.2:1. The minimum temperature was found to be 1000K.

Li et al. (2008) [16] studied the thermodynamic equilibrium for autothermal reforming of methane using Gibb's Minimization technique. They also studied the carbon dioxide reforming of methane. Hydrogen yield, conversion of methane and coke were important factors in their study. The authors found the optimal methane-carbon dioxide-oxygen ratios to be 1:0.8–1.0:0.1–0.2 at a minimum temperature of 1073K. Methods to limit coke formation were also given. It was postulated that coke could be removed by having a higher temperature for the reaction and raising the steam content in the feed. Also, lower pressures contribute to lower carbon deposition.

Chen et al. (2010) [17] studied the hydrogen production via two different methods and compared both using thermodynamic analysis. In the first method, the autothermal reforming (ATR) of methane to produce hydrogen was employed. In the second method, the partial oxidation of methane succeeded by a water gas shift reaction was considered. It is important to note that the reaction temperatures of partial oxidation and water gas shift reactor were

controlled separately and independently from each other. It was found that temperature is a crucial factor in determining hydrogen yield in the case of ATR. Effects of other parameters were also found out. It was concluded that methane conversion in the second method with partial oxidation is always higher irrespective of the reaction temperature. The other results pertain to the use of water gas shift reactor which is not of importance in the context of current study.

Freitas et al. (2012) [18] studied the oxidative reforming of methane by the thermodynamic analysis of the involved reactions using Gibbs energy minimization (at constant pressure and temperature) and entropy maximization (at constant pressure and enthalpy) methods, to determine the equilibrium compositions and equilibrium temperatures, respectively. It was found that hydrogen and syngas production were better at higher temperatures and lower pressures. Also the oxygen to fuel ratio was an important parameter in determining the product composition. The authors compared their results with published data and found close agreement. The calculated results were compared with previously published experimental and simulated data with a good agreement between them.

Nematollahi et al. (2012) [19] applied thermodynamic analysis to study combined partial oxidation and carbon dioxide reforming of methane in view of carbon formation. They employed Gibb's free energy minimization techniques on wide range of operating parameters including of pressure ranging from 1–25 bar, temperature from 600–1300 K, carbon dioxide to methane ratio 0–2 and oxygen to methane ratio 0–1. It was found that increasing pressure reduces the conversion of methane. It was also indicated that addition of oxygen to the feed mixture reduces carbon deposition.

2.2 MODELING AND SIMULATION STUDIES

Mathematical modeling of any physical process is a powerful utility that helps to study that process without having to resort to expensive real life construction of that process and conduct costly experiments. It is a theoretical tool that mathematically defines the process and helps us simulate the process on our computers.

De Groote and Froment (1996) [20] simulated the adiabatic fixed bed reactor system considering the catalytic partial oxidation process along with coke formation for the conversion

of methane to syngas at a high pressure and temperature range. The pressure in the reactor was kept at 25 bar and the temperature in the range of 808K to 1785K. The catalyst considered was Ni based and Xu and Froment kinetics were applied for steam reforming. Trimm and Lam kinetics for the oxidation of methane were applied. A one dimensional reactor model was used with material and energy balances. The operations were not isobaric and hence a pressure drop equation was also applied. Different feed conditions were provided by varying the amounts of water, carbon dioxide and so on to study the outlet values of hydrogen to carbon dioxide ratio as well as the maximum catalyst temperature. The reactor considered was an industrial reactor with a diameter of 1.2 m.

Ostrowski et al. (1998) [21] modeled the catalytic partial oxidation of methane to produce synthesis gas for a Ni/Al₂O₃ catalyst for fixed bed and fluidized bed reactors. The conditions for which the model was simulated were of industrial scale with a high pressure range of 5-30 bar and temperature range of 1023-1073 K. The reaction kinetics was taken from De Groote et al. (1996) and it was found that fluidized bed reactors produced a higher yield of syngas over fixed bed systems owing to the large dependence of the reactions on intra-particle mass transport resistance, which is lesser in fluidized state.

de Smet et al. (2001) [22] simulated the adiabatic fixed bed reactor for catalytic partial oxidation of methane to synthesis gas using a one dimensional steady state model. The catalyst considered for was Ni based. The reactions considered were the total oxidation of methane along with steam reforming and water gas shift. Water was added as a reactant. The kinetics of oxidation and steam reforming were studied and their influence on a number of output parameters was given as results. Different reforming models were applied to find the different maximum temperatures in the catalyst bed. One of the models that were used was from Xu and Froment's work on Ni catalyst [23].

Avci et al. (2001) [24] modeled an autothermal, dual catalyst fixed bed reactor with the prime motive of hydrogen production. The model configurations included using different catalyst with varying feed ratios and bed configurations. The different configurations in question are the mixing of catalysts Pt-Al₂O₃ and Ni/MgO-Al₂O₃ or placing them in series one after the other. The reactor was operated with varying feed ratios at both lab scale and industrial scale. It was found that the hydrogen production is higher when the catalysts are in a physically mixed state as

well as at low methane-to-oxygen and high steam-to-methane ratios. The optimum operating conditions for obtaining maximum hydrogen production were also investigated

Ji et al. (2003) [25] worked on a one dimensional steady state model for the partial oxidation of methane on a Ni catalyst. The kinetics used was from the work of De Groote and Froment (1996). Using this model a membrane reactor with oxygen permeable membrane was also developed. Using the simulation results outlet temperatures and flow rates were calculated, which were used in further calculating the exergies of different species. It was found that membrane reactors give a better conversion and at the same time thermodynamically a lower pressure and higher inlet temperature favours the product formation.

Halabi et al. (2008) [26] worked on the autothermal reforming process of methane with the aim of hydrogen production. A fixed bed reactor with Xu and Froment kinetics for reforming was considered. The analysis was conducted at steady state as well as dynamically. The input parameters like oxygen to carbon ratio, water to carbon ratio, temperature etc. were varied and the impact of changing these on output parameters like hydrogen yield, conversion of methane, reforming efficiency was studied. The temperature was kept at 873K while the pressure at 1.5 bar. Optimum values of the input variables were reported.

Kumar et al. (2009) [27] developed a one dimensional non-isothermal model for oxygen permeable membrane reactor for the purpose of hydrogen production. Three reactors were compared. One was a fixed bed reactor with pure oxygen in feed, the second was a fixed bed reactor with air in feed, and the third was a membrane reactor with an oxygen permeable membrane. Data given by De Groote and Froment was used for validating the model. The effect of changing inlet parameters was studied on the outlet parameters. It was found that the fixed bed reactor with pure oxygen in feed has the best performance amongst the aforesaid reactors.

Zahedi nezhad et al. (2009) [28] suggested an autothermal reformer with two distinct sections. The first section is assumed to be the combustion section while the other one has a catalytic bed. The mathematical model of such a reformer is developed by the authors. In the combustion section, temperature and composition were predicted using 108 simultaneous elementary reactions considering 28 species. The results of the simulation of the first section were taken as the starting point for the second section. A one-dimensional heterogeneous reactor

model was used for kinetic simulation of the second section. The catalyst considered was a Ni based catalyst supported on Mg- alumina spinel. Results of the model were compared with published data on ATR process.

Reese et al. (2010) [29] modeled the high pressure autothermal reforming of methane via a 1-D, heterogeneous, numerical model. The impact of changing steam to carbon ratio and oxygen to carbon ratio on output parameters was studied by the authors for different operating pressures of 6, 28 and 50 bar. A sensitivity analysis consisting of 9 model parameters was also completed. It was found that the model was sensitive to the activation energy of the endothermic reforming reactions and the ratio of oxygen to carbon. This paper was a companion paper to an experimental work by the authors wherein a lab scale reformer was constructed and tested for pressure range between 6 to 50 bar.

Scognamiglio Diego et al. (2012) [30] modeled and validated an autothermal reactor with a fixed bed of Rh catalyst. For the validation of their model they conducted experiments on a small reactor of laboratory scale. The temperature profiles of this experiment were measured with the help of an infrared camera. It was found that the temperature peaks were present on the inlet as a result of separation between spaces for oxidation and reforming reaction. The model of the authors was validated with experimental data by comparing temperature profiles with those obtained experimentally at different feed compositions, total flow rate and preheating temperatures. The validated model was used to analyze the effect of thermal conductivity and of the flow rate on overall reactor performance.

2.3 CATALYST STUDIES

A lot of work has been done in the field of finding suitable catalysts and kinetics for the reactions that are in the scope of our present study. The reactions have been studied at a laboratory scale experimentally to determine a kinetic model. These works are then utilized in modeling and simulation work.

Trimm and Lam (1980) [31] conducted their experimental work on a catalytic combustor. Their work entailed the study of methane combustion over platinum catalyst supported on porous and non-porous alumina fiber. They measured reaction kinetics at temperatures above and less

than 815 K and found that activation energy changes at the aforesaid temperature. For different types of catalysts different models were found applicable. On comparing the model with Langmuir-Hinshelwood type of model they postulated that the reaction mechanism involves reactions occurring between adsorbed methane and between the oxygen either adsorbed or in the gas phase. Their work has been used by a variety of researchers working in the field of modeling and simulation studies on Ni catalysts even though the catalyst they have used is Pt by incorporating some correction/effectiveness factors for different reactions.

Xu and Froment (1989) [23] derived intrinsic rate equations for methane steam reforming and accompanying water gas shift reaction. The catalyst used for the study was a Ni/MgAl₂O₄ catalyst. The work has been cited very frequently in literature for modeling studies as well as experimental works. Based on the rate determining steps of reactions, Xu and Froment formulated Langmuir-Hinshelwood type rate expressions. They assumed the same active sites for all the reactions. Using thermodynamic analysis they reduced the possible mechanisms, and the parameter estimation for the best model are statistically significant and thermodynamically consistent.

Heitnes et al. (1995) [32] studied the partial oxidation of methane on a number of catalyst beds- Monolithic reactor with 5% Ni catalyst and a fixed bed reactor with Ni/Al₂O₃ as catalyst. The temperature range of the experiments was 873K to 1073K at 1 bar pressure. The results were analyzed and it was predicted that the reactions occurring in both the systems consist of total combustion of methane, reforming reactions and water gas shift reaction.

Freni et al. (2000) [13] worked on collating the previous developments on processes used for syngas production. The processes that they reviewed included partial methane oxidation with or without steam. They also considered a variety of reactors including monoliths, fixed bed reactors; fluidized bed reactors etc. They also considered a number of catalysts for review including Ni based catalysts, catalysts containing noble metals like Pt, Pd etc. They also reviewed differences in mechanism for different reactions on different catalysts.

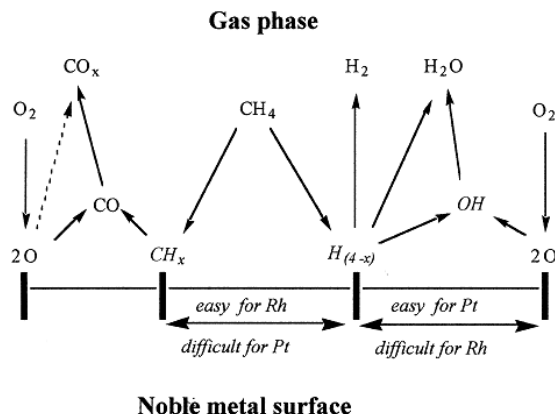


Figure 2.2: Reaction mechanism for partial oxidation of methane on different catalysts with noble metal

They also listed potential benefits of using one type of catalyst over the other, say Rh is an addition to the cost of process however, it minimizes water production and maximizes hydrogen yield.

Choudhary et al. (2006) [33] worked on CO_2 reforming with simultaneous steam reforming or partial oxidation of methane to syngas over NdCoO_3 perovskite-type mixed metal oxide catalyst. Their study was at different process conditions. For both the cases they observed almost negligible carbon deposition. They concluded that reduced NdCoO_3 perovskite-type mixed-oxide catalyst is a highly promising catalyst for carbon-free CO_2 reforming combined with steam reforming or partial oxidation of methane to syngas.

Corbo et al. (2007) [34] studied the catalytic partial oxidation reaction for hydrogen production on three catalyst types, two based on $\text{Ni-Al}_2\text{O}_3$ and one constituted by Pt supported on cerium oxide. The feedstock for the authors was propane as it is a major constituent of LPG. The same catalysts were utilized to study the partial oxidation of methane and for comparing the results to propane results. The catalytic properties were quantified in terms of yield and selectivity of hydrogen. Tests were conducted to check the durability and stability of catalyst along with the resistance to carbon deposition. It was concluded that Ni catalysts are highly selective for hydrogen. The cerium based catalyst is helpful in resisting coke deposition more than Ni.

Munera et al. (2010) [35] worked on the combination of carbon dioxide reforming and oxidation of methane with the motive of producing syngas. They used a membrane reactor. Two different types of catalysts were used. They were analyzed in a conventional reactor with a fixed bed and then used in a membrane reactor. For our purpose the results of the fixed bed reactor are of importance. Varying oxygen to methane ratios and carbon dioxide to methane ratios were supplied to identify their impact on hydrogen yield. The fresh, reduced and used catalysts were characterized using a variety of techniques like X-Ray Diffraction, laser Raman spectroscopy and XPS. The spectroscopic features were consistent with the catalytic behavior of both formulations. The best performance of the reactor was achieved on one of the catalysts and use of approximately 10% oxygen in feed.

Dantas et al. (2012) [36] studied the nickel catalysts supported on different types of supports for the methane oxidative reforming reactions. BET surface area results showed that the catalysts containing alumina presented higher surface area which favored better nickel dispersion. X-ray diffraction data from the reduced samples was used for confirmation. A literature based kinetic model was used to compare data predicted by this model with the experimental behavior. The results showed that high temperatures are optimum for maximum hydrogen production. The differences between the data and model could be attributed to the difference in catalysts over which the model equations were developed and the experiments were conducted.

2.4 CONCLUDING REMARKS

In this chapter, research work done on thermodynamic analysis and modeling and simulation studies majorly pertaining to oxidative reforming of methane was critically analyzed. Catalyst and kinetic models developed were presented in brief, with the range of operating parameters over which they were evaluated. These results would be used in subsequent chapters for selecting the appropriate constitutive relationships and also for validation of the developed model.

CHAPTER 3

THERMODYNAMIC ANALYSIS

This chapter deals with the thermodynamic analysis conducted on a system with oxidative reforming of methane. The science of thermodynamics at a basic level involves energy and its transformation.

The name thermodynamics means literally the changes in temperature (heat). However, thermodynamics is also utilized to determine the conditions under which a reaction or a set of reactions attain a state of equilibrium- a state where no visible change occurs. In dynamic equilibrium the rate of forward and backward reactions becomes equal and hence the two opposite changes occurring at a microscopic level cancel each other out on macroscopic level. Thermodynamic analysis is an important tool in the study of any reaction or a system of reactions. Thermodynamic analysis puts the theoretical limits to maximum achievable yields and conversions.

3.1 DETERMINATION OF AUTOTHERMAL POINT

As mentioned in the introduction, this work entails the study of oxidative reforming of methane. As per the definition being adopted in this work, oxidative reforming entails the region bounded by the point representing total combustion of methane where the only products are oxides of carbon and water in the form of steam on one side, and the point representing pure steam reforming with no added oxygen as the other extreme. The region of oxidative reforming has purely endothermic reactions on one end, and highly exothermic reaction on the other, with the enthalpy at a particular point determined by the supply of oxygen and water. In between these two extremities, both the types of reactions are present.

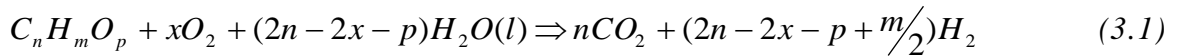
We define an autothermal point where the net enthalpy of these reactions becomes equal to zero. For this to happen, the oxygen supplied has to be in a specific ratio such that the aforesaid conditions of enthalpy are achievable. The region between the autothermal point and the point representing total combustion can be said to be the region for partial oxidation (with steam supply) where overall exothermic reaction occurs (albeit the presence of endothermic reforming

reactions). Between the autothermal point and steam reforming point, overall endothermic conditions prevail due to lower dominance of exothermic combustion reaction.

Autothermal reforming is a combination of both endothermic and exothermic reactions. In a perfectly autothermal system the heat produced in the exothermic reactions is taken by the endothermic reactions. The word ‘autothermal’ originates from the same ideology. The system of reactions regulates its enthalpies in itself. There is no requirement for supplying or taking away heat. In an idealized condition a perfect autothermal reaction will have its ΔH_{net} equal to zero. It implies that under autothermal conditions the enthalpy of exothermic and endothermic reactions is balanced in such a way that no net heat is taken or generated and the reaction is in fact truly ‘autothermal’. For the purpose of this work, the autothermal point in terms of oxygen supplied is of important concern to us. This is so because it gives us an idea of the range of oxygen ratio that is to be used for operation.

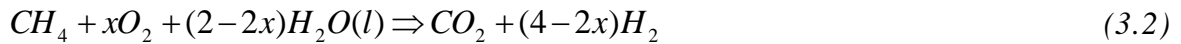
3.1.1 Idealized reaction

Ahmed and Krumpelt [37] considered a general feedstock $C_nH_mO_p$ and formulated the idealized reaction stoichiometry for the conversion of the hydrocarbon feed into carbon dioxide and hydrogen. No incomplete conversions were considered and hence no free carbon or carbon monoxide was included in the stoichiometry.



Where, x is the oxygen-to-fuel ratio.

In our case the feedstock is methane. Hence $n=1$, $m=4$, $p=0$ is taken as the special case and the overall idealized conversion reaction is:



The overall heat of reaction at 298.15 K and 1 bar for the above standard reaction is:

$$\Delta H_{R, 298K, 1bar}^{\circ} = \Delta H_{CO_2}^{\circ} + (4 - 2x)\Delta H_{H_2}^{\circ} - \Delta H_{CH_4}^{\circ} - x\Delta H_{O_2}^{\circ} - (2 - 2x)\Delta H_{H_2O}^{\circ} \quad (3.3)$$

The ΔH^0 is the standard enthalpy of formation of component in the subscript. Another important parameter is maximum hydrogen yield and maximum percentage of hydrogen in product and is given by:

$$\text{Max. H}_2 \text{ yield} = 4 - 2x$$

$$\text{Max. H}_2 \text{ percentage} = \frac{4 - 2x}{1 + (4 - 2x)} \times 100$$

Table 3.1: Standard heat of formation ^[38]

Species	Standard Heat of formation at 298.15 K (kJ/mol)
Carbon Dioxide	-393.51
Water(gas, liquid)	-241.83,-285.84
Hydrogen	0
Oxygen	0
Methane	74.86

A critical oxygen-to-fuel ratio X_c is defined to be that value of oxygen-to-fuel where the enthalpy of the idealized reaction becomes zero or the autothermal condition is achieved. It is calculated by setting the ΔH_R° zero and solving the equation for x. The value is called the critical oxygen to methane ratio or X_c .

For determining X_c for the idealized reaction at any temperature T, we require the enthalpy at T. For evaluating enthalpy as a function of temperature C_p° values are used. The dependence of enthalpy is assumed to be on temperature only and pressure variation is ignored.

National Institute of Standards of Technology (NIST), US Department of Commerce has a substantial database on a number of species. The NIST Chemistry Web-book [38] utilizes the Shomate equations where Gas Phase Heat Capacity is given as

$$C_p^\bullet = A + B*t + C*t^2 + D*t^3 + E/t^2 \quad (3.4)$$

The integration of the above equation with t, gives H° as a function of temperature. The constant of integration is evaluated by using the standard enthalpy at 298.15 K which is known.

$$H^\circ - H_{298.15}^\circ = A*t + B*t^2/2 + C*t^3/3 + D*t^4/4 - E/t + F - H \quad (3.5)$$

Where,

C_p = heat capacity (J/mol*K)

H° = standard enthalpy (kJ/mol)

t = temperature (K) / 1000

Table 3.2: Shomate equation parameters for different components ^{[39] [40]}

<u>Species</u>	<u>A</u>	<u>B</u>	<u>C</u>	<u>D</u>	<u>E</u>	<u>F</u>	<u>G</u>	<u>H</u>
Carbon Monoxide	25.56759	6.09613	4.054656	-2.6713	0.131021	-118.009	227.3665	-110.527
Water	30.092	6.832514	6.793435	-2.53448	0.082139	-250.881	223.3967	-241.826
Carbon Dioxide	24.99735	55.18696	-33.6914	7.948387	-0.13664	-403.608	228.2431	-393.522
Hydrogen	33.06618	-11.3634	11.43282	-2.77287	-0.15856	-9.9808	172.708	0
Oxygen	0.03235	8.772972	-3.98813	0.788313	-0.7416	-11.3247	236.1663	0
Methane	-0.70303	108.4773	-42.5216	5.862788	0.678565	-76.8438	158.7163	-74.8731

3.1.2 Solution methodology and results

The program to solve the enthalpy of the idealized reaction as a function of x (oxygen-to-fuel ratio) is written in MATLAB R2010b. The library function f_{zero} used to solve such kind of linear and non-linear equations is used. All used data are given.

It has been assumed that $0.0 \leq x \leq 1.0$ because if $x > 1$ then water will be obtained as a product which goes against our initial assumption of having only carbon dioxide as a product. The autothermicity of the reaction is defined using [26]:

$$\Delta H_T = \sum_i \nu_i(x) H_i(T) = 0 \quad (3.6)$$

Where, i is used to denote the five species involved.

For validation the equation is solved at 298.15K. At this temperature water is assumed to be a liquid and hence heat of formation of liquid water is used. For oxygen-to-fuel ratios greater than 1, water is assumed to be available as liquid on product side. Ahmed and Krumpelt [37] had found it to be 0.44 at the same temperature. The solution of the equation yielded a value of 0.44261 which is in close agreement.

Next, the equation is solved at different temperatures in the range of 800-1200 K and the critical value and other parameters are reported. However in this temperature range water is considered to be in gaseous state and hence the heat of formation of gaseous water is used.

Table 3.3: Results of critical oxygen-fuel ratio at different temperatures

Temperature(K)	Critical X_c	Max. H_2 yield	Max H_2 % in product
800	0.3256	3.3488	77.0054
900	0.3186	3.3627	77.0784
1000	0.3108	3.3785	77.1611
1100	0.3020	3.3960	77.2520
1200	0.2925	3.415	77.4000

In the case of methane, considering an idealized stoichiometry, it can be said that pure steam reforming occurs when the value of x is equal to zero. For values of x greater than 2.0 total combustion in excess of oxygen can be said to occur. Thus in between the range of 0.0 to 2.0 we can find the region of oxidative reforming for methane to occur. Within that range, the autothermal point is dependent on the reaction temperatures because the heat of formation of the species is a function of temperatures rendering the autothermal point to be a function of temperature alone. It can be seen that for using water as a gaseous product, the results vary from assuming it as liquid product. The range of steam to fuel ratio which is determined for the idealized stoichiometry is given below.

Table 3.4: Steam to fuel ratio corresponding to the calculated critical oxygen to methane ratio (obtained via stoichiometric balance)

Temperature(K)	Critical Oxygen to Methane Content	Steam to fuel ratio (via stoichiometry)
800	0.3256	1.3488
900	0.3186	1.3628
1000	0.3108	1.3784
1100	0.302	1.396
1200	0.2925	1.415

Thus, we have a reasonable estimate of the oxygen to fuel ratio which gives us autothermal conditions. It is essential to remember that it is an estimate as no partial conversions are considered which happen in the real situations. Also some heat loss is also there so generally the value of X_c in reality is greater than theoretical value [26]. This gives us an estimate of the range of oxygen to methane ratio that we will be working with and at the same time it provides information about steam to methane ratio. No doubt that the reaction stoichiometry is idealized and involves a lot of assumptions, but for the purpose of this current work, it provides us a good starting point. It is clear from the results obtained that the oxygen to methane ratio of around 0.3 ensures that we will be operating in the region of partial oxidation. Hence it gives us an idea of the region of oxidative reforming that we are operating in.

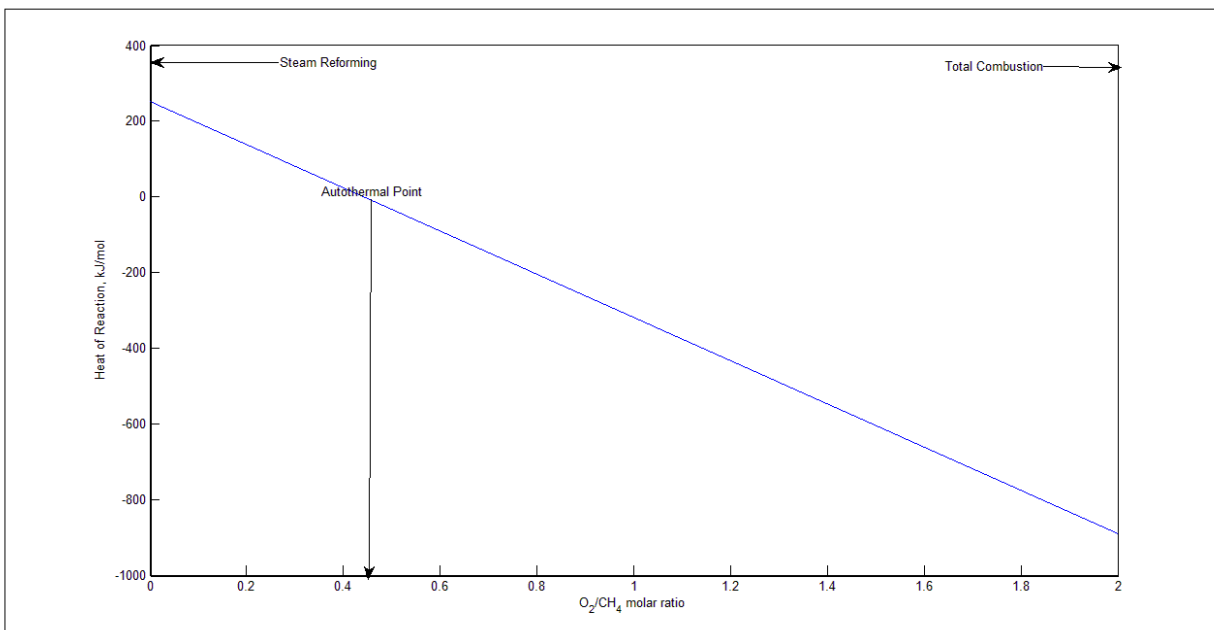


Figure 3.1: Heat of reaction during ATR of methane at 298K as a function of oxygen-to-methane ratio

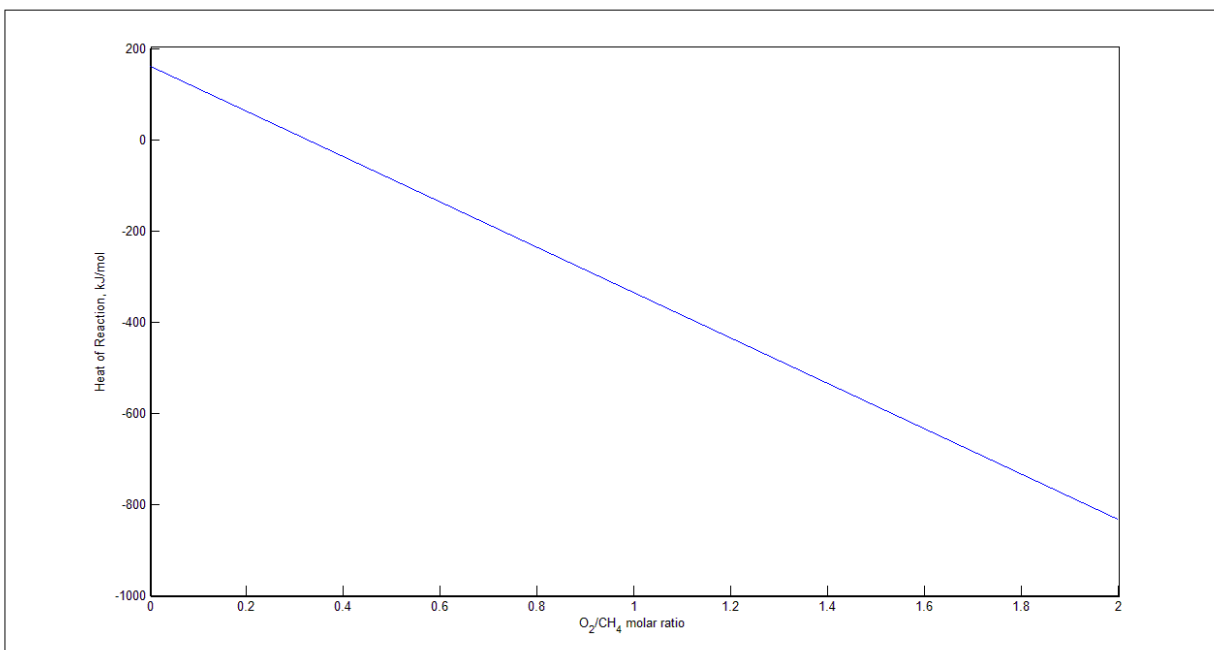


Figure 3.2: Heat of reaction during ATR of methane at 800K as a function of oxygen-to-methane ratio

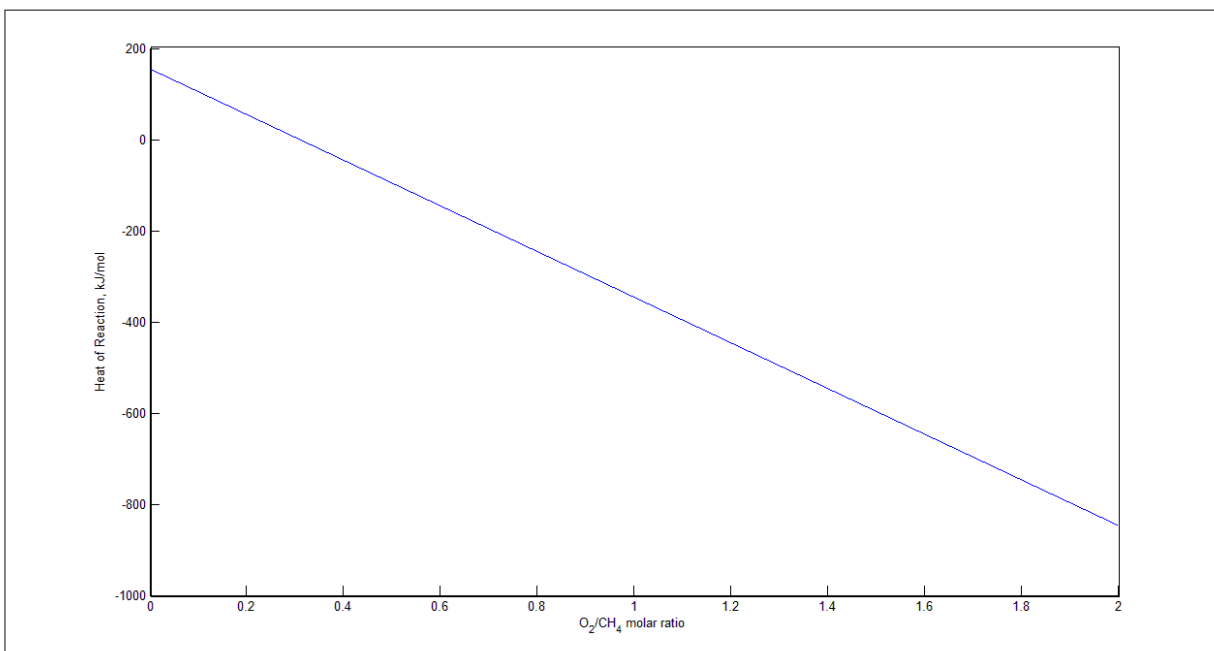


Figure 3.3: Heat of reaction during ATR of methane at 1000K as a function of oxygen-to-methane ratio

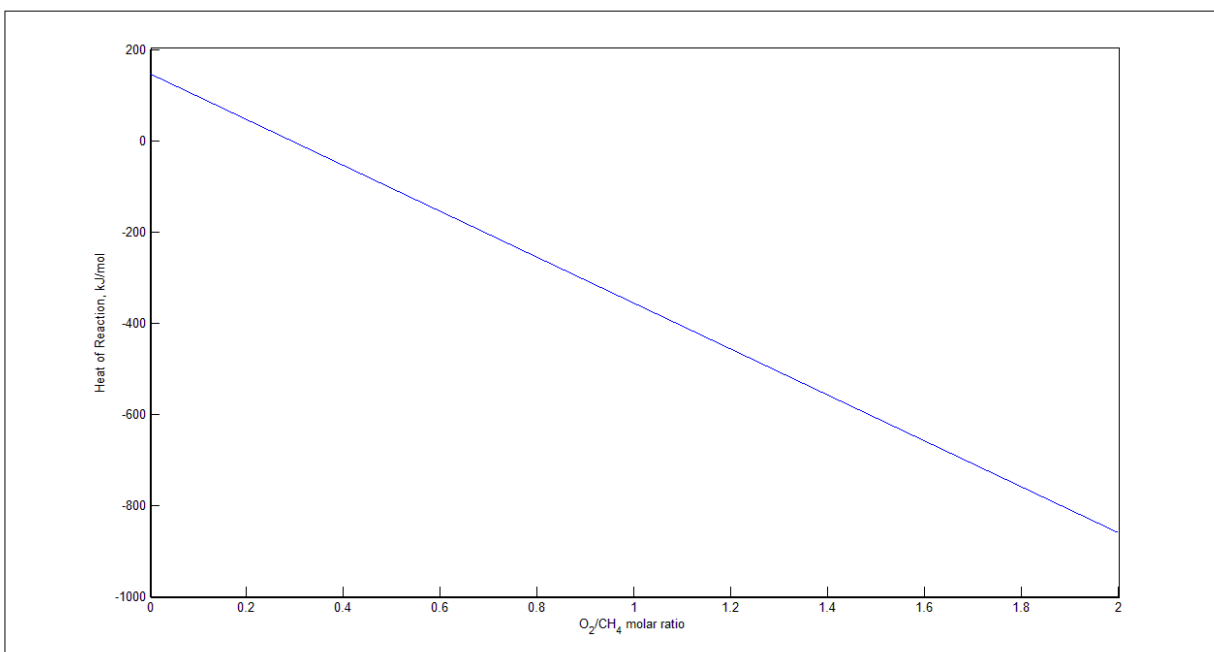


Figure 3.4: Heat of reaction during ATR of methane at 1200K as a function of oxygen-to-methane ratio

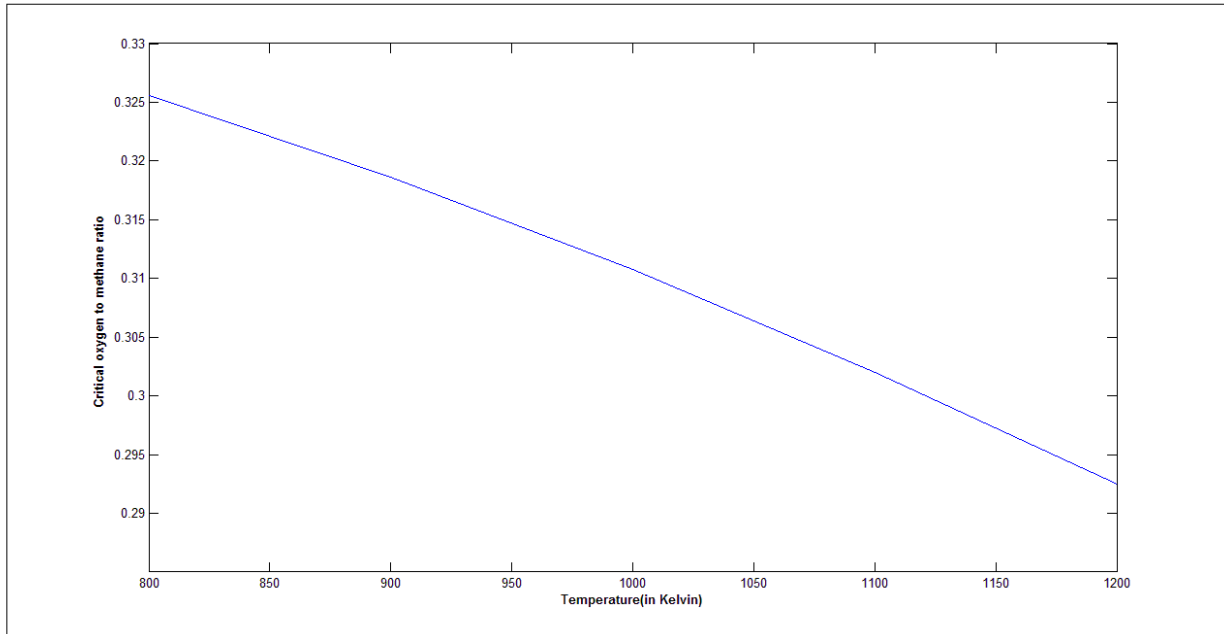


Figure 3.5: Variation of critical oxygen to fuel ratio with temperature

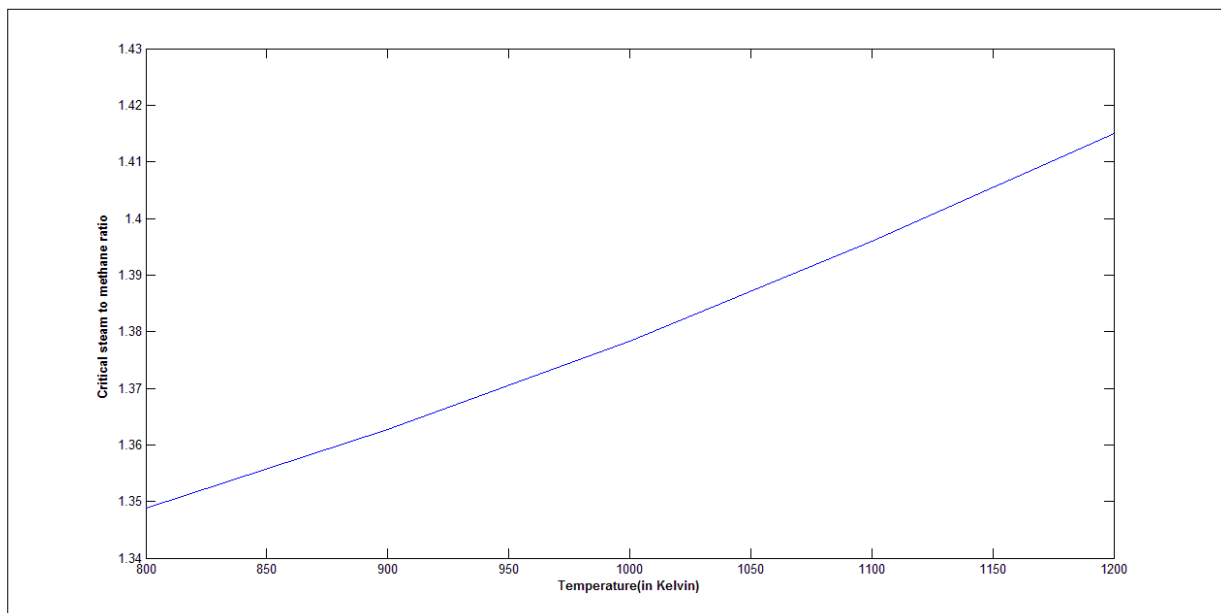


Figure 3.6: Variation of stoichiometric steam to methane requirement with temperature.

3.2 THERMODYNAMIC FEASIBILITY OF REACTIONS

Although there are a large number of reactions occurring consecutively and in parallel in any complex reaction system, it is very difficult to incorporate all the reactions into the model being developed. For the purpose of model development and thermodynamic analysis, this work contains essentially four major reactions:

Table 3.5: Reactions in oxidative reforming ^[26]

Serial	Reaction name	Reaction	$\Delta H^{o(298K)}$ (kJ/mol)
R1.	Partial Steam Reforming	$CH_4 + H_2O \leftrightarrow CO + 3H_2$	206.2
R2.	Water Gas Shift	$CO + H_2O \leftrightarrow CO_2 + H_2$	-41.1
R3.	Total Steam Reforming	$CH_4 + 2H_2O \leftrightarrow CO_2 + 4H_2$	164.9
R4.	Methane Combustion	$CH_4 + 2O_2 \rightarrow CO_2 + 2H_2O$	-802.7

Methane combustion or total oxidation is highly exothermic reaction. The water gas shift (WGS) reaction is a major influencer of an important parameter viz. $\frac{H_2}{CO}$ ratio. The $\frac{H_2}{CO}$ ratio determines the usability and applicability of syngas in different processes and industries. For pure H_2 production it can be stated that the $\frac{H_2}{CO}$ ratio approaches a large value and water gas shift dominates for changing CO to H_2 .

For a reaction in the gaseous state $aA + bB \leftrightarrow cC + dD$ the equilibrium constant can be defined in the terms of partial pressures of its reactants and products. Hence the equilibrium constant for the reaction would be:

$$K_{eq} = \frac{P_C^c P_D^d}{P_A^a P_B^b} ; \text{unit} = \text{bar}^{(d+c-b-a)}. \quad (3.7)$$

Gibb's free energy is a function of temperature and pressure. Since the standard state is defined in terms of a specified pressure of 1atm, ΔG^o is independent of pressure. Similarly the enthalpy of a reaction is assumed to be dependent only on T and its variation with P can be neglected. Using Shomate equation (3.5), we can determine H^o . On the basis of Gibbs free

energy of a reaction we can determine its feasibility. We know that a reaction is feasible as long as $\Delta G^0 < 0$. If this is not the case then the reverse of the reaction under consideration is dominant and hence the reaction under our purview is not significant and is moving in the backward of what we have assumed. The feasibility range of the series of reactions is determined by the temperature range over which all of them are feasible, or in thermodynamic terms where each and every reaction has its $\Delta G^0 < 0$. From thermodynamics it is known that:

$$\Delta S^\bullet = \int \frac{C_p}{T} dT \quad (3.8)$$

From C_p equation, Equation (3.4), the integration yields us the equation

$$\Delta S_i^\bullet = A \ln(t) + B \cdot t + C \cdot t^2/2 + D \cdot t^3/3 - E/(2 \cdot t^2) + G \quad (3.9)$$

Where, ΔS_i° = standard entropy (J/mol*K) and G is available using NIST data table or can be evaluated as a constant of integration as standard entropy at 298K is known.

From thermodynamics it is also known that:

$$\Delta G_i^\circ = H_i^\circ - T \Delta S_i^\circ \quad (3.10)$$

Where, subscript i denotes the i^{th} species.

For getting the Gibb's energy for a particular reaction ΔG_i° is multiplied by its stoichiometric coefficient and summed together.

$$\Delta G_{rj}^\bullet = \sum_i \nu_{ij} \Delta G_i^\circ \quad (3.11)$$

Where, subscript r_j denotes the j^{th} reaction and ν_{ij} denotes the stoichiometric coefficient of species i in reaction j .

Using all the above equations and NIST data for Shomate equation and solving sequentially using MATLAB R2010b we obtain the plots of Standard Gibb's free Energy as a function of temperature for all the four reactions (see Figure 3.7 to Figure 3.10).

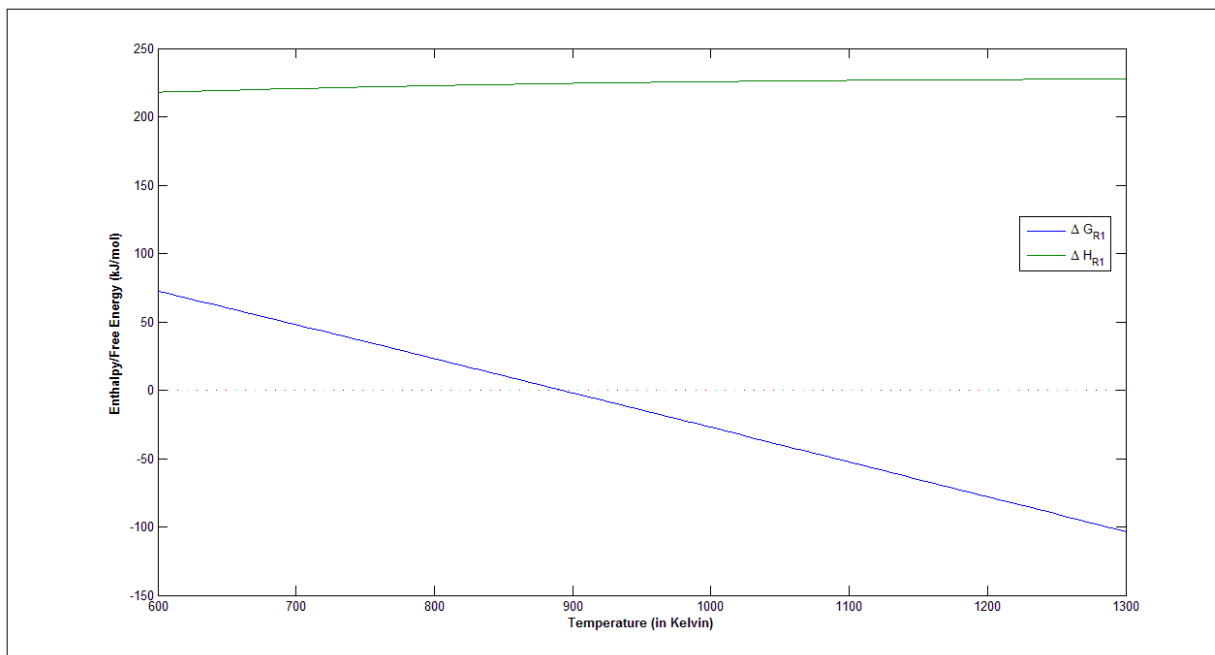


Figure 3.7: Enthalpy and Gibbs Free energy variation for R1

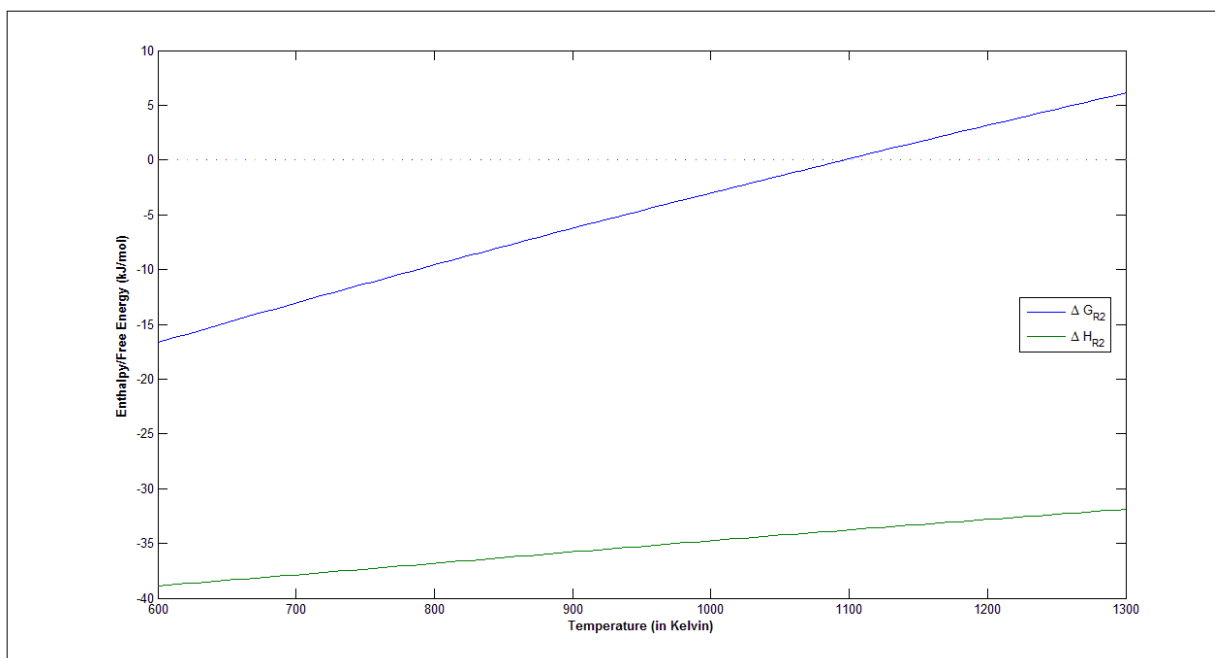


Figure 3.8: Enthalpy and Gibbs Free energy variation for R2

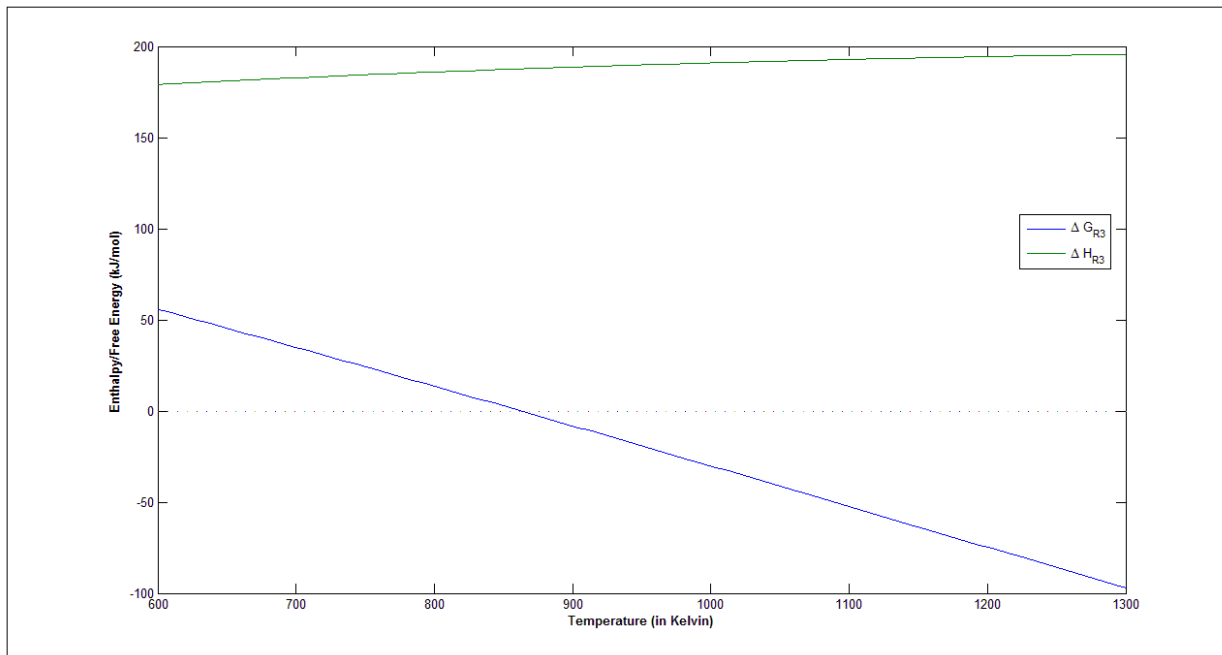


Figure 3.9: Enthalpy and Gibb's Free energy variation for R3

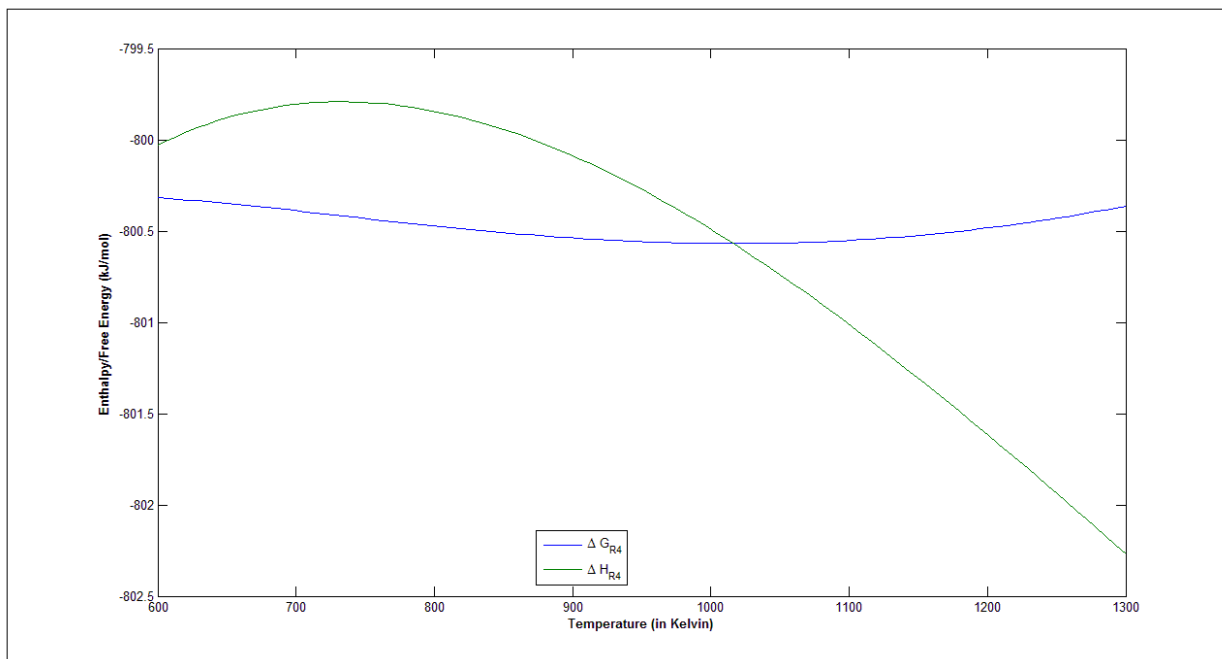


Figure 3.10: Enthalpy and Gibb's Free energy variation for R4

From these plots we can find the temperature range for the feasibility of each reaction.

Table 3.6: Feasible temperature range for the involved reactions

Reaction No.	Reaction Name	Temperature Range of feasibility
R1	Partial Steam Reforming	$T > 900\text{K}$
R2	Water Gas Shift	$T < 1100\text{K}$
R3	Total Steam Reforming	$T > 860\text{K}$
R4	Methane Oxidation	All T from 700-1200K

Thus the common range from the above table is determined to be **$T = 900\text{-}1100\text{K}$** where all the four reactions are feasible and their respective $\Delta G_{\text{rxn}}^{\circ} < 0$.

The results obtained from plots for R1, R2 and R3 are matched with Katiyar et al. [41] to verify the correctness of the procedure. These authors had obtained a feasible temperature range of 894- 1080 K using a slightly different procedure to determine K values. They relied on the Van't Hoff relation and had a different Cp equation for the components. The results are a very close match and hence the correctness of the result is verified.

From the values of Gibb's free energy the equilibrium constants are determined and plotted. ΔG° relates to equilibrium constant as:

$$\Delta G^{\circ} = -RT \ln K \quad (3.12)$$

Where, R is the Universal Gas Constant (with a value of $8.314 \text{ J mol}^{-1} \text{ K}^{-1}$)

The equilibrium constants are plotted with temperature and we can use these values in this work wherever necessary (see Figure 3.11, 3.12 and 3.13). The high equilibrium constant values for R4 meant that it should not be treated as a reversible chemical change and should be considered as an irreversible reaction.

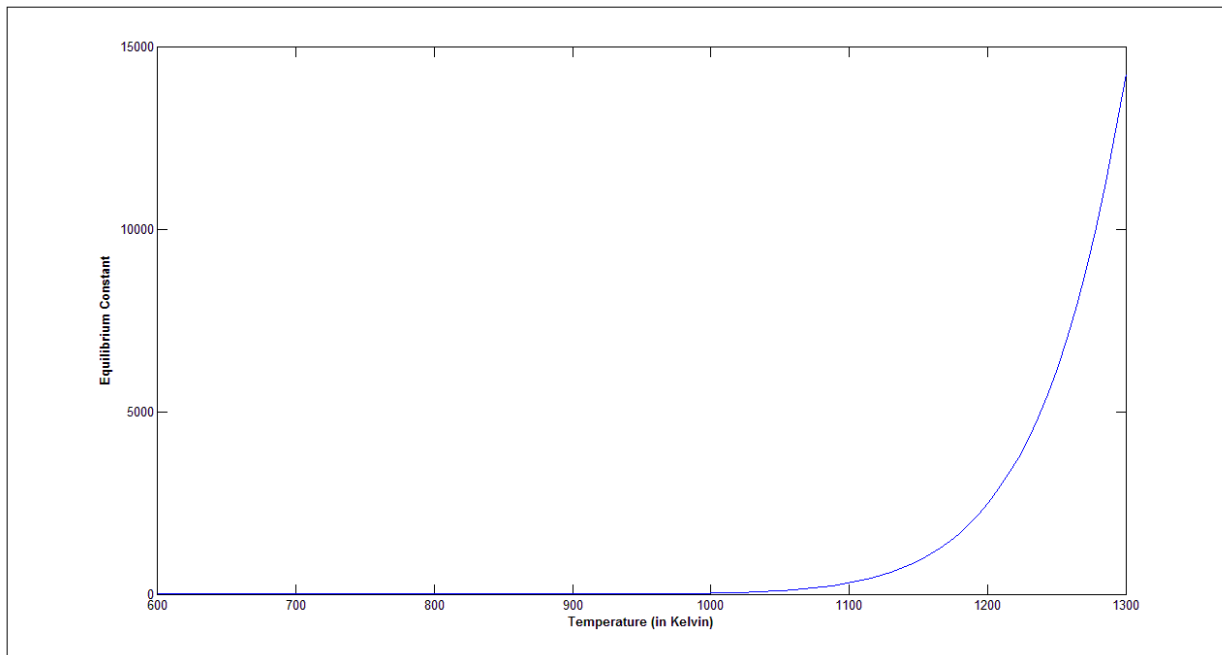


Figure 3.11: Equilibrium constant as a function of temperature for R1

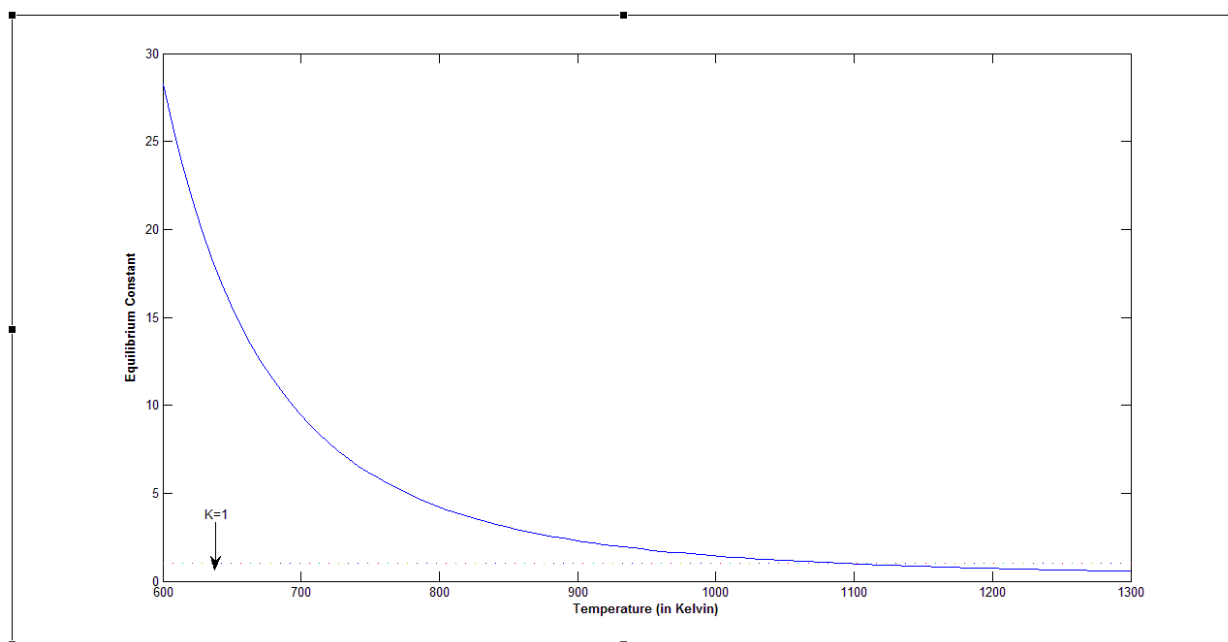


Figure 3.12; Equilibrium constant as a function of temperature for R2

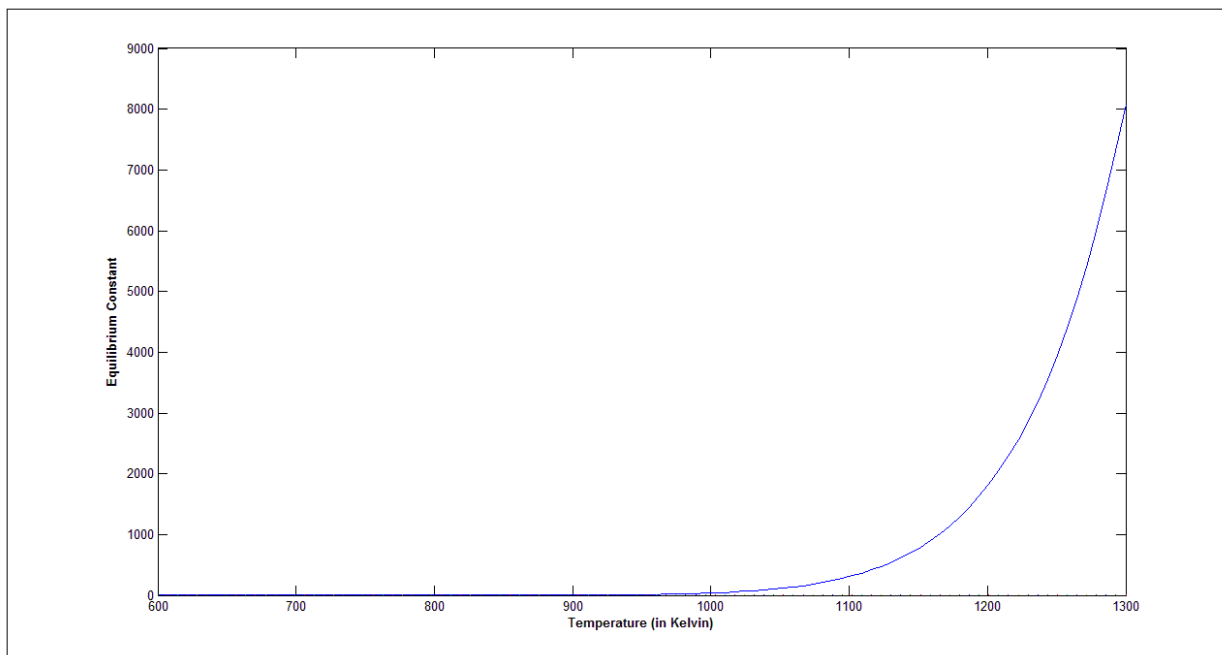


Figure 3.13: Equilibrium constant as a function of temperature for R3

3.3 GIBB'S ENERGY MINIMIZATION

Gibb's Energy Minimization is a technique used to compute equilibrium compositions of a reacting mixture [4]. Its theoretical base lies in the fact that in a reacting system which has attained equilibrium, the total Gibbs free energy will be at a minimum. The thermodynamic equilibrium condition for reactive multicomponent closed system, at constant Pressure and Temperature, with given initial composition, can be obtained by the minimization of Gibbs energy (G) of the system, with respect to the number of moles of each component in each phase [18,19]. Assuming that the gas phase is an ideal gas, the total Gibbs function for the system is given as sum of i^{th} species as:

$$G^t = \sum_{i=1}^N n_i \bar{G}_i = \sum_{i=1}^N n_i \mu_i = \sum_{i=1}^N n_i G_i^o + RT \sum_{i=1}^N n_i \ln \frac{\hat{f}_i}{f_i^o} \quad (3.13)$$

Where G^t is the total Gibbs free energy, \bar{G}_i is the partial molar Gibbs free energy of species i , G_i^o is the standard Gibbs free energy, μ_i is the chemical potential, R is the molar gas constant, T is the temperature of system, \hat{f}_i is the fugacity in system, f_i^o is the standard-state fugacity, and n_i is the mole of species i . For reaction equilibrium in gas-phase, $\hat{f}_i = y_i \hat{\phi}_i P$ and $f_i^o = P^o$, where $\hat{\phi}_i$ is the fugacity coefficient, y_i is the gaseous mole fraction of species i .

Hence,

$$G^t = \sum_{i=1}^N n_i (\Delta G_{fi}^o + RT \ln \frac{y_i \hat{\phi}_i P}{P^o}) \quad (3.14)$$

Where, ΔG_{fi}^o is the Gibbs free energy of formation at temperature T.

This is the objective function that needs to be minimized. For this minimization an inbuilt function of MATLAB R2010b *fmincon* is called and utilized. This library function is applicable for constrained minimization problems. This function attempts to find a constrained minimum of a scalar function of several variables starting at an initial estimate. This is generally referred to as constrained optimization.

The species that are considered for the study are the six species involved in the four reactions R1, R2, R3, and R4 namely carbon dioxide, water, hydrogen, carbon monoxide, methane and oxygen. For the analysis of coke production and deposition at equilibrium, seventh

specie in the form of carbon in its graphite form is included in the analysis. As for the earlier data, once more NIST data are used for carbon considering it to be in graphite form.

The constraint equation in this case is the conservation of mass of elements involved in the reaction. Writing a material balance on the number of moles of the elements involved, i.e. Carbon, Hydrogen and Oxygen in this case yields us equation (3.15) which ties the inlet number of moles of carbon, oxygen and hydrogen to the moles of these elements at any point. This constraint along with the minimization of objective function gives us the moles of each species at a point when the Gibbs free energy has been minimized, or to put simply, at equilibrium.

$$A_{eq}x = b_{eq} \quad (3.15)$$

Where, A_{eq} is the matrix of number of atoms of the k^{th} element present in each molecule of chemical species i (3 elements(C, H, O) \times 7 species); x is the number of moles of each species; b_{eq} is the inlet number of moles of each element, C,H and O.

The equation (3.15) is basically a material balance which ties the inlet number of moles of carbon, oxygen and hydrogen to the moles of these elements at equilibrium. x is subjected to a lower bound so that no mole fraction can be negative, i.e. minimum value is 0, which is a physical constraint on the system.

The motivation behind this is to find out thermodynamically, the optimum conditions at which the reactor should be operated. The operating parameters that need to be ascertained are temperature, oxygen-to-methane ratio and steam-to-methane ratio. The proposed strategy here is to vary one out of these parameters and keeping the other values constant. The effect of changing these parameters on methane conversion, hydrogen yield and hydrogen-to-carbon monoxide ratio is evaluated and the operating conditions are chosen on the same basis. The results of this analysis are reported in the fifth chapter of this thesis as they are quite detailed and require a separate chapter.

CHAPTER 4

MODEL DEVELOPMENT

The mathematical model development for the reactor in which these reactions are occurring has been considered in this chapter. The reactor is a fixed bed reactor with a catalyst bed of Ni based alumina catalyst. The kinetics available for this type of catalyst is easiest and has been widely studied. The model is validated on the basis of published data.

4.1 KINETICS

A lot of study has gone into the Ni based catalysts for reforming of methane along with oxygen [42,43]. Dissanayake et al. studied the state of the Ni/Al₂O₃ catalyst and found that their experimental bed had different regions out of which complete oxidation of methane occurred over the second region where NiO+Al₂O₃ were found. As a result of complete consumption of oxygen, the next stage of the bed comprised of Ni/Al₂O₃ phase. Here the reforming reaction of methane corresponding to thermodynamic equilibrium at bed temperature occurs.

Xu and Froment [23] studied the water gas shift reaction and the methane reforming reactions (both partial and total reforming) on a Ni/MgAl₂O₄ catalyst used with α -alumina diluent. Based on the rate determining steps of Reaction No. 1, 2 and 3, Xu and Froment formulated a Langmuir type rate expression for the three reactions as given below:

$$r_1 = \frac{\frac{k_1}{P_{H_2}^{2.5}} (P_{CH_4} P_{H_2O} - \frac{P_{H_2}^3 P_{CO}}{Keq1})}{Den^2} \quad (4.1)$$

$$r_2 = \frac{\frac{k_2}{P_{H_2}} (P_{CO} P_{H_2O} - \frac{P_{H_2} P_{CO_2}}{Keq2})}{Den^2} \quad (4.2)$$

$$r_3 = \frac{\frac{k_3}{P_{H_2}^{3.5}} (P_{CH_4} P_{H_2O}^2 - \frac{P_{H_2}^4 P_{CO_2}}{Keq3})}{Den^2} \quad (4.3)$$

Where,

$$Den = 1 + K_{CO} P_{CO} + K_{H_2} P_{H_2} + K_{CH_4} P_{CH_4} + \frac{K_{H_2O} P_{H_2O}}{P_{H_2}} \quad (4.4)$$

P_i = Partial pressure of i^{th} component

The denominator in all the three rate expressions is the same because Xu and Froment assumed that all three reactions take place on the same active sites. The kinetics proposed by Xu and Froment for methane steam reforming on Ni catalyst are well established and have been widely reported and used by many researchers[27,44,45].

The methane combustion reaction has been studied on catalysts with a noble metal base viz. Pd, Pt etc. Most notable work on methane combustion kinetics and mechanism is by Trimm and Lam [31] who considered the Pt-alumina fiber catalyst for studying the reaction. They proposed a Langmuir Hinshelwood type of model, given as follows:

$$r_4 = \frac{k_{41} M_{CH_4} M_{O_2}}{(1 + K_{CH_4}^o M_{CH_4} + K_{O_2}^o M_{O_2})^2} + \frac{k_{42} M_{CH_4} M_{O_2}^{1/2}}{(1 + K_{CH_4}^o M_{CH_4} + K_{O_2}^o M_{O_2})} \quad (4.5)$$

Where, M_i is the molar percentage of species i .

This rate expression was applicable in higher temperature range of 813K with a standard deviation of 3.3% from the experimental data. De Smet et al. [22] have modified the Trimm and Lam kinetics for Ni catalyst for use at a very high pressure. However, the kinetic parameters utilized here are the ones proposed by Trimm and Lam and this kinetic expression has been utilized by a number of researchers including Ji et.al [25], De Groote and Froment [20], Rakib et al. [46] among a few.

Table 4.1: Arrhenius Parameter and Activation Energies^[23,25]

Reaction No.	A(k _j)(mol kg _{cat} ⁻¹ s ⁻¹)	E _j (J mol ⁻¹)
1.	1.17×10 ¹⁵ bar ^{0.5}	240100
2.	5.54×10 ⁵ bar ⁻¹	67130
3.	2.83×10 ¹⁴ bar ^{0.5}	243900
4.	A(k ₄₁) = 3.14×10 ⁻⁴ A(k ₄₂) = 2.64×10 ⁻⁴	- -

Where $k_j = A_j \times \exp(-E_j / RT)$ (4.6)

Table 4.2: Van't Hoff adsorption parameters and heats of adsorption for components^[23,25]

Species	A _{di}	ΔH _{di} (J mol ⁻¹)
CH ₄ (combustion)($K^{o_{CH_4}}$)	6.67×10 ⁻²	-
O ₂ (combustion) ($K^{o_{O_2}}$)	4.34×10 ⁻⁵	-
CH ₄ (K_{CH_4})	6.65×10 ⁻⁴ bar ⁻¹	-38280
CO (K_{CO})	8.23×10 ⁻⁵ bar ⁻¹	-70650
CO ₂ (K_{CO_2})	6.12×10 ⁻⁹ bar ⁻¹	-82900
H ₂ O (K_{H_2O})	1.77×10 ⁵	88680

Where $K_i = A_{di} \times \exp(-\Delta H_{di} / RT)$ (4.7)

4.2 REACTOR MODEL

The reactor considered is a tubular reactor with constant cross sectional area and is packed with Ni catalyst supported on Mg-Al₂O₃ catalyst. The walls of the reactor are covered with insulation layer. The pure oxygen stream is mixed along with feed and steam and preheated to the desired temperature and fed into the reactor.

In order to develop a one dimensional steady state mathematical model for the reactor, component material and energy balances are written. Following postulates are assumed for this model development:

- No pressure drop in the reactor (Isobaric operation)
- No heat loss to the surroundings from the reactor (Adiabatic)
- No concentration change in the radial direction
- No temperature change in the radial direction
- No catalyst deactivation considered/No coke formation reactions

- No external mass transfer resistance of catalyst particles
- No non-ideality in flow regime



Figure 4.1: Reactor diagram

With the above assumptions mentioned a balance on an infinitesimally volume of reactor yields the following equations:

$$\frac{dF_i}{dZ} = A_c \rho_b (1 - \varepsilon_b) \sum_{j=1}^4 \nu_j r_j \quad (4.8)$$

$$\frac{dT}{dZ} = \frac{A_c \rho_b (1 - \varepsilon_b) \sum_{j=1}^4 (-\Delta H_{rj} \nu_j r_j)}{\sum_{i=1}^6 F_i C_{p_i}} \quad (4.9)$$

Where,

i = Species, CH₄, CO₂, CO, H₂, O₂, H₂O and j = Reaction number, 1-4

$A_c = \pi R^2$, where R is radius of tube

ν_{ij} = Stoichiometric coefficient of i^{th} species in reaction j

ΔH_{rj} = Enthalpy of reaction j at temperature T

F_i = Flow rate of i^{th} species

Cp_i = Heat capacity of i^{th} species

4.3 MODEL VALIDATION

The mathematical model as formulated above has been validated on the basis of outlet temperature, outlet hydrogen-carbon monoxide ratio, and outlet mole fractions of species that were in the product side of any of the reactions, viz. CO_2 , CO , H_2 and H_2O . The industrial data used by De Groote and Froment [20] has been used to validate the model. The authors carried out the autothermal reforming of natural gas on Ni based catalyst. The input feed consists of natural gas (methane), oxygen and steam.

However the authors postulated that a very small quantity of hydrogen is present in natural gas feedstock available at industrial scale. This assumption/postulate is important because at zero partial pressure of H_2 the rate of reactions by Xu Froment kinetics tends to be extremely large. For the purpose of this simulation I have taken H_2 flow rate at inlet is taken to be 10^{-8} mol/s to avoid infinite reaction rates at inlet to the reactor.

Table 4.3: Input conditions of industrial reactor ^[20]

Input parameter	Value	Unit
Methane flow rate	3483	Nm^3/h
O_2/CH_4	0.598	-
$\text{H}_2\text{O}/\text{CH}_4$	1.4	-
Pressure	25	Bar
Inlet Temperature	808	Kelvin
Diameter of reactor	1.2	Meter
Catalyst density	Not mentioned	-
Porosity of bed, ε_b	Not mentioned	-

The values of catalyst density and porosity of bed are unavailable for the industrial reactor. For this the values of density and porosity for a typically used Ni-bed ($=2100 \text{ kg/m}^3$ and 0.43, respectively) as given in literature are used [22,27].

The model equations form an Initial Value Differential Equation Problem, and can be solved using an inbuilt Ordinary Differential Equation (ODE) solver in MATLAB R2010b which utilizes the Runge-Kutta numerical methods for solving. All the IVP conditions were input. All the reaction rates were multiplied by an effectiveness factor. The effect of intra-particle diffusion

is described by using these effectiveness factors. Literature shows that effectiveness factors are actually a function of temperature, and hence they vary along the length of the reactor and thus influence the rates of reaction in a dynamic fashion along the reactor [47]. However to evaluate the functional dependence of effectiveness factor on temperature is a handful procedure in itself. Thus for the sake of simplification an average value was used for the four effectiveness factors for the four reactions. The four values of effectiveness factors used by De Groote and Froment were 0.07, 0.06, 0.7 and 0.05 for R1, R2, R3 and R4 respectively (as in Table 3.5).

Table 4.4: Comparison between model predictions with industrial data

Parameter/Species	Unit	Industrial Data [20]	Validation Run(Model)	Relative Error
Outlet Temperature	Kelvin	1223	1310.7	7.17%
Outlet H ₂ /CO	-	2.854	2.728	4.42%
Outlet <i>x</i> fraction				
CO	-	0.160	0.1702	6.38%
H ₂ O	-	0.306	0.3057	1%
H ₂	-	0.456	0.46417	1.8%

Thus, a close agreement between the two can be seen and hence it points to the applicability of our model. The errors are within acceptable limits.

This chapter contains the results of thermodynamic analysis conducted considering seven species including carbon deposition involved in oxidative reforming of methane and the results of simulation of the mathematical model developed in the previous chapter. The simulation conditions are based on the analysis of the results obtained in Chapter 3. The obtained results are also analyzed.

5.1 RESULTS OF THERMODYNAMIC ANALYSIS

The thermodynamic evaluation is carried out keeping in mind the parameters that will be required for operation. The key input variables that could be varied during the Gibb's energy minimization technique to determine mole fractions of different components at equilibrium are temperature, pressure, oxygen-to-methane ratio and steam-to-methane ratio. The parameters that are evaluated by this analysis and that are dependent on the values considered for these input variables are taken to be the conversion of methane, hydrogen to carbon monoxide ratio, (which is an important parameter for determining syngas quality), hydrogen moles being produced and the moles of coke generated at equilibrium. The strategy chalked out is to determine the best possible values of the input variables from a selected range using the results of thermodynamic analysis by studying the impact of these input variables on the agreed upon output parameters.

Table 5.1: Input variables and their possible ranges

Input variable	Range of possible values
Temperature	600-1300K
Pressure	1-25 bar
Oxygen-to-methane ratio	0.2-1.0
Steam-to-methane ratio	0-10

The range for these input variables is decided on a number of factors. In the following discussion we shall analyze how the values for different variables were reached upon. The basic approach is to study the effect of changing input values to be able to see a change in the output values.

5.1.1 Temperature Range

The temperature range is decided on the basis of the conversion. It is quite evident that at a higher temperature the conversion increases. It can be seen that at temperatures above the range of 900 K -1000 K the conversion for higher steam-to-methane ratios reaches to values exceeding 99% (See Figures 5.4, 5.8, 5.12, 5.16 and 5.20). It is important to note that these are theoretical values for equilibrium conversions and independent of reaction kinetics. At a higher temperature value, the coke yield is also reduced for every value of oxygen-to-methane ratio and steam-to-methane ratio (See Figures 5.1, 5.5, 5.9, 5.13 and 5.17). Thermodynamically, it can be generalized that a higher temperature is aiding the overall conversion process and minimizing the production of coke. This is also strengthening the initial analysis on the temperature feasibility range which found the reactions R1, R2, R3 and R4 to be proceeding in the forward direction (and hence aiding overall methane conversion in the range of 900-1100K). Hence, it has been ascertained that a temperature range of 900-1200K would be suitable for the best performance of the reactor.

5.1.2 Steam-to-Methane Ratio

It can be seen from the conversion at any oxygen content that increasing the steam-to-methane ratio increases the conversion at the same temperature (See Figures 5.4, 5.8, 5.12, 5.16 and 5.20). However, it needs to be pointed out that beyond a certain value of steam content, at higher temperatures that have been selected in the previous section, the conversion is already at its theoretical peaks and the additional steam has no visible effect. Similar is the effect seen in carbon content. At higher values of steam to methane ratio, the coke formation are reduced considerably (See Figures 5.1, 5.5, 5.9, 5.13 and 5.17). Thus from these two effects alone, it would seem that a higher steam content is beneficial to us. When the factor of hydrogen to carbon monoxide ratio is brought into the picture it is evident that as a general trend a higher steam ratio leads to higher hydrogen to carbon monoxide ratio, the only visible exception to the trend being keeping the steam supply to zero. (See Figures 5.3, 5.7, 5.11, 5.15 and 5.19) Thus, a higher value of steam-to-methane ratio makes the theoretical hydrogen to carbon monoxide content too high. Based on this a range of 0.5-3 is chosen for steam-to-methane content.

5.1.3 Oxygen-to-Methane Ratio

For determining the optimum oxygen-to-methane ratio we can see from the plots that increasing oxygen content means better conversion, lower coke content and suitable hydrogen-to-carbon monoxide ratios. The plots are for a constant steam to methane ratio with varying oxygen content. The analysis was done on an oxygen ratio of 0.2-1.0 widening the range as determined by the autothermal point in section 3.1. The conversion and coke content at the chosen temperature range, do not amount to a practical difference (See Figures 5.21, 5.22, 5.25, and 5.26). However, when we analyze the hydrogen moles produced there is a visible decline in production of hydrogen with increasing oxygen-to-methane ratio (See Figures 5.23 and 5.24). Based on this analysis an oxygen-methane ratio greater than 0.5 is chosen which also satisfies the region for oxidative reforming.

5.1.4 Pressure Range

The analysis of pressure range is based on literature review and Le Chatelier's principle which dictates the equilibrium extent of any reaction. Freitas et al. [18] showed that the conversion is lowered at higher pressure. Even though the increased pressure also reduces coke formation, at the temperature range that has been selected, the coke formation is low enough to work at a lower pressure. Thus the optimum pressure for better conversion is 1 bar.

Thus, on the basis of the thermodynamic analysis the optimum conditions for the operation of the reactor were determined. The parameters that were optimized were temperature, pressure, oxygen-to-methane ratio and steam-to-methane ratio. This optimization relied on the equilibrium values of methane conversion, carbon generation, hydrogen-carbon monoxide ratio and moles of hydrogen produced. The initial analysis on the temperature feasibility of reactions as well as the determination of autothermal point was crucial as initial pointers. The obtained values of input parameters provide us with values to efficiently simulate the model developed previously.

Table 5.2: Values obtained for input parameters by analysis

Parameter	Value	Unit
Temperature	900-1200	Kelvin
Pressure	1	Bar
Steam: Methane Ratio	0.5-3	-
Oxygen: Methane Ratio	0.5-1.2	-

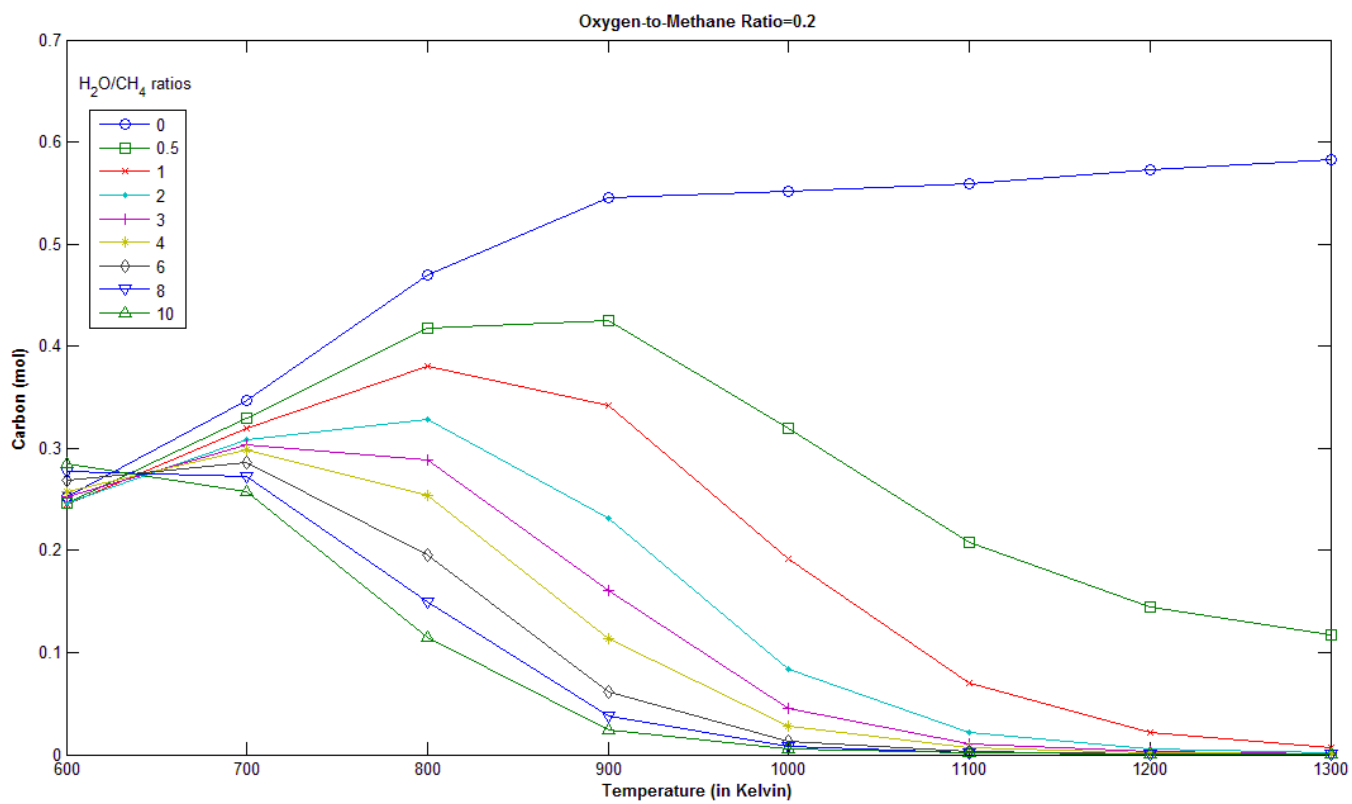


Figure 5.1: Coke formation at different steam/methane ratios with oxygen/methane=0.2

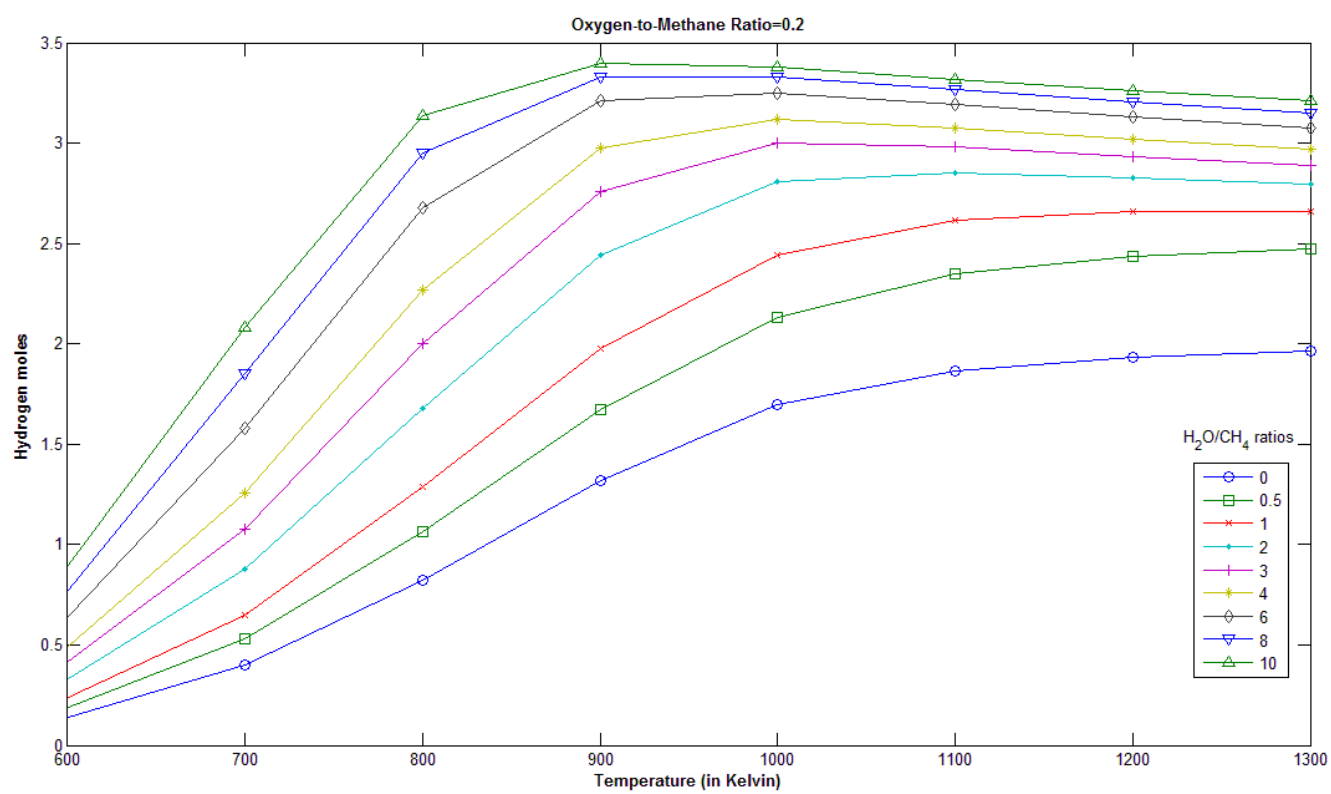


Figure 5.2: Hydrogen moles at different steam/methane ratios with oxygen/methane=0.2

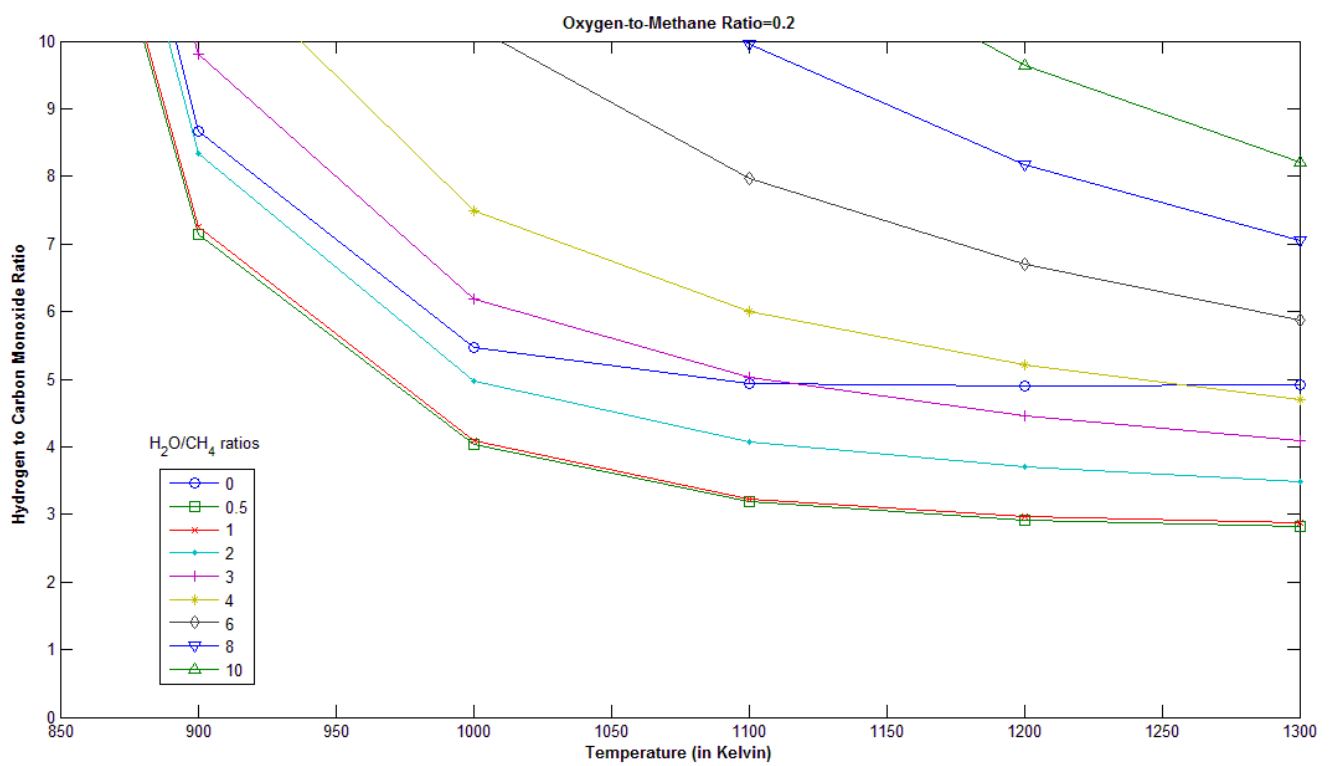


Figure 5.3: Hydrogen/Carbon Monoxide ratio at different steam/methane ratios with oxygen/methane=0.2

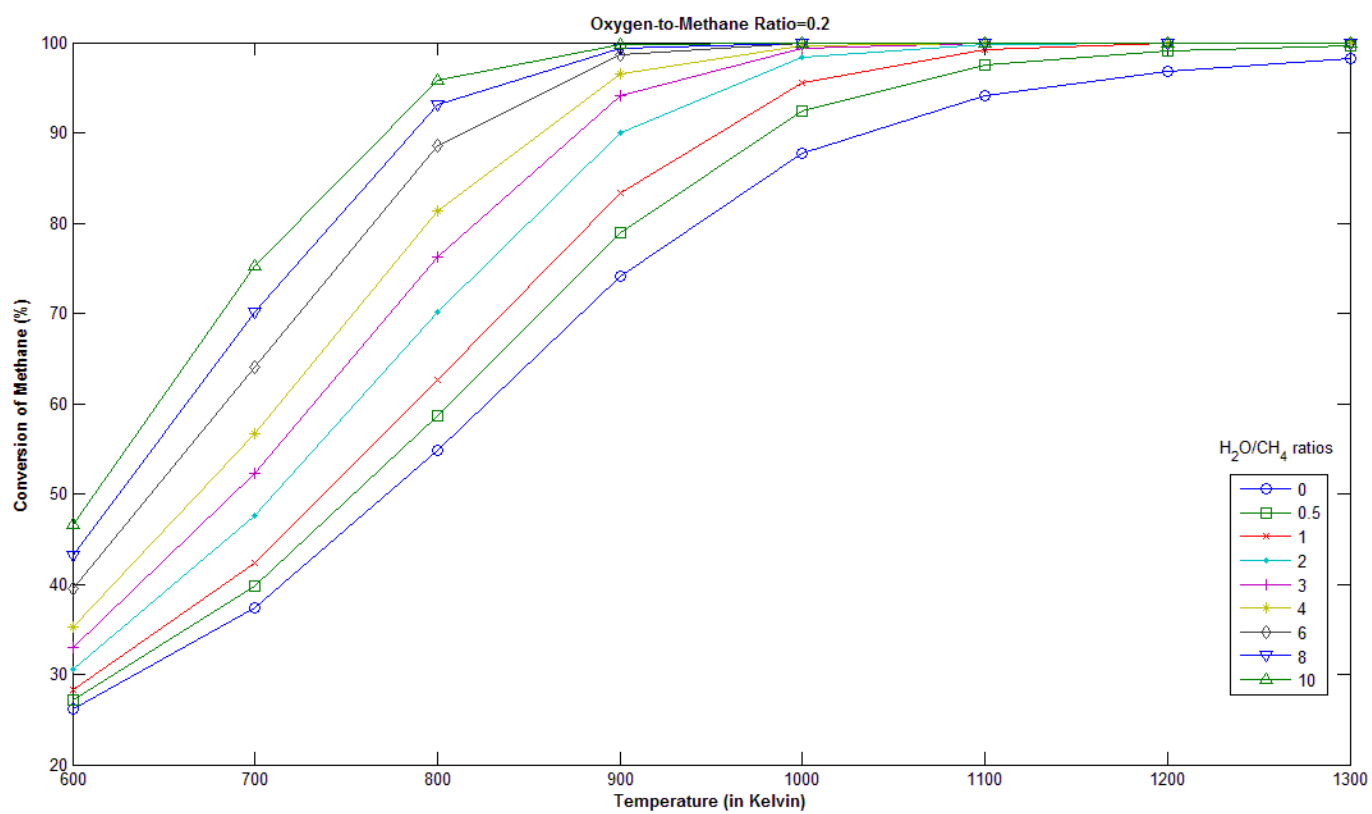


Figure 5.4: Conversion of methane at different steam/methane ratios with oxygen/methane=0.2

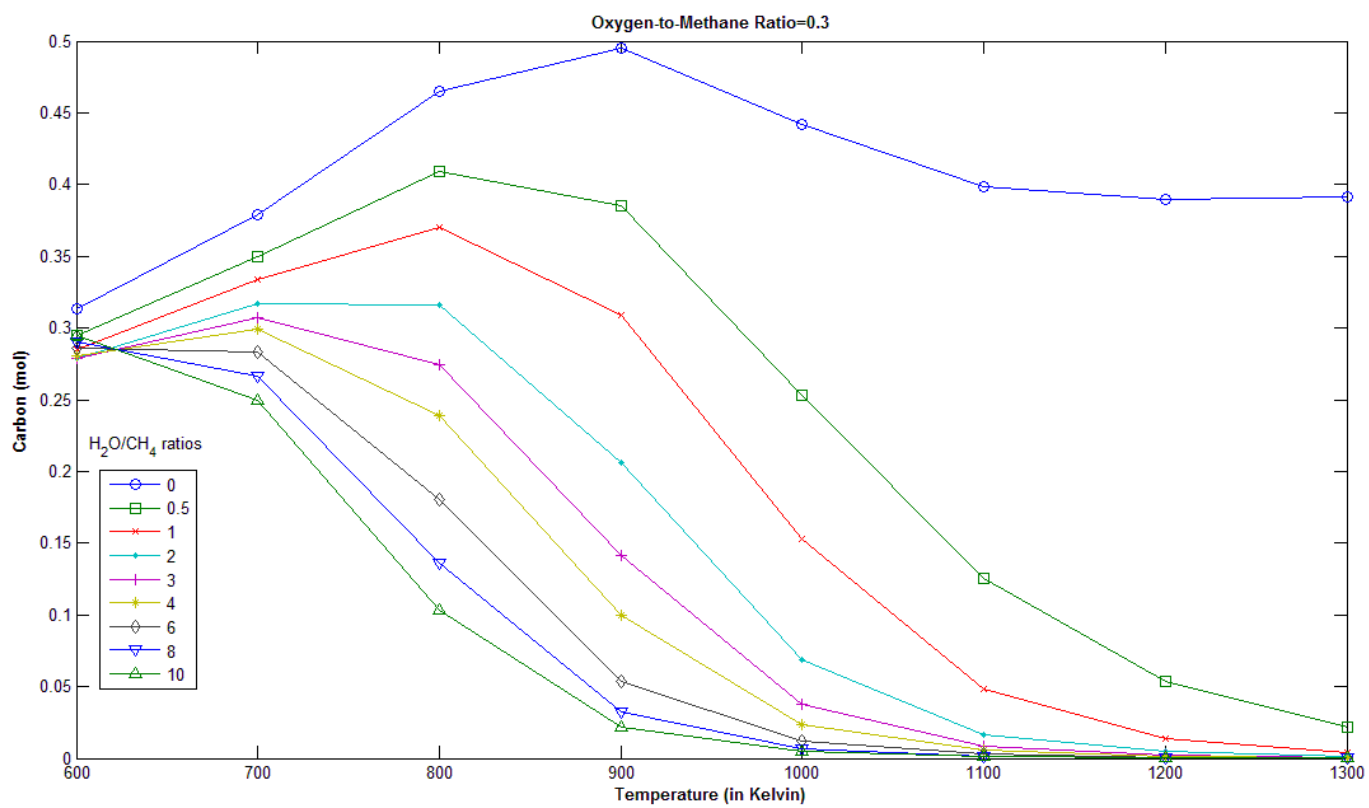


Figure 5.5: Coke formation at different steam/methane ratios with oxygen/methane=0.3

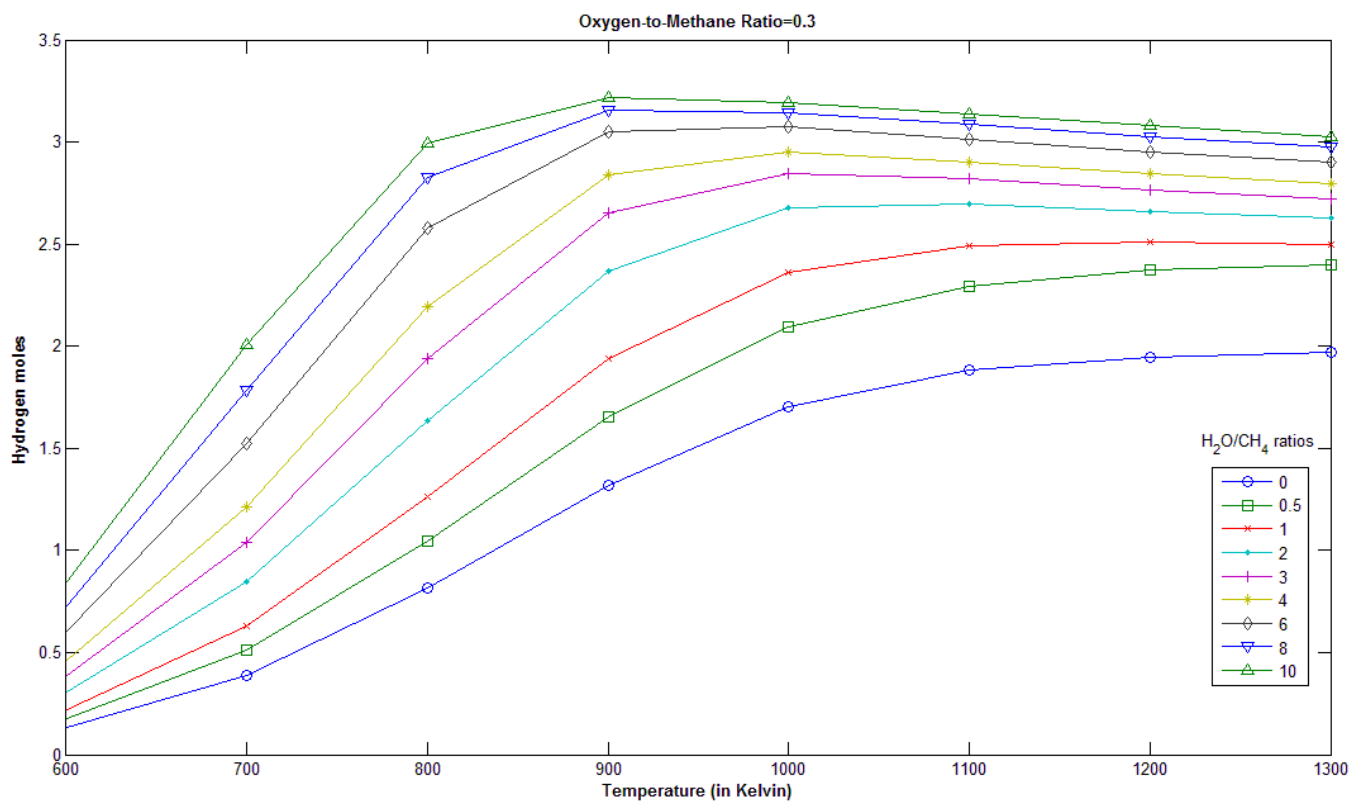


Figure 5.6: Hydrogen moles at different steam/methane ratios with oxygen/methane=0.3

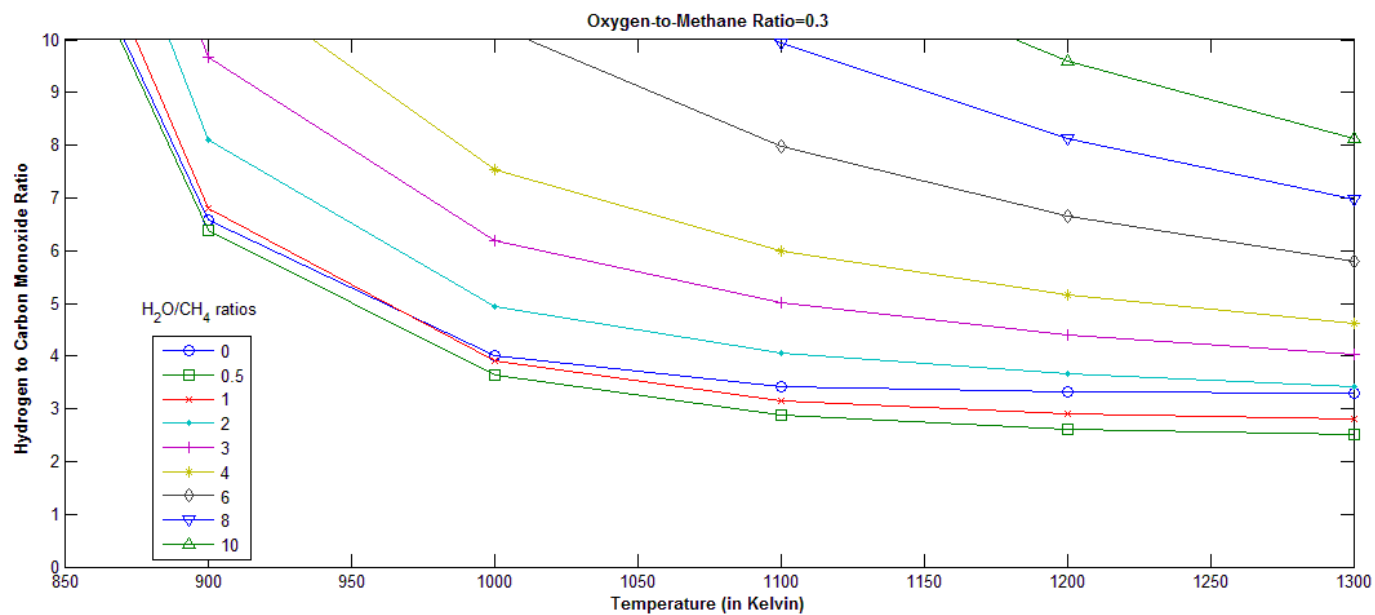


Figure 5.7: Hydrogen/Carbon Monoxide ratio at different steam/methane ratios with oxygen/methane=0.3

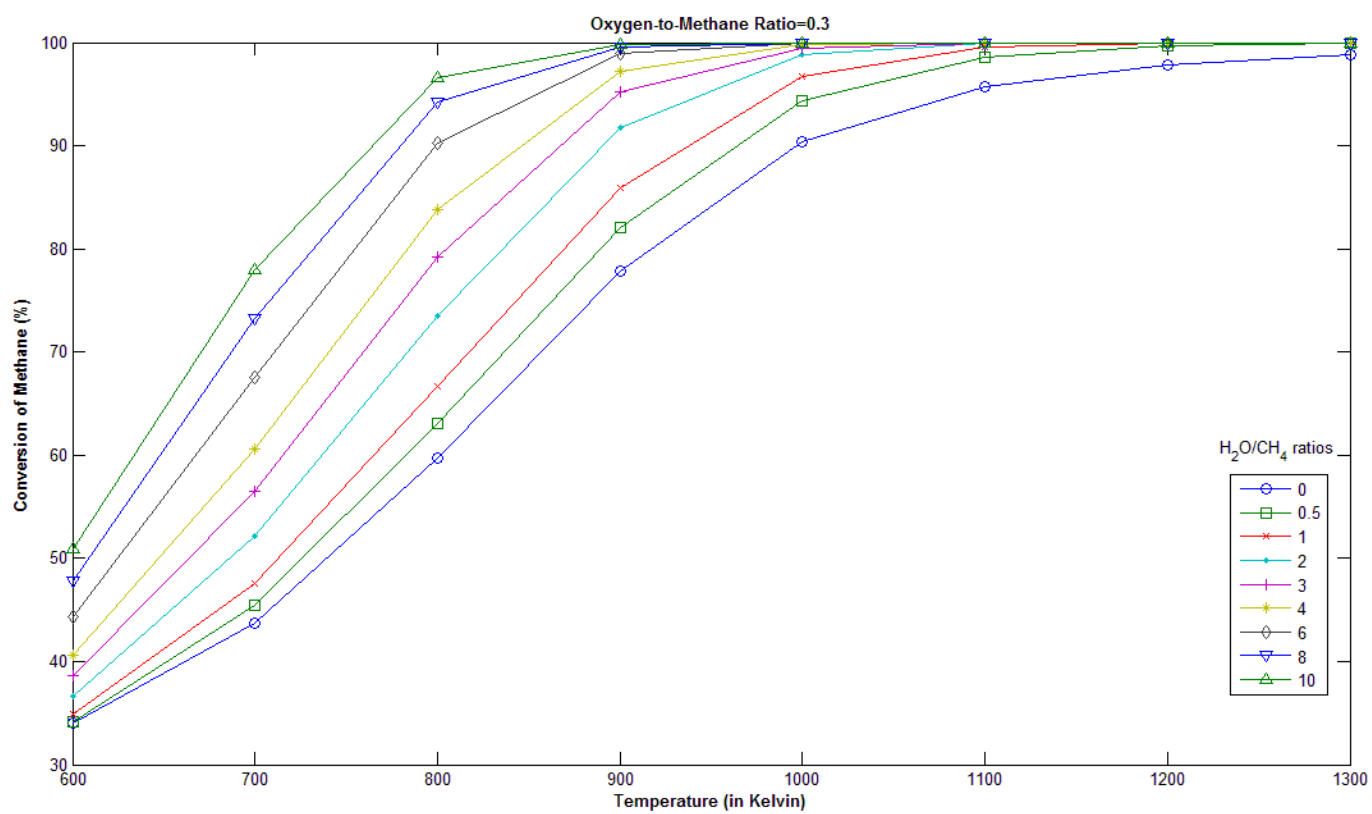


Figure 5.8: Conversion of methane at different steam/methane ratios with oxygen/methane=0.3

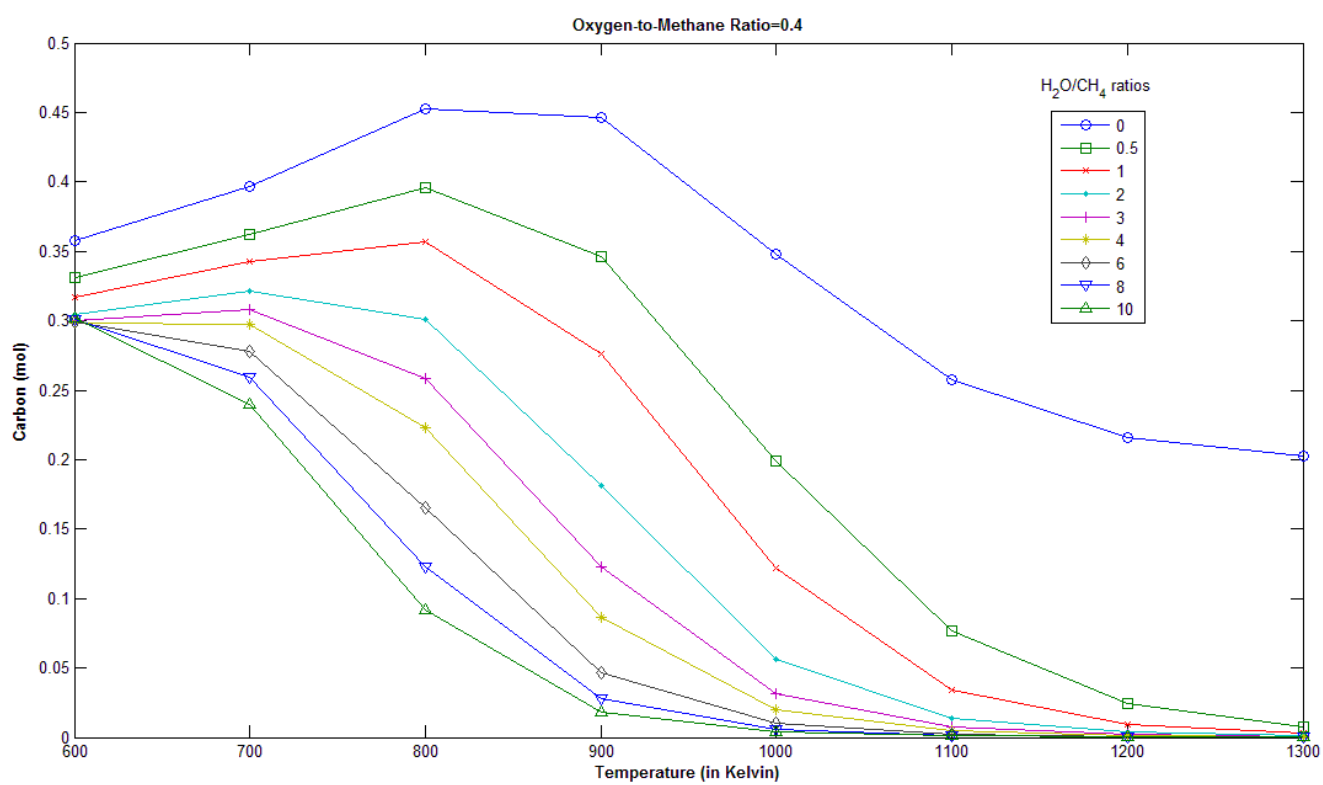


Figure 5.9: Coke formation at different steam/methane ratios with oxygen/methane=0.4

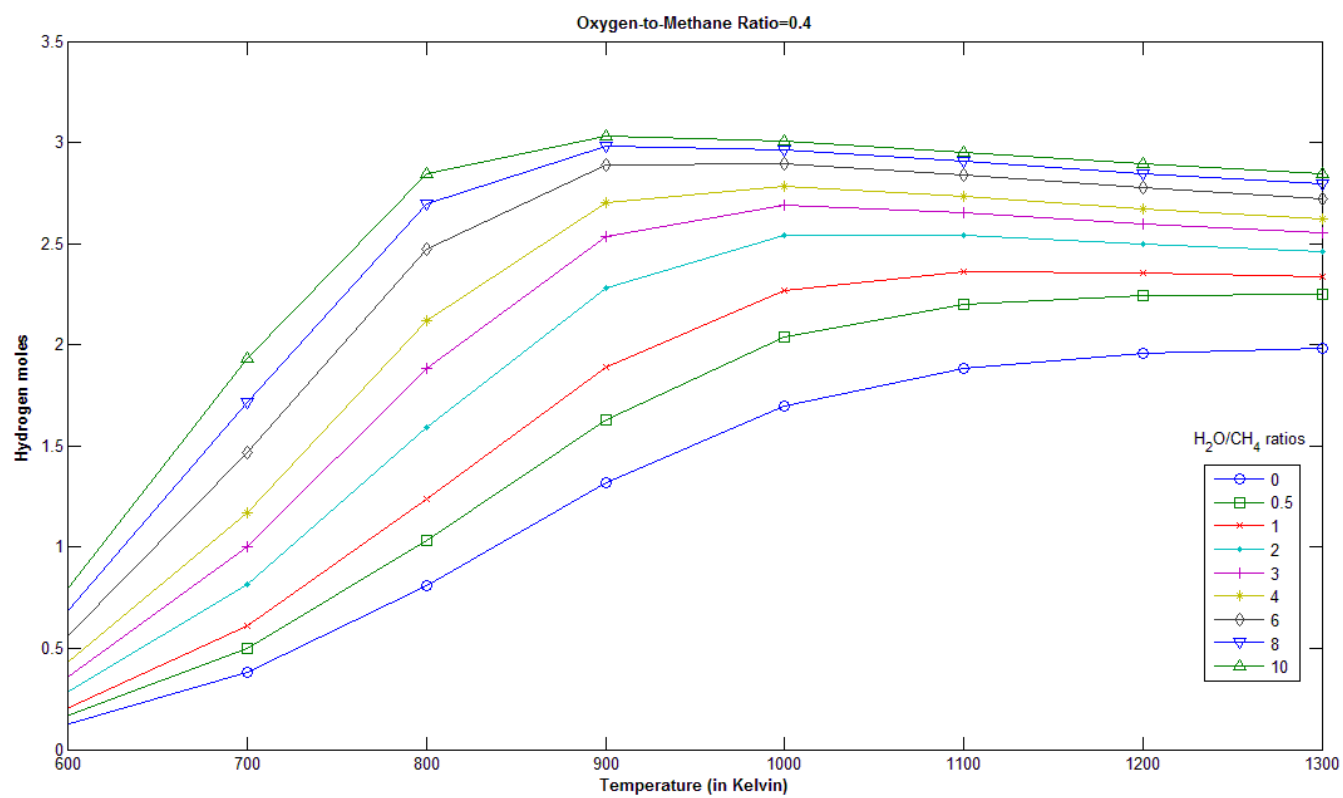


Figure 5.10: Hydrogen moles at different steam/methane ratios with oxygen/methane=0.4

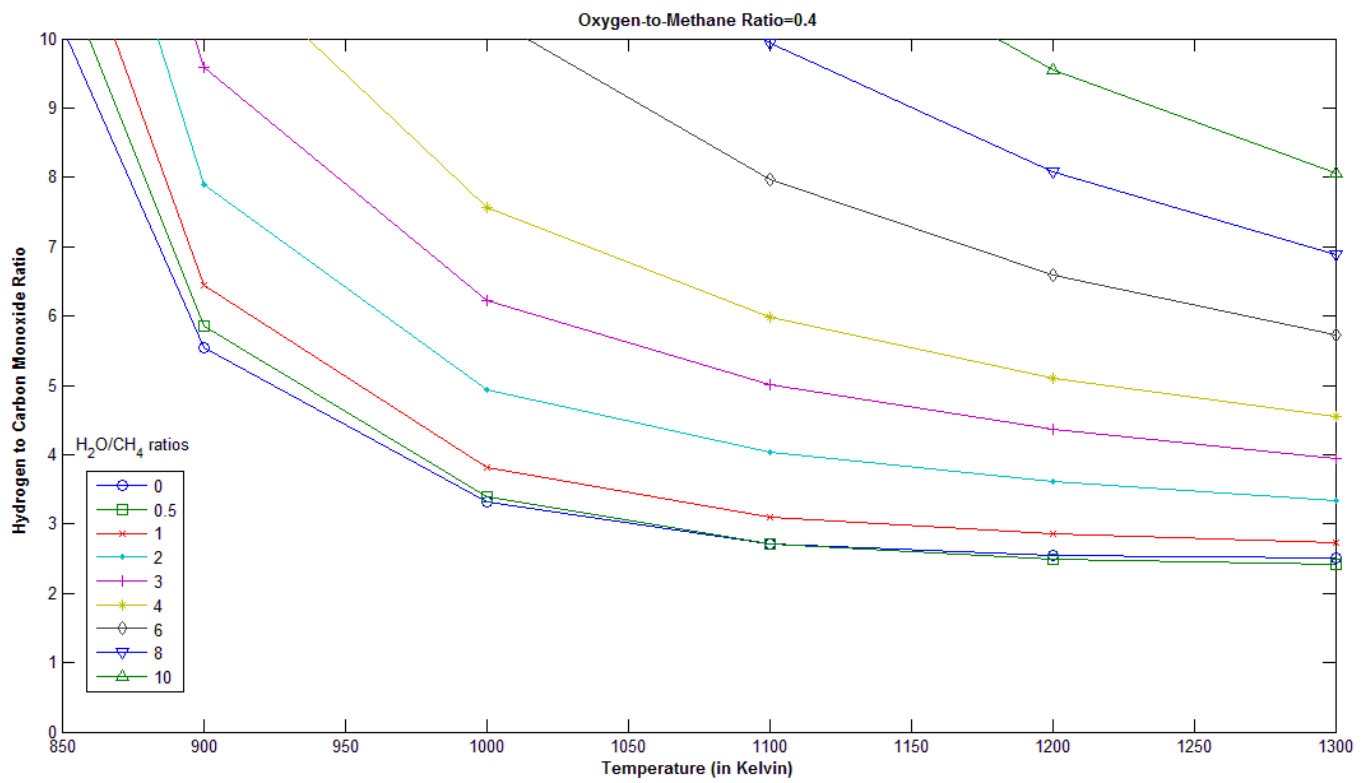


Figure 5.11: Hydrogen/Carbon Monoxide ratio at different steam/methane ratios with oxygen/methane=0.4

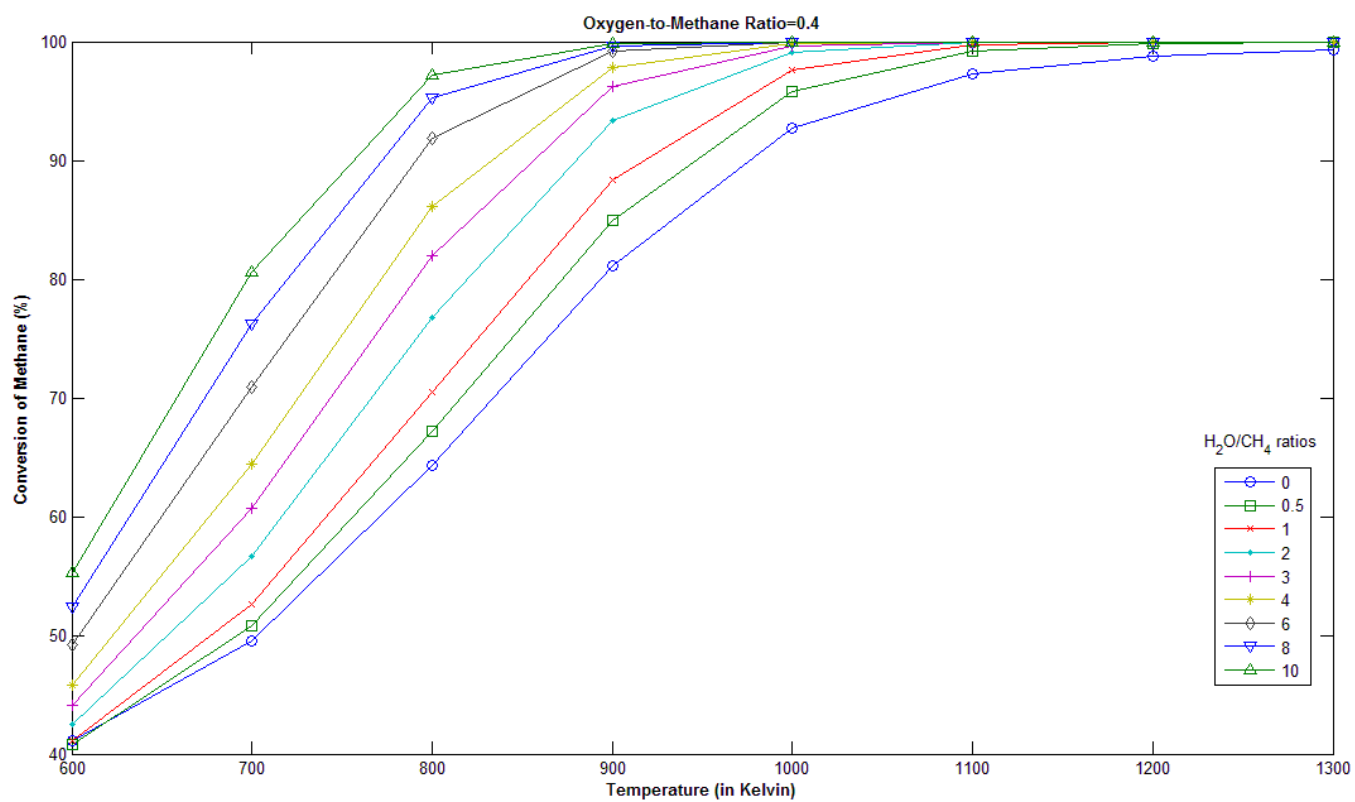


Figure 5.12: Conversion of methane at different steam/methane ratios with oxygen/methane=0.4

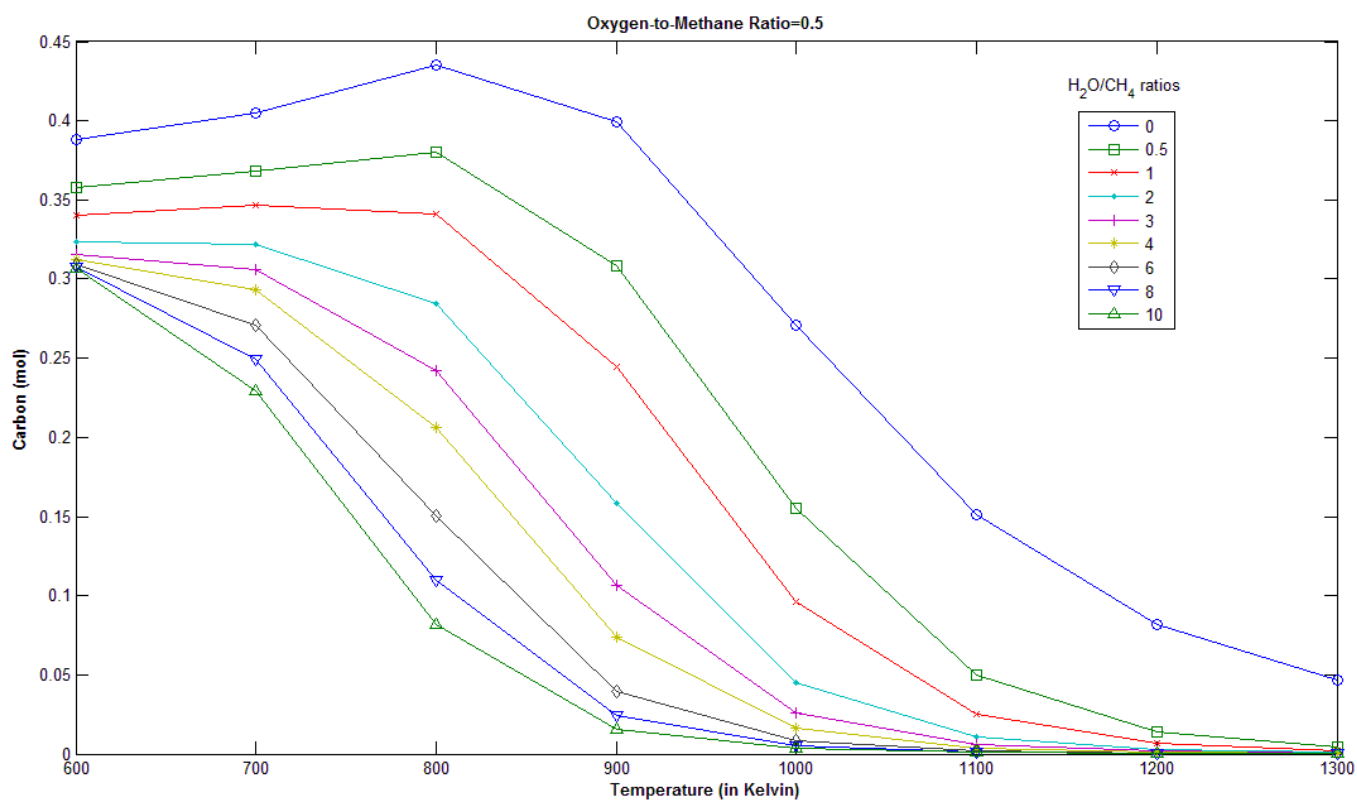


Figure 5.13: Coke formation at different steam/methane ratios with oxygen/methane=0.5

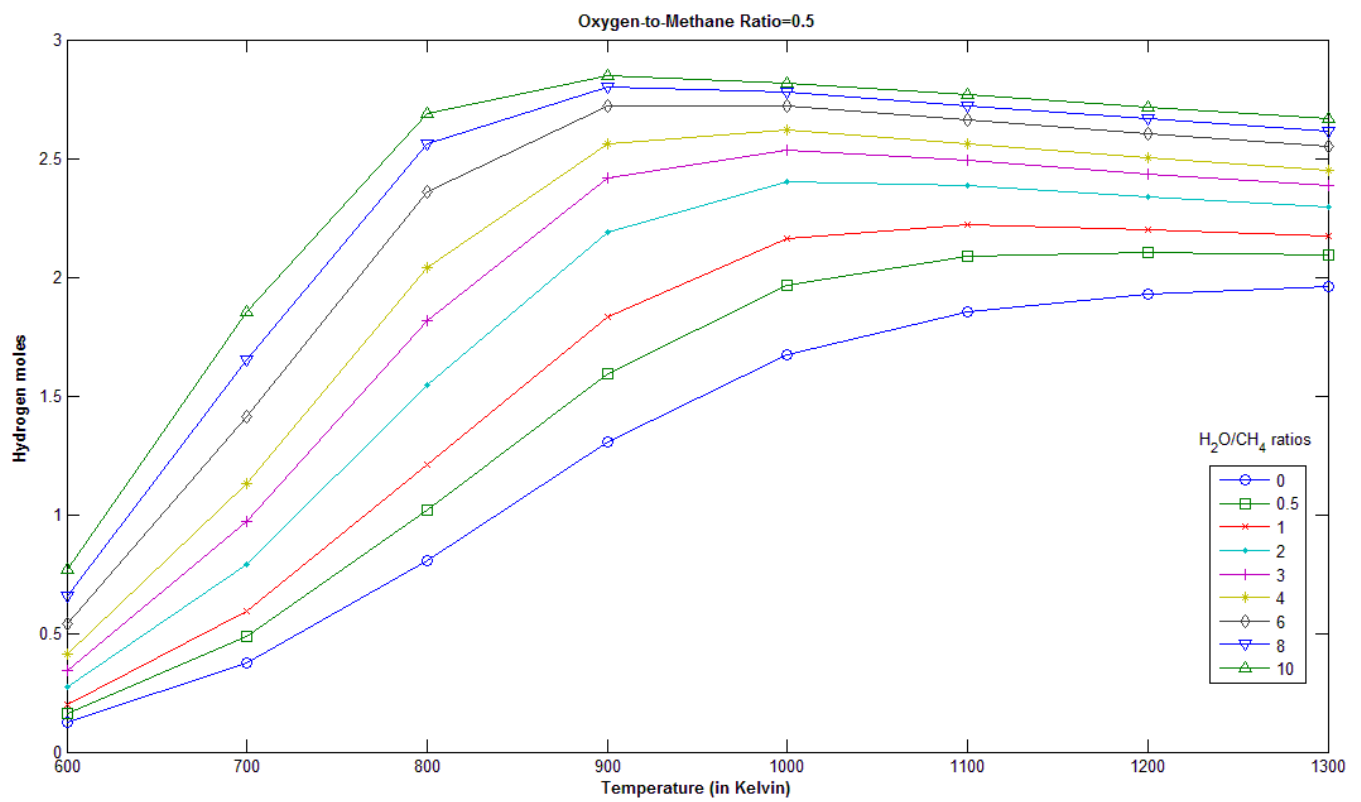


Figure 5.14 : Hydrogen moles at different steam/methane ratios with oxygen/methane=0.5

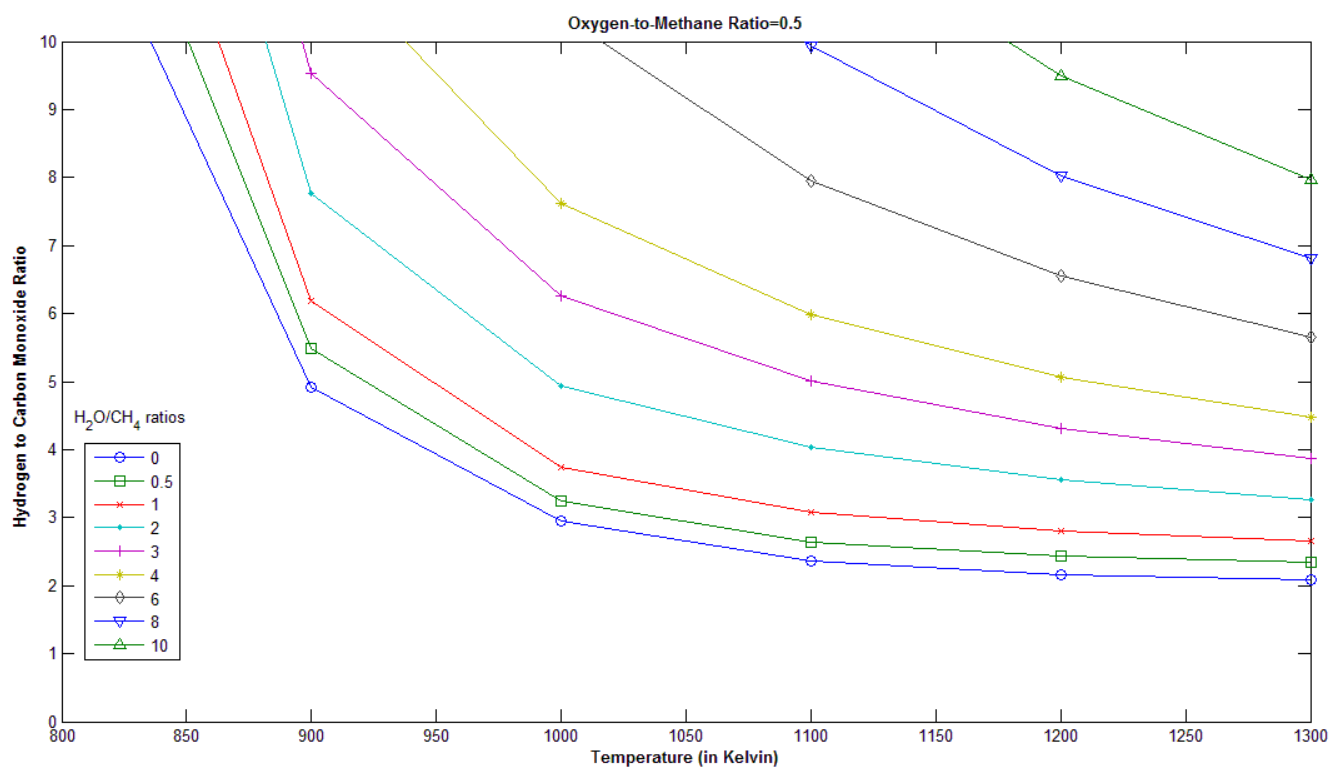


Figure 5.15: Hydrogen/Carbon Monoxide ratio at different steam/methane ratios with oxygen/methane=0.5

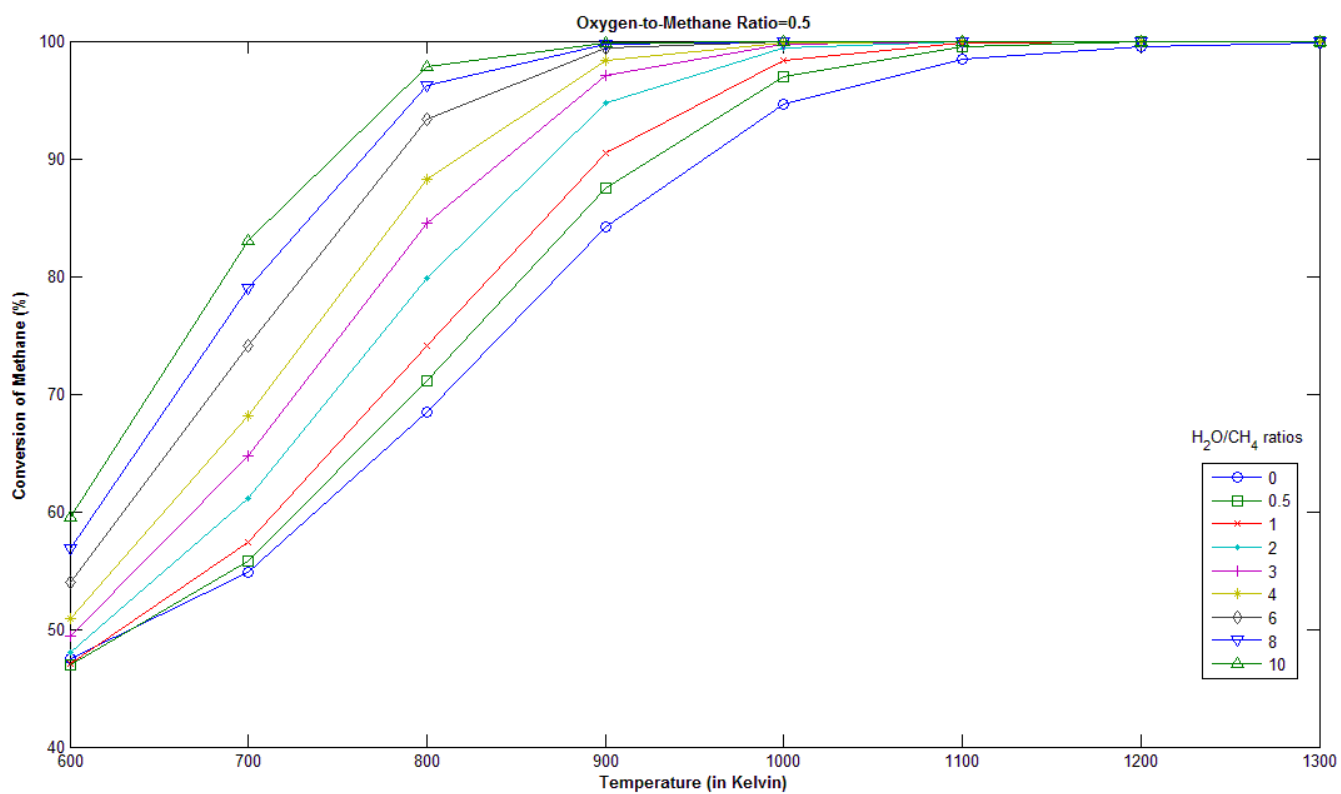


Figure 5.16: Conversion of methane at different steam/methane ratios with oxygen/methane=0.5

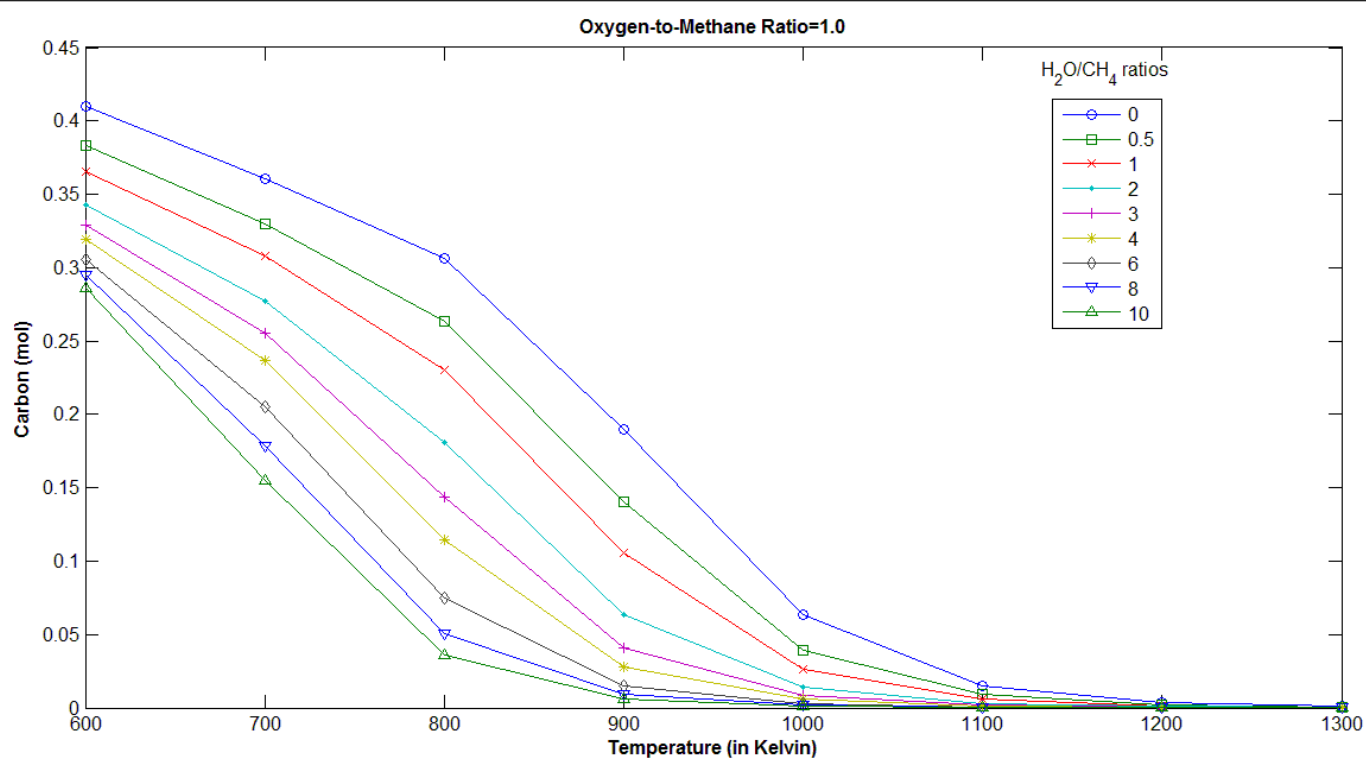


Figure 5.17: Coke formation at different steam/methane ratios with oxygen/methane=1.0

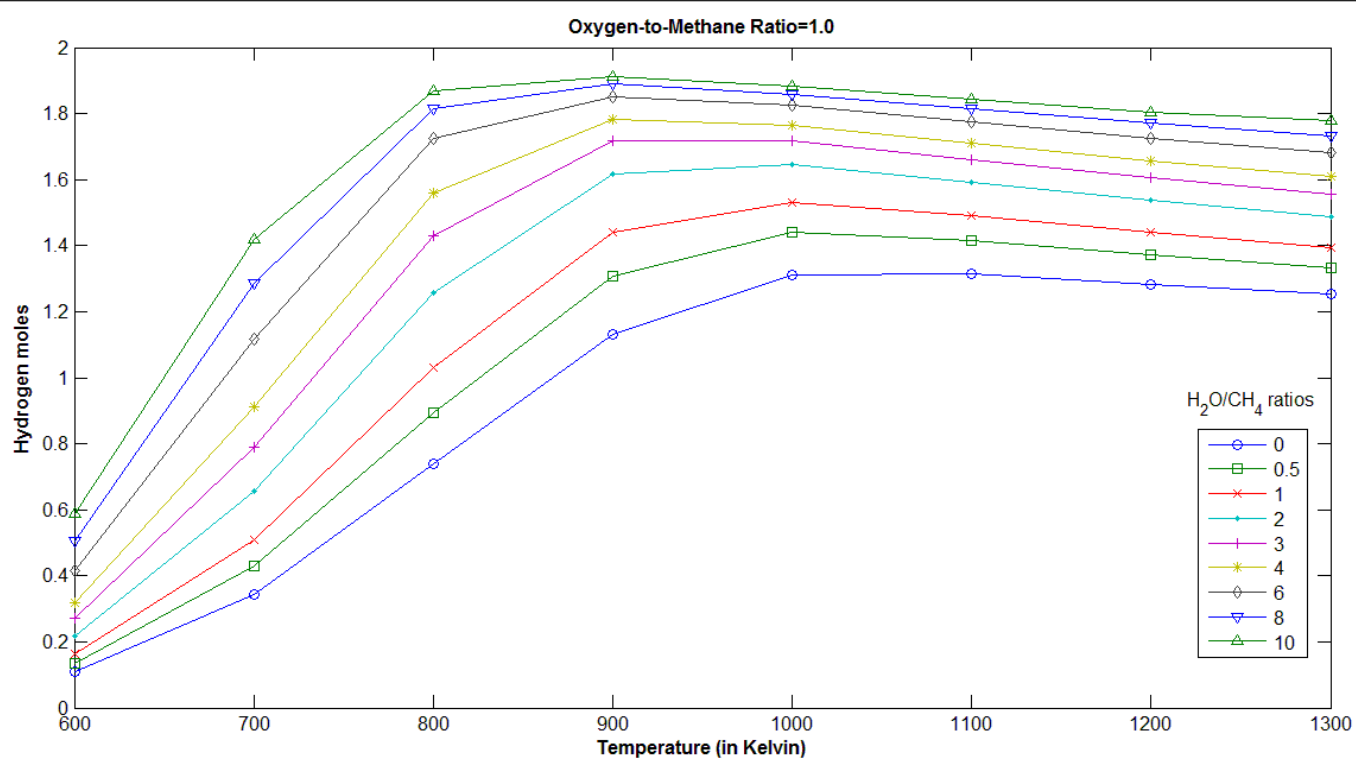


Figure 5.18: Hydrogen moles at different steam/methane ratios with oxygen/methane=1.0

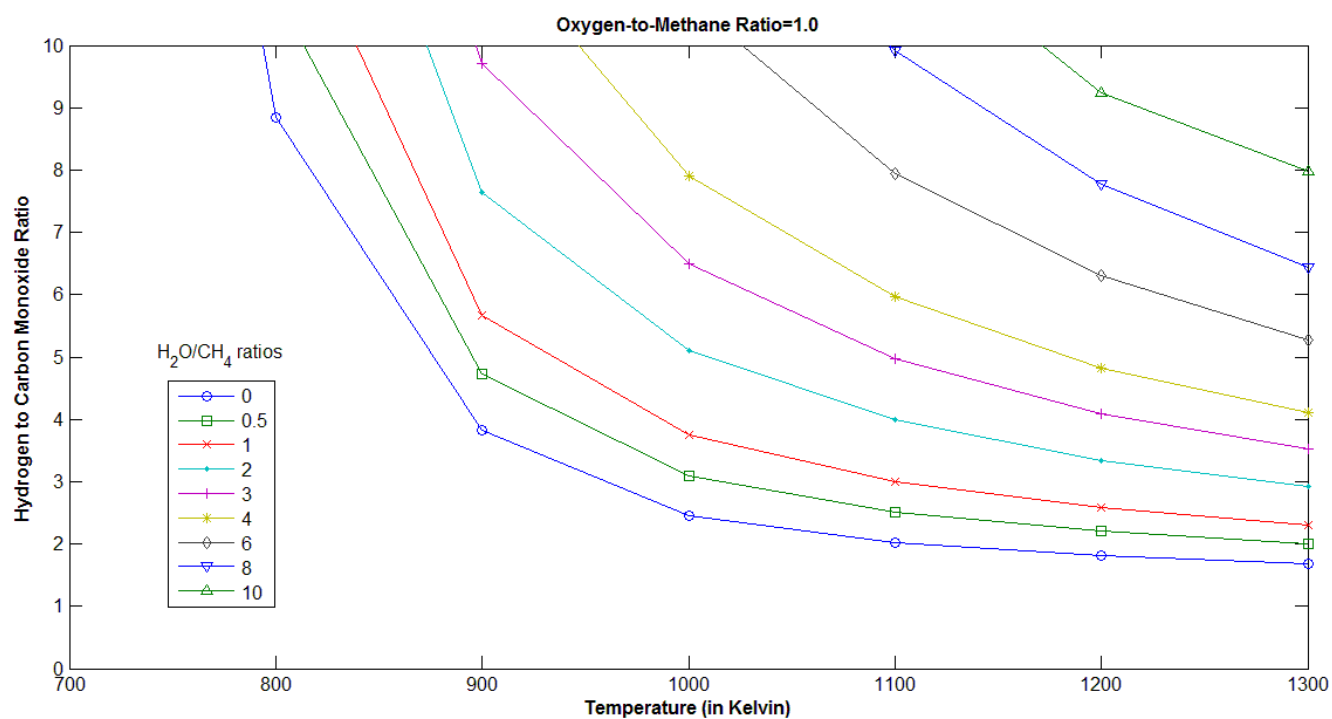


Figure 5.19: Hydrogen/Carbon Monoxide ratio at different steam/methane ratios with oxygen/methane=1.0

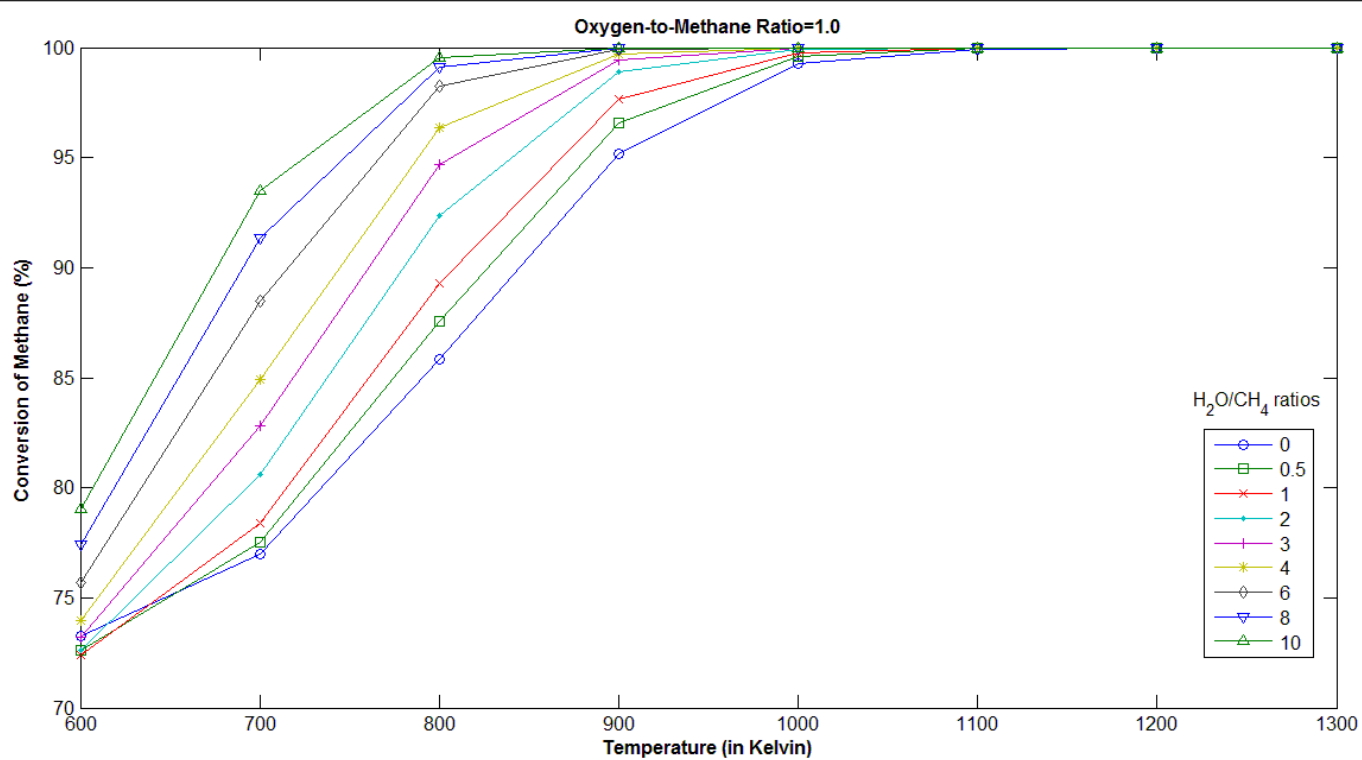


Figure 5.20: Conversion of methane at different steam/methane ratios with oxygen/methane=1.0

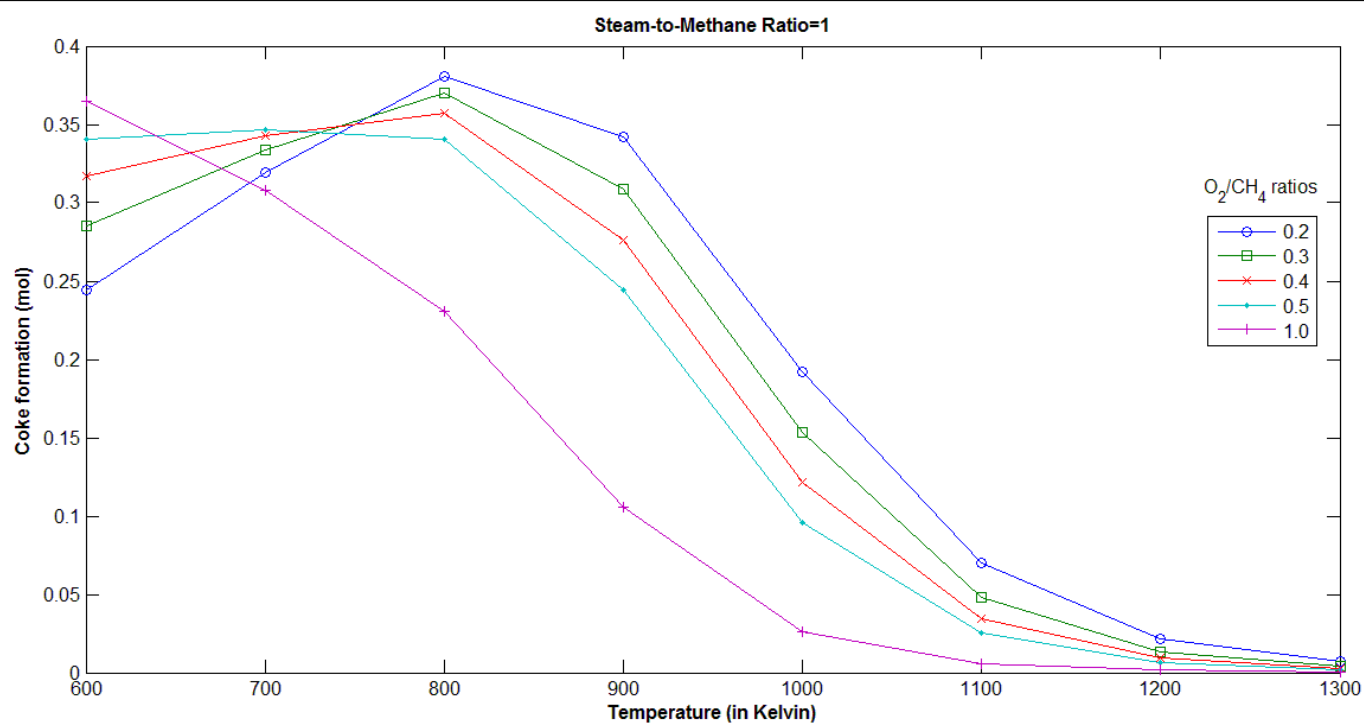


Figure 5.21: Effect of changing oxygen/methane ratio on coke formation at steam/methane=1.0

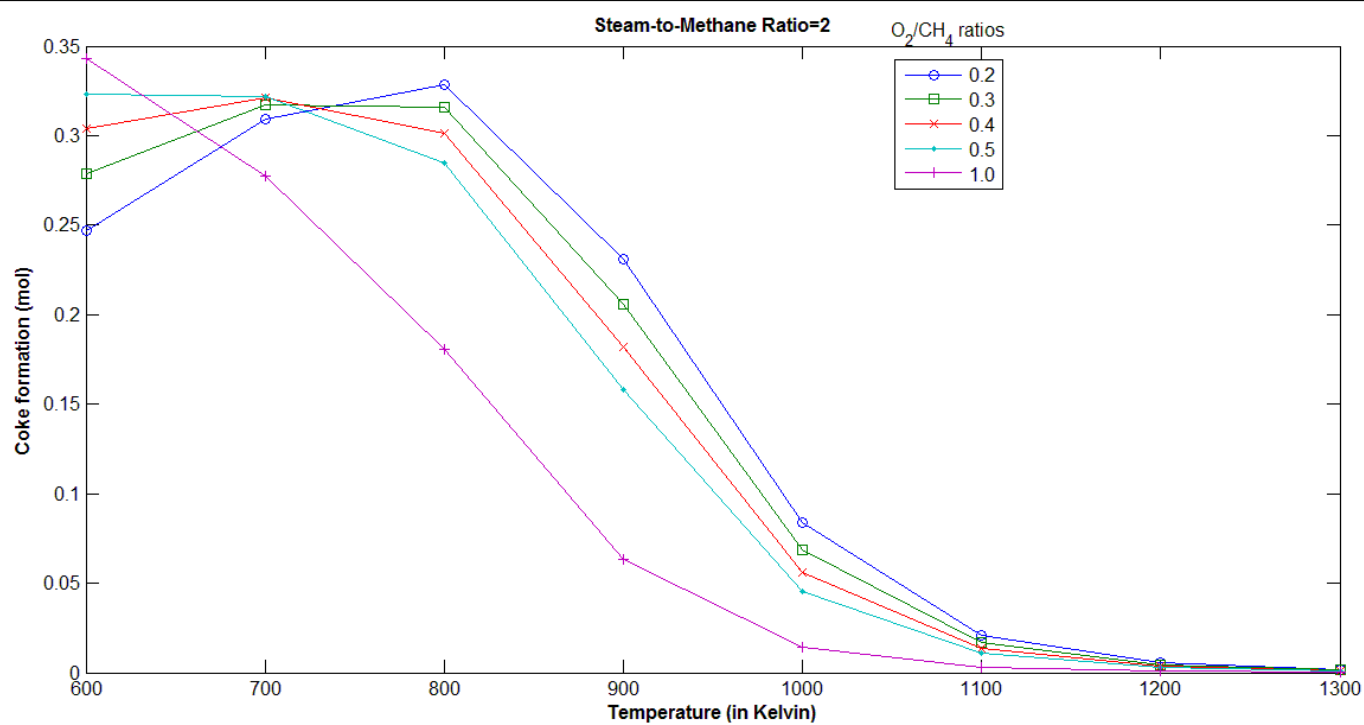


Figure 5.22: Effect of changing oxygen/methane ratio on coke formation at steam/methane=2.0

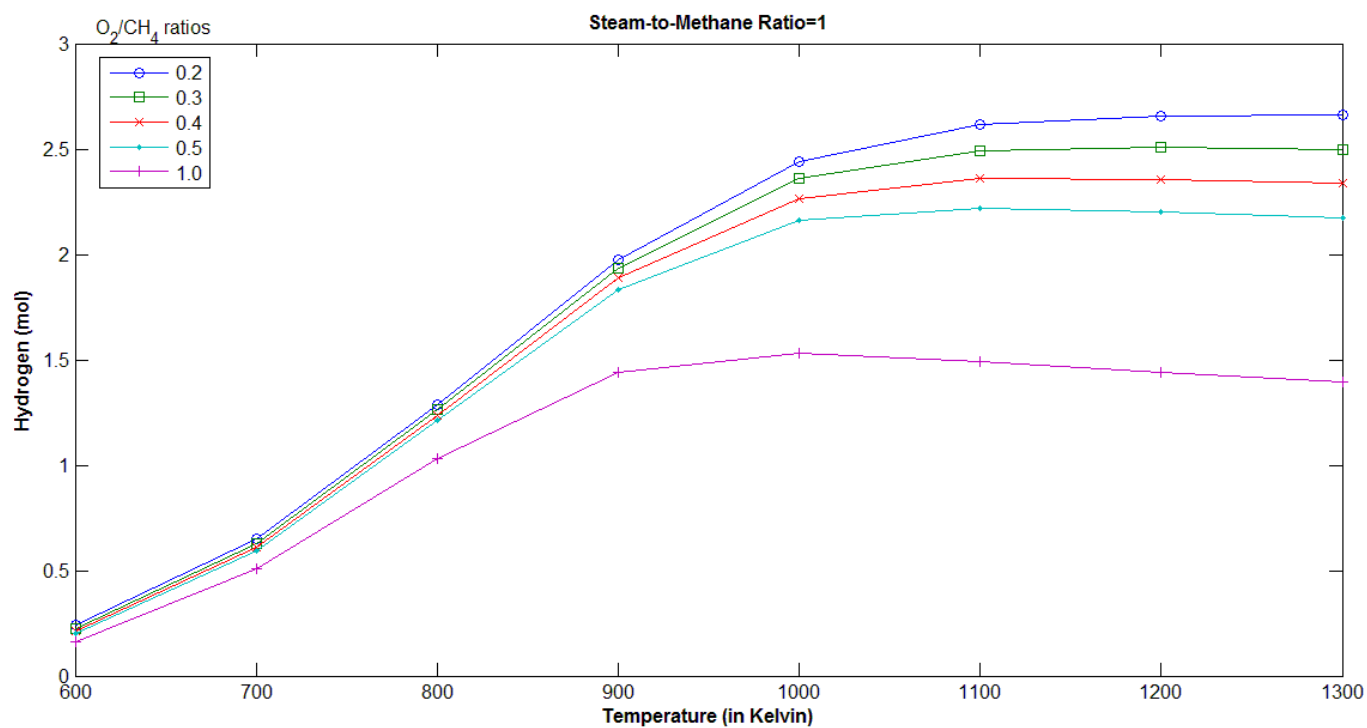


Figure 5.23: Effect of changing oxygen/methane ratio on hydrogen moles at steam/methane=1.0

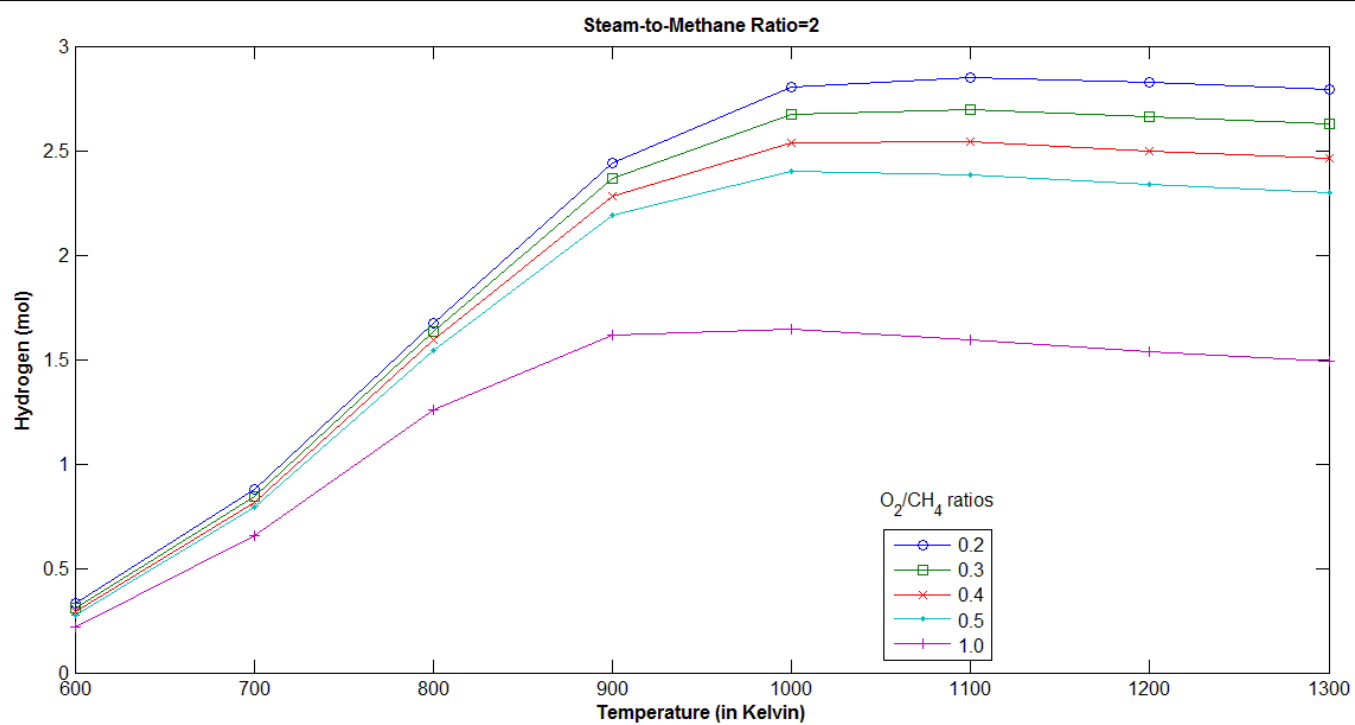


Figure 5.24: Effect of changing oxygen/methane ratio on hydrogen moles at steam/methane=2.0

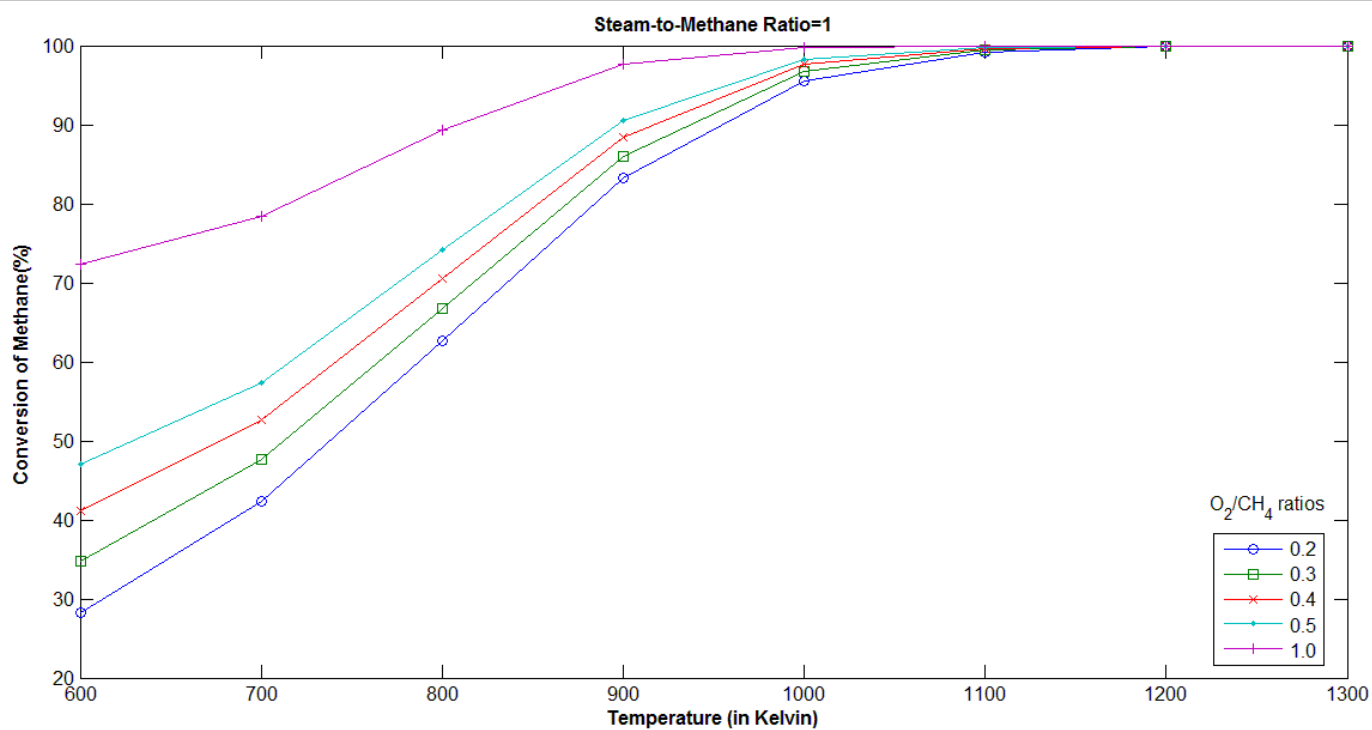


Figure 5.25: Effect of changing oxygen/methane ratio on methane conversion at steam/methane=1.0

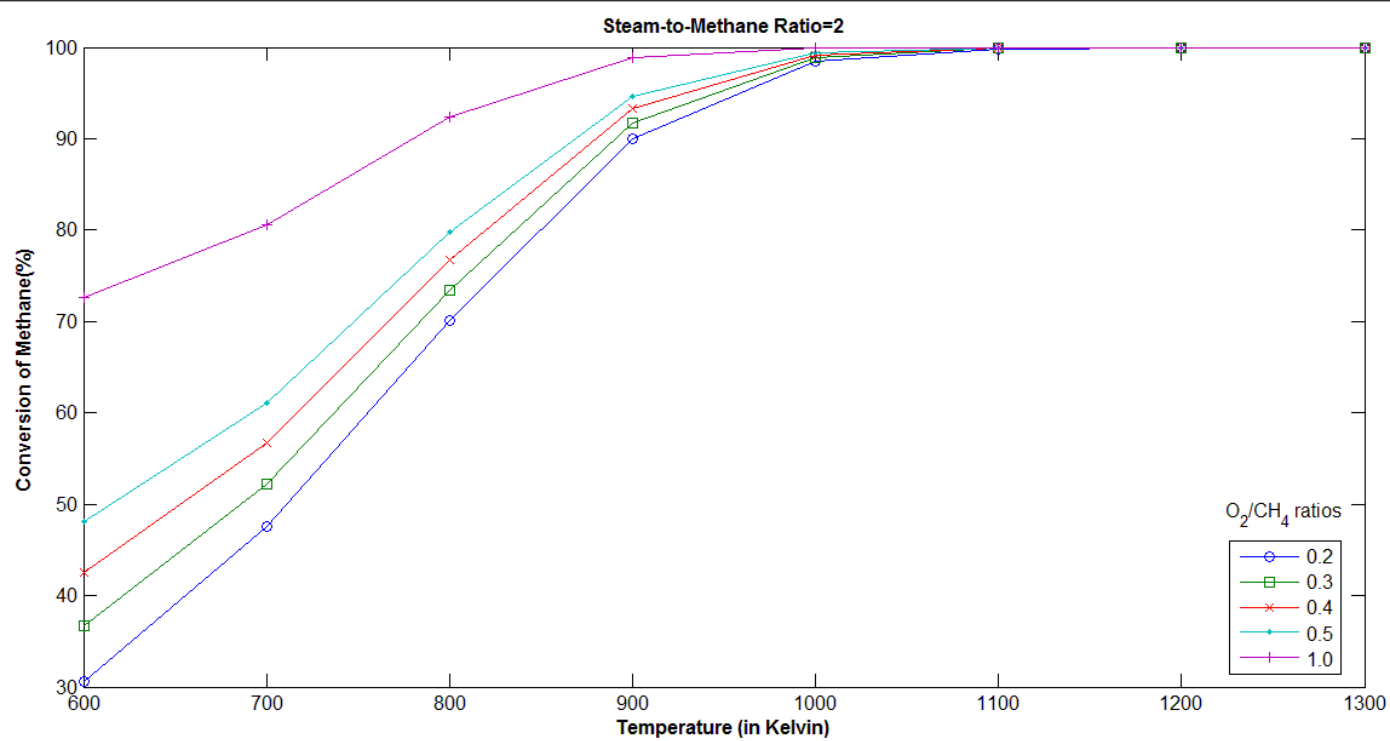


Figure 5.26: Effect of changing oxygen/methane ratio on methane conversion at steam/methane=2.0

5.2 MODEL SIMULATION

The simulation for the study of the reactor has been done by using the reactor specifications used by Kumar et al. [27] who have utilized the specifications of Ji et al. [25] The specifications are tabulated below:

Table 5.3: Initial flow rates for simulation of model ^[27]

Parameter	Value	Unit
Initial methane flow rate	2.50×10^{-3}	mol s^{-1}
Initial CO flow rate	0.00	mol s^{-1}
Initial CO ₂ flow rate	0.00	mol s^{-1}
Initial H ₂ flow rate	10^{-10}	mol s^{-1}

The hydrogen flow rate is taken tending to zero because there is no hydrogen in feed. However, the Xu and Froment kinetics used for reforming reaction will be mathematically NaN (Not a Number, mathematically speaking) if the hydrogen partial pressure is zero. Thus, to avoid indeterminate flow rates at the start, this assumption has to be taken. Mathematically, this value is trivial to cause any change of result to the simulation. For the reactor and catalyst specifications once again values from Kumar et al. have been used to know a feasible range. These values have been used in an experimental setup by Ji et al.

Table 5.4: Reactor specifications for simulation of model

Parameter	Value	Unit
Reactor diameter	24	mm
Catalyst density	2100	kg m^{-3}
Void fraction of packing	0.43	-
Length	1	metre

Table 5.5: Operating conditions for simulation of model

Parameter	Value	Unit
Pressure	1	bar
Temperature	900	Kelvin
Steam-to-methane ratio	1.5	-
Oxygen-to-methane ratio	0.6	-

Steam content and oxygen content for the purpose of the study is kept variable within the range determined by the thermodynamic analysis. The operating parameters i.e. temperature is also variable in view of the thermodynamic study. The effectiveness factors reported by De Groote and Froment are used for the simulation. The results of simulation are given in graphical form in figures 5.27 to 5.42.

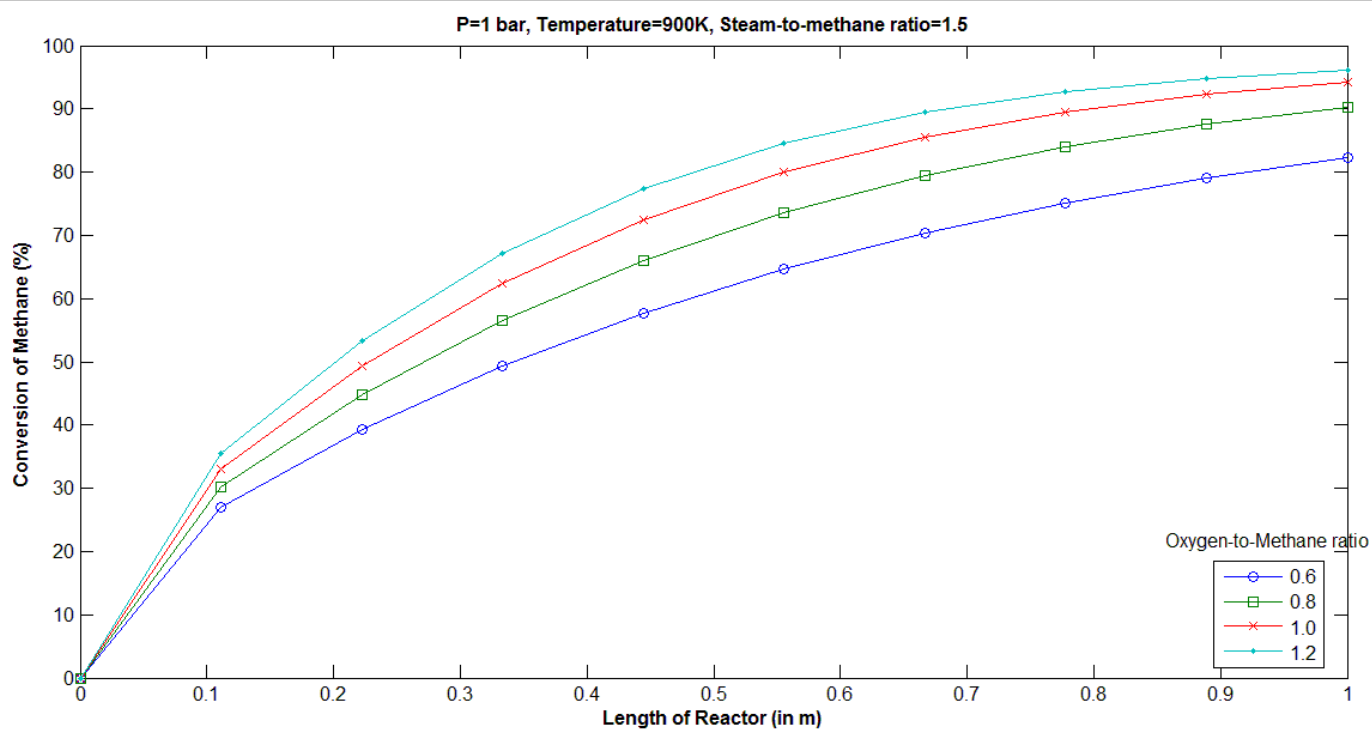


Figure 5.27: Conversion at different positions with varying oxygen content

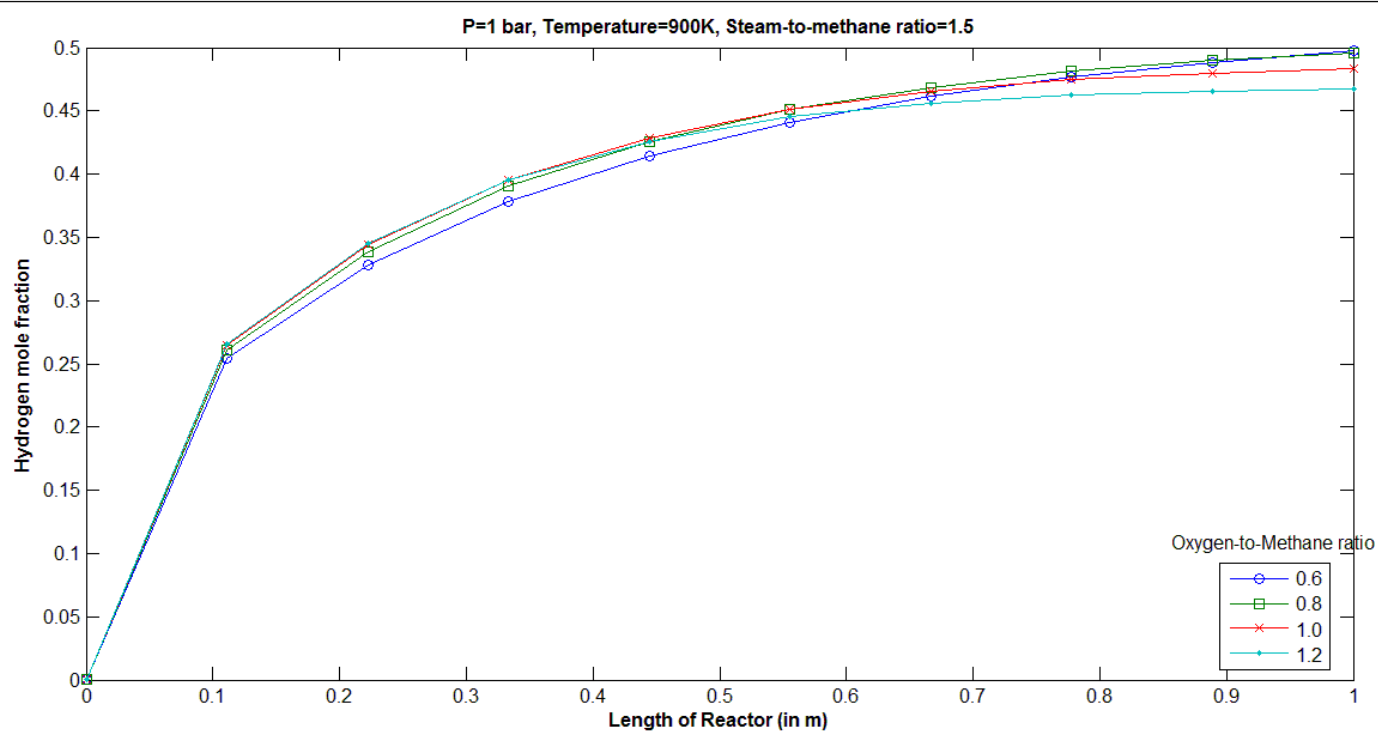


Figure 5.28: Hydrogen mole fraction at different positions with varying oxygen content

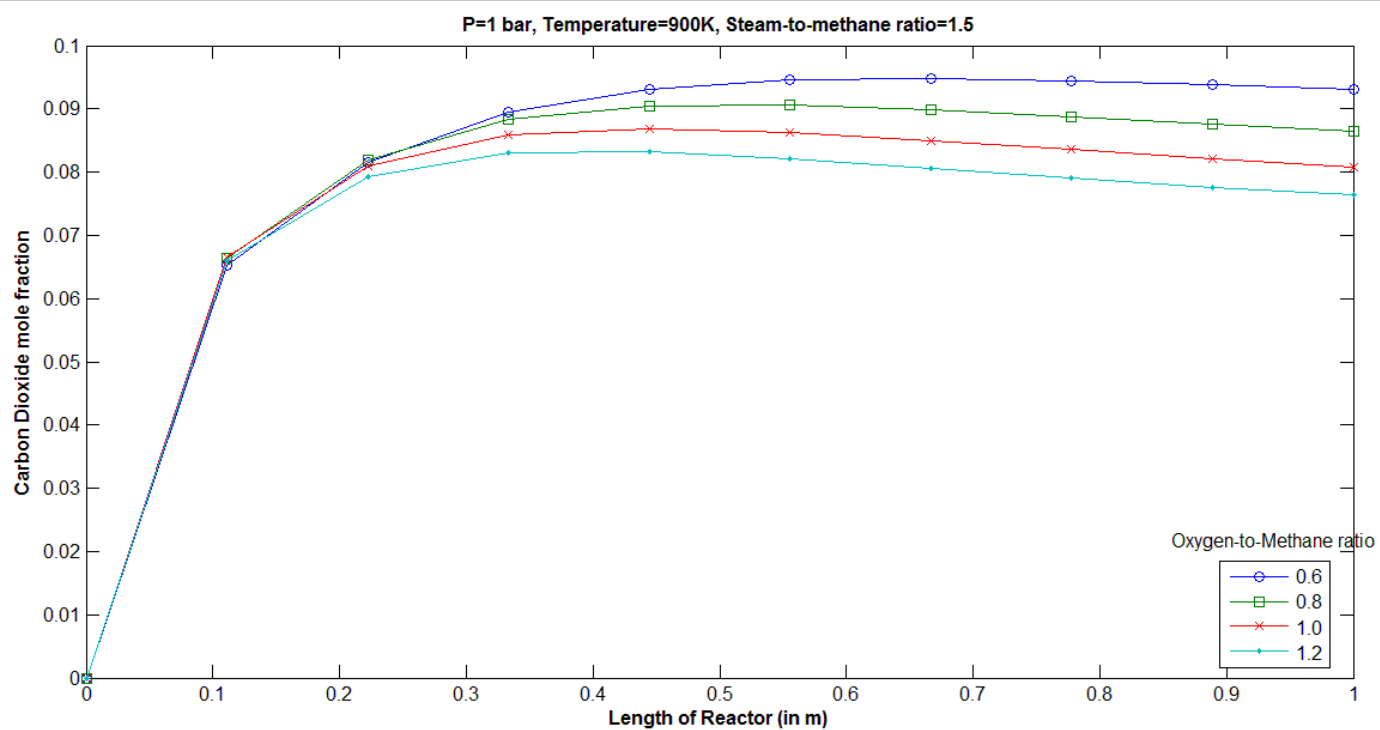


Figure 5.29: CO₂ mole fraction at different positions with varying oxygen content

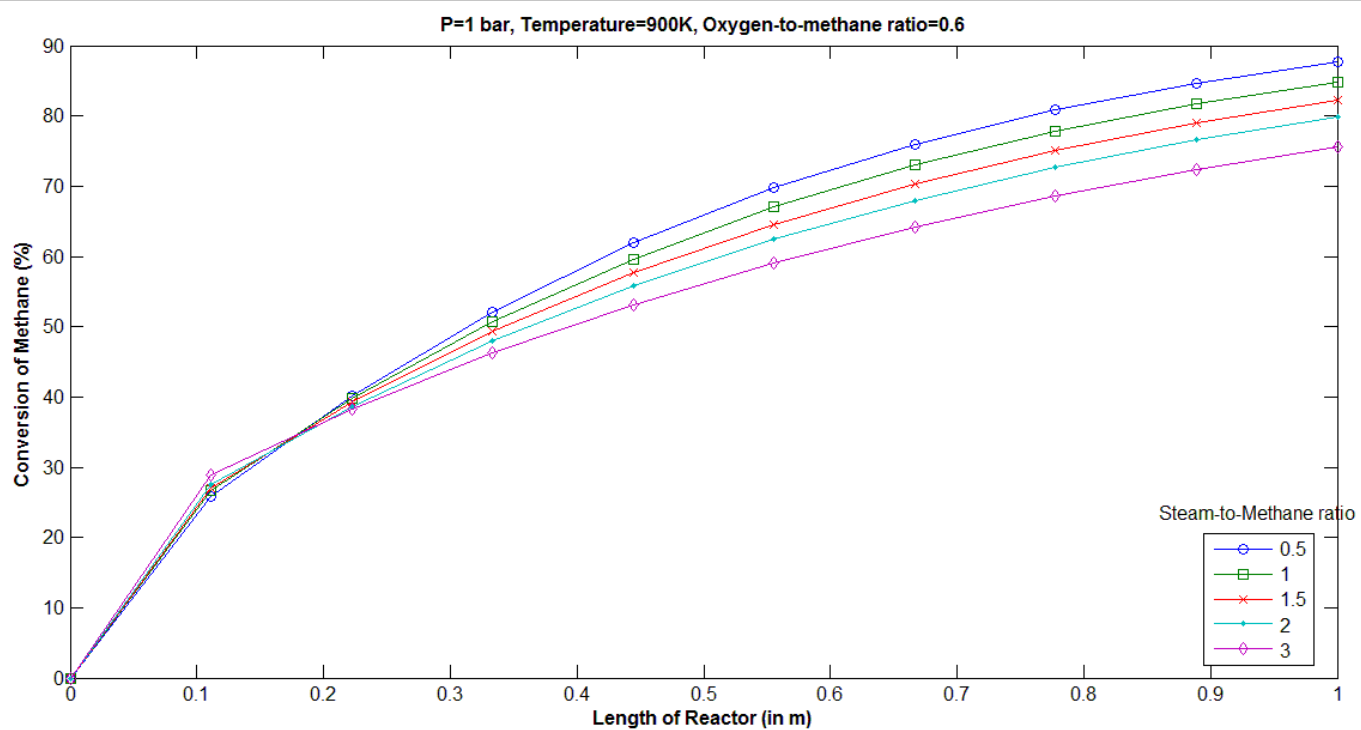


Figure 5.30: CO mole fraction at different positions with varying oxygen content

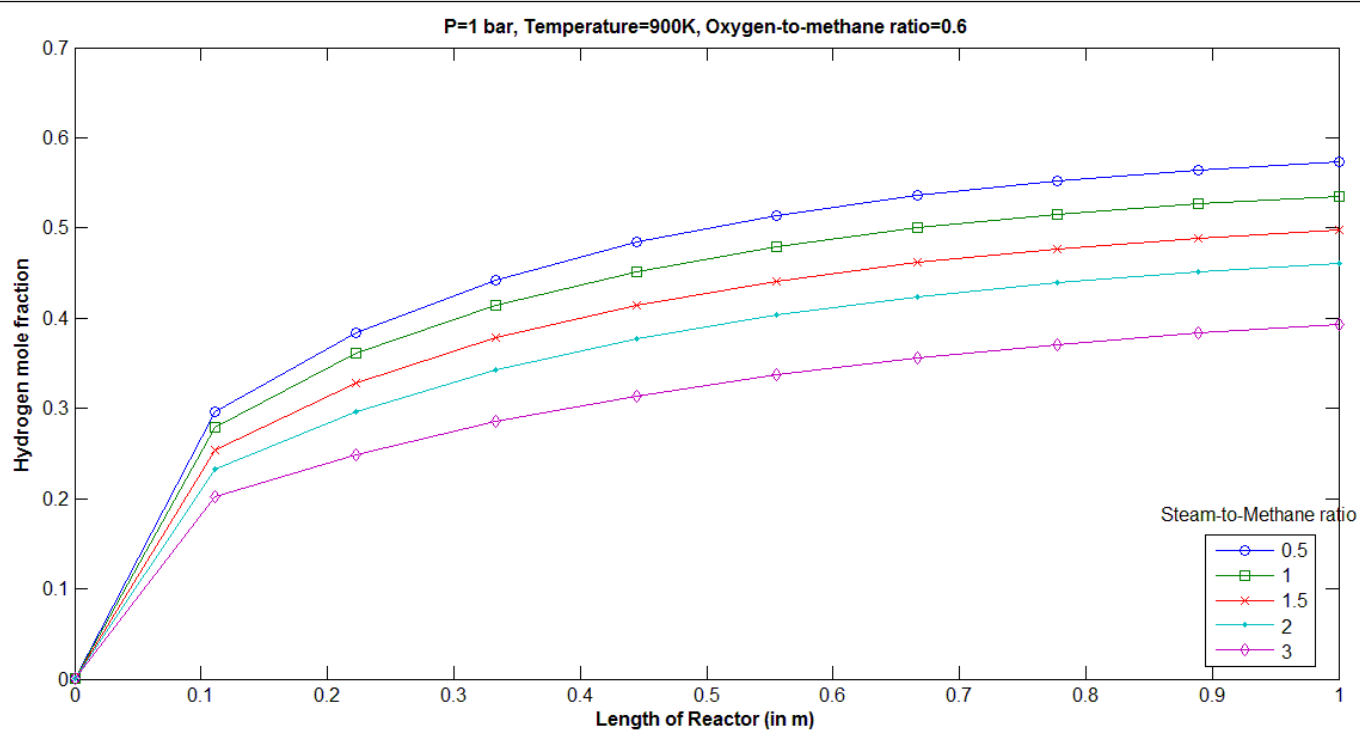


Figure 5.31: Hydrogen mole fraction at different positions with varying steam content

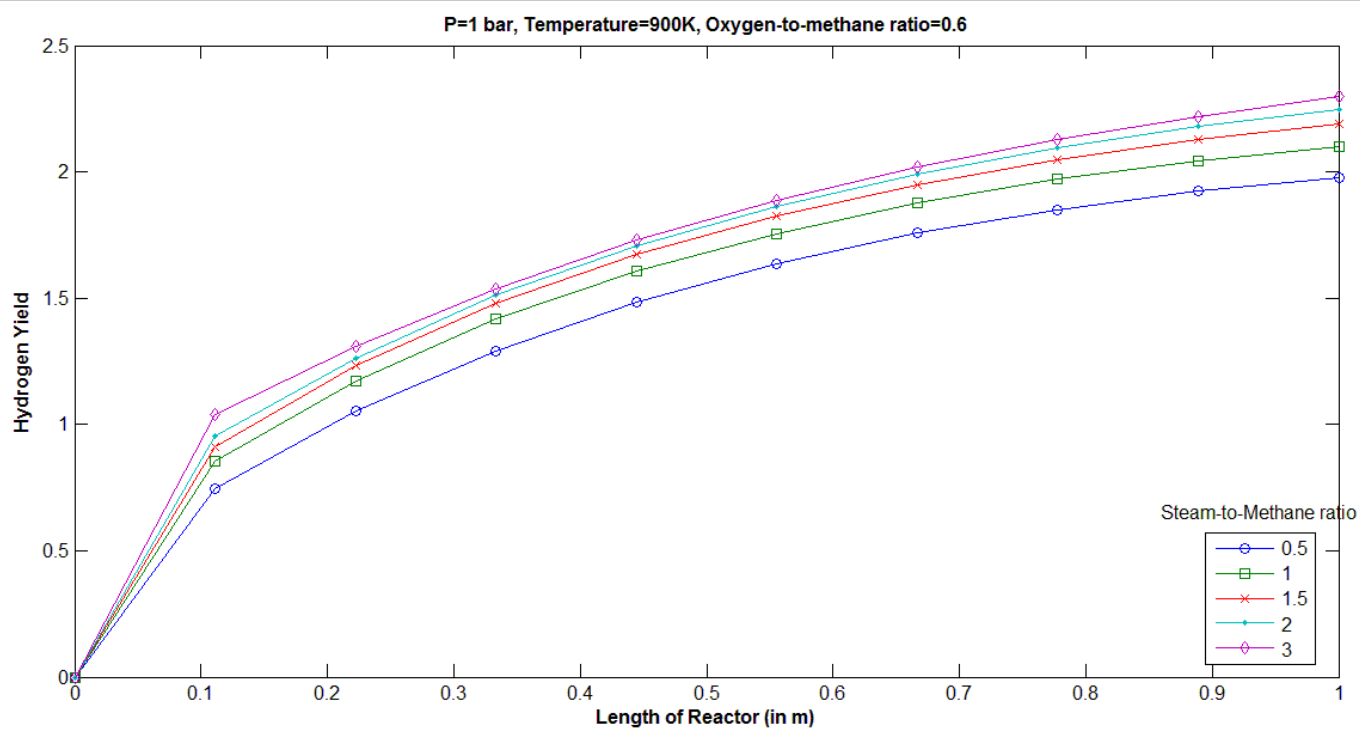


Figure 5.32: Hydrogen yield at different positions with varying steam content

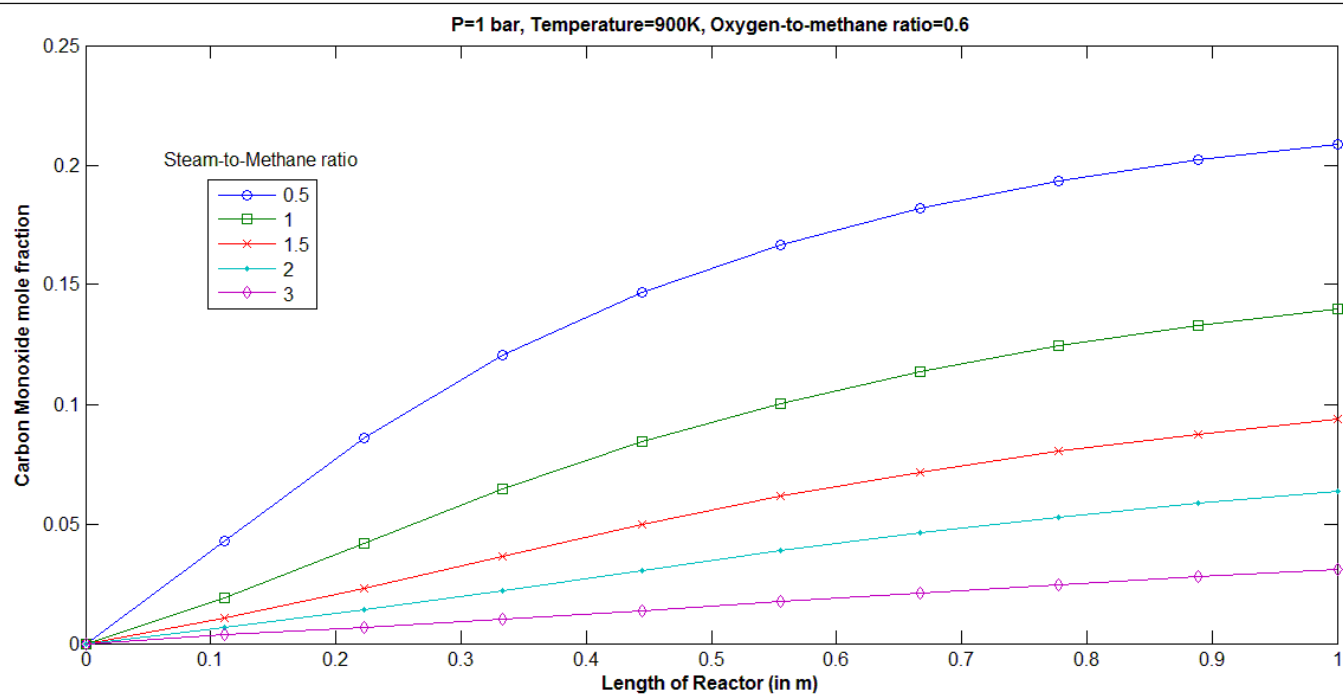


Figure 5.33: CO mole fraction at different positions with varying steam content

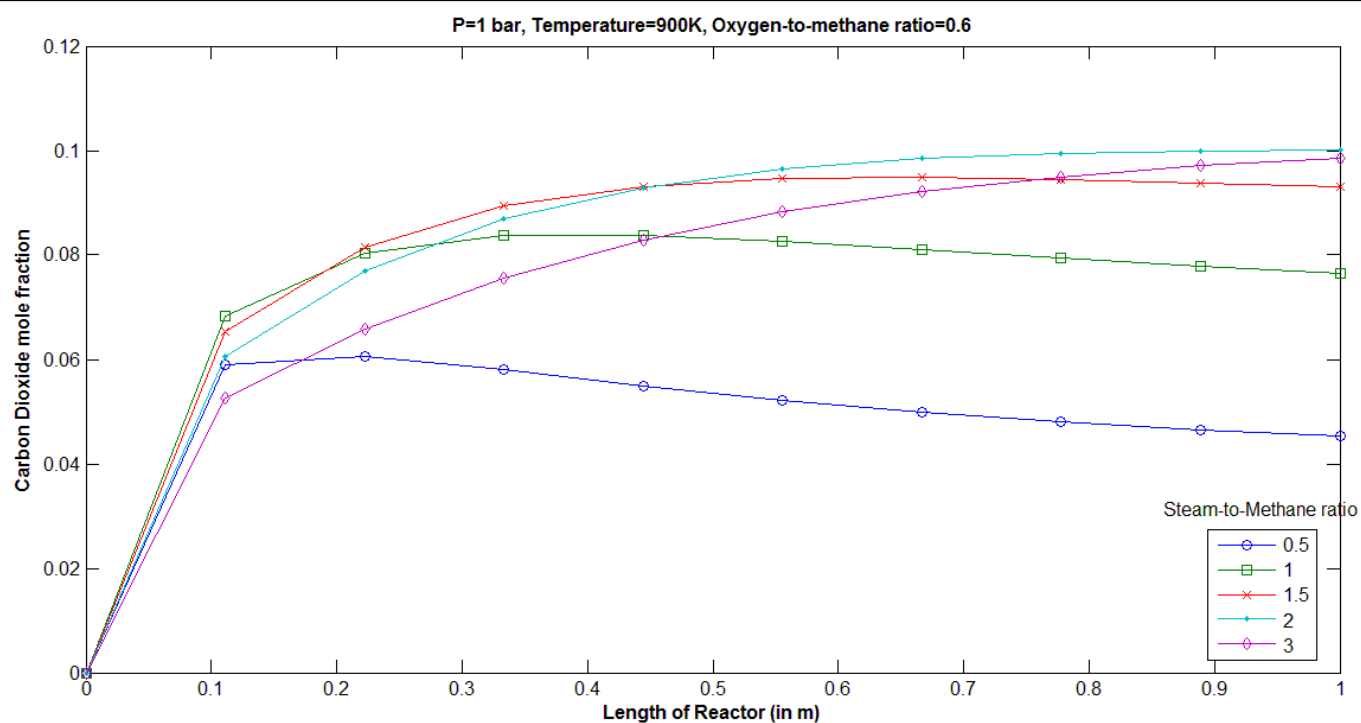


Figure 5.34: CO₂ mole fraction at different positions with varying steam content

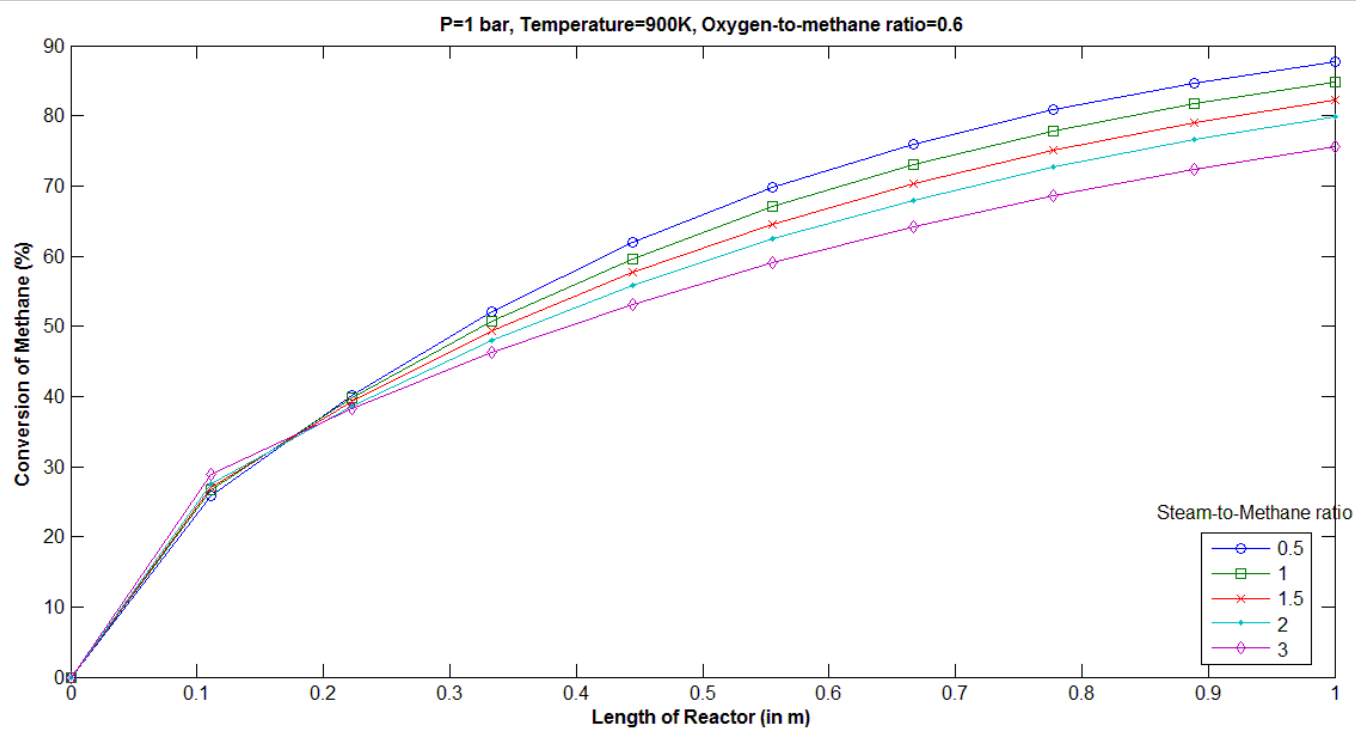


Figure 5.35: Conversion at different positions with varying steam content

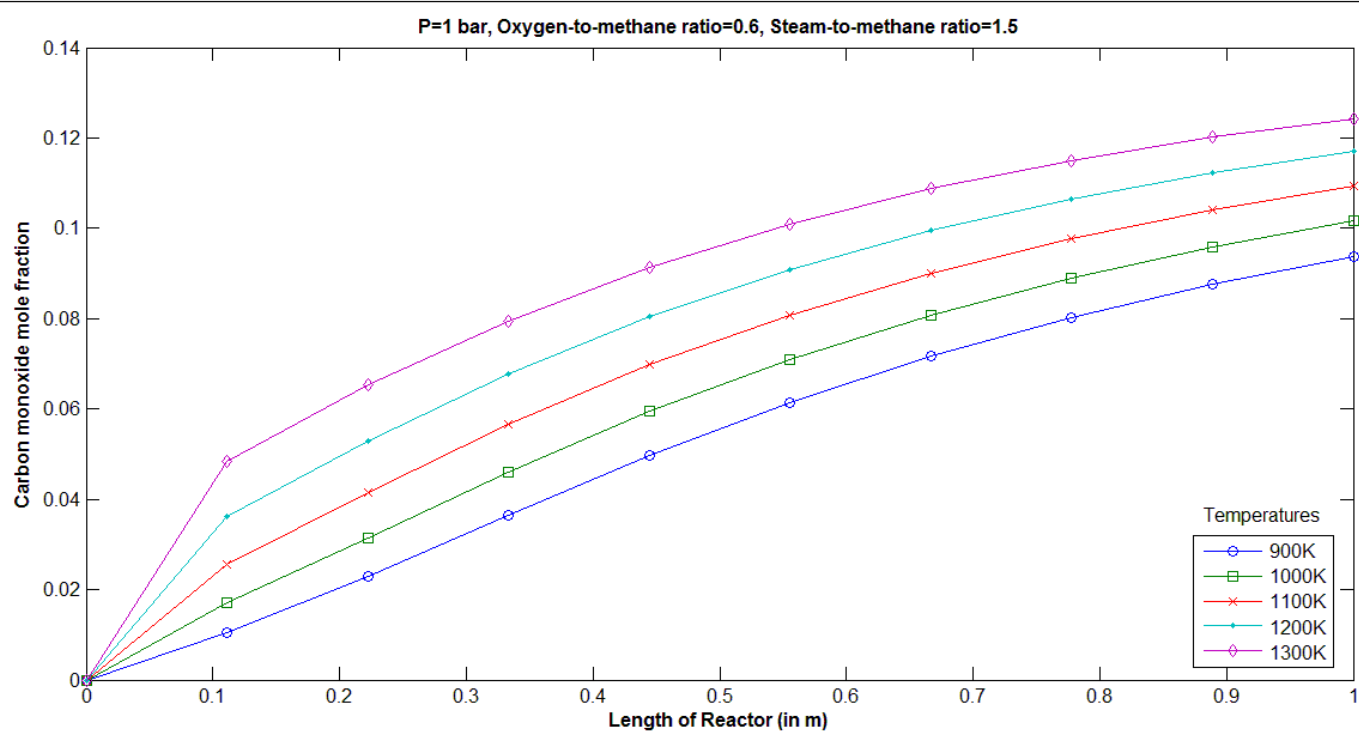


Figure 5.36: CO mole fraction at different positions with varying temperatures

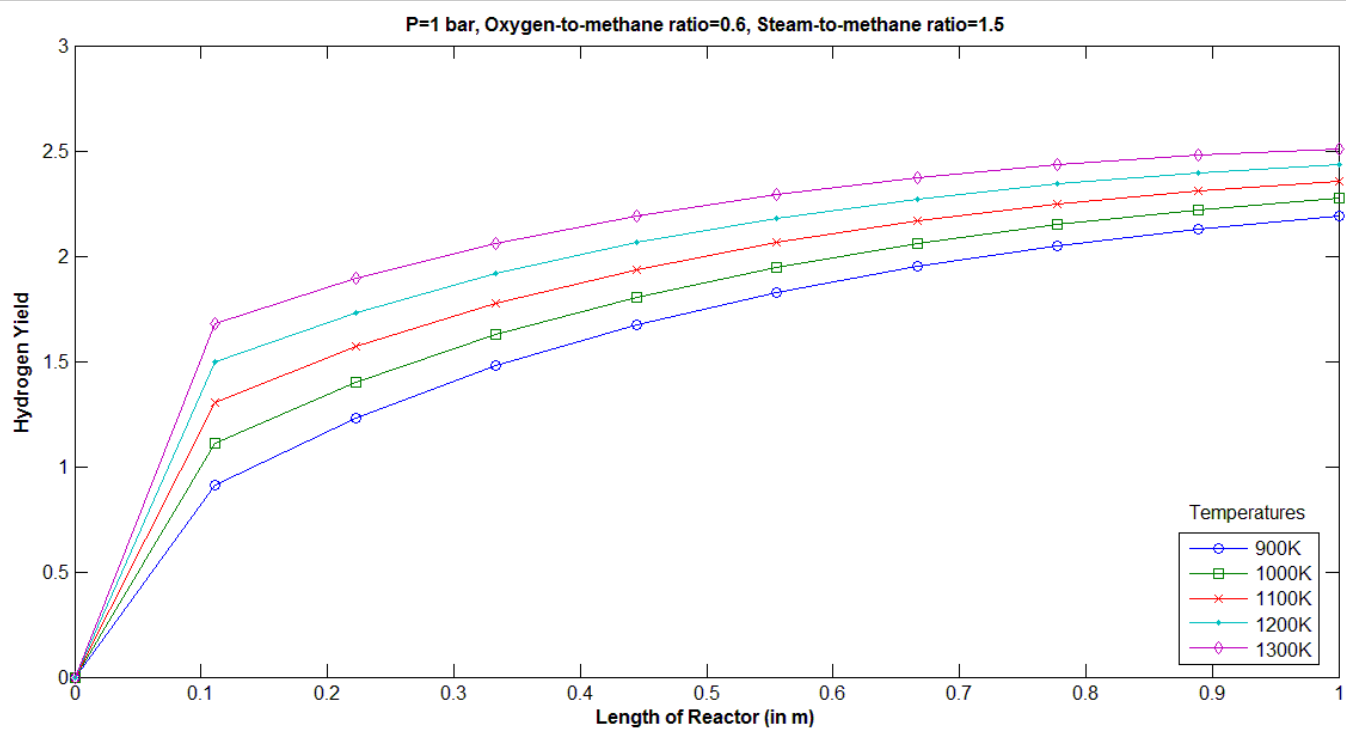


Figure 5.37: Hydrogen yield at different positions with varying temperatures

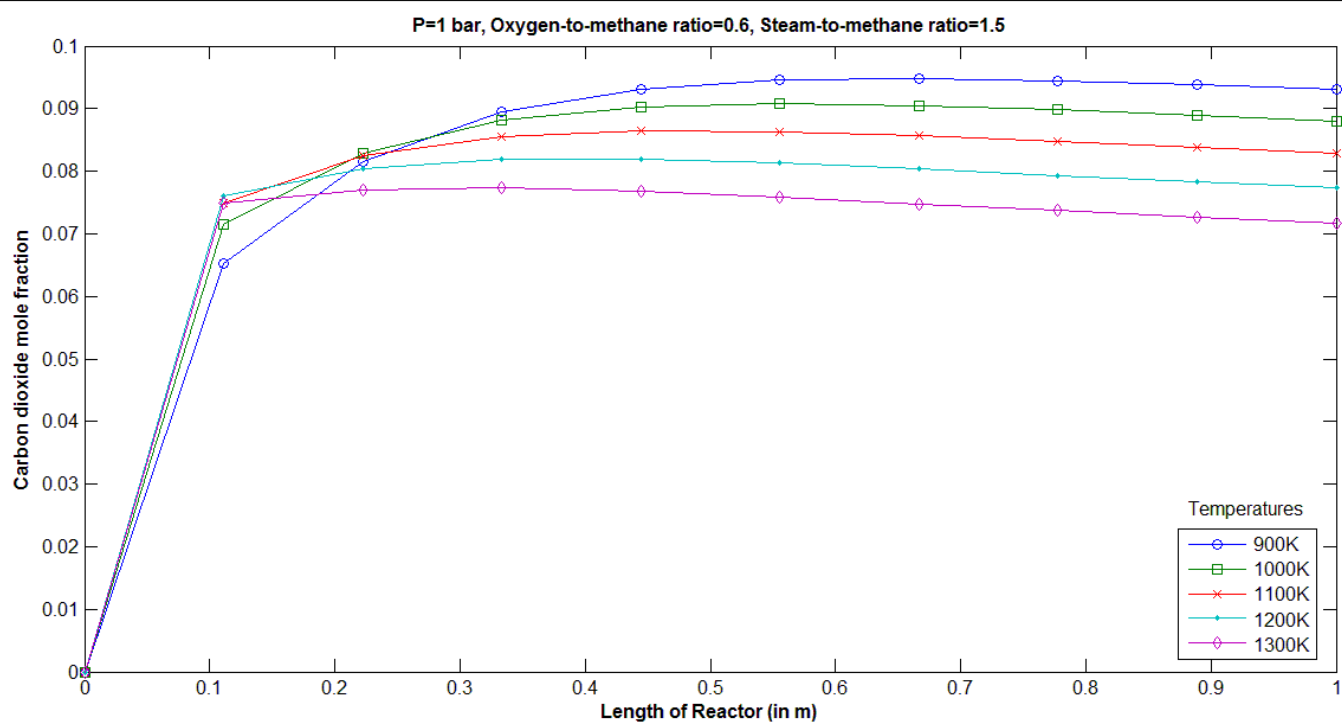


Figure 5.38: CO₂ mole fraction at different positions with varying temperatures

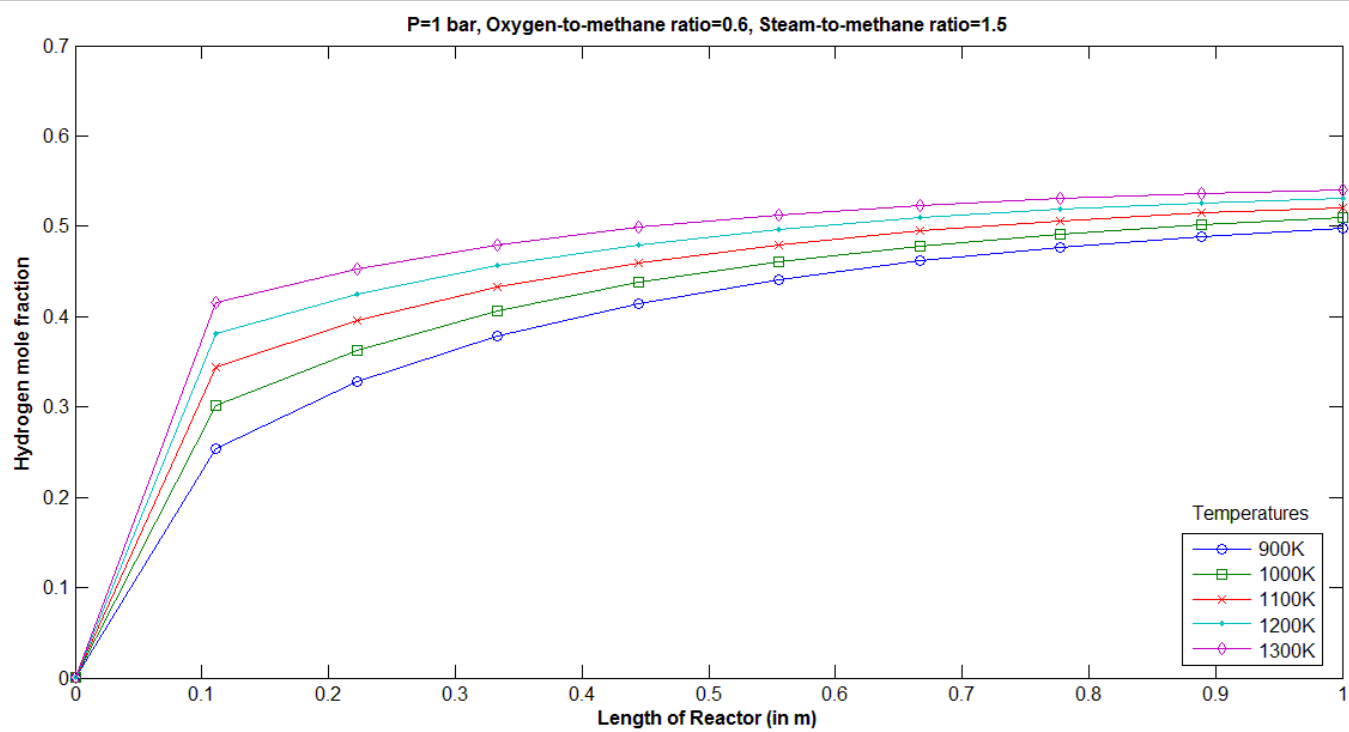


Figure 5.39: Hydrogen mole fraction at different positions with varying temperatures

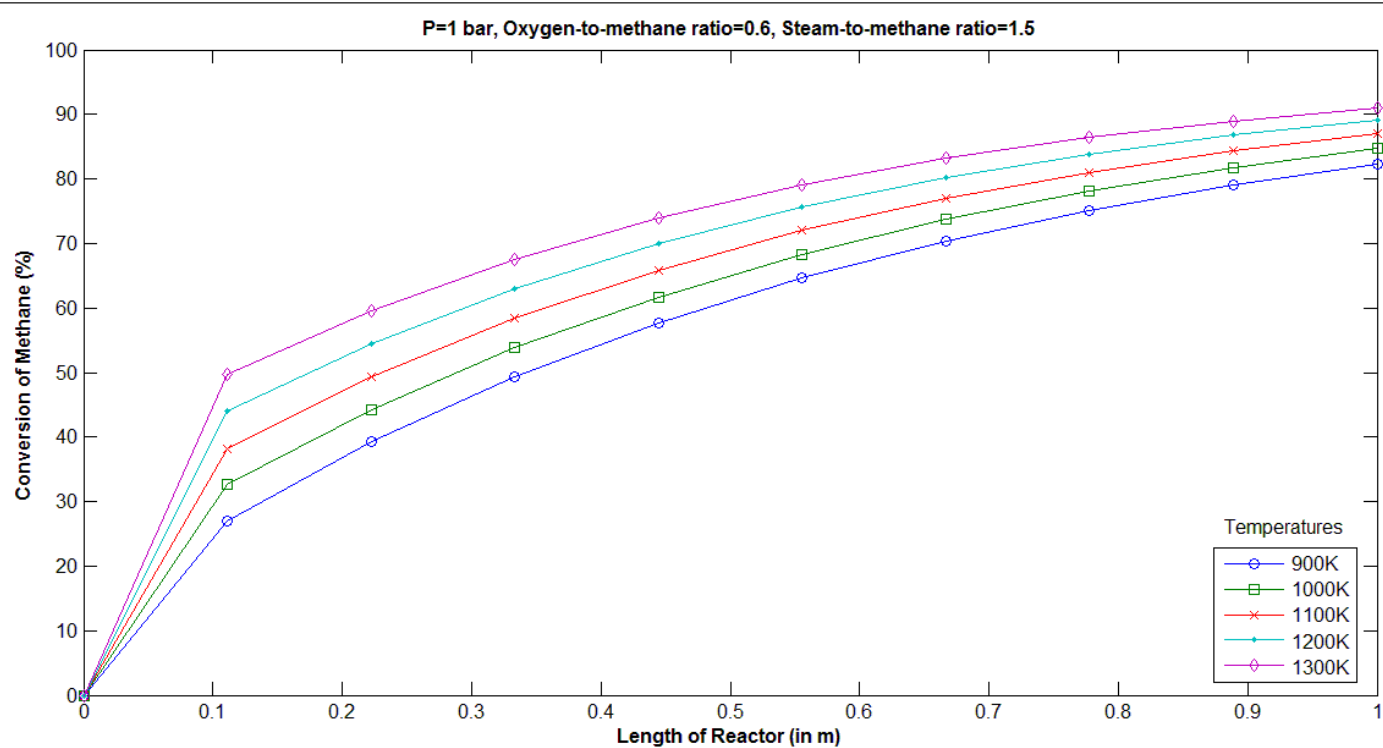


Figure 5.40: Conversion at different positions with varying temperatures

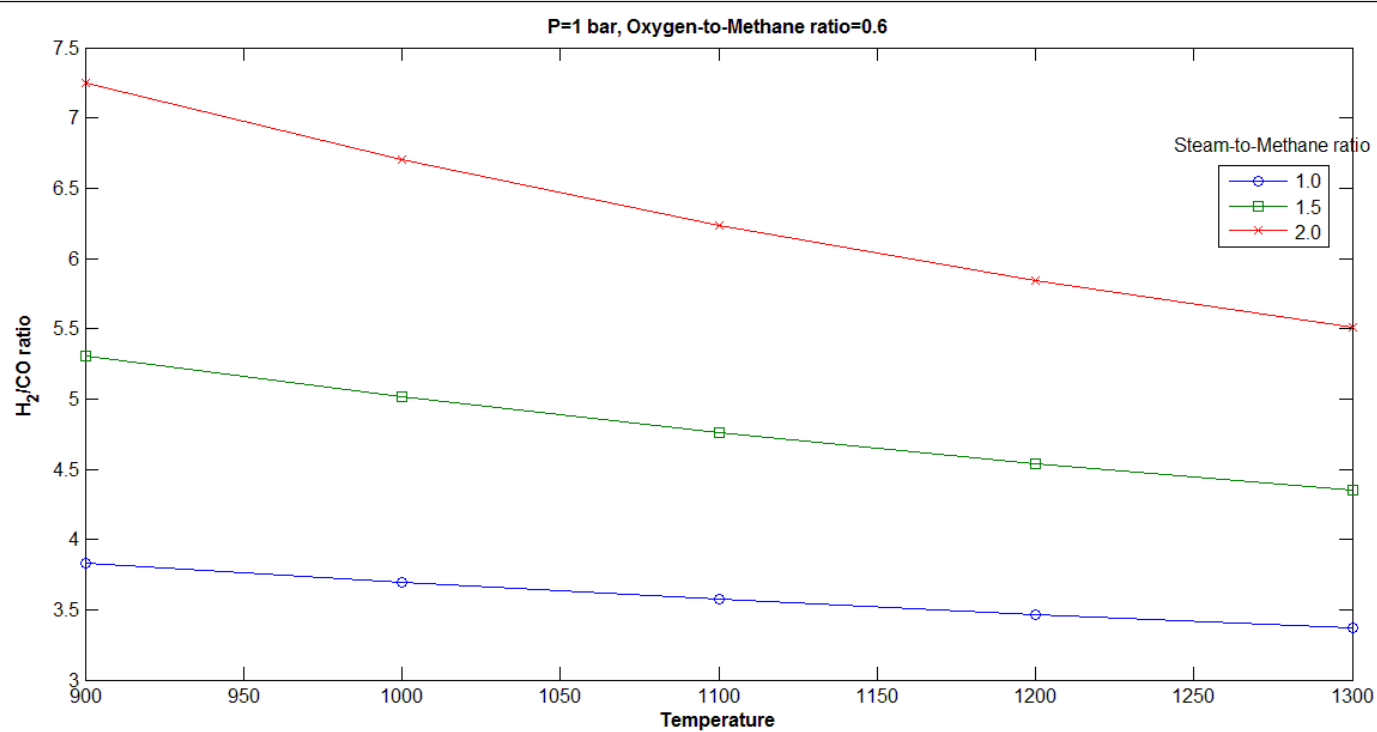


Figure 5.41: H₂/CO ratios at different temperatures with varying steam content

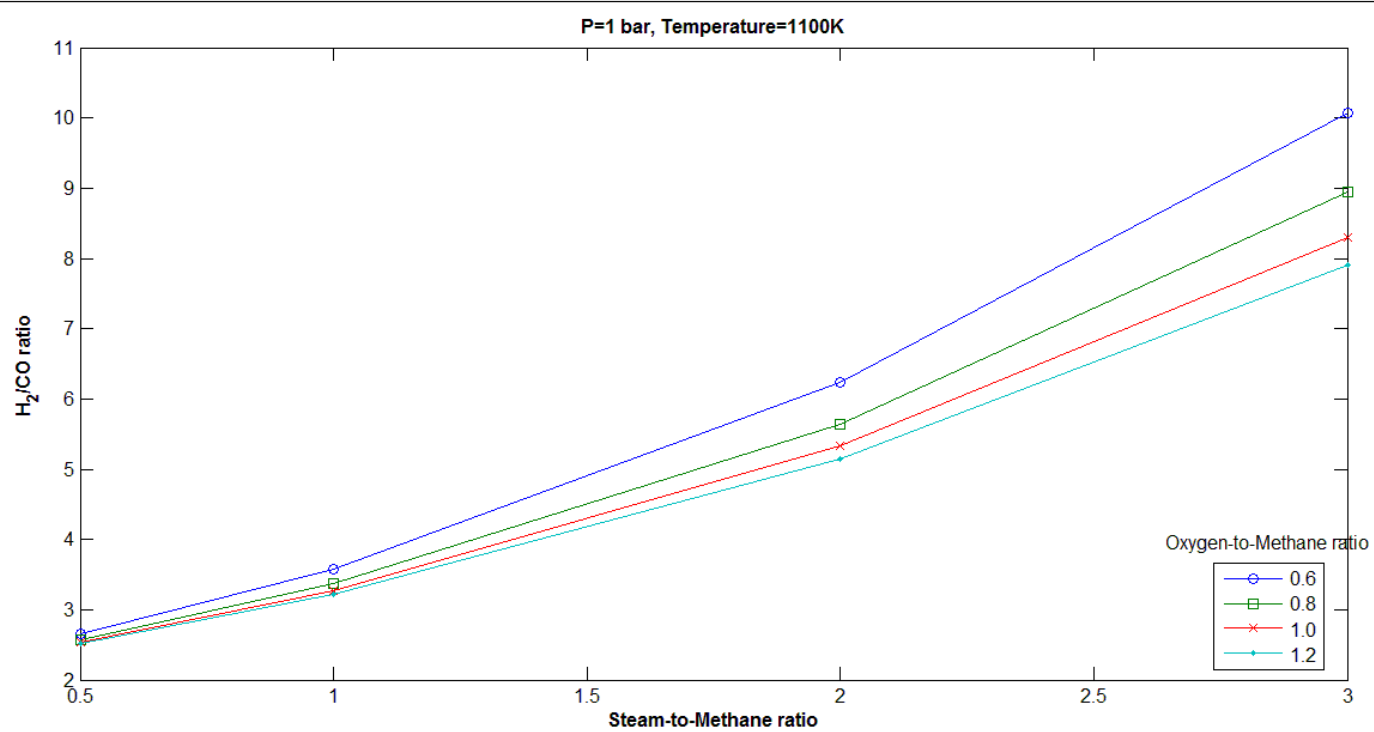


Figure 5.42: H_2/CO ratios at different steam content with varying oxygen content

The simulations can be divided into three major portions for the sake of ease of classification and understanding. The first part evaluates changes in the output parameters by varying oxygen to methane ratio. For this part the steam ratio is fixed at 0.6 while the temperature was taken to be 900K for the sake of maximum applicability of Trimm and Lam kinetics which were derived in the temperature range of 800K. The evaluated parameters are defined as follows:

$$Conversion = X_{CH_4} = \frac{F_{CH_4 @ z=0} - F_{CH_4 @ z=L}}{F_{CH_4 @ z=0}} \times 100\% \quad (5.1)$$

$$Yield = Y_{H_2} = \frac{F_{H_2 @ z=L} - F_{H_2 @ z=0}}{F_{CH_4 @ z=0}} \quad (5.2)$$

The mole fraction of any of the six species is defined as:

$$x_i = \frac{F_i}{\sum_{i=1}^6 F_i} \quad (5.3)$$

It was found that the conversion of methane increases with increasing oxygen ratio (see Figure 5.27). This is expected because the methane combustion reaction is an irreversible reaction with a large equilibrium constant. The oxygen supplied is consumed in that reaction, and hence increases the percentage of methane consumed overall. The hydrogen mole fractions for a lower oxygen ratio was initially lower (see Figure 5.28); however at the outlet of the reactor it increases above the mole fractions obtained with higher oxygen content. Increasing oxygen to methane ratio also increases the yield of carbon monoxide produced (see Figure 5.30). This increase reduces visibly as the oxygen content is increased. The higher moles of carbon monoxide (see Figure 5.29) can be explained by the higher moles of produced carbon dioxide during combustion reaction which then contributes to the reverse water gas shift reaction leading to higher carbon monoxide at the outlet. The trend of higher oxygen to methane ratio leading to lower mole fraction of carbon dioxide at the outlet also supports this explanation.

The second part of this simulation is done to analyse the effect of changing steam to methane ratios on output parameters. As the results suggest, increasing the amount of steam

supplied reduces the conversion of methane at the same constant oxygen to methane ratio and keeping the temperature constant, although this difference is not large and within a ten percent band for the simulated conditions (see Figure 5.35). This difference is further reduced on increasing the temperature. The hydrogen yield obtained is improved marginally on increasing the steam supplied (see Figure 5.32). The hydrogen mole fraction obtained at the outlet brings out the fact even more clearly that reducing the steam supplied produces a better hydrogen production (see Figure 5.31). The carbon monoxide mole fraction is reduced on increasing the supply of steam (see Figure 5.33). There is a very clear trend in falling carbon monoxide moles throughout the reactor on increasing steam supplied. For carbon dioxide, the trend is not that clear throughout the length of the reactor (see Figure 5.34), however, at the outlet it is clear that increasing the supplied steam to methane ratio causes more moles of carbon dioxide to be formed.

The third part of this simulation evaluates the effect of increasing temperatures on various outlet parameters, keeping the oxygen to methane ratio at 0.6 and steam to methane ratio at 1.5 . In this case the trends are very uniform throughout the reactor. For the conversion of methane the outlet conversion is higher at higher temperatures, as was indicated by thermodynamic study as well (see Figure 5.40). The hydrogen yield is better at higher temperatures owing to a better conversion of methane (see Figure 5.37). The outlet hydrogen mole fraction is also higher for higher temperatures, however the difference is not significant (see Figure 5.39). The carbon monoxide clearly shows an increasing trend with temperature (see Figure 5.36). The trend for carbon dioxide is not uniform throughout the length of the reactor, but at the outlet position, it is clearly visible that carbon dioxide production tapers off at higher temperatures (see Figure 5.38). It is clearly indicated that a higher temperature is useful to us.

The study would be incomplete without studying the effect of changing the different parameters on hydrogen to carbon monoxide ratio which is a crucial property for synthesis gas. The simulation study on the hydrogen to carbon monoxide ratio points to the fact that a higher temperature coupled with a low steam to methane ratio would bring the outlet gas composition within the desired range for syngas for Fischer Tropsch synthesis. A second analysis on the effect of oxygen input to this ratio shows that higher oxygen supply reduces the outlet hydrogen to carbon monoxide ratio. However, this effect is less pronounced at lower steam to methane

ratios and becomes significantly clear at higher steam supply at input conditions (see Figures 5.41 and 5.42).

CHAPTER 6

CONCLUSIONS AND RECOMMENDATIONS

The conclusions are enumerated under two heads, the first drawn from results of thermodynamic analysis and the second from the modeling and simulation of oxidative reforming of methane.

Thermodynamic Analysis

On the basis of $\Delta G < 0$, the temperature feasibility of reactions was determined in Section 3.2 to be 900K-1100K. This range was extended to 600-1300K for thermodynamic analysis based upon Gibb's free energy minimization, which was conducted by optimization tool *fmincon* in MATLAB. From this thermodynamic analysis it has been found that an increasing temperature enhances the conversion and decreases the coke formation. Theoretically, at temperatures around 1000K the conversion is quite high of the order of 95%. Thus, for simulation runs a temperature range of 900K -1200K was chosen.

Thermodynamically it has been shown that increasing the steam content also increases the conversion and reduces the coke formation. However, the hydrogen to carbon monoxide ratio increases as well. Thus, a limit of 5 was set on hydrogen to carbon monoxide ratio and hence steam ratio for simulation was limited to 0.5-3.0.

The oxygen content for autothermal operation was determined as a function of temperature in Section 3.1. This serves as defining the lower bound on the oxygen content for purposes of thermodynamic analysis. Increasing oxygen-to-methane ratio improves conversion, lowers coke deposition and brings the hydrogen to carbon monoxide ratio to lower values. Consequently, increasing it also causes a reduction in the number of moles of hydrogen produced. Thus, there is a tradeoff and for this reason the oxygen to methane ratio was kept between 0.5-1.2 for simulation studies to study its effect on output parameters.

The low pressure operation (1 bar) was determined on the basis of literature survey which pointed out theoretical benefits of enhanced conversion when operating at lower pressure. This is

also supported by Le Chateliers principle which dictates that lowering pressure would enhance the forward reaction because of increase in number of moles due to forward reaction of methane.

Modeling and Simulation

A steady state one-dimensional, non-isothermal, mathematical model for oxidative reforming of methane in a fixed bed reactor has been developed. This model utilizes the Xu and Froment kinetics for steam reforming and water gas shift reactions, and that of Trimm and Lam for methane combustion. In the reactor Ni based alumina catalyst is used. Variation of physical properties with temperature has also been accounted for. Variables' values at the inlet to the reactor have been taken as the input to the model, which constitute an initial value problem. Therefore this has been solved using *ode23s* solver in MATLAB. Model has been validated with the experimental data of De Groote and Froment. Using the output from the solver, methane conversion, hydrogen yield, mole fractions of hydrogen, carbon monoxide and carbon dioxide, and hydrogen to carbon monoxide ratio beside others have been computed.

The simulation results show that a higher oxygen supply leads to better conversion of methane (although the difference is not too large), lower carbon dioxide mole fraction and higher carbon monoxide mole fraction. The hydrogen mole fraction is also lowered to a limited extent at the outlet of the reactor. Thus, operating with higher oxygen to methane ratio lowers the hydrogen to carbon monoxide ratio, enhancing the applicability of outlet gas for gas to liquid (GTL) technologies. However, it is important to keep in mind the fact that a higher oxygen supply adds to the cost, and lowers the number of moles of hydrogen produced (as ascertained by thermodynamic analysis). Thus, based on these facts, it can be postulated that oxygen to methane ratio should be kept at reasonably high levels (say >0.5) to aid in conversion and better hydrogen/carbon monoxide ratio, but at the same time, an upper limit is required. Based on this logic the optimum oxygen to methane ratio for operation of reactor should be 0.8.

A higher temperature of operation implies higher carbon monoxide moles in outlet gas, marginally better hydrogen yield, and lower carbon dioxide mole fraction. The dependence of conversion and outlet hydrogen mole fraction on temperature is less significant. A higher temperature also reduces the hydrogen to carbon monoxide ratio in the outlet gas. Hence for a sufficiently high conversion, a temperature range of 1000-1100K is adequate.

The increasing steam supply lowers the outlet conversion slightly, as well as lowers the mole fraction of carbon monoxide. The mole fraction of carbon dioxide is increased and hydrogen yield is marginally improved. The hydrogen mole fraction also drops off. Once again the hydrogen to carbon monoxide ratio becomes an important parameter and it is found that a lower steam supply lowers the outlet hydrogen-to-carbon monoxide ratio. Based on model simulation ratio at the chosen temperature range (1000-1100K) and the oxygen to methane ratio (0.8) the hydrogen to carbon monoxide ratio varies from 2.7 to 9 when the steam to methane ratio is varied from 0.5 to 3.0. Hence, the steam content can be seen as a controlling parameter for hydrogen/carbon monoxide ratio, depending on the usage. GTL applications require this ratio to be around 2-2.5.

In summary, thermodynamic analysis predicted the theoretical ranges for the operating conditions, which were then utilized to simulate the developed mathematical model. On the basis of results obtained it can be summarized that the reaction operation at 1 bar pressure at temperature 1000-1100K and oxygen to methane ratio of 0.8 is versatile and satisfactory. At this configuration, the minimum hydrogen to carbon monoxide ratio in the outlet was found to be 2.7 at steam to methane ratio of 0.5. This ratio can be further altered as desired by using another separation unit. It is further stated that this operation requires low P and reasonable temperature. Thus, it is preferable to be used in practice.

REFERENCES

- [1]. *BP Statistical Review fo World Energy June 2012*. s.l. : BP, 2012.
- [2]. Global Warming FAQ's. **Easterling, David and Karl, Tom**. *National Oceanic and Atmospheric Administration, National Climatic Data Center*. [Online]
<http://www.ncdc.noaa.gov/cmb-faq/globalwarming.html>.
- [3]. *New and improved catalytic priocesses for clean fuel*. **Maxwell, I. E. and Naber, J. E.** 1992, Caltalyst Letters, Vol. 12, pp. 105-116.
- [4]. *Perry's chemical engineers' handbook*. **Perry, Robert H.; Green, Don W. and Maloney, James O'**. 7th. s.l. : McGraw-Hill, 1997. 0-07-049841-5.
- [5]. *Syngas production for gas-to-liquids applications:technologies, issues and outlook*. **Wilhelm, D. J.; Simbeck, D. R.; Karp, A. D. and Dickenson, R. L.** 2001, Fuel Processing Technology, Vol. 71, pp. 139-148.
- [6]. *New catalytic routes for syngas and hydrogen production*. **Pena, M. A.; Gomez, J. P. and Fierro, J. L.G.** 1996, Applied Catalyts A: Gen., Vol. 144, pp. 7-57.
- [7]. *Gas to liquids: A technology for natural gas industrialization in Bolivia*. **Velasco, J. A.; Lopez, L.; Velasquez, M.; Boutonnet, M.; Cabrera, S. and Jaras, S.** 2011, Journal of Natural Gas Science and Engineering, Vol. 3, pp. 423-459.
- [8]. Preliminary screeneing- technical and economic assessment of synthesis gas to fuels and chemicals with emphaissis on biomass derived syngas. **Spath, P. L. and Dayton, D. C.** *National Renewable Energy Labaratory*. December 2003. NREL/TP-510-34929.
- [9]. *Catalytic partial oxidation of natural gas to syngas*. **Bhardwaj, S. S. and Schmidt, L. D.** 1995, Fuel Porcessing Technology, Vol. 42, pp. 109-127.
- [10]. *Modelling of packed bed membrane reactors for autothermal production of ultrapure hydroge*. **Tiemersma, T. P.; Patil, C. S.; Annaland, M. van Sint and Kuipers, J. A.M.** 2006, Chemical Engineering Science, Vol. 61, pp. 1602-1616.

- [11]. *New aspects of syngas production and use*. **Rostrup-Nielsen, Jens R.** 2000, Catalysis Today, Vol. 63, pp. 159-164.
- [12]. *Technologies for large scale gas conversion*. **Aasberg-Petersen, K.; Bak Hansen, J. H.; Christensen, T. S.; Dybkjaer, I.; Seier Christensen, P.; Stub Nielsen, C.; Winter Madsen, S. E. L. and Rostrup-Nielsen, J.R.** 2001, Applied Catalysis A: General, Vol. 221, pp. 379-387.
- [13]. *Hydrogen production from methane through catalytic partial oxidation reactions*. **Freni, S.; Calogero, G. and Cavallaro, S.,** 2000, Journal of Power Sources, Vol. 87, pp. 28-38.
- [14]. *Thermodynamic analysis of hydrogen production by partial oxidation reforming*. **Lutz, Andrew E.; Bradshaw, Robert W.; Bromberg, Leslie and Rabinovich, Alex** 2004, International Journal of Hydrogen Energy, Vol. 29, pp. 809-816.
- [15]. *Thermodynamic equilibrium analysis of combined carbon dioxide reforming with partial oxidation of methane to syngas*. **Amin, Nor Aishah and Yaw, Tung Chun** 2007, International Journal of Hydrogen Energy, Vol. 32, pp. 1789–1798.
- [16]. *Thermodynamic analysis of autothermal steam and CO₂ reforming of methane*. **Li, Yunhua; Wang, Yaquan; Zhang, Xiangwen and Mi, Zhentao** 2008, International Journal of Hydrogen Energy, Vol. 33, pp. 2507-2514.
- [17]. *Thermodynamic analysis of hydrogen production from methane via autothermal reforming and partial oxidation followed by water gas shift reaction*. **Chen, Wei-Hsen; Lin, Mu-Rong; Lu, Jau-Jang; Chao, Yu and Leu, Tzong-Shyng** 2010, International Journal of Hydrogen Energy, Vol. 35, pp. 11787-11797.
- [18]. *Oxidative reforming of methane for hydrogen and synthesis gas production: Thermodynamic equilibrium analysis*. **Freitas, Antonio C. D. and Guirardello, Reginaldo.** 2012, Journal of Natural Gas Chemistry, Vol. 21, pp. 571-580.
- [19]. *Thermodynamic analysis of combined reforming process using Gibbs energy minimization method: In view of solid carbon formation*. **Nematollahi, Behzad; Rezaei, Mehran; Nemati, Ebrahim Lay and Khajenoori, Majid** 2012, Journal of Natural Gas Chemistry, Vol. 21, pp. 694–702.

[20]. *Simulation of the catalytic partial oxidation of methane to synthesis gas*. **De Groote, Ann M. and Froment, Gilbert F.** 1996, Applied Catalysis A: General, Vol. 138, pp. 245-264.

[21]. *Comparative study of the catalytic partial oxidation of methane to synthesis gas in fixed-bed and fluidized-bed membrane reactors Part I: A modeling approach*. **Ostrowski, T.; Giroir-Fendler, A.; Mirodatos, C. and Mleczko, L.** 1998, Catalysis Today, Vol. 40, pp. 181-190.

[22]. *Design of adiabatic fixed-bed reactors for the partial oxidation of methane to synthesis gas. Application to production of methanol and hydrogen-for-fuel-cells*. **de Smet, C. R.H.; de Croon, M. H.J.M.; Berger, R. J.; Marin, G. B. and Schouten, J. C.** 2001, Chemical Engineering Science, Vol. 56, pp. 4849-4861.

[23]. *Methane Steam Reforming, Methanation and Water-Gas Shift: 1. Intrinsic Kinetics*. **Xu, Jianguo and Froment, Gilbert F.** 1989, A.I.Ch.E Journal, Vol. 35, pp. 88-96.

[24]. *Heterogeneous reactor modeling for simulation of catalytic oxidation and steam reforming of methane*. **Avci, A. K.; Trimm, D. L. and Onsan, Z.** 2001, Chemical Engineering Science, Vol. 56, pp. 641-649.

[25]. *Simulation and thermodynamic analysis of conventional and oxygen permeable CPO reactors*. **Ji, Peijun; Kooi, H. J. van der and Arons, J. de Swaan.** 2003, Chemical Engineering Science, Vol. 58, pp. 2921-2930.

[26]. *Modeling and analysis of autothermal reforming of methane to hydrogen in a fixed bed reformer*. **Halabi, M. H.; de Croon, M. H.J.M.; Schaff, J. van der; Cobden, P. D. and Schouten, J. C.** 2008, Chemical Engineering Journal, Vol. 137, pp. 568-578.

[27]. *Hydrogen production by partial oxidation of methane: Modeling and Simulation*. **Kumar, Shashi; Kumar, Surendra and Prajapati, Jitendra K.** 2009, International Journal of Hydrogen Energy, Vol. 34, pp. 6655-6668.

[28]. *Autothermal reforming of methane to synthesis gas: Modeling and simulation*. **Zahedi nezhad, M.; Rowshanzamir, S. and Eikani, M.** 2009, International Journal of Hydrogen Energy, Vol. 34, pp. 1292-1300.

- [29]. *Kinetic modeling of high pressure autothermal reforming*. **Reese, Mark A.; Turn, Scott Q. and Cui, Hong** 2010, Journal of Power Sources, Vol. 195, pp. 553-558.
- [30]. *Modelling and simulation of a catalytic autothermal methane reformer with Rh catalyst*. **Scognamiglio, Diego; Russo, L.; Maffetonne, P. L.; Salemm, L.; Simeone, M. and Crescitelli, S.** 2012, International journal of Hydrogen Energy, Vol. 37, pp. 263-175.
- [31]. *Combustion of methane on platinum-alumina fibre catalysts-I: Kinetics and mechanism*. **Trimm, D. L. and Lam, C. W.** 1980, Chemical Engineering Science, Vol. 35, pp. 1405-1413.
- [32]. *Catalytic partial oxidation of methane to synthesis gas*. **Heitnes, K.; Lindberg, S.; Rokstad, O. A. and Holmen, A.** 1995, Catalysis Today, Vol. 24, pp. 211-216.
- [33]. *CO₂ reforming of methane combined with steam reforming or partial oxidation of methane to syngas over NdCoO₃ perovskite-type mixed metal-oxide catalyst*. **Choudhary, Vasant R. and Mondal, Kartick C.** 2006, Applied Energy, Vol. 83, pp. 1024–1032.
- [34]. *Hydrogen production by catalytic partial oxidation of methane and propane on Ni and Pt catalysts*. **Corbo, Pasquale and Migliardini, Fortunato.** 2007, International Journal of Hydrogen Energy, Vol. 32, pp. 55-66.
- [35]. *Combined oxidation and reforming of methane to produce pure H₂ in a membrane reactor*. **Munera, J. F.; Carrara, C.; Cornaglia, L. M. and Lombardo, E. A.** 2010, Chemical Engineering Journal, Vol. 161, pp. 204-211.
- [36]. *Hydrogen production from oxidative reforming of methane on supported nickel catalysts: An experimental and modeling study*. **Dantas, S. C.; Resende, K. A.; Rossi, R. L.; Assis, A. J. and Hori, C. E.** 2012, Chemical Engineering Journal, Vol. 197, pp. 407–413.
- [37]. *Hydrogen from hydrocarbon fuels for fuel cells*. **Ahmed, S. and Krumpelt, M.** 2001, International Journal of Hydrogen Energy, Vol. 26, pp. 291-301.
- [38]. NIST Chemistry Webbook-NIST Standard Reference Database Number 69. *NIST: National Institute of Standards and Technology, US Department of Commerce*. [Online] National Institute of Standards and Technology. <http://webbook.nist.gov/chemistry/> .

- [39]. *NIST-JANAF Thermochemical Tables*. **Chase, M.W. Jr.** 1998, J. Phys. Chem. Ref. Data, Monograph 9, Vol. Fourth Ed., pp. 1-1951. Data compilation copyright by the U.S. Secretary of Commerce on behalf of the U.S.A.
- [40]. **Cox, J. D., Wagman, D. D., and Medvedev, V. A.** *CODATA Key Values for Thermodynamics*. New York : Hemisphere Publishing Corp., 1984. Data compilation copyright by the U.S. Secretary of Commerce on behalf of the U.S.A.
- [41]. *Comparative thermodynamic analysis of adsorption, membrane and adsorption-membrane hybrid reactor systems for methanol steam reforming*. **Katiyar, Nisha; Kumar, Shashi; and Kumar, Surendra** 2013, International Journal of Hydrogen Energy, Vol. 38, pp. 1363-1375.
- [42]. *Partial oxidation of methane to carbon monoxide and hydrogen over a Ni-Al₂O₃ catalyst*. **Dissanayake, Dhammike; Rosynek, Michael P.; Kharas, Karl C.C. and Lunsford, Jack H.** 1991, Journal of Catalysis, Vol. 132, pp. 117-127.
- [43]. *Catalytic and thermodynamic approach of the oxyreforming reaction of methane*. **Vermeiren, W.J.M.; Blomsma, E. and Jacobs, P.A.** 1992, Catal.Today, Vol. 13, pp. 427-436.
- [44]. *A simulation study of the steam reforming of methane in a dense tubular membrane reactor*. **Gallucci, Fausto; Paturzo, Luca and Basile, Angelo** 2004, International Journal of Hydrogen Energy, Vol. 29, pp. 611-617.
- [45]. *Methane steam reforming modeling in a palladium membrane reactor*. **Fernandes, Fabiano A.N. and Soares Jr., Aldo B.** 2006, Fuel, Vol. 85, pp. 569-573.
- [46]. *Modeling of a Fluidized Bed Membrane Reactor for the Steam Reforming of Methane: Advantages of Oxygen Addition for Favorable Hydrogen Production*. **Rakib, M. A. and Alhumaizi, K.** 2005, Energy & Fuels, Vol. 19, pp. 2129-2139.
- [47]. *Effect of intraparticle transport limitations on temperature profiles and catalytic performance of the reverse-flow reactor for the partial oxidation of methane to synthesis gas*. **Gosiewski, K., Bartmann, Ulrich; Moszczynski, Marek and Mleczko, Leslaw** 1999, Chemical Engineering Science, Vol. 54, pp. 4589-4602.



INDIAN INSTITUTE OF TECHNOLOGY

CANDIDATE'S DECLARATION

I hereby declare that the work being presented in the dissertation titled "Oxidative Reforming of Methane : Thermodynamic and Modeling Study" in partial fulfillment of the requirements for the award of Integrated Dual Degree (With M.Tech Specialization in Hydrocarbon Engineering) and submitted in the department of Chemical Engineering of the Indian Institute of Technology Roorkee, Roorkee is an authentic record of my own work under the supervision of Dr.(Mrs.) Shashi, Associate Professor, Department of Chemical Engineering, Indian Institute of Technology Roorkee, Roorkee, India.

The matter presented in this report has not been submitted by me for the award of any other degree of this or any other institute

Date:

Place: IIT Roorkee

(Abhinav Malhotra)

CERTIFICATE

This is to certify that the above statement made by the candidate is correct to the best of my knowledge and belief.

Date:

(Dr. Shashi)

Associate Professor,
Chemical Engineering Department,
Indian Institute of Technology
Roorkee-247667

ACKNOWLEDGEMENTS

I wish to express my sincere gratitude to my mentor and guide Dr.Shashi, Associate Professor, Department of Chemical Engineering, Indian Institute of Technology Roorkee, Roorkee for providing me an opportunity to work under her illuminating guidance. Her vast knowledge and constant understanding and support at every stage of the present work have proved to be extremely beneficial to me. More than anything her supportive nature not only to me, but to every one of her students makes her a true teacher.

I would also like to thank Dr. Surendra Kumar, Professor, Department of Chemical Engineering for his inspiring words of wisdom.

I would also express my gratitude to my parents,Dr. Suresh Malhotra and Dr. Sita Malhotra, and my brother, Dr. Suhail Malhotra for things that would take pages to fill. I wish to make you prouder.

I would also take a moment to thank all the friends that I made here in Roorkee. I had the best times of my life and thanks to all of you.

Abhinav Malhotra

CONTENTS

DECLARATION	i
ACKNOWLEDGEMENTS	iii
CONTENTS	v
LIST OF FIGURES	vii
LIST OF TABLES	xi
ABSTRACT.....	xiii
CHAPTER 1: INTRODUCTION.....	1
1.1 SYNGAS AND HYDROGEN	2
1.2 APPLICATION OF SYNGAS	3
1.3 REFORMING PROCESSES	5
1.4 FIXED BED REACTOR SYSTEM	10
1.5 OBJECTIVES.....	10
1.6 ORGANIZATION OF THESIS	11
CHAPTER 2: LITERATURE REVIEW.....	13
2.1 THERMODYNAMIC STUDIES	14
2.2 MODELING AND SIMULATION STUDIES	15
2.3 CATALYST STUDIES	18
2.4 CONCLUDING REMARKS.....	21
CHAPTER 3: THERMODYNAMIC ANALYSIS.....	23
3.1 DETERMINATION OF AUTOTHERMAL POINT	23
3.2 THERMODYNAMIC FEASIBILITY OF REACTIONS	34
3.3 GIBB'S ENERGY MINIMIZATION	44
CHAPTER 4: MODEL DEVELOPMENT	47
4.1 KINETICS	47
4.2 REACTOR MODEL	49
4.3 MODEL VALIDATION	51
CHAPTER 5: RESULTS AND DISCUSSION	53
5.1 RESULTS OF THERMODYNAMIC ANALYSIS	53
5.2 MODEL SIMULATION	109
CHAPTER 6: CONCLUSIONS AND RECOMMENDATIONS	147
REFERENCES.....	151

LIST OF FIGURES

Figure No.	Title	Page No.
1.1	FLOW SCHEME FOR FT SYNTHESIS	4
1.2	SYNGAS UTILIZATION ROUTES	5
1.3	INCREASING ENTHALPIES IN DIFFERENT REFORMING PROCESSES WITH OXIDATIVE REFORMING REGION SHOWN	9
2.1	THERMODYNAMIC REPRESENTATION OF METHANE OXIDATION	13
2.2	REACTION MECHANISM FOR PARTIAL OXIDATION OF METHANE ON DIFFERENT CATALYSTS WITH NOBLE METAL	20
3.1	HEAT OF REACTION DURING ATR OF METHANE AT 298K AS A FUNCTION OF OXYGEN-TO-METHANE RATIO	29
3.2	HEAT OF REACTION DURING ATR OF METHANE AT 800K AS A FUNCTION OF OXYGEN-TO-METHANE RATIO	29
3.3	HEAT OF REACTION DURING ATR OF METHANE AT 1000K AS A FUNCTION OF OXYGEN-TO-METHANE RATIO	31
3.4	HEAT OF REACTION DURING ATR OF METHANE AT 1200K AS A FUNCTION OF OXYGEN-TO-METHANE RATIO	31
3.5	VARIATION OF CRITICAL OXYGEN TO FUEL RATIO WITH TEMPERATURE	33
3.6	VARIATION OF STOICHIOMETRIC STEAM TO METHANE REQUIREMENT WITH TEMPERATURE	33
3.7	ENTHALPY AND GIBB'S FREE ENERGY VARIATION FOR R1	34
3.8	ENTHALPY AND GIBB'S FREE ENERGY VARIATION FOR R2	34
3.9	ENTHALPY AND GIBB'S FREE ENERGY VARIATION FOR R3	37
3.10	ENTHALPY AND GIBB'S FREE ENERGY VARIATION FOR R4	37
3.11	EQUILIBRIUM CONSTANT AS A FUNCTION OF TEMPERATURE FOR R1	41
3.12	EQUILIBRIUM CONSTANT AS A FUNCTION OF TEMPERATURE FOR R2	41
3.13	EQUILIBRIUM CONSTANT AS A FUNCTION OF TEMPERATURE FOR R3	43
4.1	REACTOR DIAGRAM	50
5.1	COKE FORMATION AT DIFFERENT STEAM/METHANE RATIOS WITH OXYGEN/METHANE=0.2	57
5.2	HYDROGEN MOLES AT DIFFERENT STEAM/METHANE RATIOS WITH OXYGEN/METHANE=0.2	59
5.3	HYDROGEN/CARBON MONOXIDE RATIO AT DIFFERENT STEAM/METHANE RATIOS WITH OXYGEN/METHANE=0.2	61
5.4	CONVERSION OF METHANE AT DIFFERENT STEAM/METHANE RATIOS WITH OXYGEN/METHANE=0.2	63
5.5	COKE FORMATION AT DIFFERENT STEAM/METHANE RATIOS WITH OXYGEN/METHANE=0.3	65
5.6	HYDROGEN MOLES AT DIFFERENT STEAM/METHANE RATIOS WITH OXYGEN/METHANE=0.3	67
5.7	HYDROGEN/CARBON MONOXIDE RATIO AT DIFFERENT STEAM/METHANE RATIOS WITH OXYGEN/METHANE=0.3	69
5.8	CONVERSION OF METHANE AT DIFFERENT STEAM/METHANE RATIOS WITH OXYGEN/METHANE=0.3	71
5.9	COKE FORMATION AT DIFFERENT STEAM/METHANE RATIOS WITH OXYGEN/METHANE=0.4	73

5.10	HYDROGEN MOLES AT DIFFERENT STEAM/METHANE RATIOS WITH OXYGEN/METHANE=0.4	75
5.11	HYDROGEN/CARBON MONOXIDE RATIO AT DIFFERENT STEAM/METHANE RATIOS WITH OXYGEN/METHANE=0.4	77
5.12	CONVERSION OF METHANE AT DIFFERENT STEAM/METHANE RATIOS WITH OXYGEN/METHANE=0.4	79
5.13	COKE FORMATION AT DIFFERENT STEAM/METHANE RATIOS WITH OXYGEN/METHANE=0.5	81
5.14	HYDROGEN MOLES AT DIFFERENT STEAM/METHANE RATIOS WITH OXYGEN/METHANE=0.5	83
5.15	HYDROGEN/CARBON MONOXIDE RATIO AT DIFFERENT STEAM/METHANE RATIOS WITH OXYGEN/METHANE=0.5	87
5.16	CONVERSION OF METHANE AT DIFFERENT STEAM/METHANE RATIOS WITH OXYGEN/METHANE=0.5	89
5.17	COKE FORMATION AT DIFFERENT STEAM/METHANE RATIOS WITH OXYGEN/METHANE=1.0	91
5.18	HYDROGEN MOLES AT DIFFERENT STEAM/METHANE RATIOS WITH OXYGEN/METHANE=1.0	93
5.19	HYDROGEN/CARBON MONOXIDE RATIO AT DIFFERENT STEAM/METHANE RATIOS WITH OXYGEN/METHANE=1.0	95
5.20	CONVERSION OF METHANE AT DIFFERENT STEAM/METHANE RATIOS WITH OXYGEN/METHANE=1.0	97
5.21	EFFECT OF CHANGING OXYGEN/METHANE RATIO ON COKE FORMATION AT STEAM/METHANE=1.0	99
5.22	EFFECT OF CHANGING OXYGEN/METHANE RATIO ON COKE FORMATION AT STEAM/METHANE=2.0	101
5.23	EFFECT OF CHANGING OXYGEN/METHANE RATIO ON HYDROGEN MOLES AT STEAM/METHANE=1.0	103
5.24	EFFECT OF CHANGING OXYGEN/METHANE RATIO ON HYDROGEN MOLES AT STEAM/METHANE=2.0	105
5.25	EFFECT OF CHANGING OXYGEN/METHANE RATIO ON METHANE CONVERSION AT STEAM/METHANE=1.0	107
5.26	EFFECT OF CHANGING OXYGEN/METHANE RATIO ON METHANE CONVERSION AT STEAM/METHANE=2.0	111
5.27	CONVERSION AT DIFFERENT POSITIONS WITH VARYING OXYGEN CONTENT	113
5.28	HYDROGEN MOLE FRACTION AT DIFFERENT POSITIONS WITH VARYING OXYGEN CONTENT	115
5.29	CO ₂ MOLE FRACTION AT DIFFERENT POSITIONS WITH VARYING OXYGEN CONTENT	117
5.30	CO MOLE FRACTION AT DIFFERENT POSITIONS WITH VARYING OXYGEN CONTENT	119
5.31	HYDROGEN MOLE FRACTION AT DIFFERENT POSITIONS WITH VARYING STEAM CONTENT	121
5.32	HYDROGEN YIELD AT DIFFERENT POSITIONS WITH VARYING STEAM CONTENT	123
5.33	CO MOLE FRACTION AT DIFFERENT POSITIONS WITH VARYING STEAM CONTENT	125
5.34	CO ₂ MOLE FRACTION AT DIFFERENT POSITIONS WITH VARYING STEAM CONTENT	127
5.35	CONVERSION AT DIFFERENT POSITIONS WITH VARYING STEAM CONTENT	129

5.36	CO MOLE FRACTION AT DIFFERENT POSITIONS WITH VARYING TEMPERATURES	131
5.37	HYDROGEN YIELD AT DIFFERENT POSITIONS WITH VARYING TEMPERATURES	133
5.35	CO ₂ MOLE FRACTION AT DIFFERENT POSITIONS WITH VARYING TEMPERATURES	135
5.39	HYDROGEN MOLE FRACTION AT DIFFERENT POSITIONS WITH VARYING TEMPERATURES	137
5.40	CONVERSION AT DIFFERENT POSITIONS WITH VARYING TEMPERATURES	139
5.41	H ₂ /CO RATIOS AT DIFFERENT TEMPERATURES WITH VARYING STEAM CONTENT	141
5.42	H ₂ /CO RATIOS AT DIFFERENT STEAM CONTENT WITH VARYING OXYGEN CONTENT	143

LIST OF TABLES

Table No.	Title	Page No.
1.1	MAJOR REACTIONS IN SMR	6
3.1	STANDARD HEAT OF FORMATION	25
3.2	SHOMATE EQUATION PARAMETERS FOR DIFFERENT COMPONENTS	26
3.3	RESULTS OF CRITICAL OXYGEN-FUEL RATIO AT DIFFERENT TEMPERATURES	27
3.4	STEAM TO FUEL RATIO CORRESPONDING TO THE CALCULATED CRITICAL OXYGEN TO METHANE RATIO (OBTAINED VIA STOICHIOMETRIC BALANCE)	27
3.5	REACTIONS IN OXIDATIVE REFORMING	34
3.6	FEASIBLE TEMPERATURE RANGE FOR THE INVOLVED REACTIONS	40
4.1	ARRHENIUS PARAMETER AND ACTIVATION ENERGIES	49
4.2	VAN'T HOFF ADSORPTION PARAMETERS AND HEATS OF ADSORPTION FOR COMPONENTS	49
4.3	INPUT CONDITIONS OF INDUSTRIAL REACTOR	51
4.4	COMPARISON BETWEEN MODEL PREDICTIONS WITH INDUSTRIAL DATA	52
5.1	INPUT VARIABLES AND THEIR POSSIBLE RANGES	53
5.2	VALUES OBTAINED FOR INPUT PARAMETERS BY ANALYSIS	55
5.3	INITIAL FLOW RATES FOR SIMULATION OF MODEL	109
5.4	REACTOR SPECIFICATIONS FOR SIMULATION OF MODEL	109
5.5	OPERATING CONDITIONS FOR SIMULATION OF MODEL	109

ABSTRACT

Energy is the pivot upon which our modern society is hinged. Everything in this world depends on energy. Traditionally fossil fuels found in the nature have been the relied and trusted sources of energy. All our modern technologies are developed to run on fossil fuels, be it a thermal power generation plant running on coal or the engine of a car, designed to draw power from crude oil derivatives. Now we know that excessive use of fossil fuel has a huge environmental cost attached with it. The rapidly changing climatic scenario, melting of polar ice caps and rise in sea levels are offshoots of global warming. Our over dependence on fossil fuel adds to it.

Hydrogen has been touted as the fuel of the future owing to its large calorific value and harmless by products of its combustion. Reforming of natural gas is a process by which industrial scale production of hydrogen can be carried out. Syngas is another fuel of a similar origin. It is a majorly a mixture of hydrogen and carbon monoxide in varying proportions. It finds its applications in Gas to liquid (GTL) fuel production. Syngas is an important feedstock for a large number of industrial products including ammonia, methanol, urea etc.

Oxidative reforming involves addition of steam and oxygen to methane (natural gas) at a sufficiently high temperature in presence of a catalyst to produce hydrogen and carbon monoxide along with other side products. It comprises of both endothermic reforming reactions and exothermic combustion reaction. In a perfect autothermal system, the amount of added oxygen is fixed in such a way that the net $\Delta H = 0$ for the system. This point acts as the lower bound for the amount of oxygen considered in this study. For an estimate on the temperature range over which the considered reactions occur, the region where $\Delta G < 0$ is evaluated, which comes out to 900-1100 K. Based on these values as a pointer, a thermodynamic analysis by minimizing the Gibb's free energies is conducted to find out the equilibrium moles of each species including carbon. The results of thermodynamic analysis act as a starting point for the simulation study. It is found that at temperatures exceeding 1000K the theoretical conversion is sufficiently high and coke deposited is in miniscule amount. A large range of steam to methane ratio was evaluated and ultimately a range of 0.5-3.0 was selected for simulation study on the basis of conversion, coke formation and H_2/CO ratio. The large values of H_2/CO ratio were not considered relevant since

the primary motive was to study the syngas production. At those high ratios, it is beneficial to go for pure hydrogen production. O_2/CH_4 ratio was upper bounded by considering the fact that the number of hydrogen moles produced drops off with an increase in oxygen supplied.

The steady state one-dimensional, non-isothermal model was developed. Nickel based catalyst was selected and a fixed tubular reactor system was considered. The kinetic model was based on the experimental works of Xu and Froment (on steam reforming reactions), and Trimm and Lam (on methane combustion). The industrial data of De Groote and Froment was used for validation. On the basis of simulation of model for a low pressure operation, it was concluded that a temperature of 1000K- 1100K with an O_2/CH_4 ratio of 0.8 is suitable for syngas production, with varying H_2/CO ratios. The minimum H_2/CO for this configuration was found to be 2.7 when the steam to methane ratio was taken as 0.5 and a peak value of $H_2/CO=9.1$ was found with steam to methane ratio=3.0. This ratio can be further altered as desired by using another separation unit. It is further stated that this operation requires low pressure and reasonable temperature. Thus, it is preferable to be used in practice.

CHAPTER 1

INTRODUCTION

Today, we live in a modern 21st century society where everything is growing at a rapid pace. Scientific development has ushered in an era of technological growth and economic prosperity. We as humans have access to comforts and amenities. However, all of our modern society-its growth, prosperity and progress is hinged upon one crucial requirement- the need for energy.

The energy requirement of the world has been increasing over the past few years at an average annual rate of 2.5%. The most widely used sources of energy are the fossil fuels including natural gas, coal, crude oil and crude oil based products. For the year 2011 the consumption of oil increased marginally at a rate of 0.6 million barrels per day to attain a value of 88 million barrels per day. Natural Gas consumption of the world increased by 2.2 % to reach a high of 3222 billion cubic metres and production by 3% for a value of 2954.8 billion cubic metres. Coal consumption for the same year jumped by a hefty 5.4% [1]. From the statistics available, it is evident that the demand for energy and hence our limited fuel sources is constantly increasing. We are dependent on fossil fuels for a majority of our energy requirement.

The use of fossil fuels entails with it an environmental cost especially in the form of greenhouse emissions. Climatic variations are one of the biggest risks created by the modern human growth. Greenhouse effect is leading to an overall increase in the temperature of the Earth. The greenhouse emissions contribute to the global warming of Earth by trapping the heat of the Sun. Carbon dioxide is largely produced in the combustion of all fossil fuels. Before the Industrial Revolution, the carbon dioxide levels in our atmosphere were about 280 parts per million by volume (ppmv), and current levels are greater than 380 ppmv. The major reason of concern is the fact that these levels have been increasing at a rate of 1.9 ppm yr⁻¹ since 2000 [2]. The global concentration of CO₂ in our atmosphere today far exceeds the natural range over the last 650,000 years of 180 to 300 ppmv. These increasing temperatures lead to a rising sea levels, impacting the lives of millions of people living on coastal lands and islands.

Hence, the burgeoning demand makes not only the economics of the energy supply an important issue, the question of sustainability of the energy source has become a big topic for debate nowadays. The issue of sustainability makes the case for hydrogen as an energy source. Hydrogen is clean burning fuel as it produces water as a by-product in place of harmful greenhouse gases. Another option is the development of syngas as a source to produce fuels via Fischer-Tropsch synthesis. As the fuels by the second route do not contain sulfur and other heteroatoms, they are a cleaner option to be used especially in internal combustion engines. Using these fuels there is a lesser production of harmful contaminants in the air [3].

1.1 SYNGAS AND HYDROGEN

Hydrogen is the simplest element consisting of just one proton in its nucleus. It is found in trace amount as gas in our atmosphere but is found in abundance in a combined form with oxygen (i.e. as water) on Earth. Hydrogen is rich in energy. Its heat of combustion is 141.8 MJ/kg, while for natural gas it depends on the source and quality but taking the higher heating value for its main constituent methane we can take a value of approximately 55.4 MJ/kg [4]. The value for coal and liquid fuels is even lower. This shows that a plethora of energy is available in hydrogen fuel.

The two major sources of hydrogen are the petrochemical sector and the electrolysis of water. Production of hydrogen from other hydrocarbons like naphtha, coal, heavy oil etc. has achieved a certain degree of importance in the last few years. The major driving force in this regard has been the rising demand for hydrogen in refineries and petrochemical complexes. Processes like hydrotreating, hydrocracking used for fuel upgradation utilize hydrogen. In the petrochemical industry hydrogen finds wide applications in production of important chemicals like ammonia, methanol etc. and also in hydrocarbon synthesis via Fischer Tropsch processes. Another method to produce hydrogen is via electrolysis of water. This method is energy intensive and a large amount of current has to be passed before water molecule is split. For the utilization of hydrogen fuel cells have been suggested as a good alternative. The principle behind the fuel cells was discovered by Swiss scientist Christian Schönbein. In a fuel cell hydrogen is combusted to release electricity.

Synthesis Gas is a mixture of carbon monoxide and hydrogen in varying ratios. Synthesis gas or Syngas, as it is most commonly called, is the name that is attributed to a gas mixture of Carbon monoxide and Hydrogen in varying proportions. This important factor, more easily named as the hydrogen-to-carbon monoxide ratio is a determining factor of the usability and property of the available synthesis gas. The heating value, density and other important properties are determined by this ratio. For example the Fischer Tropsch Process requires an optimum value of this ratio to be less than 3.5 [5]. This ratio can be varied by changing temperatures, steam content in the steam reforming process among others.

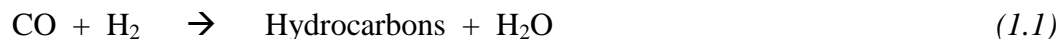
The name synthesis gas is given because it is widely used as an intermediate to create or synthesize synthetic fuels and for producing ammonia or methanol. Syngas is also used as intermediate in producing synthetic petroleum for use as a fuel or lubricant via the Fischer–Tropsch process. Syngas consists primarily of hydrogen, carbon monoxide, and very often some carbon dioxide, and has lesser energy density than that of natural gas. Syngas is combustible and often used as a fuel in internal combustion engines or as an intermediate for the production of other chemicals. The heating value of syngas depends on the proportion of carbon monoxide and hydrogen in the gas.

Out of all the production methods reforming of natural gas is the one that is widely implemented in the industry. Natural gas (which primarily contains methane) is the major feed for production of hydrogen and syngas owing to its large availability. Coal is also widely available but investment in a coal based syngas production unit is three times larger than that of a natural-gas dependent plant [6]. Thus it is an issue of a large capital investment v/s a higher operating costs. Economic analysis can determine which type of feed based plant should be setup. Since it is a gaseous fuel, natural gas has a large transportation and storage cost as compared to fuels like petroleum, which adds to the production cost of hydrogen and syngas. Liquid fuels have a higher energy density and thus the cost per unit energy produced is lower in the case of liquid fuels.

1.2 APPLICATION OF SYNGAS

Methane which is the primary constituent of natural gas is an important feedstock for manufacturing a large number of industrial chemicals as well as used in Gas-to-Liquid (GTL)

process. The major GTL process that has become ubiquitous is the Fischer-Tropsch (FT) synthesis. Methane is converted to syngas majorly via the reforming process and the syngas is used in FT synthesis to produce a wide array of liquid hydrocarbons. Group VIII transition metals are used as catalysts for the conversion process.



Another route is by first converting syngas to methanol using Cu/ZnO as a catalyst and then in a series conversion over a Zeolite ZSM-5 catalyst.

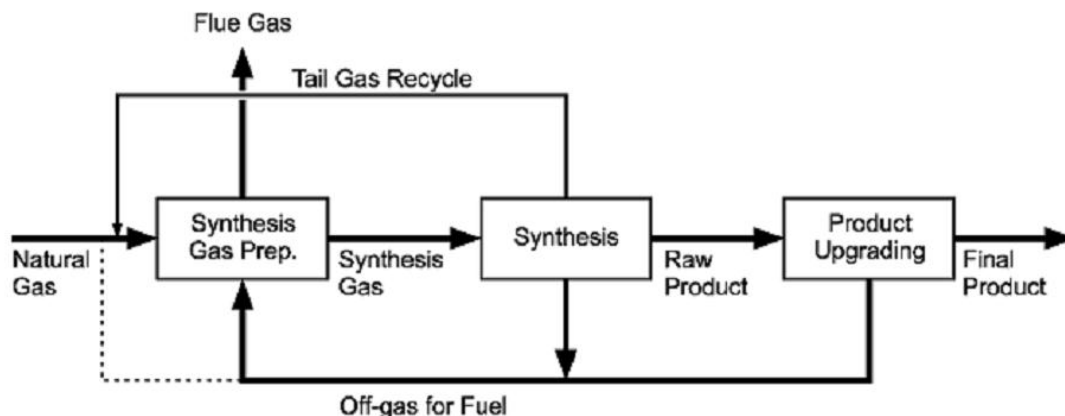


Figure 1.1: Flow Scheme for FT synthesis^[3]

Technologies required for the conversion and utilization of natural gas by converting it to syngas are well established. Syngas is then used as a feedstock for important chemicals. Ammonia synthesis is another large consumer of syngas. The world production of ammonia in the calendar year '08 was 133 MT with an average growth rate of 2.4% over the previous 5 years. Similarly another important chemical is methanol whose annual production in 2010 was 45 MT. The total natural gas required for producing these two chemicals amounts to 100 billion Nm³ annually [7]. Thus the areas where syngas is used are:

- Urea manufacture
- Gasoline blends

-
- The diagram illustrates various chemical synthesis routes, primarily centered around Syngas and Methanol.
- Syngas ($\text{CO} + \text{H}_2$)** is a central intermediate that can be converted into:
- Fischer-Tropsch:** Produces Waxes, Diesel, Olefins, and Gasoline. Catalysts: Fe , Co , Ru .
 - Mixed Alcohols:** Produced via Alkylated, ZnO , Cu , and MoS_2 .
 - Isosynthesis:** Produces C_4 using ThO_2 or ZrO_2 .
 - H_2 :** Produced from N_2 over Fe/FeO (with K_2O , Al_2O_3 , CaO) or via H_2O WGS Purify.
 - Oxosynthesis:** Produces Aldehydes and Alcohols using $\text{HO}(\text{CO})_2\text{P}(\text{Ph})_2$ or $\text{HO}(\text{CO})_2\text{P}(\text{Ph})_3$.
 - Methanol:** Produced using Co or Rh .
- Methanol** is a central intermediate that can be converted into:
- MTBE:** Produced via Isobutylene and acid ion exchange.
 - Acetic Acid:** Produced via Carboxylation ($\text{CH}_3\text{OH} + \text{CO}$) using Co , Rh , or Ni .
 - zeolites:** Produces Olefins and Gasoline.
 - MTO/MTG:** Produces Olefins and Gasoline.
 - DME:** Produced using Al_2O_3 .
 - Direct Use:** Produces M100, M85, and DMFC.

1.3 REFORMING PROCESSES

Reforming has been the cornerstone of natural gas conversion to syngas. The first step towards reforming was Steam Methane Reforming (SMR). It was developed in 1885 but

implemented at a large scale by BASF. There are a large number of reforming processes which can be classified on the basis of the use of air/oxygen and steam. In this work we will be focusing more on the oxidative reforming. However to gain a perspective of what oxidative reforming comprises of, and the differences between oxidative reforming and other reforming processes, it is essential to have a brief overview about them.

1.3.1 Steam Methane Reforming (SMR)

Steam Methane Reforming is the oldest and widely used process for industrial reforming. As the name entails steam is added in this type of reforming process. Owing to the stability of the methane molecule, somewhat severe conditions are requisite for the reforming process. The major reactions involved in the steam reforming are:

Table 1.1: Major Reactions in SMR

Reaction name	Reaction	ΔH_{298K}° (kJ/mol)
Partial Steam Reforming	$CH_4 + H_2O \leftrightarrow CO + 3H_2$	206.2
Water Gas Shift	$CO + H_2O \leftrightarrow CO_2 + H_2$	-41.1

The overall SMR is an endothermic reaction and hence a higher temperature pushes the reaction forward. Primarily a Ni/Al₂O₃ catalyst is used for conversion [9]. External heat needs to be supplied for optimum conversion which adds to the cost [10] as it is clearly evident that it is a highly endothermic process. For a complete GTL system based on natural gas as a feedstock, the SMR unit alone accounts for a major fraction of the total cost. The benefit lies in the fact that no oxygen is needed thus savings can be achieved on reducing the equipment necessary for the same. Further the temperature needed in SRM is lowest when compared to all other reforming processes. Thus, it helps save cost by savings on the material of construction and the insulation cost. The H₂/CO ratio in this case is higher than those required for FT synthesis and is applicable for hydrogen production.

1.3.2 Dry Reforming of Methane (DRM)

Dry reforming of methane, as the name suggests does not require steam to be provided as a reactant. The water in the steam reforming reactions is replaced by carbon dioxide.



The dry reforming of methane utilizes the greenhouse gas carbon dioxide and hence is a topic which receives a great deal of attention. It consumes one of the greenhouse gases to yield hydrogen. However, the H_2/CO ratio in this process is low (~ 1) which makes it suitable for applications other than hydrogen production like downstream conversion in FT synthesis.

The aforesaid reforming methods do not require oxygen for the reforming process. In the next section we will be covering the reforming methods that require air/oxygen as a feed and briefly analyze the advantages and disadvantages of the reforming processes. However, the industrial applicability of this method has been limited till now [11]. Developing this method holds huge potential for environmental sustainability by converting two undesirable greenhouse gases into an eco-friendly fuel in terms of emissions in the form of hydrogen.

1.3.3 Oxidative Reforming

When oxygen is supplied in conjunction with natural gas to achieve the reforming reactions, it is termed as the oxidative reforming process. The supplied oxygen can be in the form of pure oxygen or as air. The former requires equipment to produce pure oxygen which is most commonly achieved by liquefaction of air. This method is cost intensive. However, using pure oxygen gives better selectivity and gets rid of the wasted volume of inert gases like nitrogen which make up almost three-fourth of atmosphere. The drawback is additional equipment and capital cost along with cooling costs if liquefaction of air is employed as the method of choice for the production of pure oxygen.

1.3.3.1 Partial Oxidation of Methane (POX)

Partial Oxidation of Methane can be carried out via two basic routes- one without the use of catalyst wherein it is named as a direct oxidation process and second with the use of catalyst, with the title of catalytic partial oxidation. The two methods differ in the use of catalysts-the former employs no catalyst and relies on the direct combustion of methane, while the latter employs a catalyst bed to tilt the balance in the favour of reactions that are favourable and reducing the coke deposited. A simplified view of the reactions can be presented as:



This is a very simplified view of the highly exothermic incomplete combustion reaction. In reality the reaction products of combustion will also include water in its vapour state i.e. as steam. In the presence of water/steam the endothermic steam reforming reaction will also play its part; especially, if the catalyst is also being used, like the case in catalytic partial oxidation reforming.



The first commercial POX technologies were developed by Shell and Texaco and use a burner. This technology is also used in Shell's GTL-plant in Malaysia. The disadvantages of this technology are the very high reactor outlet temperature (± 1600 K), the high required O_2/CH_4 ratio (~ 0.7) with the accompanying moderate syngas selectivity ($< 90\%$) [12]. Some points in favour of POX include a H_2/CO ratio of around 2 which is suitable for FT synthesis. Also the equipment required to produce oxygen increases the cost. It can work without the need of external heat due to the intrinsic exothermicity of the combustion reactions. Unlike the autothermal reformer, for the control of heat, tube wall heating/cooling is employed in a partial oxidation reactor. Insulation may be used to ensure near adiabatic conditions. POX is able to sustain without external heating due to combustion reaction and without cooling due to endothermic steam reforming reaction.

1.3.3.2 Autothermal Reforming of Methane (ATR)

An ideal autothermal reforming reaction, as the name suggests does not require any external control of temperature. This happens because the endothermic steam reforming reactions are coupled with the exothermic methane combustion reaction. The ratio of steam to fuel and oxygen to fuel is set in such a way that the overall enthalpy of the reaction system is zero. The H_2/CO ratio obtained in this process is favourable for the GTL need. The controlled coupling of the endothermic reactions with the exothermic ones ensures that the temperature is lower than POX where steam is not supplied in feed. The energy requirement is lower because of the opposing contributions to enthalpy of the two sets of reactions. The gas space velocity is also higher in comparison to a traditional steam reformer [13]. However, autothermal reforming has a limited industrial application. There are limited tried catalysts for the same. Also, need for pure oxygen adds to the cost of operation.

Thus, in oxidative reforming we can see that oxygen is supplied in the feed which ensures the fact that the exothermic methane combustion will take place. Water may or may not be supplied with the feed. Not supplying water does not imply that the endothermic steam reforming reactions will not occur. The combustion product will include water which will ensure some endothermicity in the reacting mixture even in the absence of feed steam. A perfect ATR adjusts the supplied oxygen and steam values in such a way that the overall enthalpy of the reacting system is zero. It is also possible to supply steam in the feed in a proportion that the overall reaction is exothermic. Thus on that basis we can draw the following schematic for a system with oxidative reforming. The POX lies between total combustion and ATR conditions. The region for oxidative reforming can be defined as the one from Steam reforming to Total combustion, excluding both the limiting points.

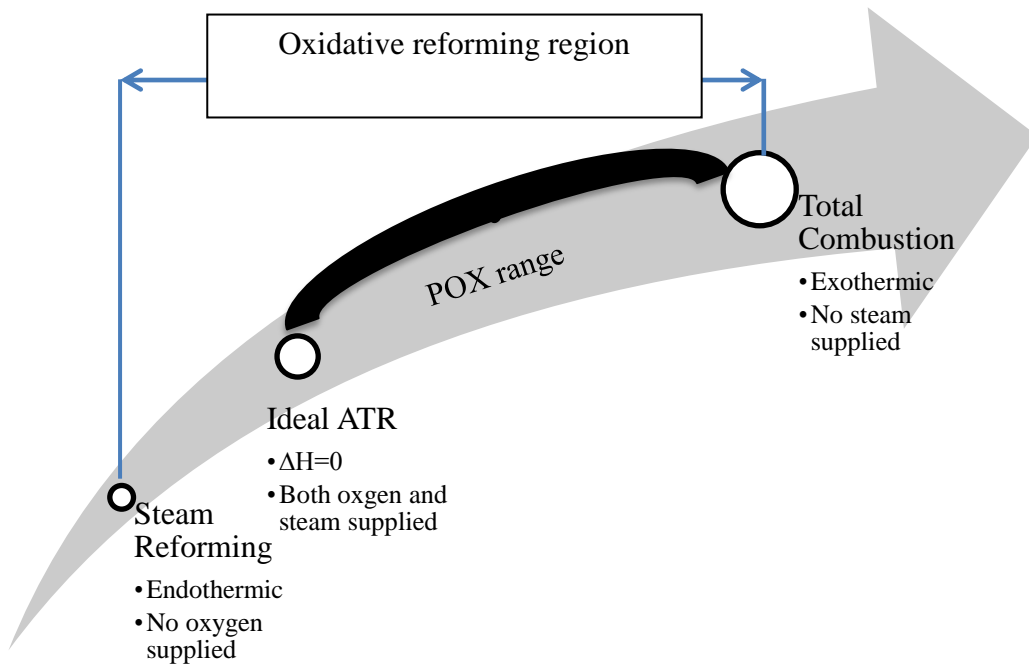


Figure 1.3: Increasing enthalpies in different reforming processes with oxidative reforming region shown

1.4 FIXED BED REACTOR SYSTEM

A fixed bed reactor in its most common form consists of a cylindrical column with a bed of catalyst particles in place. The catalyst bed is stagnant and the flow rates of the reacting streams are kept sufficiently low to prevent the bed from having an increased voidage, and become fluidized. It is a continuous reactor with the feed constantly entering and after conversion leaving. At steady state operation, the accumulation term in the mass and energy balances is neglected and no change in conversion is assumed with time. Steady state assumption makes the modeling of a fixed bed reactor easier. Most of the industrial and experimental reformers are fixed bed type owing to stability and ease of operation. Also a quicker startup if the catalyst bed needs to be changed can be initiated. For continuous operation two parallel fixed bed reactors are operated so that one of them can be taken out of operation for catalyst removal and/or regeneration and the other reactor ensures continuity of operation with minimum down time. Thus, the ease of operation, wide acceptance and easy availability are some of the reasons that have made a fixed bed reactor the basic reactor for all chemical industries.

1.5 OBJECTIVES

The objectives that were formulated for this work are as follows:

- Evaluation of oxygen-to-fuel ratio to obtain theoretical autothermal point for oxidative reforming region.
- A thermodynamic analysis of the reactions under consideration to find the feasibility range of different reactions.
- Thermodynamic analysis by Gibb's energy minimization for the determination of optimum operating parameters for the reactor using optimization tools in MATLAB.
- Collating kinetic data for different reactions under consideration using previously published research works.
- Formulating a one dimensional, steady state, non-isothermal mathematical model for a tubular reformer where oxidative reforming is being carried out.
- Solving the formulated equations using differential equation solver in MATLAB.
- Validating the model using an experimental/industrial data set.

- Using the operating parameters determined by thermodynamic analysis, simulate the mathematical model around that range of parameters to find the effect of varying the operating conditions on output parameters (e.g. methane conversion, hydrogen-to-carbon monoxide ratio etc.)

1.6 ORGANIZATION OF THESIS

Chapter 1 includes a brief introduction on the need for reforming natural gas to hydrogen and syngas. It also enumerates the different reforming routes and the objectives of this work. Chapter 2 contains a brief literature review. Chapter 3 pertains to the thermodynamic analysis of oxidative reforming of methane. Chapter 4 contains the mathematical model and validation of the model of oxidative reforming. Chapter 5 contains the results and discussions of the thermodynamic analysis and the simulation of the model prepared in the previous chapter. Chapter 6 concludes the work and makes recommendations for future work.

This chapter deals with the crucial research works done in the past in the area of modeling and simulation studies of the oxidative reforming as well as thermodynamic analysis of the reactions involved in the oxidative reforming. For the sake of avoiding superfluous information, the literature review has been focused on the objectives of this thesis.

The chapter is divided into three sections on the basis of the content that each section covers. The first section deals with the works of past on the thermodynamic analysis of reactions, mostly pertaining to reforming reactions. In some cases, however, the papers cited do not cover oxidative reforming. Their study is crucial to understand the methodology of thermodynamic analysis and using it as a tool to further its use in the scope of the current thesis. The second section deals with the important works on modeling and simulation of oxidative reforming. The final section is smaller and comprises of research work done on the catalysts for oxidative reforming processes.

2.1 THERMODYNAMIC STUDIES

Thermodynamic analysis is an important tool in the study of any reaction or a system of reactions. Thermodynamic analysis puts the theoretical limits to maximum achievable yields and conversions.

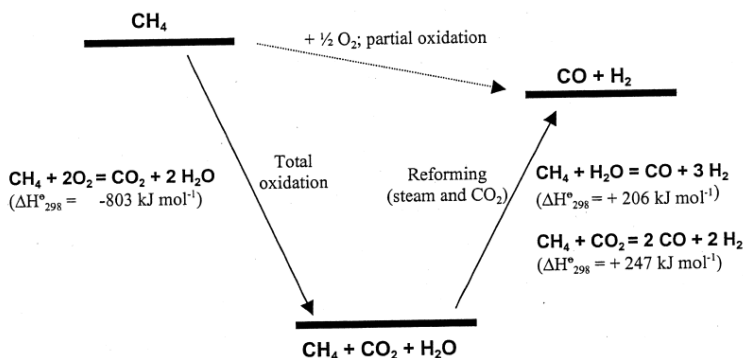


Figure 2.1: Thermodynamic representation of methane oxidation

Lutz et al. (2004) [14] conducted the thermodynamic analysis for producing hydrogen via partial oxidation route. In their analysis the authors have considered a global balance on the reactions which assists in giving the upper limits in theory to the steam-carbon and oxygen-carbon ratios. The equilibrium analysis provides a closer to reality estimate to product compositions and the efficiency of the process. The equilibrium calculations were cross checked with experimental data of a diesel fuel based reformer and as expected, it was found that the reformer efficiency was lower than that predicted by the equilibrium analysis. This goes on to show that thermodynamic analysis provides the theoretical maximum limits to our process.

Amin et al. (2007) [15] studied the combined reforming of methane with carbon dioxide and oxygen. The authors relied on an equilibrium analysis using Gibb's free energy minimization technique using Lagrange's multiplier method. It was found that at the equilibrium, the product compositions were highly dependent on the amount of methane, carbon dioxide and oxygen provided in the feed. Initial temperature was another determining factor. The analysis pointed out that the oxidation reaction was dominant at lower temperatures while carbon dioxide reforming was highly dependent on the oxygen to fuel ratio. The work eventually concluded with the optimum proportions of methane-carbon dioxide-oxygen which were found to be in the range of 1:0.2:1. The minimum temperature was found to be 1000K.

Li et al. (2008) [16] studied the thermodynamic equilibrium for autothermal reforming of methane using Gibb's Minimization technique. They also studied the carbon dioxide reforming of methane. Hydrogen yield, conversion of methane and coke were important factors in their study. The authors found the optimal methane-carbon dioxide-oxygen ratios to be 1:0.8–1.0:0.1–0.2 at a minimum temperature of 1073K. Methods to limit coke formation were also given. It was postulated that coke could be removed by having a higher temperature for the reaction and raising the steam content in the feed. Also, lower pressures contribute to lower carbon deposition.

Chen et al. (2010) [17] studied the hydrogen production via two different methods and compared both using thermodynamic analysis. In the first method, the autothermal reforming (ATR) of methane to produce hydrogen was employed. In the second method, the partial oxidation of methane succeeded by a water gas shift reaction was considered. It is important to note that the reaction temperatures of partial oxidation and water gas shift reactor were

controlled separately and independently from each other. It was found that temperature is a crucial factor in determining hydrogen yield in the case of ATR. Effects of other parameters were also found out. It was concluded that methane conversion in the second method with partial oxidation is always higher irrespective of the reaction temperature. The other results pertain to the use of water gas shift reactor which is not of importance in the context of current study.

Freitas et al. (2012) [18] studied the oxidative reforming of methane by the thermodynamic analysis of the involved reactions using Gibbs energy minimization (at constant pressure and temperature) and entropy maximization (at constant pressure and enthalpy) methods, to determine the equilibrium compositions and equilibrium temperatures, respectively. It was found that hydrogen and syngas production were better at higher temperatures and lower pressures. Also the oxygen to fuel ratio was an important parameter in determining the product composition. The authors compared their results with published data and found close agreement. The calculated results were compared with previously published experimental and simulated data with a good agreement between them.

Nematollahi et al. (2012) [19] applied thermodynamic analysis to study combined partial oxidation and carbon dioxide reforming of methane in view of carbon formation. They employed Gibb's free energy minimization techniques on wide range of operating parameters including of pressure ranging from 1–25 bar, temperature from 600–1300 K, carbon dioxide to methane ratio 0–2 and oxygen to methane ratio 0–1. It was found that increasing pressure reduces the conversion of methane. It was also indicated that addition of oxygen to the feed mixture reduces carbon deposition.

2.2 MODELING AND SIMULATION STUDIES

Mathematical modeling of any physical process is a powerful utility that helps to study that process without having to resort to expensive real life construction of that process and conduct costly experiments. It is a theoretical tool that mathematically defines the process and helps us simulate the process on our computers.

De Groote and Froment (1996) [20] simulated the adiabatic fixed bed reactor system considering the catalytic partial oxidation process along with coke formation for the conversion

of methane to syngas at a high pressure and temperature range. The pressure in the reactor was kept at 25 bar and the temperature in the range of 808K to 1785K. The catalyst considered was Ni based and Xu and Froment kinetics were applied for steam reforming. Trimm and Lam kinetics for the oxidation of methane were applied. A one dimensional reactor model was used with material and energy balances. The operations were not isobaric and hence a pressure drop equation was also applied. Different feed conditions were provided by varying the amounts of water, carbon dioxide and so on to study the outlet values of hydrogen to carbon dioxide ratio as well as the maximum catalyst temperature. The reactor considered was an industrial reactor with a diameter of 1.2 m.

Ostrowski et al. (1998) [21] modeled the catalytic partial oxidation of methane to produce synthesis gas for a Ni/Al₂O₃ catalyst for fixed bed and fluidized bed reactors. The conditions for which the model was simulated were of industrial scale with a high pressure range of 5-30 bar and temperature range of 1023-1073 K. The reaction kinetics was taken from De Groote et al. (1996) and it was found that fluidized bed reactors produced a higher yield of syngas over fixed bed systems owing to the large dependence of the reactions on intra-particle mass transport resistance, which is lesser in fluidized state.

de Smet et al. (2001) [22] simulated the adiabatic fixed bed reactor for catalytic partial oxidation of methane to synthesis gas using a one dimensional steady state model. The catalyst considered for was Ni based. The reactions considered were the total oxidation of methane along with steam reforming and water gas shift. Water was added as a reactant. The kinetics of oxidation and steam reforming were studied and their influence on a number of output parameters was given as results. Different reforming models were applied to find the different maximum temperatures in the catalyst bed. One of the models that were used was from Xu and Froment's work on Ni catalyst [23].

Avci et al. (2001) [24] modeled an autothermal, dual catalyst fixed bed reactor with the prime motive of hydrogen production. The model configurations included using different catalyst with varying feed ratios and bed configurations. The different configurations in question are the mixing of catalysts Pt-Al₂O₃ and Ni/MgO-Al₂O₃ or placing them in series one after the other. The reactor was operated with varying feed ratios at both lab scale and industrial scale. It was found that the hydrogen production is higher when the catalysts are in a physically mixed state as

well as at low methane-to-oxygen and high steam-to-methane ratios. The optimum operating conditions for obtaining maximum hydrogen production were also investigated

Ji et al. (2003) [25] worked on a one dimensional steady state model for the partial oxidation of methane on a Ni catalyst. The kinetics used was from the work of De Groote and Froment (1996). Using this model a membrane reactor with oxygen permeable membrane was also developed. Using the simulation results outlet temperatures and flow rates were calculated, which were used in further calculating the exergies of different species. It was found that membrane reactors give a better conversion and at the same time thermodynamically a lower pressure and higher inlet temperature favours the product formation.

Halabi et al. (2008) [26] worked on the autothermal reforming process of methane with the aim of hydrogen production. A fixed bed reactor with Xu and Froment kinetics for reforming was considered. The analysis was conducted at steady state as well as dynamically. The input parameters like oxygen to carbon ratio, water to carbon ratio, temperature etc. were varied and the impact of changing these on output parameters like hydrogen yield, conversion of methane, reforming efficiency was studied. The temperature was kept at 873K while the pressure at 1.5 bar. Optimum values of the input variables were reported.

Kumar et al. (2009) [27] developed a one dimensional non-isothermal model for oxygen permeable membrane reactor for the purpose of hydrogen production. Three reactors were compared. One was a fixed bed reactor with pure oxygen in feed, the second was a fixed bed reactor with air in feed, and the third was a membrane reactor with an oxygen permeable membrane. Data given by De Groote and Froment was used for validating the model. The effect of changing inlet parameters was studied on the outlet parameters. It was found that the fixed bed reactor with pure oxygen in feed has the best performance amongst the aforesaid reactors.

Zahedi nezhad et al. (2009) [28] suggested an autothermal reformer with two distinct sections. The first section is assumed to be the combustion section while the other one has a catalytic bed. The mathematical model of such a reformer is developed by the authors. In the combustion section, temperature and composition were predicted using 108 simultaneous elementary reactions considering 28 species. The results of the simulation of the first section were taken as the starting point for the second section. A one-dimensional heterogeneous reactor

model was used for kinetic simulation of the second section. The catalyst considered was a Ni based catalyst supported on Mg- alumina spinel. Results of the model were compared with published data on ATR process.

Reese et al. (2010) [29] modeled the high pressure autothermal reforming of methane via a 1-D, heterogeneous, numerical model. The impact of changing steam to carbon ratio and oxygen to carbon ratio on output parameters was studied by the authors for different operating pressures of 6, 28 and 50 bar. A sensitivity analysis consisting of 9 model parameters was also completed. It was found that the model was sensitive to the activation energy of the endothermic reforming reactions and the ratio of oxygen to carbon. This paper was a companion paper to an experimental work by the authors wherein a lab scale reformer was constructed and tested for pressure range between 6 to 50 bar.

Scognamiglio Diego et al. (2012) [30] modeled and validated an autothermal reactor with a fixed bed of Rh catalyst. For the validation of their model they conducted experiments on a small reactor of laboratory scale. The temperature profiles of this experiment were measured with the help of an infrared camera. It was found that the temperature peaks were present on the inlet as a result of separation between spaces for oxidation and reforming reaction. The model of the authors was validated with experimental data by comparing temperature profiles with those obtained experimentally at different feed compositions, total flow rate and preheating temperatures. The validated model was used to analyze the effect of thermal conductivity and of the flow rate on overall reactor performance.

2.3 CATALYST STUDIES

A lot of work has been done in the field of finding suitable catalysts and kinetics for the reactions that are in the scope of our present study. The reactions have been studied at a laboratory scale experimentally to determine a kinetic model. These works are then utilized in modeling and simulation work.

Trimm and Lam (1980) [31] conducted their experimental work on a catalytic combustor. Their work entailed the study of methane combustion over platinum catalyst supported on porous and non-porous alumina fiber. They measured reaction kinetics at temperatures above and less

than 815 K and found that activation energy changes at the aforesaid temperature. For different types of catalysts different models were found applicable. On comparing the model with Langmuir-Hinshelwood type of model they postulated that the reaction mechanism involves reactions occurring between adsorbed methane and between the oxygen either adsorbed or in the gas phase. Their work has been used by a variety of researchers working in the field of modeling and simulation studies on Ni catalysts even though the catalyst they have used is Pt by incorporating some correction/effectiveness factors for different reactions.

Xu and Froment (1989) [23] derived intrinsic rate equations for methane steam reforming and accompanying water gas shift reaction. The catalyst used for the study was a Ni/MgAl₂O₄ catalyst. The work has been cited very frequently in literature for modeling studies as well as experimental works. Based on the rate determining steps of reactions, Xu and Froment formulated Langmuir-Hinshelwood type rate expressions. They assumed the same active sites for all the reactions. Using thermodynamic analysis they reduced the possible mechanisms, and the parameter estimation for the best model are statistically significant and thermodynamically consistent.

Heitnes et al. (1995) [32] studied the partial oxidation of methane on a number of catalyst beds- Monolithic reactor with 5% Ni catalyst and a fixed bed reactor with Ni/Al₂O₃ as catalyst. The temperature range of the experiments was 873K to 1073K at 1 bar pressure. The results were analyzed and it was predicted that the reactions occurring in both the systems consist of total combustion of methane, reforming reactions and water gas shift reaction.

Freni et al. (2000) [13] worked on collating the previous developments on processes used for syngas production. The processes that they reviewed included partial methane oxidation with or without steam. They also considered a variety of reactors including monoliths, fixed bed reactors; fluidized bed reactors etc. They also considered a number of catalysts for review including Ni based catalysts, catalysts containing noble metals like Pt, Pd etc. They also reviewed differences in mechanism for different reactions on different catalysts.

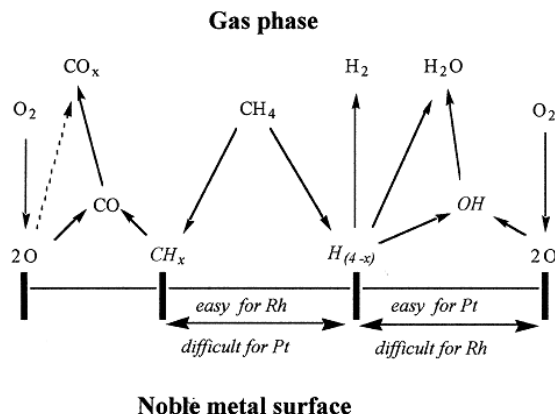


Figure 2.2: Reaction mechanism for partial oxidation of methane on different catalysts with noble metal

They also listed potential benefits of using one type of catalyst over the other, say Rh is an addition to the cost of process however, it minimizes water production and maximizes hydrogen yield.

Choudhary et al. (2006) [33] worked on CO₂ reforming with simultaneous steam reforming or partial oxidation of methane to syngas over NdCoO₃ perovskite-type mixed metal oxide catalyst. Their study was at different process conditions. For both the cases they observed almost negligible carbon deposition. They concluded that reduced NdCoO₃ perovskite-type mixed-oxide catalyst is a highly promising catalyst for carbon-free CO₂ reforming combined with steam reforming or partial oxidation of methane to syngas.

Corbo et al. (2007) [34] studied the catalytic partial oxidation reaction for hydrogen production on three catalyst types, two based on Ni–Al₂O₃ and one constituted by Pt supported on cerium oxide. The feedstock for the authors was propane as it is a major constituent of LPG. The same catalysts were utilized to study the partial oxidation of methane and for comparing the results to propane results. The catalytic properties were quantified in terms of yield and selectivity of hydrogen. Tests were conducted to check the durability and stability of catalyst along with the resistance to carbon deposition. It was concluded that Ni catalysts are highly selective for hydrogen. The cerium based catalyst is helpful in resisting coke deposition more than Ni.

Munera et al. (2010) [35] worked on the combination of carbon dioxide reforming and oxidation of methane with the motive of producing syngas. They used a membrane reactor. Two different types of catalysts were used. They were analyzed in a conventional reactor with a fixed bed and then used in a membrane reactor. For our purpose the results of the fixed bed reactor are of importance. Varying oxygen to methane ratios and carbon dioxide to methane ratios were supplied to identify their impact on hydrogen yield. The fresh, reduced and used catalysts were characterized using a variety of techniques like X-Ray Diffraction, laser Raman spectroscopy and XPS. The spectroscopic features were consistent with the catalytic behavior of both formulations. The best performance of the reactor was achieved on one of the catalysts and use of approximately 10% oxygen in feed.

Dantas et al. (2012) [36] studied the nickel catalysts supported on different types of supports for the methane oxidative reforming reactions. BET surface area results showed that the catalysts containing alumina presented higher surface area which favored better nickel dispersion. X-ray diffraction data from the reduced samples was used for confirmation. A literature based kinetic model was used to compare data predicted by this model with the experimental behavior. The results showed that high temperatures are optimum for maximum hydrogen production. The differences between the data and model could be attributed to the difference in catalysts over which the model equations were developed and the experiments were conducted.

2.4 CONCLUDING REMARKS

In this chapter, research work done on thermodynamic analysis and modeling and simulation studies majorly pertaining to oxidative reforming of methane was critically analyzed. Catalyst and kinetic models developed were presented in brief, with the range of operating parameters over which they were evaluated. These results would be used in subsequent chapters for selecting the appropriate constitutive relationships and also for validation of the developed model.

CHAPTER 3

THERMODYNAMIC ANALYSIS

This chapter deals with the thermodynamic analysis conducted on a system with oxidative reforming of methane. The science of thermodynamics at a basic level involves energy and its transformation.

The name thermodynamics means literally the changes in temperature (heat). However, thermodynamics is also utilized to determine the conditions under which a reaction or a set of reactions attain a state of equilibrium- a state where no visible change occurs. In dynamic equilibrium the rate of forward and backward reactions becomes equal and hence the two opposite changes occurring at a microscopic level cancel each other out on macroscopic level. Thermodynamic analysis is an important tool in the study of any reaction or a system of reactions. Thermodynamic analysis puts the theoretical limits to maximum achievable yields and conversions.

3.1 DETERMINATION OF AUTOTHERMAL POINT

As mentioned in the introduction, this work entails the study of oxidative reforming of methane. As per the definition being adopted in this work, oxidative reforming entails the region bounded by the point representing total combustion of methane where the only products are oxides of carbon and water in the form of steam on one side, and the point representing pure steam reforming with no added oxygen as the other extreme. The region of oxidative reforming has purely endothermic reactions on one end, and highly exothermic reaction on the other, with the enthalpy at a particular point determined by the supply of oxygen and water. In between these two extremities, both the types of reactions are present.

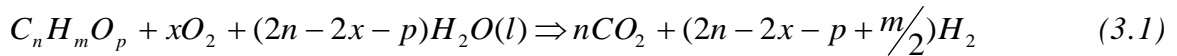
We define an autothermal point where the net enthalpy of these reactions becomes equal to zero. For this to happen, the oxygen supplied has to be in a specific ratio such that the aforesaid conditions of enthalpy are achievable. The region between the autothermal point and the point representing total combustion can be said to be the region for partial oxidation (with steam supply) where overall exothermic reaction occurs (albeit the presence of endothermic reforming

reactions). Between the autothermal point and steam reforming point, overall endothermic conditions prevail due to lower dominance of exothermic combustion reaction.

Autothermal reforming is a combination of both endothermic and exothermic reactions. In a perfectly autothermal system the heat produced in the exothermic reactions is taken by the endothermic reactions. The word ‘autothermal’ originates from the same ideology. The system of reactions regulates its enthalpies in itself. There is no requirement for supplying or taking away heat. In an idealized condition a perfect autothermal reaction will have its ΔH_{net} equal to zero. It implies that under autothermal conditions the enthalpy of exothermic and endothermic reactions is balanced in such a way that no net heat is taken or generated and the reaction is in fact truly ‘autothermal’. For the purpose of this work, the autothermal point in terms of oxygen supplied is of important concern to us. This is so because it gives us an idea of the range of oxygen ratio that is to be used for operation.

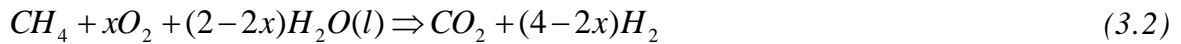
3.1.1 Idealized reaction

Ahmed and Krumpelt [37] considered a general feedstock $C_nH_mO_p$ and formulated the idealized reaction stoichiometry for the conversion of the hydrocarbon feed into carbon dioxide and hydrogen. No incomplete conversions were considered and hence no free carbon or carbon monoxide was included in the stoichiometry.



Where, x is the oxygen-to-fuel ratio.

In our case the feedstock is methane. Hence $n=1$, $m=4$, $p=0$ is taken as the special case and the overall idealized conversion reaction is:



The overall heat of reaction at 298.15 K and 1 bar for the above standard reaction is:

$$\Delta H_{R, 298K, 1bar}^{\circ} = \Delta H_{CO_2}^{\circ} + (4 - 2x)\Delta H_{H_2}^{\circ} - \Delta H_{CH_4}^{\circ} - x\Delta H_{O_2}^{\circ} - (2 - 2x)\Delta H_{H_2O}^{\circ} \quad (3.3)$$

The ΔH^0 is the standard enthalpy of formation of component in the subscript. Another important parameter is maximum hydrogen yield and maximum percentage of hydrogen in product and is given by:

$$\text{Max. H}_2 \text{ yield} = 4 - 2x$$

$$\text{Max. H}_2 \text{ percentage} = \frac{4 - 2x}{1 + (4 - 2x)} \times 100$$

Table 3.1: Standard heat of formation ^[38]

Species	Standard Heat of formation at 298.15 K (kJ/mol)
Carbon Dioxide	-393.51
Water(gas, liquid)	-241.83,-285.84
Hydrogen	0
Oxygen	0
Methane	74.86

A critical oxygen-to-fuel ratio X_c is defined to be that value of oxygen-to-fuel where the enthalpy of the idealized reaction becomes zero or the autothermal condition is achieved. It is calculated by setting the ΔH_R° zero and solving the equation for x. The value is called the critical oxygen to methane ratio or X_c .

For determining X_c for the idealized reaction at any temperature T, we require the enthalpy at T. For evaluating enthalpy as a function of temperature C_p° values are used. The dependence of enthalpy is assumed to be on temperature only and pressure variation is ignored.

National Institute of Standards of Technology (NIST), US Department of Commerce has a substantial database on a number of species. The NIST Chemistry Web-book [38] utilizes the Shomate equations where Gas Phase Heat Capacity is given as

$$C_p^\bullet = A + B*t + C*t^2 + D*t^3 + E/t^2 \quad (3.4)$$

The integration of the above equation with t, gives H° as a function of temperature. The constant of integration is evaluated by using the standard enthalpy at 298.15 K which is known.

$$H^\circ - H_{298.15}^\circ = A*t + B*t^2/2 + C*t^3/3 + D*t^4/4 - E/t + F - H \quad (3.5)$$

Where,

C_p = heat capacity (J/mol*K)

H° = standard enthalpy (kJ/mol)

t = temperature (K) / 1000

Table 3.2: Shomate equation parameters for different components ^{[39] [40]}

<u>Species</u>	<u>A</u>	<u>B</u>	<u>C</u>	<u>D</u>	<u>E</u>	<u>F</u>	<u>G</u>	<u>H</u>
Carbon Monoxide	25.56759	6.09613	4.054656	-2.6713	0.131021	-118.009	227.3665	-110.527
Water	30.092	6.832514	6.793435	-2.53448	0.082139	-250.881	223.3967	-241.826
Carbon Dioxide	24.99735	55.18696	-33.6914	7.948387	-0.13664	-403.608	228.2431	-393.522
Hydrogen	33.06618	-11.3634	11.43282	-2.77287	-0.15856	-9.9808	172.708	0
Oxygen	0.03235	8.772972	-3.98813	0.788313	-0.7416	-11.3247	236.1663	0
Methane	-0.70303	108.4773	-42.5216	5.862788	0.678565	-76.8438	158.7163	-74.8731

3.1.2 Solution methodology and results

The program to solve the enthalpy of the idealized reaction as a function of x (oxygen-to-fuel ratio) is written in MATLAB R2010b. The library function f_{zero} used to solve such kind of linear and non-linear equations is used. All used data are given.

It has been assumed that $0.0 \leq x \leq 1.0$ because if $x > 1$ then water will be obtained as a product which goes against our initial assumption of having only carbon dioxide as a product. The autothermicity of the reaction is defined using [26]:

$$\Delta H_T = \sum_i \nu_i(x) H_i(T) = 0 \quad (3.6)$$

Where, i is used to denote the five species involved.

For validation the equation is solved at 298.15K. At this temperature water is assumed to be a liquid and hence heat of formation of liquid water is used. For oxygen-to-fuel ratios greater than 1, water is assumed to be available as liquid on product side. Ahmed and Krumpelt [37] had found it to be 0.44 at the same temperature. The solution of the equation yielded a value of 0.44261 which is in close agreement.

Next, the equation is solved at different temperatures in the range of 800-1200 K and the critical value and other parameters are reported. However in this temperature range water is considered to be in gaseous state and hence the heat of formation of gaseous water is used.

Table 3.3: Results of critical oxygen-fuel ratio at different temperatures

Temperature(K)	Critical X_c	Max. H_2 yield	Max H_2 % in product
800	0.3256	3.3488	77.0054
900	0.3186	3.3627	77.0784
1000	0.3108	3.3785	77.1611
1100	0.3020	3.3960	77.2520
1200	0.2925	3.415	77.4000

In the case of methane, considering an idealized stoichiometry, it can be said that pure steam reforming occurs when the value of x is equal to zero. For values of x greater than 2.0 total combustion in excess of oxygen can be said to occur. Thus in between the range of 0.0 to 2.0 we can find the region of oxidative reforming for methane to occur. Within that range, the autothermal point is dependent on the reaction temperatures because the heat of formation of the species is a function of temperatures rendering the autothermal point to be a function of temperature alone. It can be seen that for using water as a gaseous product, the results vary from assuming it as liquid product. The range of steam to fuel ratio which is determined for the idealized stoichiometry is given below.

Table 3.4: Steam to fuel ratio corresponding to the calculated critical oxygen to methane ratio (obtained via stoichiometric balance)

Temperature(K)	Critical Oxygen to Methane Content	Steam to fuel ratio (via stoichiometry)
800	0.3256	1.3488
900	0.3186	1.3628
1000	0.3108	1.3784
1100	0.302	1.396
1200	0.2925	1.415

Thus, we have a reasonable estimate of the oxygen to fuel ratio which gives us autothermal conditions. It is essential to remember that it is an estimate as no partial conversions are considered which happen in the real situations. Also some heat loss is also there so generally the value of X_c in reality is greater than theoretical value [26]. This gives us an estimate of the range of oxygen to methane ratio that we will be working with and at the same time it provides information about steam to methane ratio. No doubt that the reaction stoichiometry is idealized and involves a lot of assumptions, but for the purpose of this current work, it provides us a good starting point. It is clear from the results obtained that the oxygen to methane ratio of around 0.3 ensures that we will be operating in the region of partial oxidation. Hence it gives us an idea of the region of oxidative reforming that we are operating in.

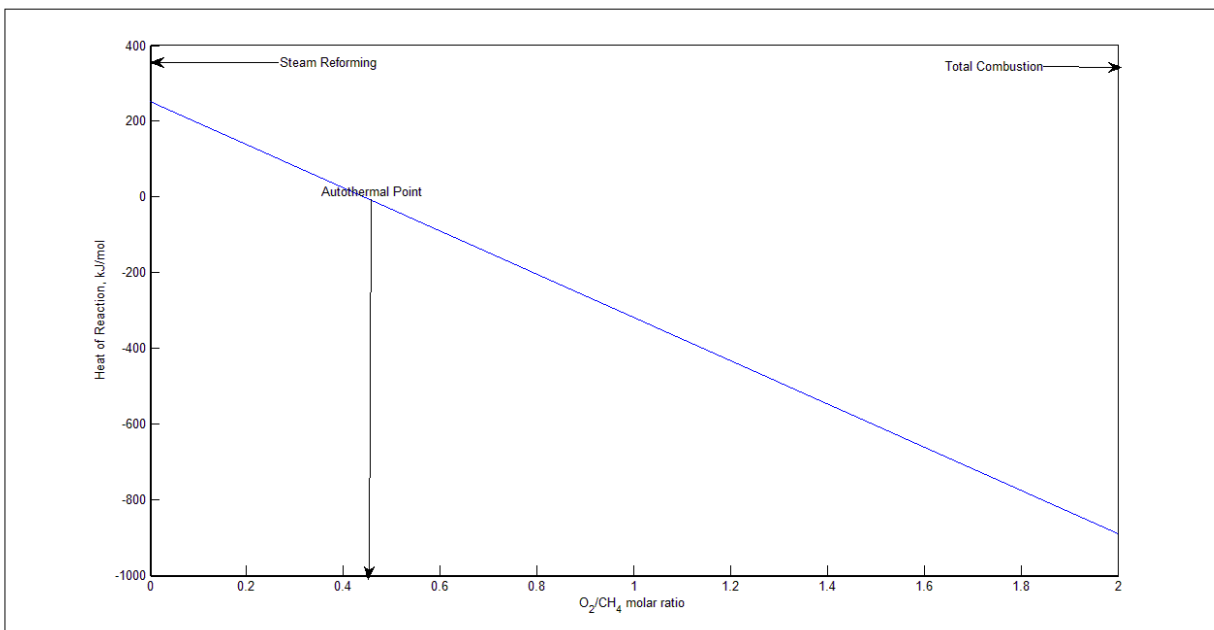


Figure 3.1: Heat of reaction during ATR of methane at 298K as a function of oxygen-to-methane ratio

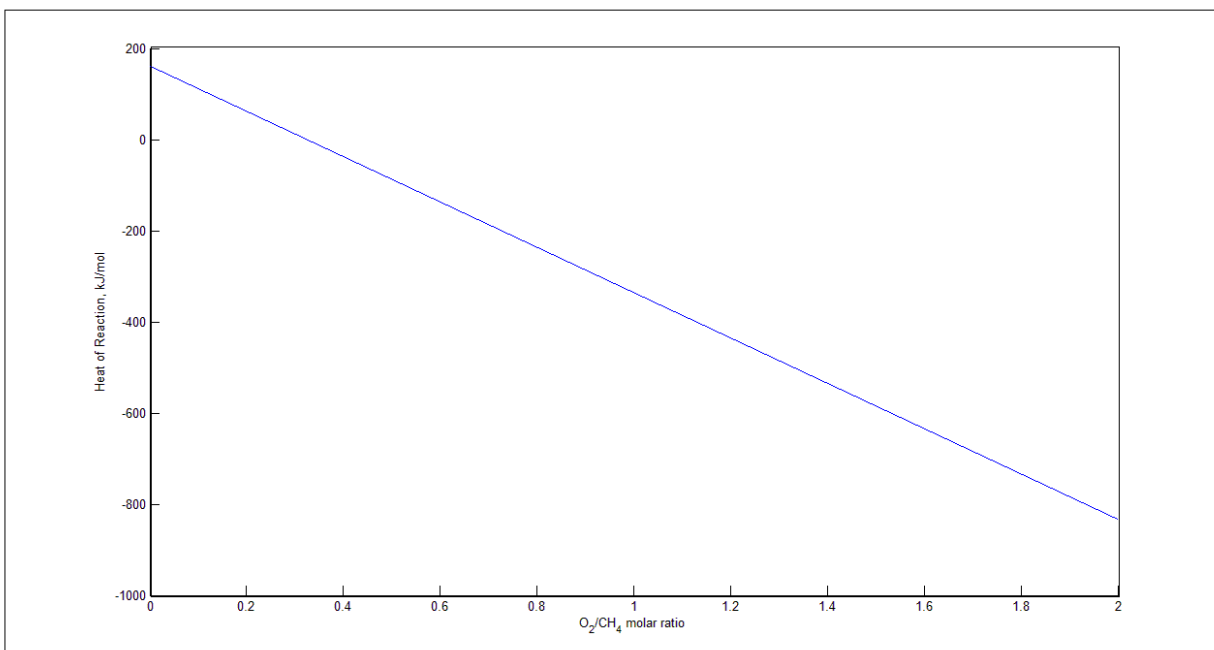


Figure 3.2: Heat of reaction during ATR of methane at 800K as a function of oxygen-to-methane ratio

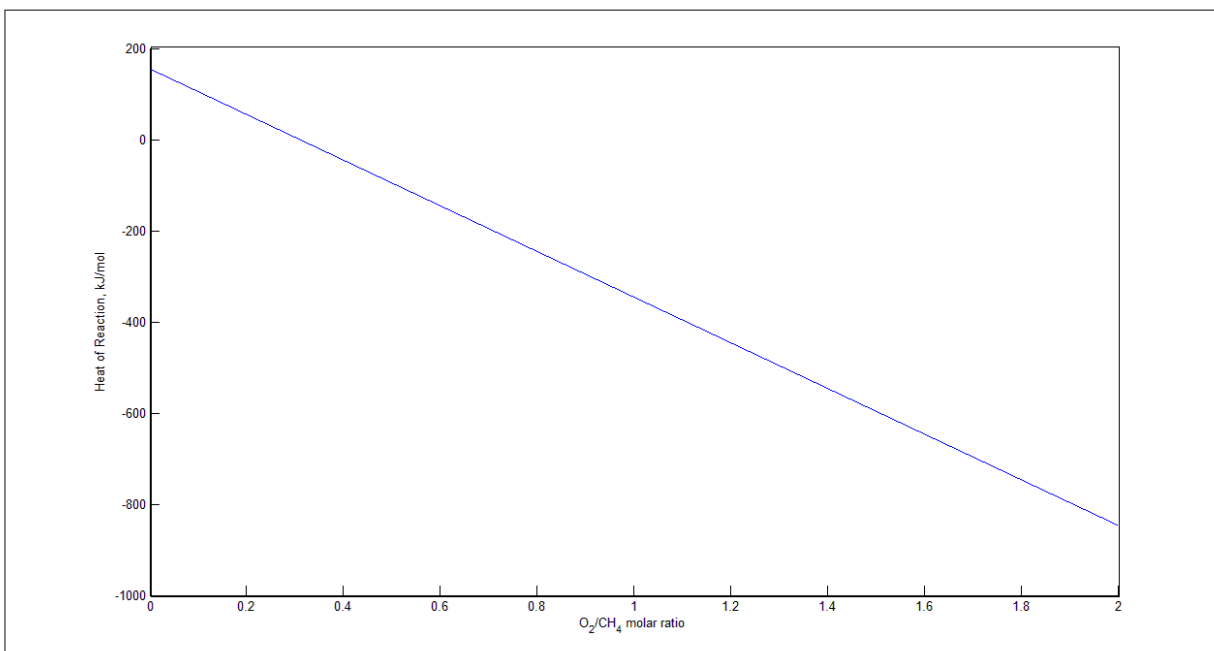


Figure 3.3: Heat of reaction during ATR of methane at 1000K as a function of oxygen-to-methane ratio

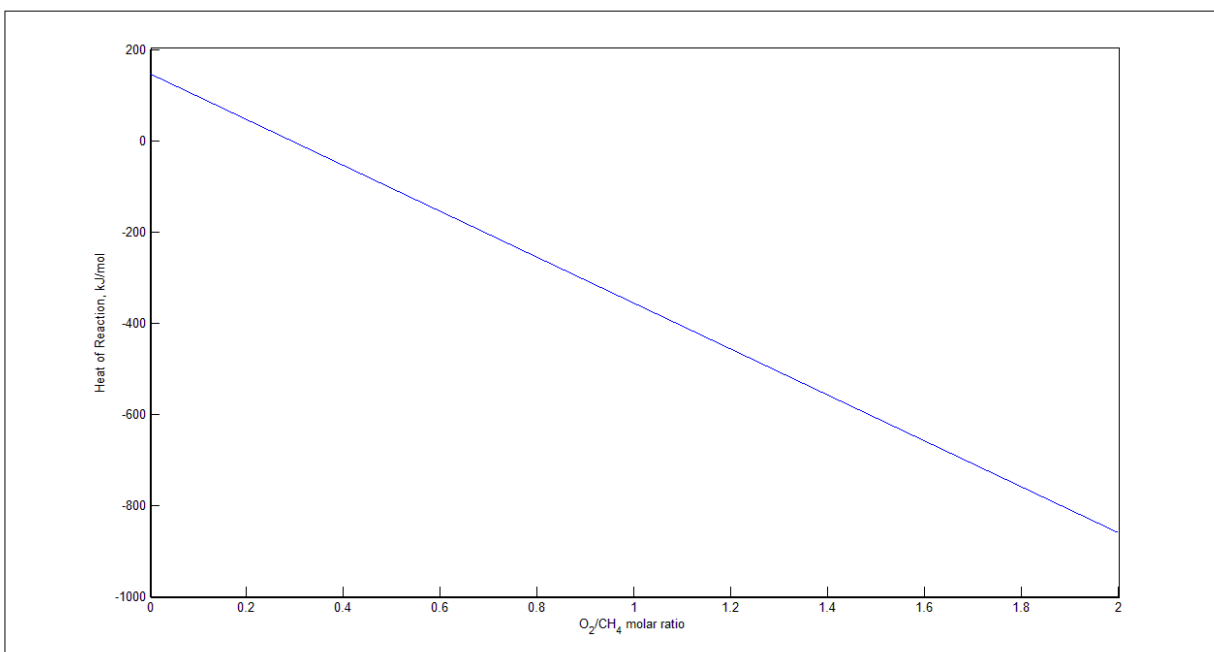


Figure 3.4: Heat of reaction during ATR of methane at 1200K as a function of oxygen-to-methane ratio

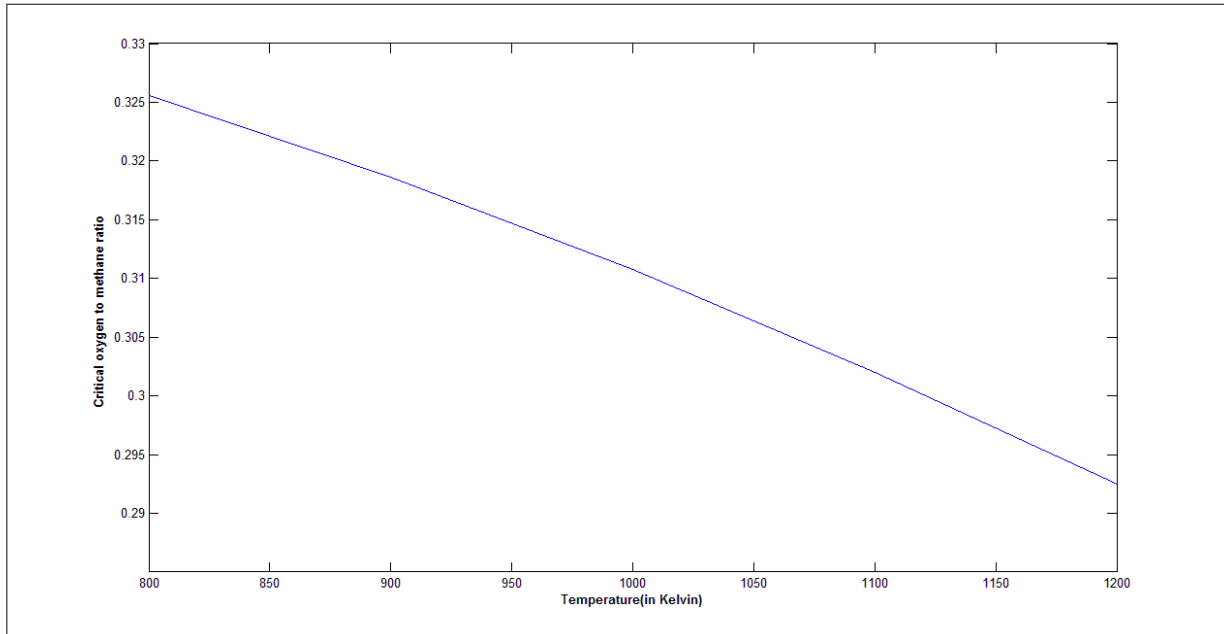


Figure 3.5: Variation of critical oxygen to fuel ratio with temperature

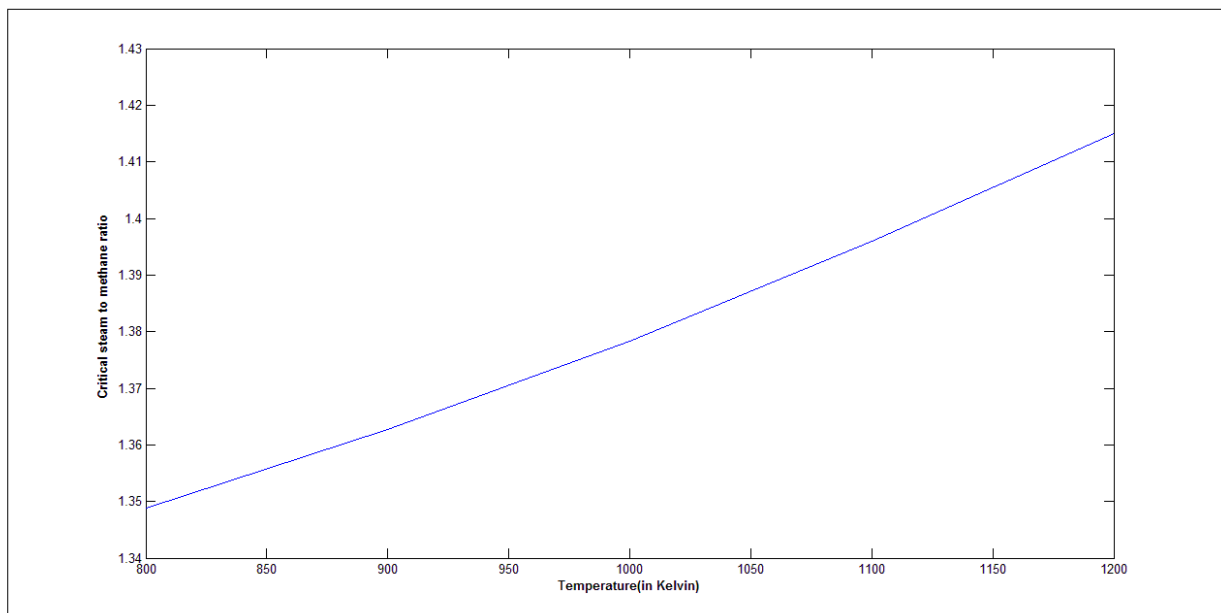


Figure 3.6: Variation of stoichiometric steam to methane requirement with temperature.

3.2 THERMODYNAMIC FEASIBILITY OF REACTIONS

Although there are a large number of reactions occurring consecutively and in parallel in any complex reaction system, it is very difficult to incorporate all the reactions into the model being developed. For the purpose of model development and thermodynamic analysis, this work contains essentially four major reactions:

Table 3.5: Reactions in oxidative reforming ^[26]

Serial	Reaction name	Reaction	$\Delta H^{o(298K)}$ (kJ/mol)
R1.	Partial Steam Reforming	$CH_4 + H_2O \leftrightarrow CO + 3H_2$	206.2
R2.	Water Gas Shift	$CO + H_2O \leftrightarrow CO_2 + H_2$	-41.1
R3.	Total Steam Reforming	$CH_4 + 2H_2O \leftrightarrow CO_2 + 4H_2$	164.9
R4.	Methane Combustion	$CH_4 + 2O_2 \rightarrow CO_2 + 2H_2O$	-802.7

Methane combustion or total oxidation is highly exothermic reaction. The water gas shift (WGS) reaction is a major influencer of an important parameter viz. $\frac{H_2}{CO}$ ratio. The $\frac{H_2}{CO}$ ratio determines the usability and applicability of syngas in different processes and industries. For pure H_2 production it can be stated that the $\frac{H_2}{CO}$ ratio approaches a large value and water gas shift dominates for changing CO to H_2 .

For a reaction in the gaseous state $aA + bB \leftrightarrow cC + dD$ the equilibrium constant can be defined in the terms of partial pressures of its reactants and products. Hence the equilibrium constant for the reaction would be:

$$K_{eq} = \frac{P_C^c P_D^d}{P_A^a P_B^b} ; \text{unit} = \text{bar}^{(d+c-b-a)}. \quad (3.7)$$

Gibb's free energy is a function of temperature and pressure. Since the standard state is defined in terms of a specified pressure of 1atm, ΔG^o is independent of pressure. Similarly the enthalpy of a reaction is assumed to be dependent only on T and its variation with P can be neglected. Using Shomate equation (3.5), we can determine H^o . On the basis of Gibbs free

energy of a reaction we can determine its feasibility. We know that a reaction is feasible as long as $\Delta G^0 < 0$. If this is not the case then the reverse of the reaction under consideration is dominant and hence the reaction under our purview is not significant and is moving in the backward of what we have assumed. The feasibility range of the series of reactions is determined by the temperature range over which all of them are feasible, or in thermodynamic terms where each and every reaction has its $\Delta G^0 < 0$. From thermodynamics it is known that:

$$\Delta S^\bullet = \int \frac{C_p}{T} dT \quad (3.8)$$

From C_p equation, Equation (3.4), the integration yields us the equation

$$\Delta S_i^\bullet = A \ln(t) + B \cdot t + C \cdot t^2/2 + D \cdot t^3/3 - E/(2 \cdot t^2) + G \quad (3.9)$$

Where, ΔS_i^\bullet = standard entropy (J/mol*K) and G is available using NIST data table or can be evaluated as a constant of integration as standard entropy at 298K is known.

From thermodynamics it is also known that:

$$\Delta G_i^\bullet = H_i^\bullet - T \Delta S_i^\bullet \quad (3.10)$$

Where, subscript i denotes the i^{th} species.

For getting the Gibb's energy for a particular reaction ΔG_i^\bullet is multiplied by its stoichiometric coefficient and summed together.

$$\Delta G_{rj}^\bullet = \sum_i \nu_{ij} \Delta G_i^\bullet \quad (3.11)$$

Where, subscript r_j denotes the j^{th} reaction and ν_{ij} denotes the stoichiometric coefficient of species i in reaction j .

Using all the above equations and NIST data for Shomate equation and solving sequentially using MATLAB R2010b we obtain the plots of Standard Gibb's free Energy as a function of temperature for all the four reactions (see Figure 3.7 to Figure 3.10).

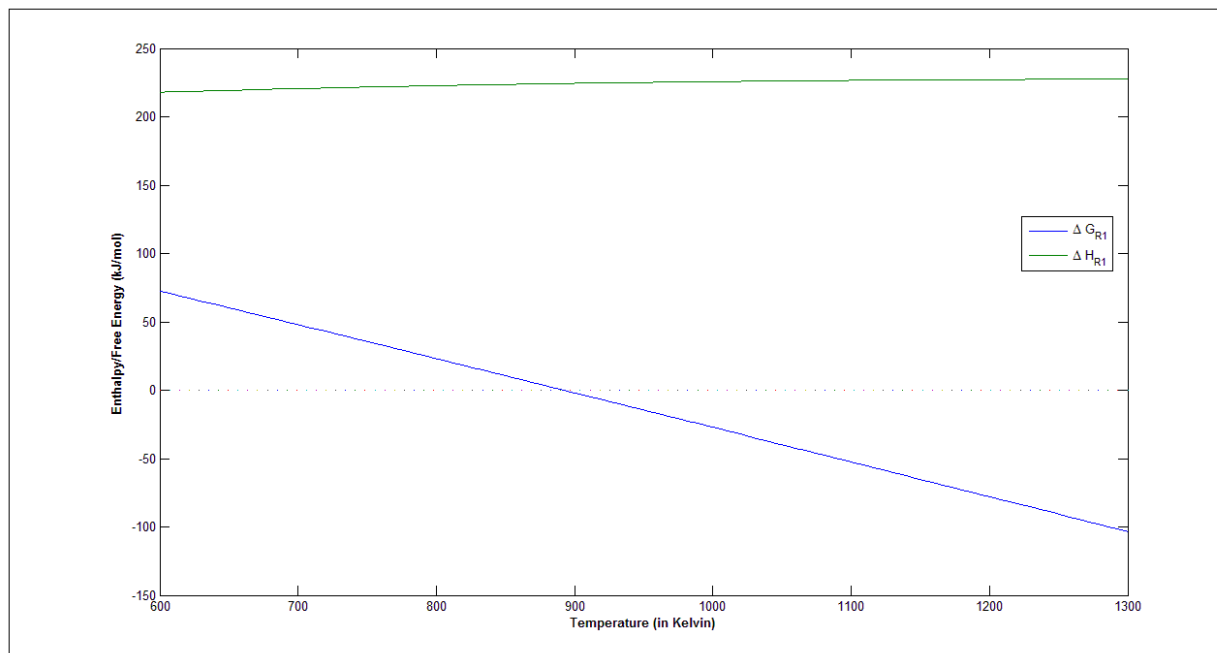


Figure 3.7: Enthalpy and Gibbs Free energy variation for R1

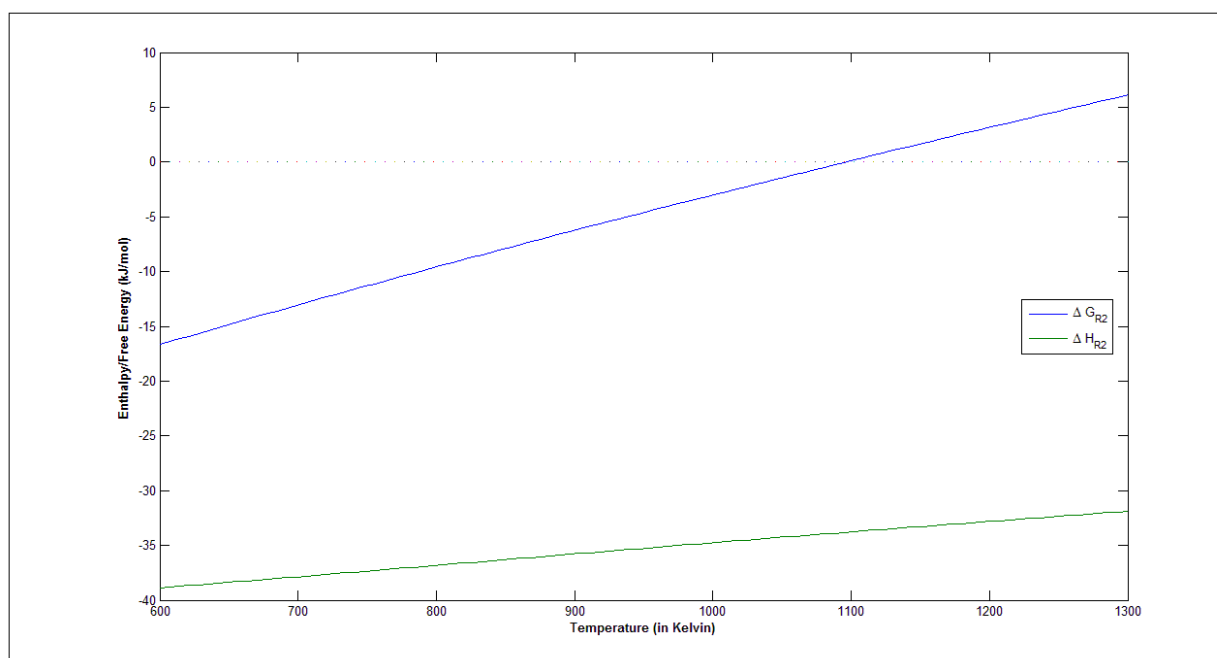


Figure 3.8: Enthalpy and Gibbs Free energy variation for R2

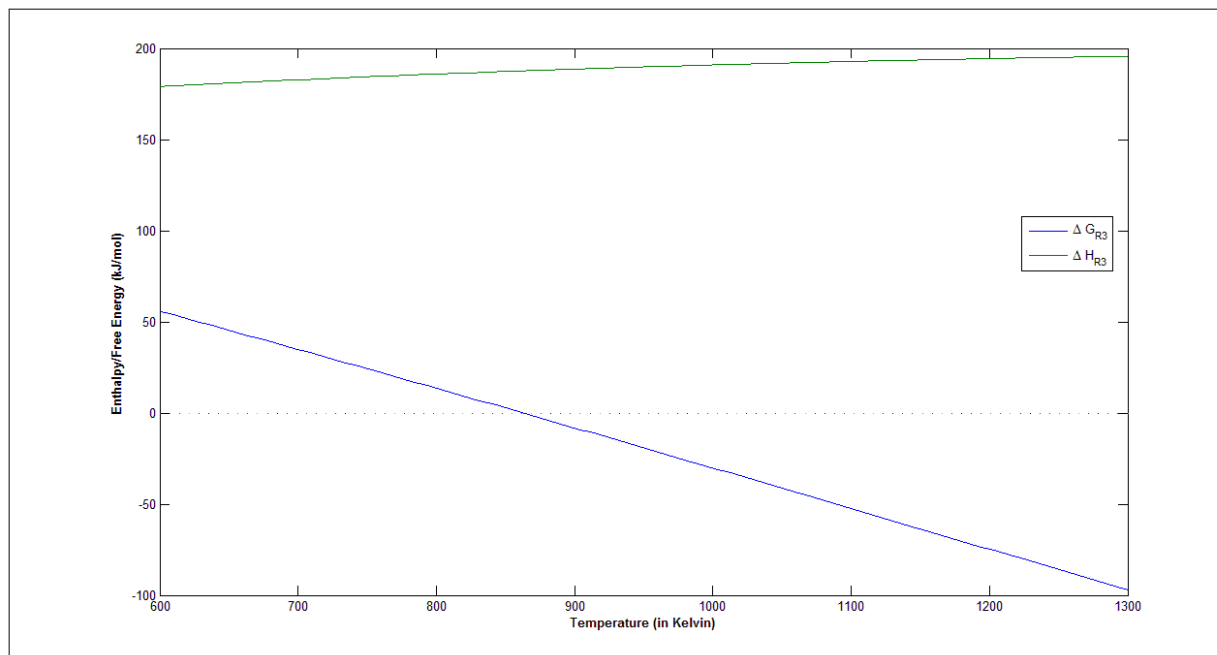


Figure 3.9: Enthalpy and Gibb's Free energy variation for R3

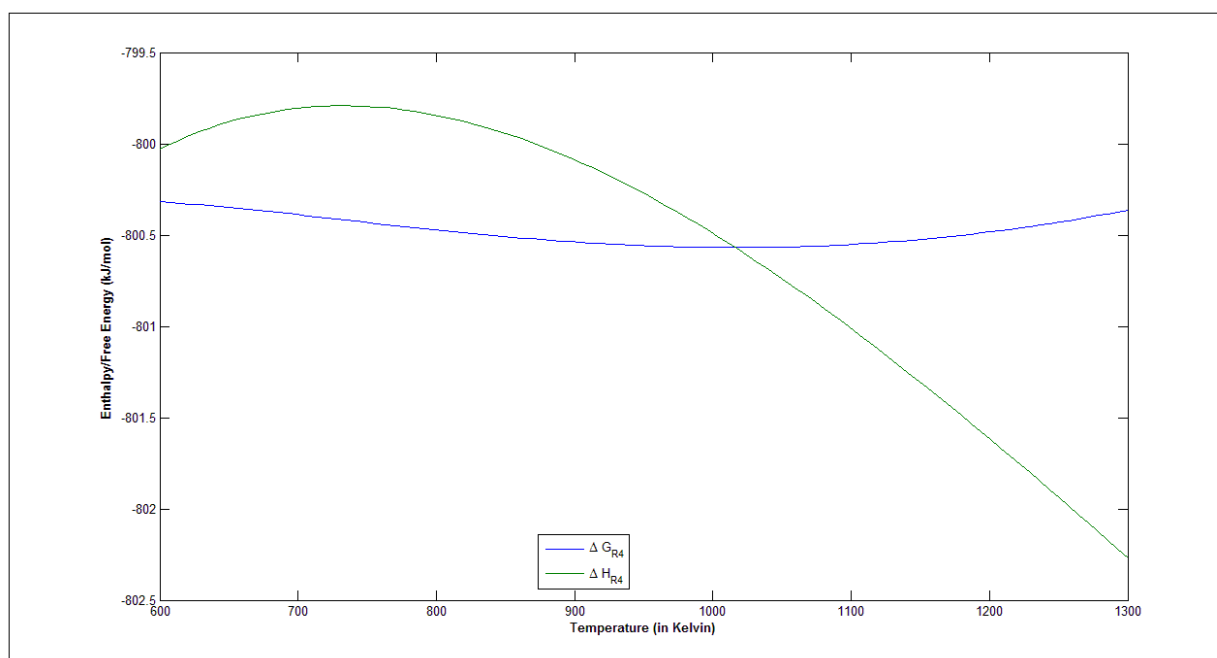


Figure 3.10: Enthalpy and Gibb's Free energy variation for R4

From these plots we can find the temperature range for the feasibility of each reaction.

Table 3.6: Feasible temperature range for the involved reactions

Reaction No.	Reaction Name	Temperature Range of feasibility
R1	Partial Steam Reforming	$T > 900\text{K}$
R2	Water Gas Shift	$T < 1100\text{K}$
R3	Total Steam Reforming	$T > 860\text{K}$
R4	Methane Oxidation	All T from 700-1200K

Thus the common range from the above table is determined to be **$T = 900\text{-}1100\text{K}$** where all the four reactions are feasible and their respective $\Delta G_{\text{rxn}}^{\circ} < 0$.

The results obtained from plots for R1, R2 and R3 are matched with Katiyar et al. [41] to verify the correctness of the procedure. These authors had obtained a feasible temperature range of 894- 1080 K using a slightly different procedure to determine K values. They relied on the Van't Hoff relation and had a different Cp equation for the components. The results are a very close match and hence the correctness of the result is verified.

From the values of Gibb's free energy the equilibrium constants are determined and plotted. ΔG° relates to equilibrium constant as:

$$\Delta G^{\circ} = -RT \ln K \quad (3.12)$$

Where, R is the Universal Gas Constant (with a value of $8.314 \text{ J mol}^{-1} \text{ K}^{-1}$)

The equilibrium constants are plotted with temperature and we can use these values in this work wherever necessary (see Figure 3.11, 3.12 and 3.13). The high equilibrium constant values for R4 meant that it should not be treated as a reversible chemical change and should be considered as an irreversible reaction.

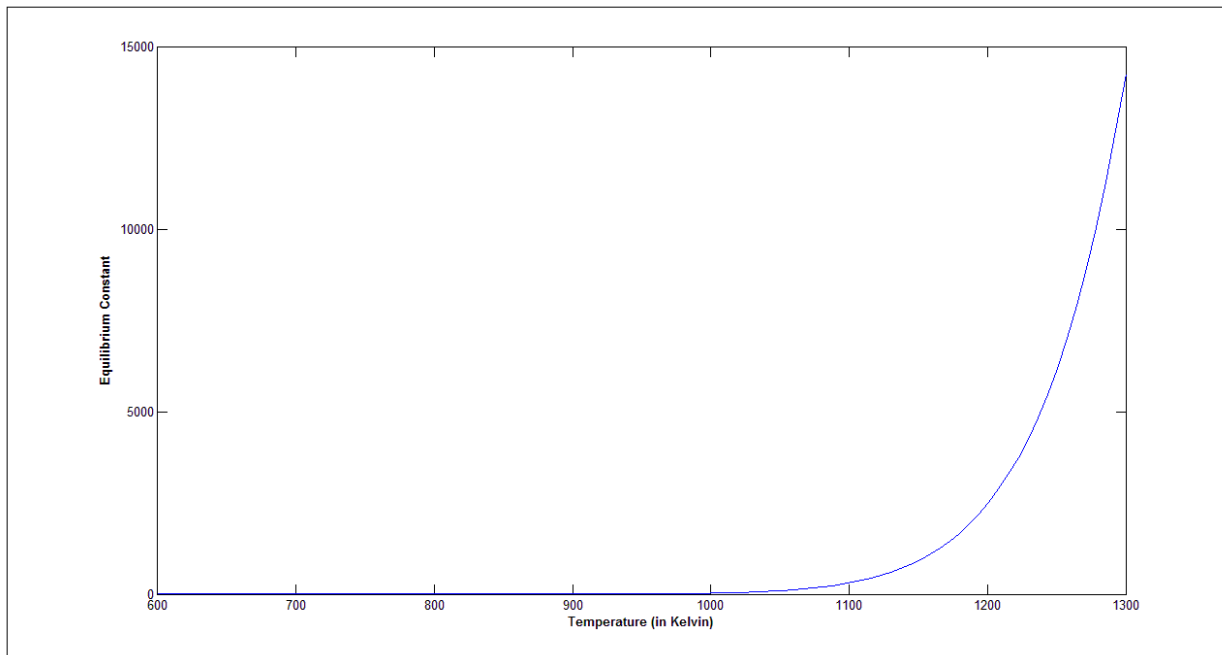


Figure 3.11: Equilibrium constant as a function of temperature for R1

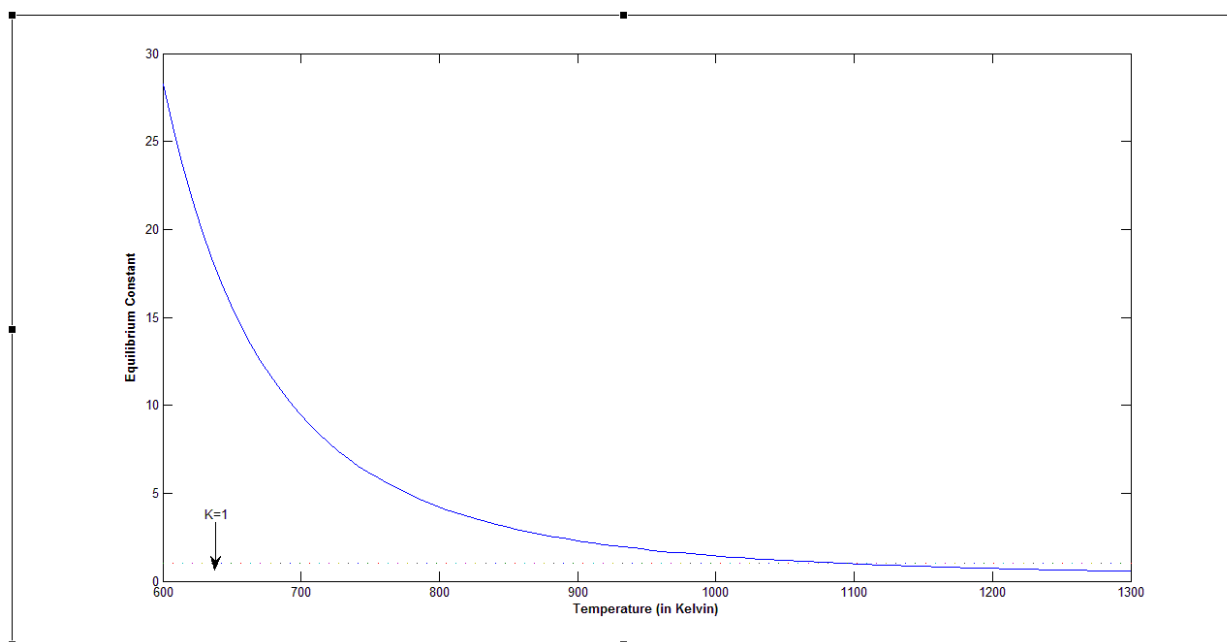


Figure 3.12; Equilibrium constant as a function of temperature for R2

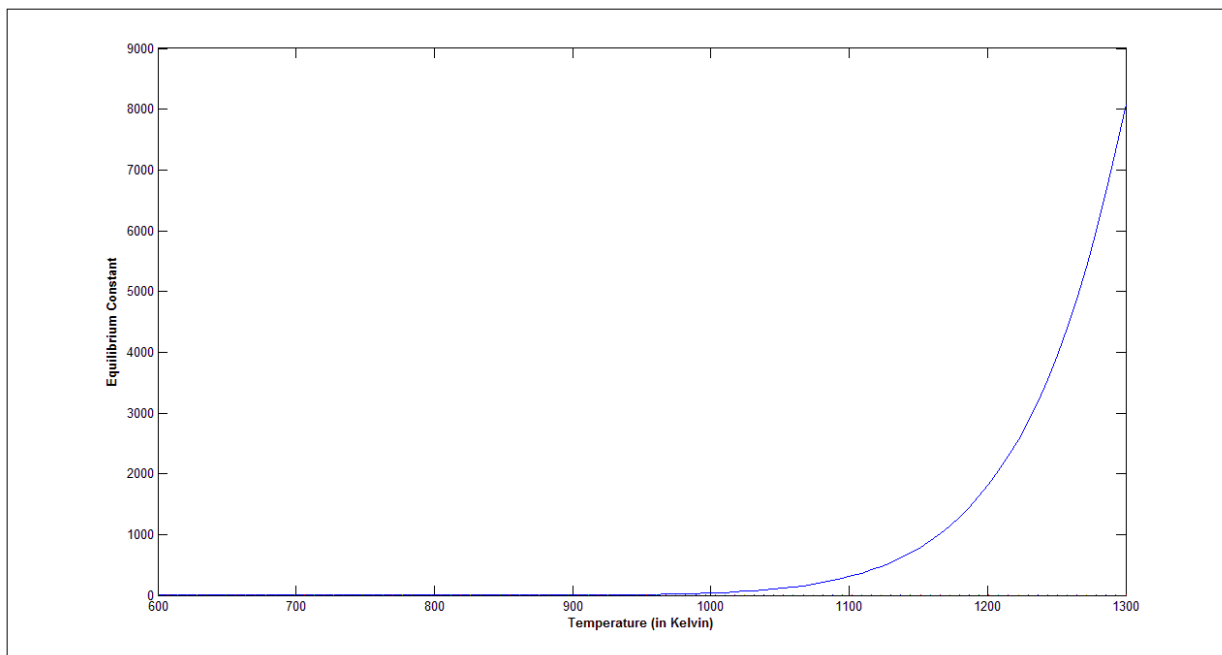


Figure 3.13: Equilibrium constant as a function of temperature for R3

3.3 GIBB'S ENERGY MINIMIZATION

Gibb's Energy Minimization is a technique used to compute equilibrium compositions of a reacting mixture [4]. Its theoretical base lies in the fact that in a reacting system which has attained equilibrium, the total Gibbs free energy will be at a minimum. The thermodynamic equilibrium condition for reactive multicomponent closed system, at constant Pressure and Temperature, with given initial composition, can be obtained by the minimization of Gibbs energy (G) of the system, with respect to the number of moles of each component in each phase [18,19]. Assuming that the gas phase is an ideal gas, the total Gibbs function for the system is given as sum of i^{th} species as:

$$G^t = \sum_{i=1}^N n_i \bar{G}_i = \sum_{i=1}^N n_i \mu_i = \sum_{i=1}^N n_i G_i^o + RT \sum_{i=1}^N n_i \ln \frac{\hat{f}_i}{f_i^o} \quad (3.13)$$

Where G^t is the total Gibbs free energy, \bar{G}_i is the partial molar Gibbs free energy of species i , G_i^o is the standard Gibbs free energy, μ_i is the chemical potential, R is the molar gas constant, T is the temperature of system, \hat{f}_i is the fugacity in system, f_i^o is the standard-state fugacity, and n_i is the mole of species i . For reaction equilibrium in gas-phase, $\hat{f}_i = y_i \hat{\phi}_i P$ and $f_i^o = P^o$, where $\hat{\phi}_i$ is the fugacity coefficient, y_i is the gaseous mole fraction of species i .

Hence,

$$G^t = \sum_{i=1}^N n_i (\Delta G_{fi}^o + RT \ln \frac{y_i \hat{\phi}_i P}{P^o}) \quad (3.14)$$

Where, ΔG_{fi}^o is the Gibbs free energy of formation at temperature T.

This is the objective function that needs to be minimized. For this minimization an inbuilt function of MATLAB R2010b *fmincon* is called and utilized. This library function is applicable for constrained minimization problems. This function attempts to find a constrained minimum of a scalar function of several variables starting at an initial estimate. This is generally referred to as constrained optimization.

The species that are considered for the study are the six species involved in the four reactions R1, R2, R3, and R4 namely carbon dioxide, water, hydrogen, carbon monoxide, methane and oxygen. For the analysis of coke production and deposition at equilibrium, seventh

specie in the form of carbon in its graphite form is included in the analysis. As for the earlier data, once more NIST data are used for carbon considering it to be in graphite form.

The constraint equation in this case is the conservation of mass of elements involved in the reaction. Writing a material balance on the number of moles of the elements involved, i.e. Carbon, Hydrogen and Oxygen in this case yields us equation (3.15) which ties the inlet number of moles of carbon, oxygen and hydrogen to the moles of these elements at any point. This constraint along with the minimization of objective function gives us the moles of each species at a point when the Gibbs free energy has been minimized, or to put simply, at equilibrium.

$$A_{eq}x = b_{eq} \quad (3.15)$$

Where, A_{eq} is the matrix of number of atoms of the k^{th} element present in each molecule of chemical species i (3 elements(C, H, O) \times 7 species); x is the number of moles of each species; b_{eq} is the inlet number of moles of each element, C,H and O.

The equation (3.15) is basically a material balance which ties the inlet number of moles of carbon, oxygen and hydrogen to the moles of these elements at equilibrium. x is subjected to a lower bound so that no mole fraction can be negative, i.e. minimum value is 0, which is a physical constraint on the system.

The motivation behind this is to find out thermodynamically, the optimum conditions at which the reactor should be operated. The operating parameters that need to be ascertained are temperature, oxygen-to-methane ratio and steam-to-methane ratio. The proposed strategy here is to vary one out of these parameters and keeping the other values constant. The effect of changing these parameters on methane conversion, hydrogen yield and hydrogen-to-carbon monoxide ratio is evaluated and the operating conditions are chosen on the same basis. The results of this analysis are reported in the fifth chapter of this thesis as they are quite detailed and require a separate chapter.

CHAPTER 4

MODEL DEVELOPMENT

The mathematical model development for the reactor in which these reactions are occurring has been considered in this chapter. The reactor is a fixed bed reactor with a catalyst bed of Ni based alumina catalyst. The kinetics available for this type of catalyst is easiest and has been widely studied. The model is validated on the basis of published data.

4.1 KINETICS

A lot of study has gone into the Ni based catalysts for reforming of methane along with oxygen [42,43]. Dissanayake et al. studied the state of the Ni/Al₂O₃ catalyst and found that their experimental bed had different regions out of which complete oxidation of methane occurred over the second region where NiO+Al₂O₃ were found. As a result of complete consumption of oxygen, the next stage of the bed comprised of Ni/Al₂O₃ phase. Here the reforming reaction of methane corresponding to thermodynamic equilibrium at bed temperature occurs.

Xu and Froment [23] studied the water gas shift reaction and the methane reforming reactions (both partial and total reforming) on a Ni/MgAl₂O₄ catalyst used with α -alumina diluent. Based on the rate determining steps of Reaction No. 1, 2 and 3, Xu and Froment formulated a Langmuir type rate expression for the three reactions as given below:

$$r_1 = \frac{\frac{k_1}{P_{H_2}^{2.5}} (P_{CH_4} P_{H_2O} - \frac{P_{H_2}^3 P_{CO}}{Keq1})}{Den^2} \quad (4.1)$$

$$r_2 = \frac{\frac{k_2}{P_{H_2}} (P_{CO} P_{H_2O} - \frac{P_{H_2} P_{CO_2}}{Keq2})}{Den^2} \quad (4.2)$$

$$r_3 = \frac{\frac{k_3}{P_{H_2}^{3.5}} (P_{CH_4} P_{H_2O}^2 - \frac{P_{H_2}^4 P_{CO_2}}{Keq3})}{Den^2} \quad (4.3)$$

Where,

$$Den = 1 + K_{CO} P_{CO} + K_{H_2} P_{H_2} + K_{CH_4} P_{CH_4} + \frac{K_{H_2O} P_{H_2O}}{P_{H_2}} \quad (4.4)$$

P_i = Partial pressure of i^{th} component

The denominator in all the three rate expressions is the same because Xu and Froment assumed that all three reactions take place on the same active sites. The kinetics proposed by Xu and Froment for methane steam reforming on Ni catalyst are well established and have been widely reported and used by many researchers[27,44,45].

The methane combustion reaction has been studied on catalysts with a noble metal base viz. Pd, Pt etc. Most notable work on methane combustion kinetics and mechanism is by Trimm and Lam [31] who considered the Pt-alumina fiber catalyst for studying the reaction. They proposed a Langmuir Hinshelwood type of model, given as follows:

$$r_4 = \frac{k_{41} M_{CH_4} M_{O_2}}{(1 + K_{CH_4}^o M_{CH_4} + K_{O_2}^o M_{O_2})^2} + \frac{k_{42} M_{CH_4} M_{O_2}^{1/2}}{(1 + K_{CH_4}^o M_{CH_4} + K_{O_2}^o M_{O_2})} \quad (4.5)$$

Where, M_i is the molar percentage of species i .

This rate expression was applicable in higher temperature range of 813K with a standard deviation of 3.3% from the experimental data. De Smet et al. [22] have modified the Trimm and Lam kinetics for Ni catalyst for use at a very high pressure. However, the kinetic parameters utilized here are the ones proposed by Trimm and Lam and this kinetic expression has been utilized by a number of researchers including Ji et.al [25], De Groote and Froment [20], Rakib et al. [46] among a few.

Table 4.1: Arrhenius Parameter and Activation Energies^[23,25]

Reaction No.	A(k _j)(mol kg _{cat} ⁻¹ s ⁻¹)	E _j (J mol ⁻¹)
1.	1.17×10 ¹⁵ bar ^{0.5}	240100
2.	5.54×10 ⁵ bar ⁻¹	67130
3.	2.83×10 ¹⁴ bar ^{0.5}	243900
4.	A(k ₄₁) = 3.14×10 ⁻⁴ A(k ₄₂) = 2.64×10 ⁻⁴	- -

Where $k_j = A_j \times \exp(-E_j / RT)$ (4.6)

Table 4.2: Van't Hoff adsorption parameters and heats of adsorption for components^[23,25]

Species	A _{di}	ΔH _{di} (J mol ⁻¹)
CH ₄ (combustion)($K^{o_{CH_4}}$)	6.67×10 ⁻²	-
O ₂ (combustion) ($K^{o_{O_2}}$)	4.34×10 ⁻⁵	-
CH ₄ (K_{CH_4})	6.65×10 ⁻⁴ bar ⁻¹	-38280
CO (K_{CO})	8.23×10 ⁻⁵ bar ⁻¹	-70650
CO ₂ (K_{CO_2})	6.12×10 ⁻⁹ bar ⁻¹	-82900
H ₂ O (K_{H_2O})	1.77×10 ⁵	88680

Where $K_i = A_{di} \times \exp(-\Delta H_{di} / RT)$ (4.7)

4.2 REACTOR MODEL

The reactor considered is a tubular reactor with constant cross sectional area and is packed with Ni catalyst supported on Mg-Al₂O₃ catalyst. The walls of the reactor are covered with insulation layer. The pure oxygen stream is mixed along with feed and steam and preheated to the desired temperature and fed into the reactor.

In order to develop a one dimensional steady state mathematical model for the reactor, component material and energy balances are written. Following postulates are assumed for this model development:

- No pressure drop in the reactor (Isobaric operation)
- No heat loss to the surroundings from the reactor (Adiabatic)
- No concentration change in the radial direction
- No temperature change in the radial direction
- No catalyst deactivation considered/No coke formation reactions

- No external mass transfer resistance of catalyst particles
- No non-ideality in flow regime



Figure 4.1: Reactor diagram

With the above assumptions mentioned a balance on an infinitesimally volume of reactor yields the following equations:

$$\frac{dF_i}{dZ} = A_c \rho_b (1 - \varepsilon_b) \sum_{j=1}^4 \nu_j r_j \quad (4.8)$$

$$\frac{dT}{dZ} = \frac{A_c \rho_b (1 - \varepsilon_b) \sum_{j=1}^4 (-\Delta H_{rj} \nu_j r_j)}{\sum_{i=1}^6 F_i C_{p_i}} \quad (4.9)$$

Where,

i = Species, CH₄, CO₂, CO, H₂, O₂, H₂O and j = Reaction number, 1-4

$A_c = \pi R^2$, where R is radius of tube

ν_{ij} = Stoichiometric coefficient of i^{th} species in reaction j

ΔH_{rj} = Enthalpy of reaction j at temperature T

F_i = Flow rate of i^{th} species

Cp_i = Heat capacity of i^{th} species

4.3 MODEL VALIDATION

The mathematical model as formulated above has been validated on the basis of outlet temperature, outlet hydrogen-carbon monoxide ratio, and outlet mole fractions of species that were in the product side of any of the reactions, viz. CO_2 , CO , H_2 and H_2O . The industrial data used by De Groote and Froment [20] has been used to validate the model. The authors carried out the autothermal reforming of natural gas on Ni based catalyst. The input feed consists of natural gas (methane), oxygen and steam.

However the authors postulated that a very small quantity of hydrogen is present in natural gas feedstock available at industrial scale. This assumption/postulate is important because at zero partial pressure of H_2 the rate of reactions by Xu Froment kinetics tends to be extremely large. For the purpose of this simulation I have taken H_2 flow rate at inlet is taken to be 10^{-8} mol/s to avoid infinite reaction rates at inlet to the reactor.

Table 4.3: Input conditions of industrial reactor ^[20]

Input parameter	Value	Unit
Methane flow rate	3483	Nm^3/h
O_2/CH_4	0.598	-
$\text{H}_2\text{O}/\text{CH}_4$	1.4	-
Pressure	25	Bar
Inlet Temperature	808	Kelvin
Diameter of reactor	1.2	Meter
Catalyst density	Not mentioned	-
Porosity of bed, ε_b	Not mentioned	-

The values of catalyst density and porosity of bed are unavailable for the industrial reactor. For this the values of density and porosity for a typically used Ni-bed ($=2100 \text{ kg/m}^3$ and 0.43, respectively) as given in literature are used [22,27].

The model equations form an Initial Value Differential Equation Problem, and can be solved using an inbuilt Ordinary Differential Equation (ODE) solver in MATLAB R2010b which utilizes the Runge-Kutta numerical methods for solving. All the IVP conditions were input. All the reaction rates were multiplied by an effectiveness factor. The effect of intra-particle diffusion

is described by using these effectiveness factors. Literature shows that effectiveness factors are actually a function of temperature, and hence they vary along the length of the reactor and thus influence the rates of reaction in a dynamic fashion along the reactor [47]. However to evaluate the functional dependence of effectiveness factor on temperature is a handful procedure in itself. Thus for the sake of simplification an average value was used for the four effectiveness factors for the four reactions. The four values of effectiveness factors used by De Groote and Froment were 0.07, 0.06, 0.7 and 0.05 for R1, R2, R3 and R4 respectively (as in Table 3.5).

Table 4.4: Comparison between model predictions with industrial data

Parameter/Species	Unit	Industrial Data [20]	Validation Run(Model)	Relative Error
Outlet Temperature	Kelvin	1223	1310.7	7.17%
Outlet H ₂ /CO	-	2.854	2.728	4.42%
Outlet <i>x</i> fraction				
CO	-	0.160	0.1702	6.38%
H ₂ O	-	0.306	0.3057	1%
H ₂	-	0.456	0.46417	1.8%

Thus, a close agreement between the two can be seen and hence it points to the applicability of our model. The errors are within acceptable limits.

This chapter contains the results of thermodynamic analysis conducted considering seven species including carbon deposition involved in oxidative reforming of methane and the results of simulation of the mathematical model developed in the previous chapter. The simulation conditions are based on the analysis of the results obtained in Chapter 3. The obtained results are also analyzed.

5.1 RESULTS OF THERMODYNAMIC ANALYSIS

The thermodynamic evaluation is carried out keeping in mind the parameters that will be required for operation. The key input variables that could be varied during the Gibb's energy minimization technique to determine mole fractions of different components at equilibrium are temperature, pressure, oxygen-to-methane ratio and steam-to-methane ratio. The parameters that are evaluated by this analysis and that are dependent on the values considered for these input variables are taken to be the conversion of methane, hydrogen to carbon monoxide ratio, (which is an important parameter for determining syngas quality), hydrogen moles being produced and the moles of coke generated at equilibrium. The strategy chalked out is to determine the best possible values of the input variables from a selected range using the results of thermodynamic analysis by studying the impact of these input variables on the agreed upon output parameters.

Table 5.1: Input variables and their possible ranges

Input variable	Range of possible values
Temperature	600-1300K
Pressure	1-25 bar
Oxygen-to-methane ratio	0.2-1.0
Steam-to-methane ratio	0-10

The range for these input variables is decided on a number of factors. In the following discussion we shall analyze how the values for different variables were reached upon. The basic approach is to study the effect of changing input values to be able to see a change in the output values.

5.1.1 Temperature Range

The temperature range is decided on the basis of the conversion. It is quite evident that at a higher temperature the conversion increases. It can be seen that at temperatures above the range of 900 K -1000 K the conversion for higher steam-to-methane ratios reaches to values exceeding 99% (See Figures 5.4, 5.8, 5.12, 5.16 and 5.20). It is important to note that these are theoretical values for equilibrium conversions and independent of reaction kinetics. At a higher temperature value, the coke yield is also reduced for every value of oxygen-to-methane ratio and steam-to-methane ratio (See Figures 5.1, 5.5, 5.9, 5.13 and 5.17). Thermodynamically, it can be generalized that a higher temperature is aiding the overall conversion process and minimizing the production of coke. This is also strengthening the initial analysis on the temperature feasibility range which found the reactions R1, R2, R3 and R4 to be proceeding in the forward direction (and hence aiding overall methane conversion in the range of 900-1100K). Hence, it has been ascertained that a temperature range of 900-1200K would be suitable for the best performance of the reactor.

5.1.2 Steam-to-Methane Ratio

It can be seen from the conversion at any oxygen content that increasing the steam-to-methane ratio increases the conversion at the same temperature (See Figures 5.4, 5.8, 5.12, 5.16 and 5.20). However, it needs to be pointed out that beyond a certain value of steam content, at higher temperatures that have been selected in the previous section, the conversion is already at its theoretical peaks and the additional steam has no visible effect. Similar is the effect seen in carbon content. At higher values of steam to methane ratio, the coke formation are reduced considerably (See Figures 5.1, 5.5, 5.9, 5.13 and 5.17). Thus from these two effects alone, it would seem that a higher steam content is beneficial to us. When the factor of hydrogen to carbon monoxide ratio is brought into the picture it is evident that as a general trend a higher steam ratio leads to higher hydrogen to carbon monoxide ratio, the only visible exception to the trend being keeping the steam supply to zero. (See Figures 5.3, 5.7, 5.11, 5.15 and 5.19) Thus, a higher value of steam-to-methane ratio makes the theoretical hydrogen to carbon monoxide content too high. Based on this a range of 0.5-3 is chosen for steam-to-methane content.

5.1.3 Oxygen-to-Methane Ratio

For determining the optimum oxygen-to-methane ratio we can see from the plots that increasing oxygen content means better conversion, lower coke content and suitable hydrogen-to-carbon monoxide ratios. The plots are for a constant steam to methane ratio with varying oxygen content. The analysis was done on an oxygen ratio of 0.2-1.0 widening the range as determined by the autothermal point in section 3.1. The conversion and coke content at the chosen temperature range, do not amount to a practical difference (See Figures 5.21, 5.22, 5.25, and 5.26). However, when we analyze the hydrogen moles produced there is a visible decline in production of hydrogen with increasing oxygen-to-methane ratio (See Figures 5.23 and 5.24). Based on this analysis an oxygen-methane ratio greater than 0.5 is chosen which also satisfies the region for oxidative reforming.

5.1.4 Pressure Range

The analysis of pressure range is based on literature review and Le Chatelier's principle which dictates the equilibrium extent of any reaction. Freitas et al. [18] showed that the conversion is lowered at higher pressure. Even though the increased pressure also reduces coke formation, at the temperature range that has been selected, the coke formation is low enough to work at a lower pressure. Thus the optimum pressure for better conversion is 1 bar.

Thus, on the basis of the thermodynamic analysis the optimum conditions for the operation of the reactor were determined. The parameters that were optimized were temperature, pressure, oxygen-to-methane ratio and steam-to-methane ratio. This optimization relied on the equilibrium values of methane conversion, carbon generation, hydrogen-carbon monoxide ratio and moles of hydrogen produced. The initial analysis on the temperature feasibility of reactions as well as the determination of autothermal point was crucial as initial pointers. The obtained values of input parameters provide us with values to efficiently simulate the model developed previously.

Table 5.2: Values obtained for input parameters by analysis

Parameter	Value	Unit
Temperature	900-1200	Kelvin
Pressure	1	Bar
Steam: Methane Ratio	0.5-3	-
Oxygen: Methane Ratio	0.5-1.2	-

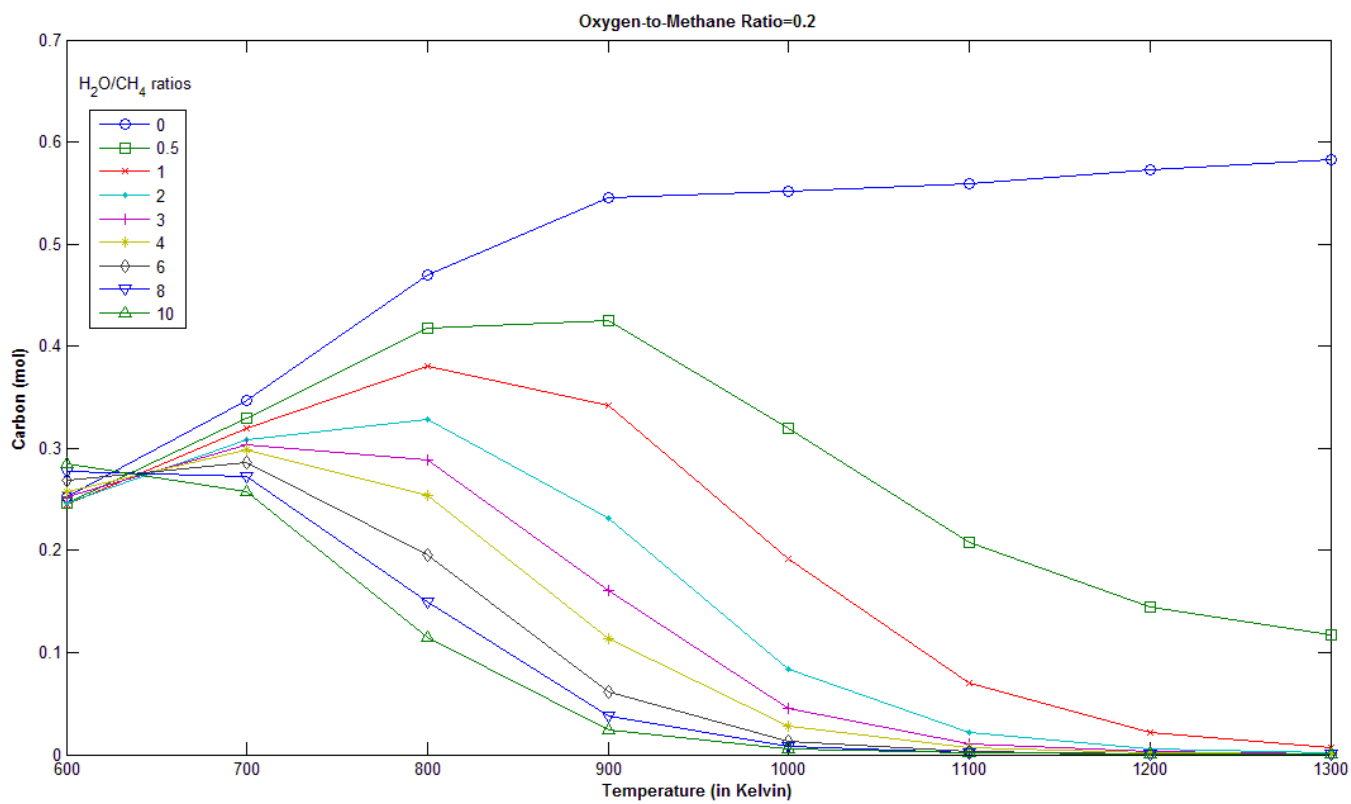


Figure 5.1: Coke formation at different steam/methane ratios with oxygen/methane=0.2

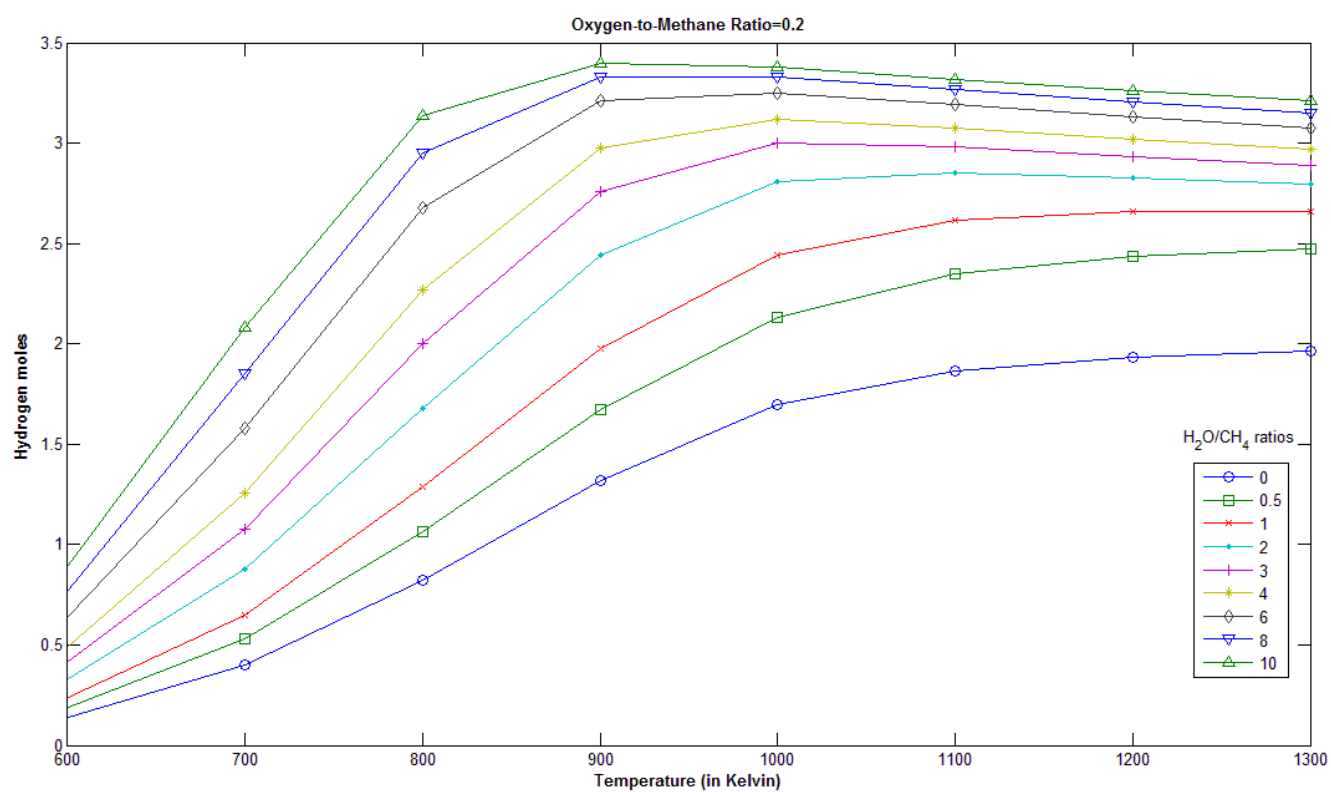


Figure 5.2: Hydrogen moles at different steam/methane ratios with oxygen/methane=0.2

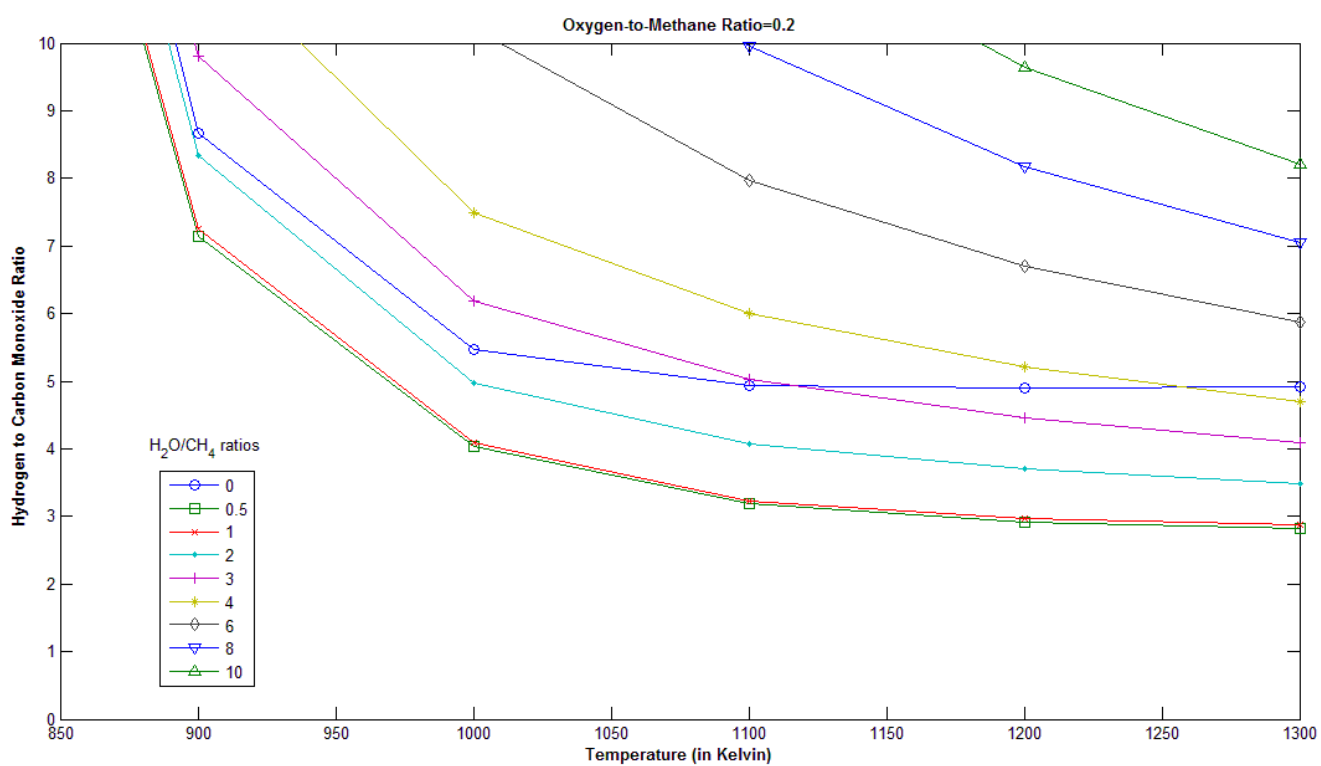


Figure 5.3: Hydrogen/Carbon Monoxide ratio at different steam/methane ratios with oxygen/methane=0.2

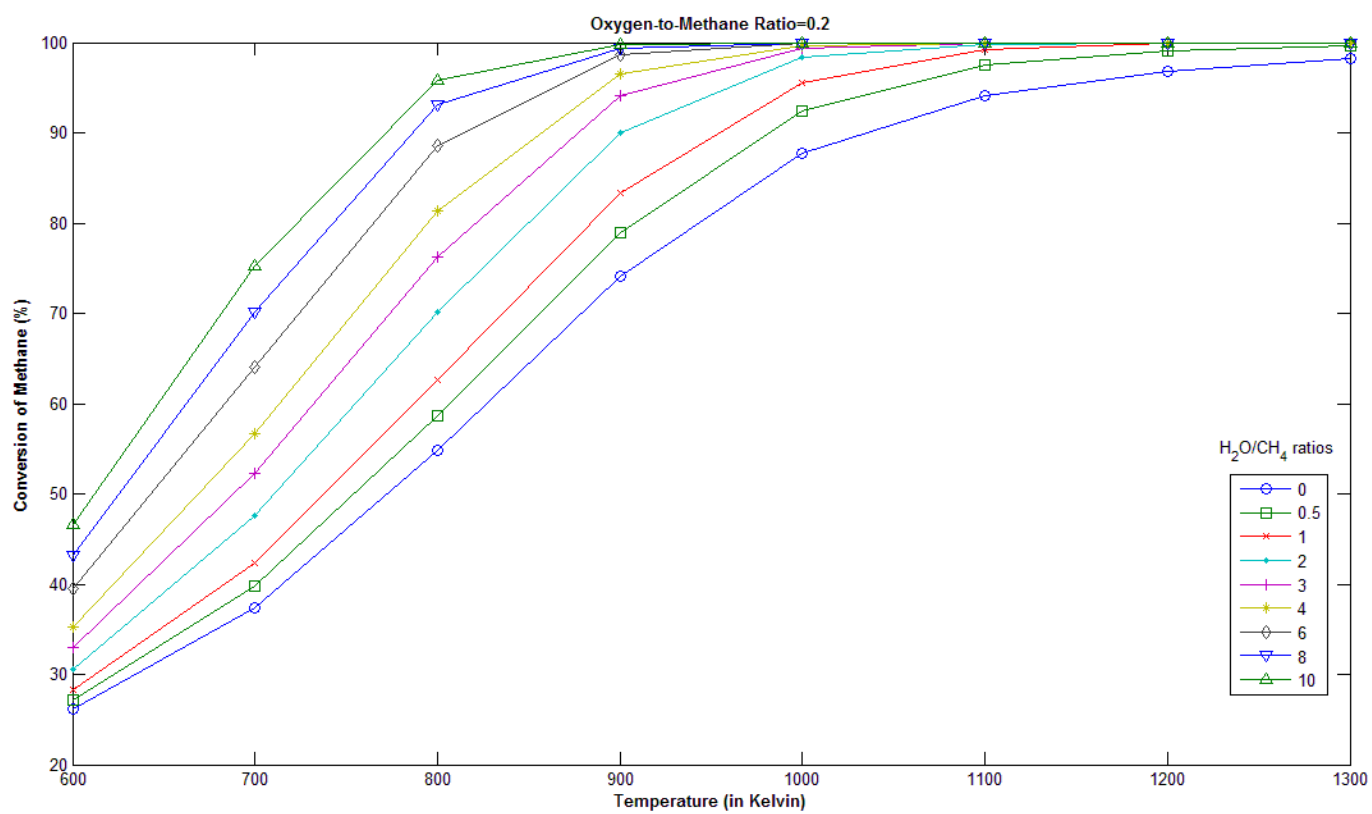


Figure 5.4: Conversion of methane at different steam/methane ratios with oxygen/methane=0.2

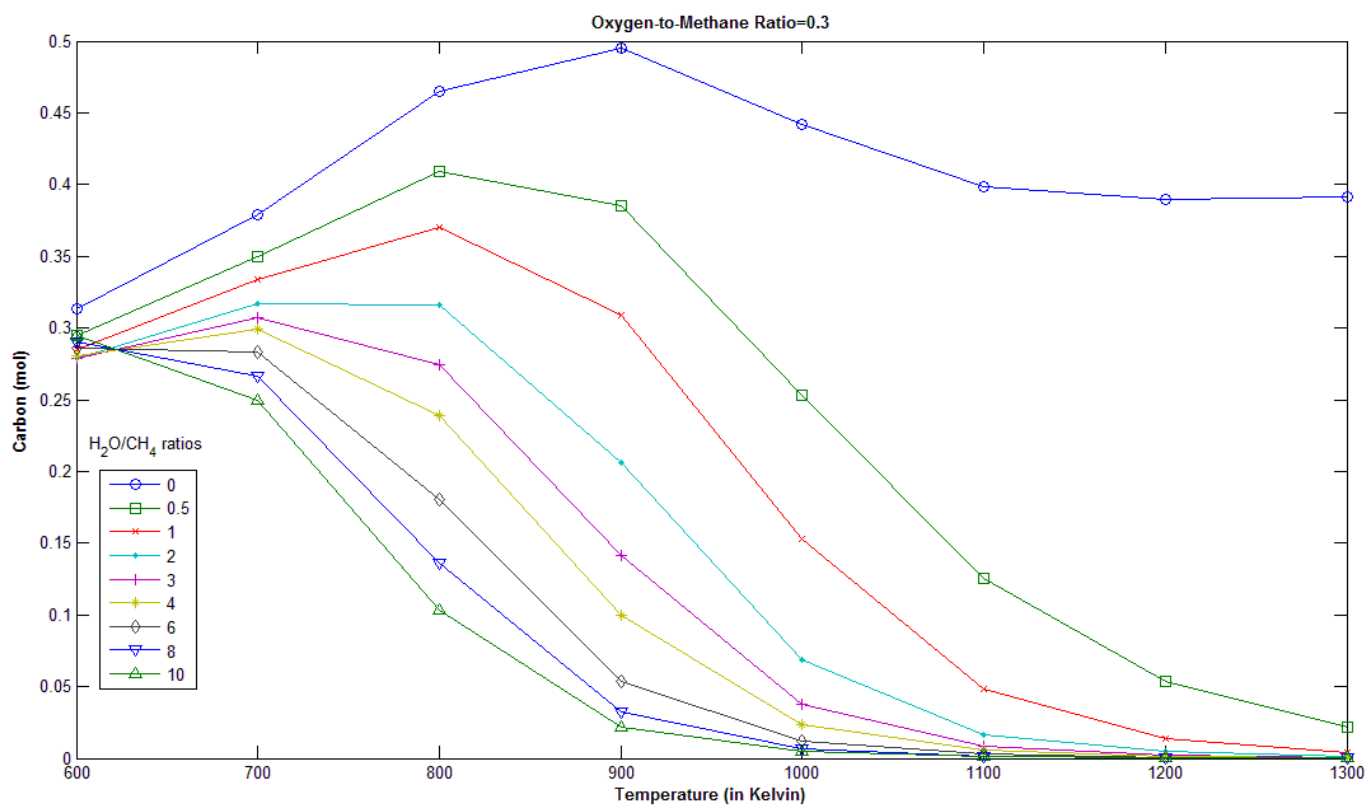


Figure 5.5: Coke formation at different steam/methane ratios with oxygen/methane=0.3

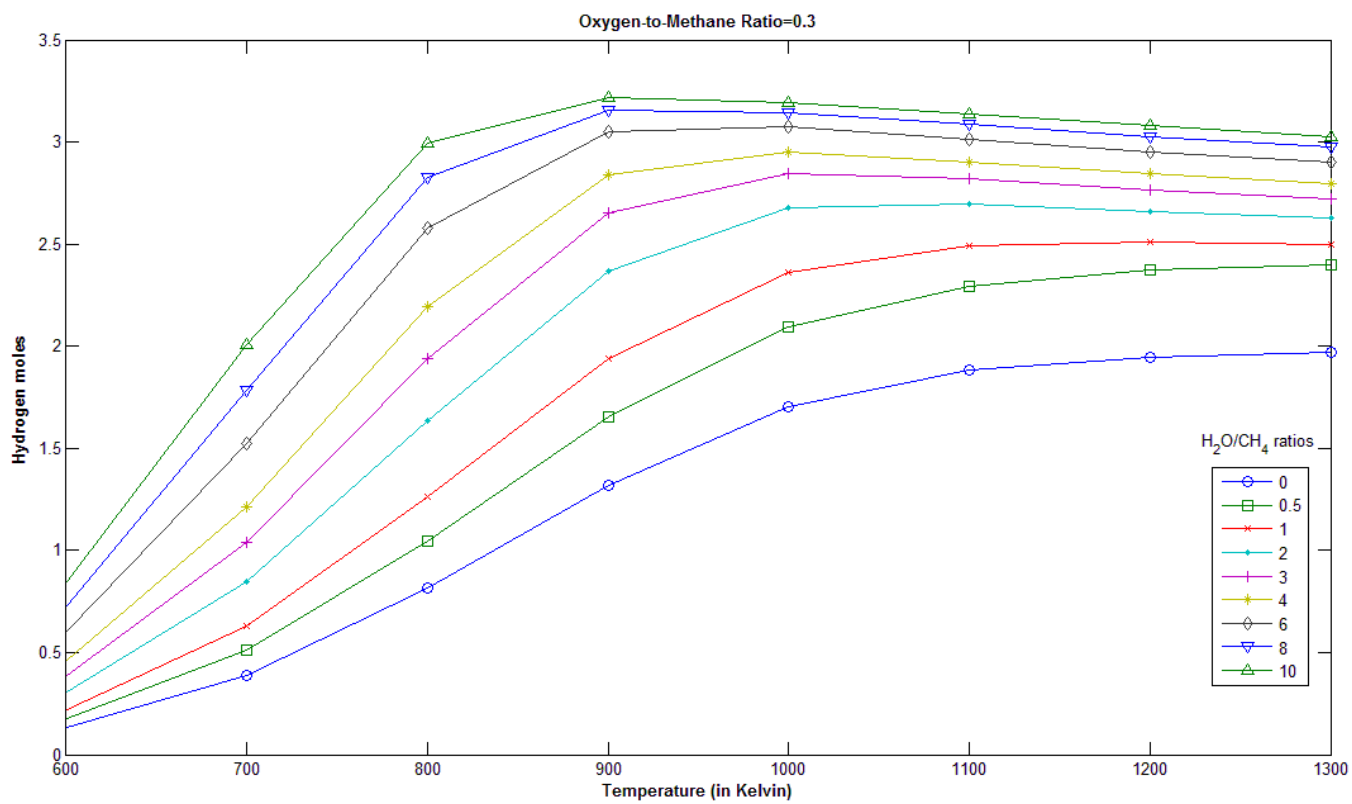


Figure 5.6: Hydrogen moles at different steam/methane ratios with oxygen/methane=0.3

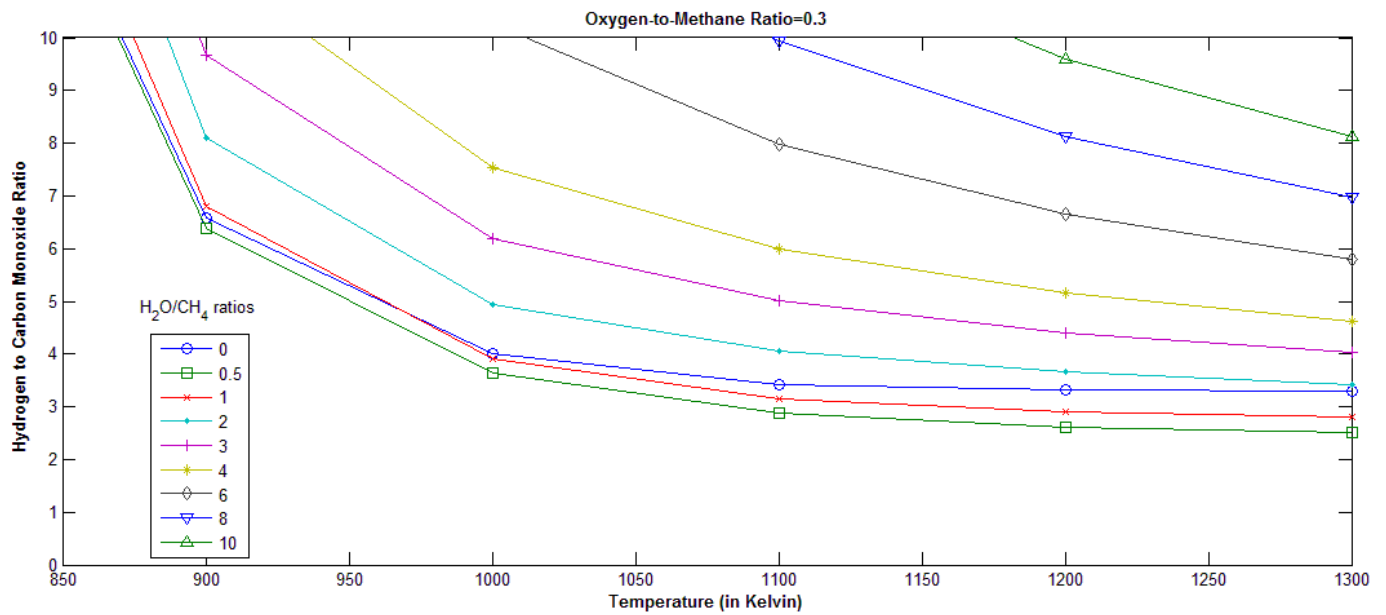


Figure 5.7: Hydrogen/Carbon Monoxide ratio at different steam/methane ratios with oxygen/methane=0.3

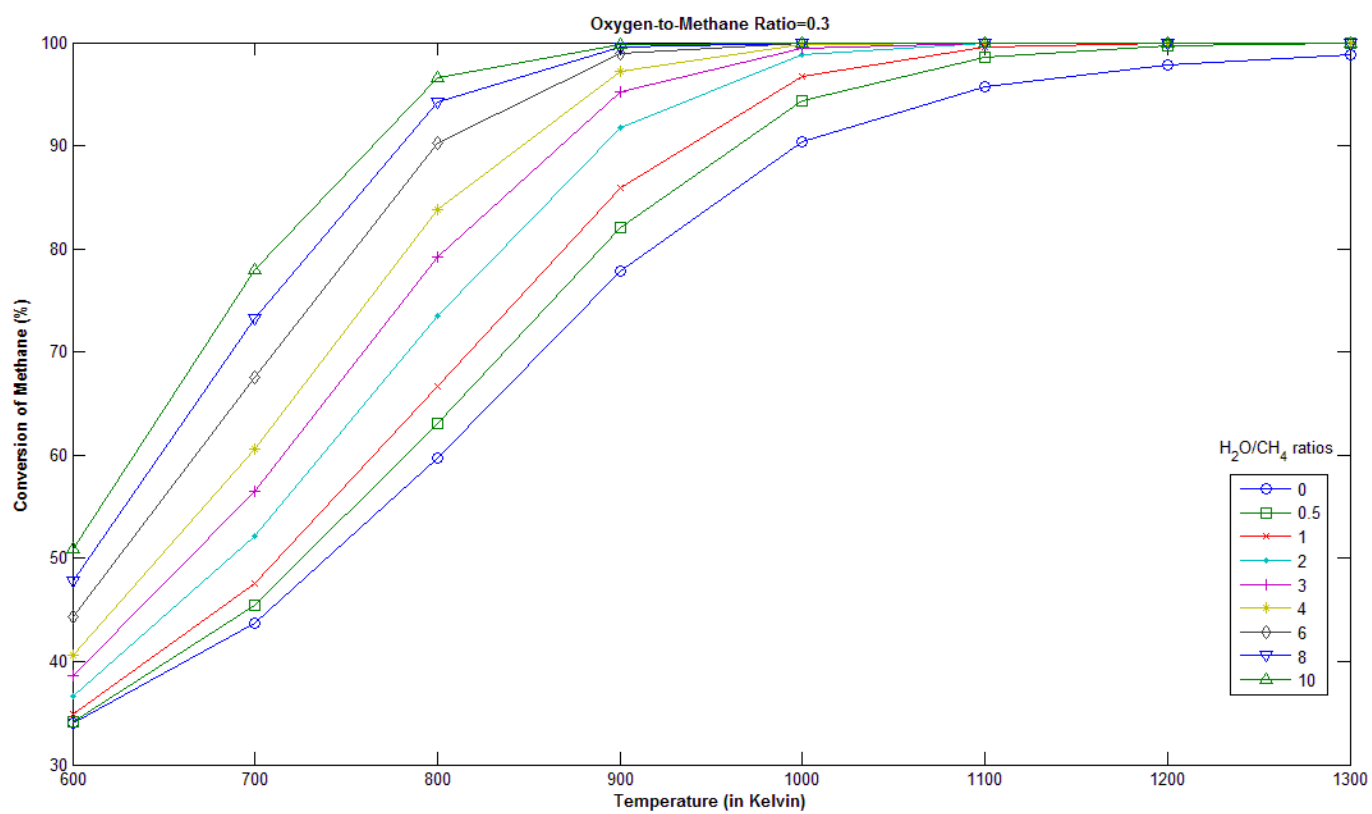


Figure 5.8: Conversion of methane at different steam/methane ratios with oxygen/methane=0.3

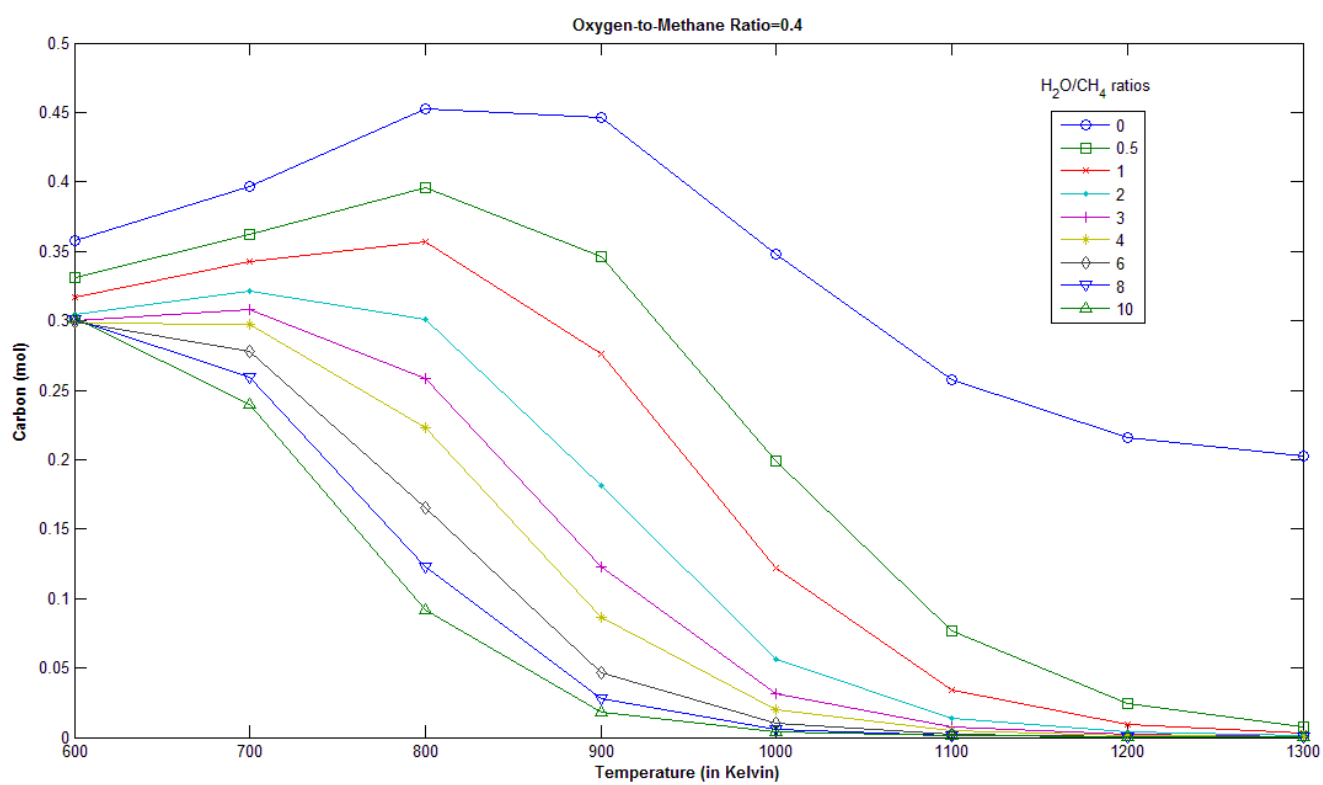


Figure 5.9: Coke formation at different steam/methane ratios with oxygen/methane=0.4

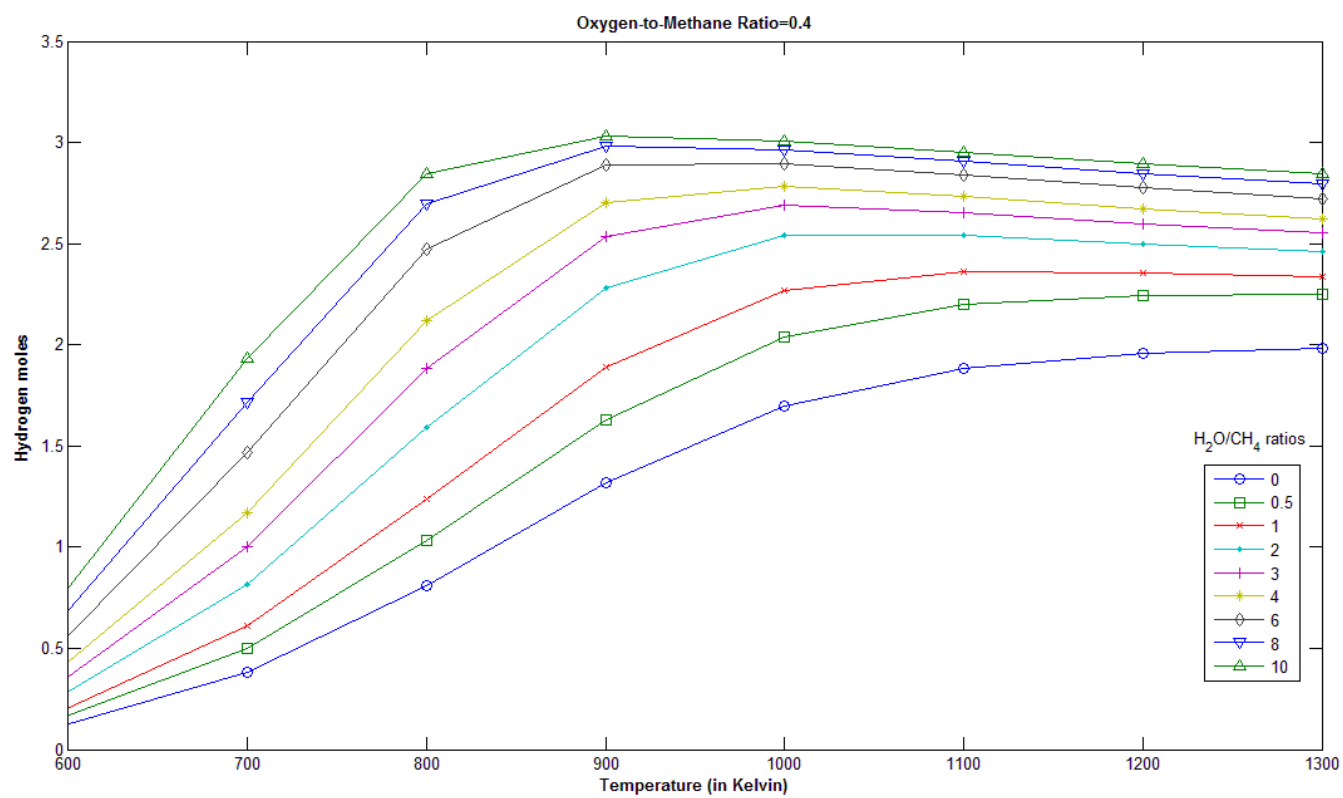


Figure 5.10: Hydrogen moles at different steam/methane ratios with oxygen/methane=0.4

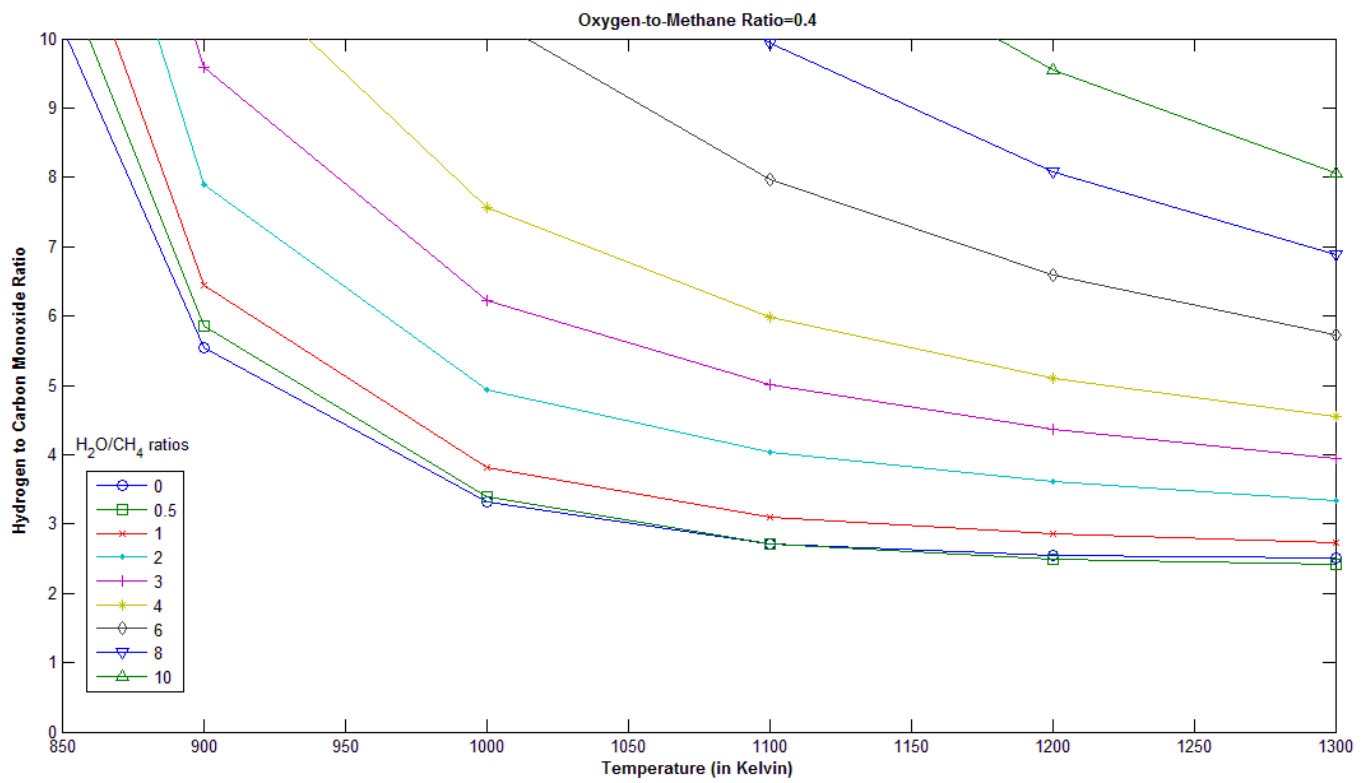


Figure 5.11: Hydrogen/Carbon Monoxide ratio at different steam/methane ratios with oxygen/methane=0.4

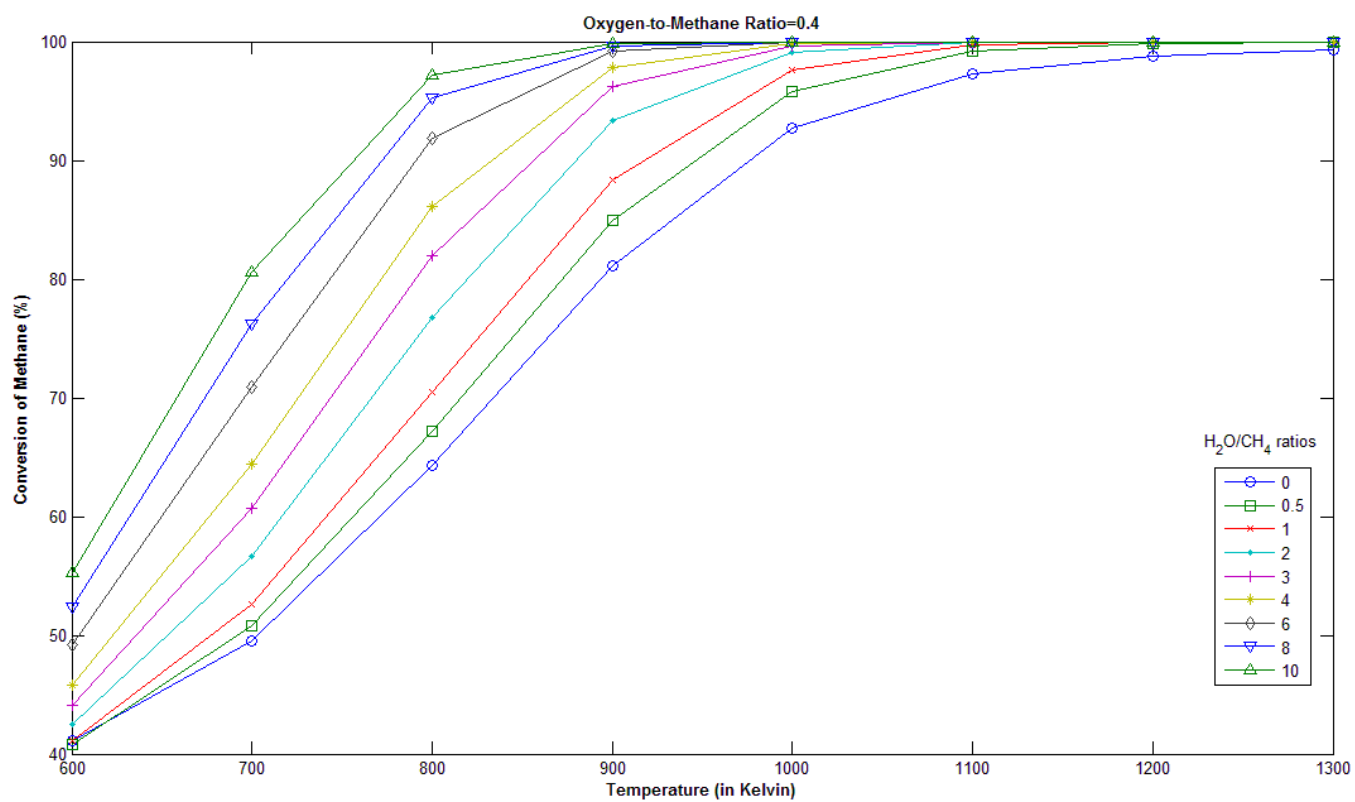


Figure 5.12: Conversion of methane at different steam/methane ratios with oxygen/methane=0.4

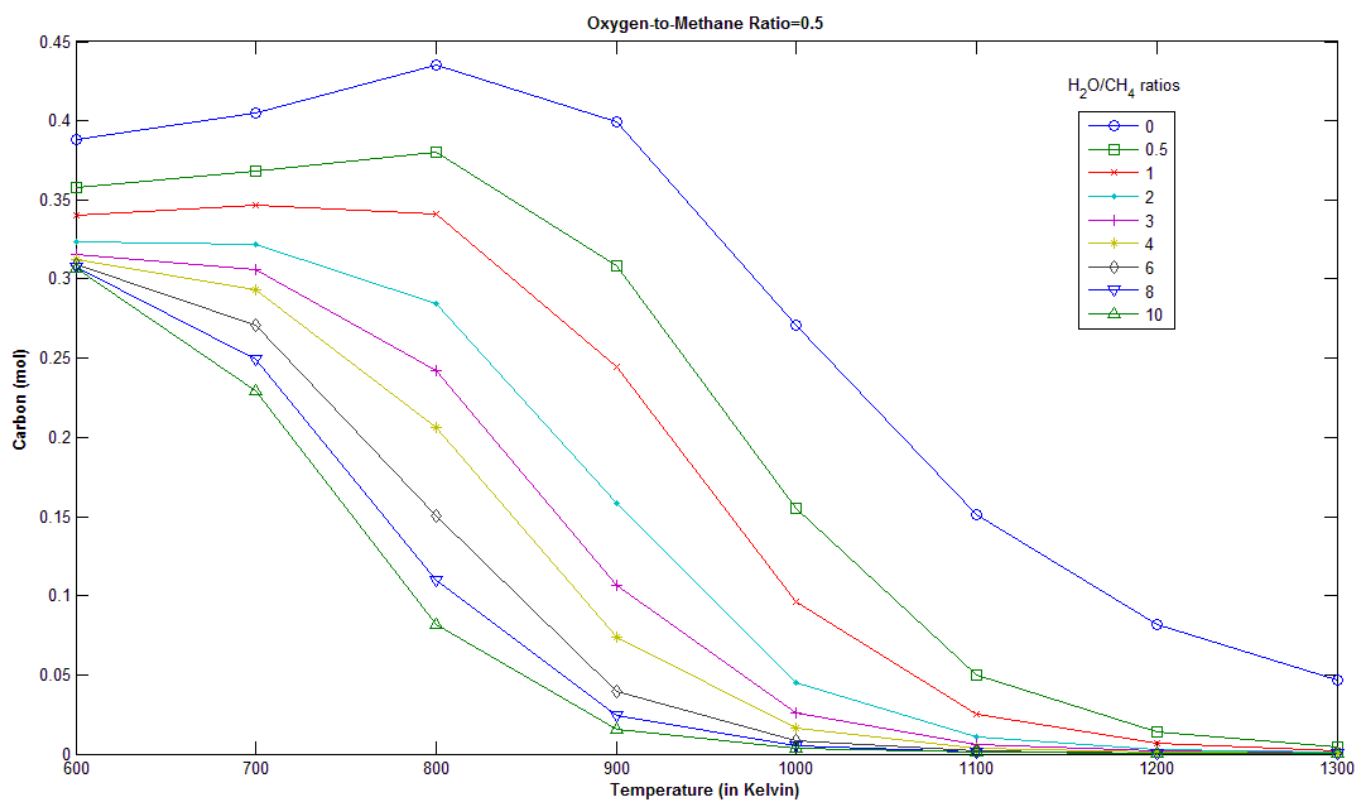


Figure 5.13: Coke formation at different steam/methane ratios with oxygen/methane=0.5

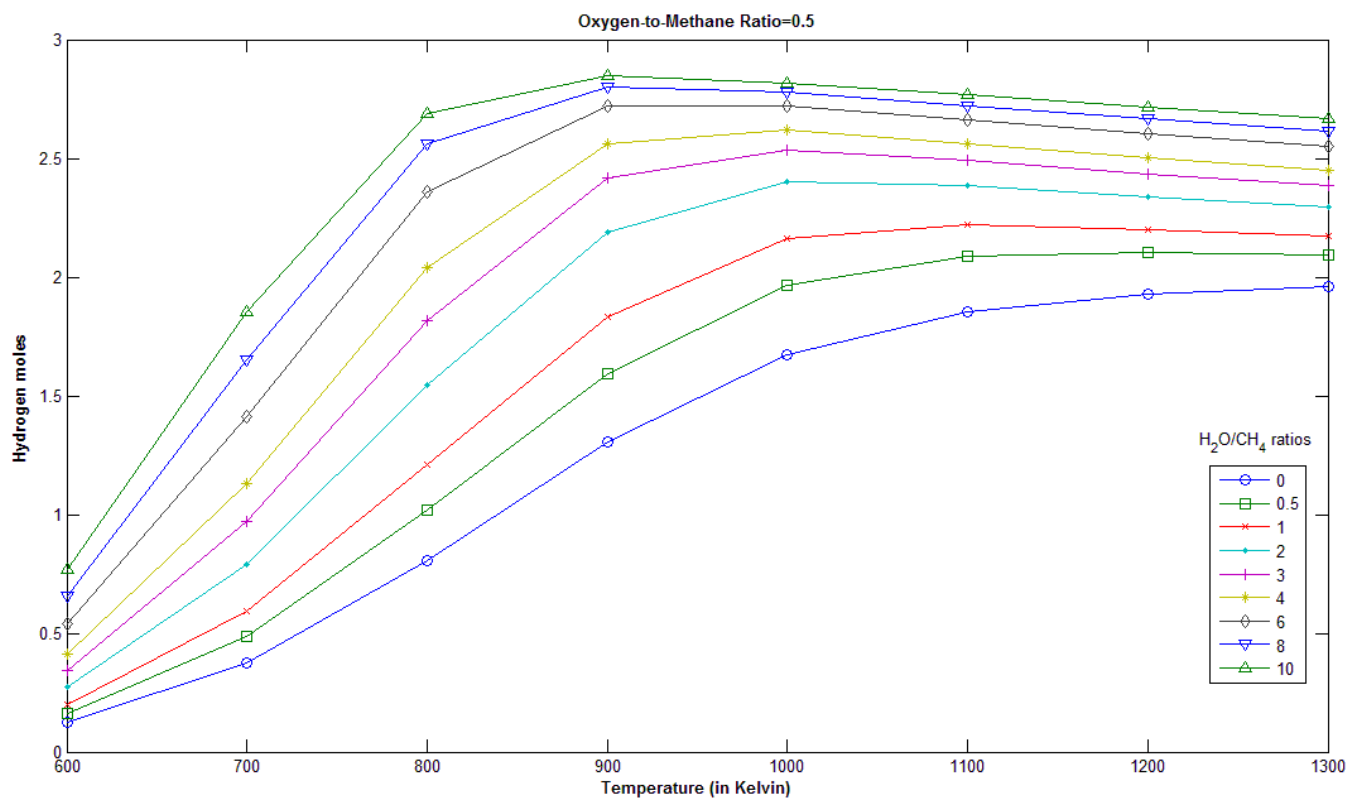


Figure 5.14 : Hydrogen moles at different steam/methane ratios with oxygen/methane=0.5

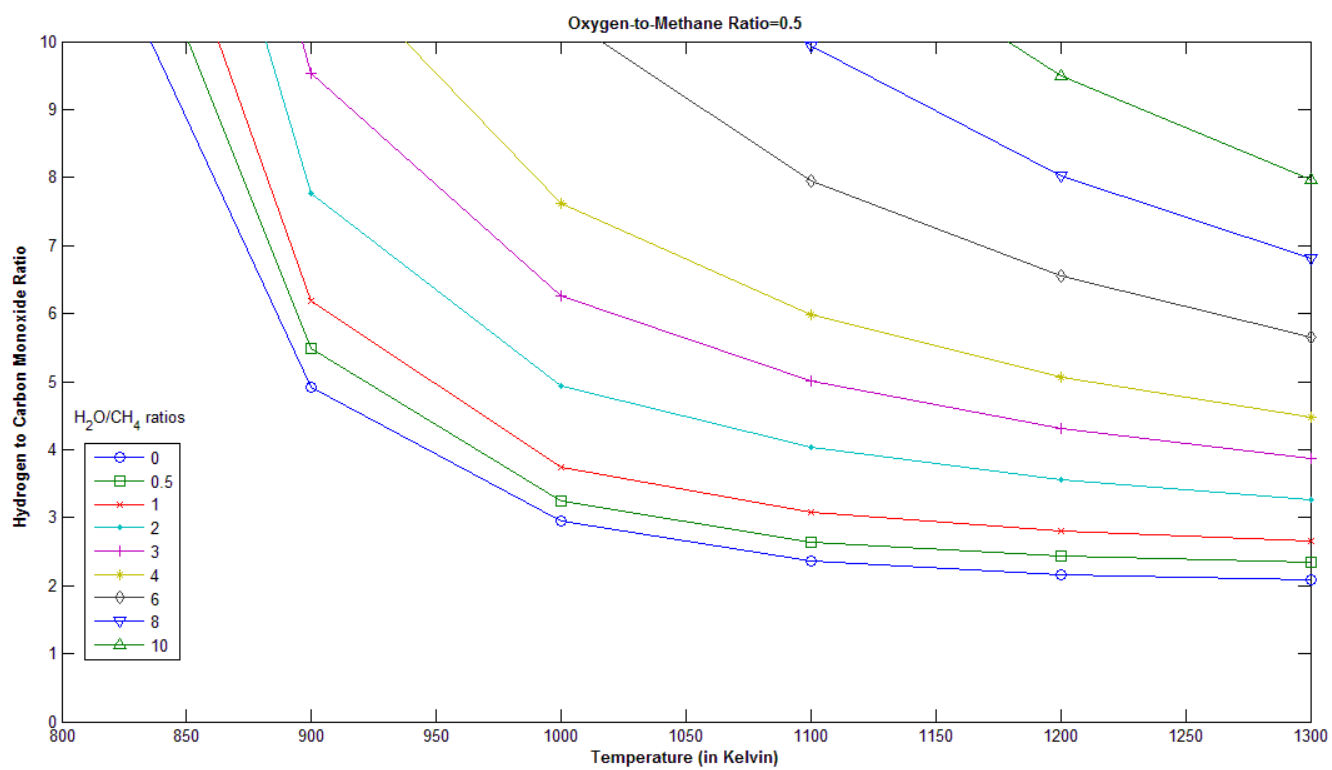


Figure 5.15: Hydrogen/Carbon Monoxide ratio at different steam/methane ratios with oxygen/methane=0.5

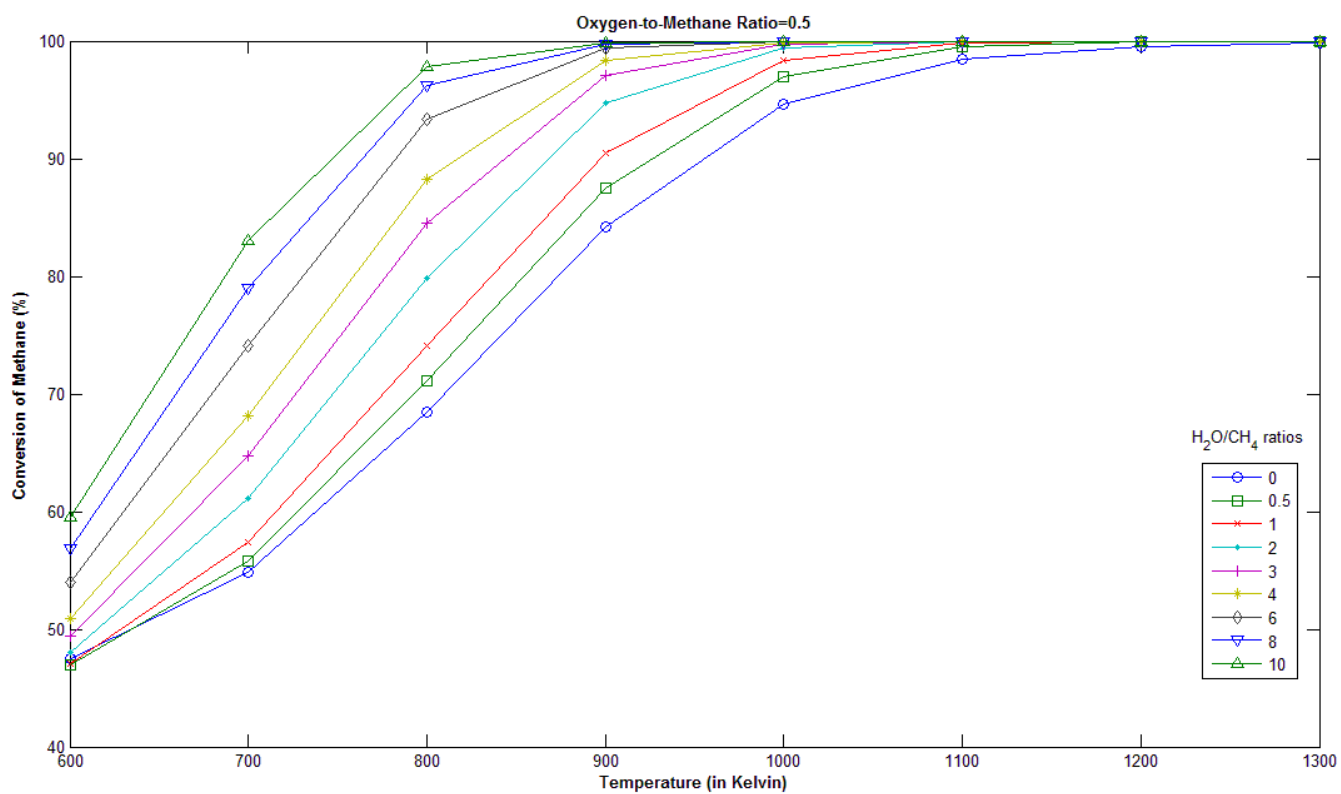


Figure 5.16: Conversion of methane at different steam/methane ratios with oxygen/methane=0.5

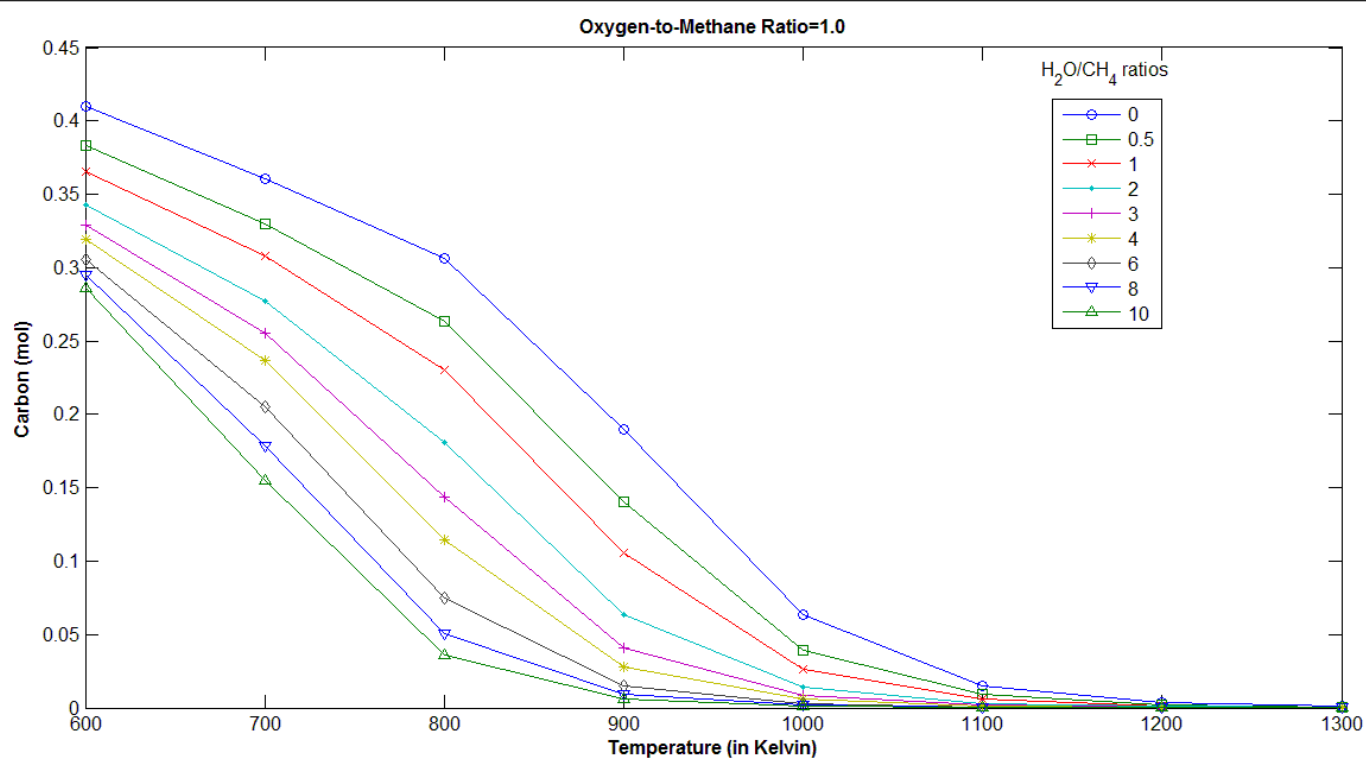


Figure 5.17: Coke formation at different steam/methane ratios with oxygen/methane=1.0

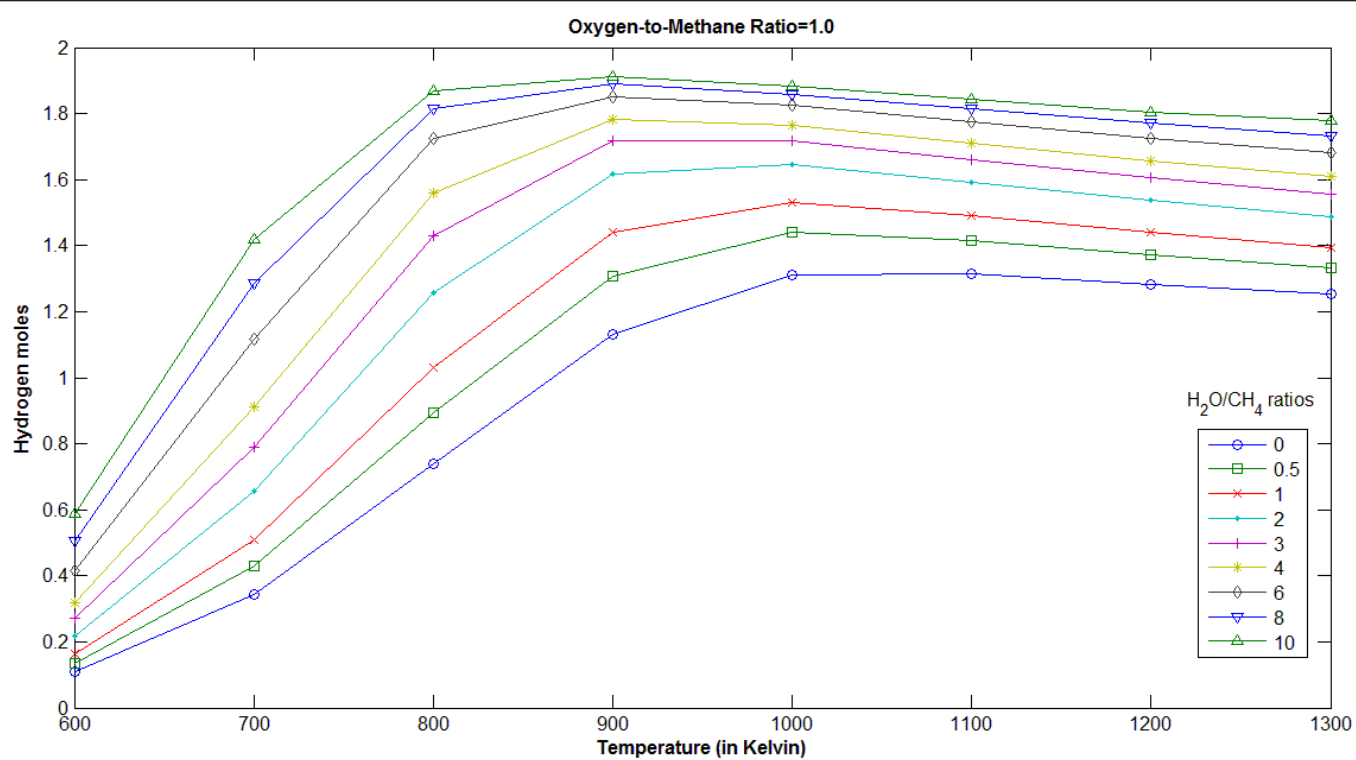


Figure 5.18: Hydrogen moles at different steam/methane ratios with oxygen/methane=1.0

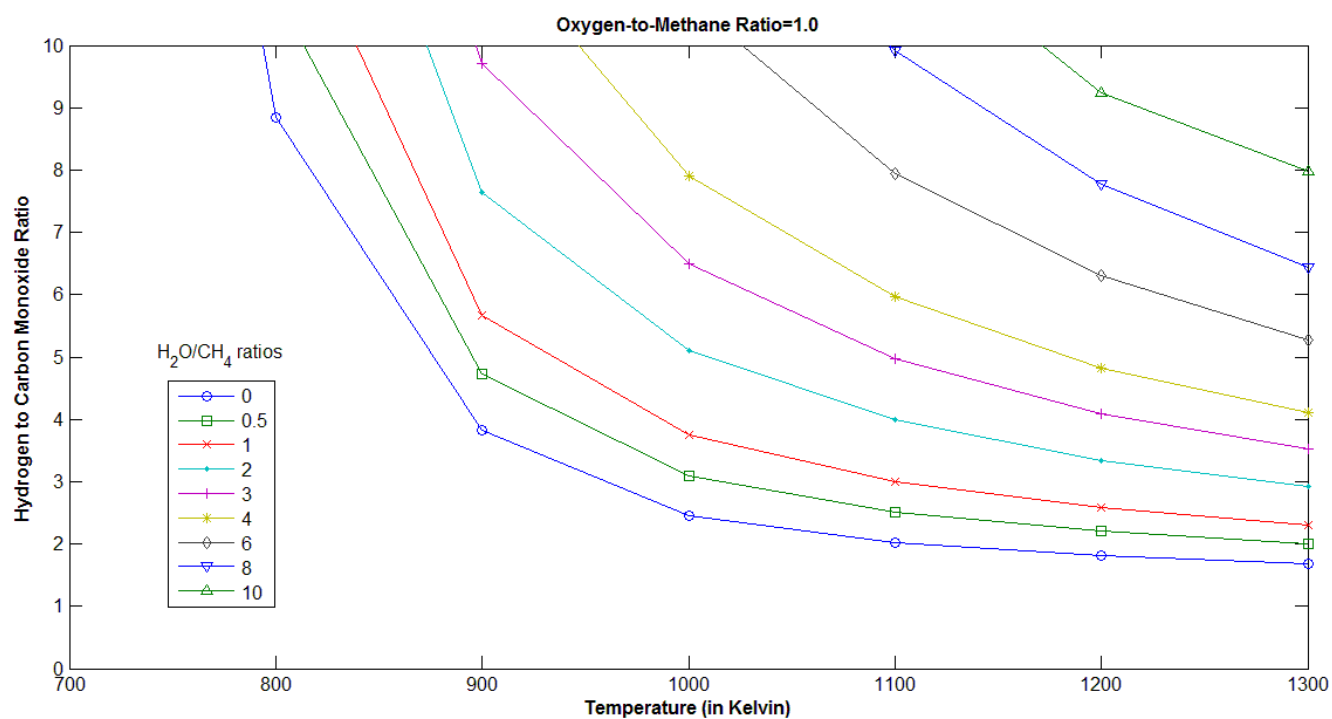


Figure 5.19: Hydrogen/Carbon Monoxide ratio at different steam/methane ratios with oxygen/methane=1.0

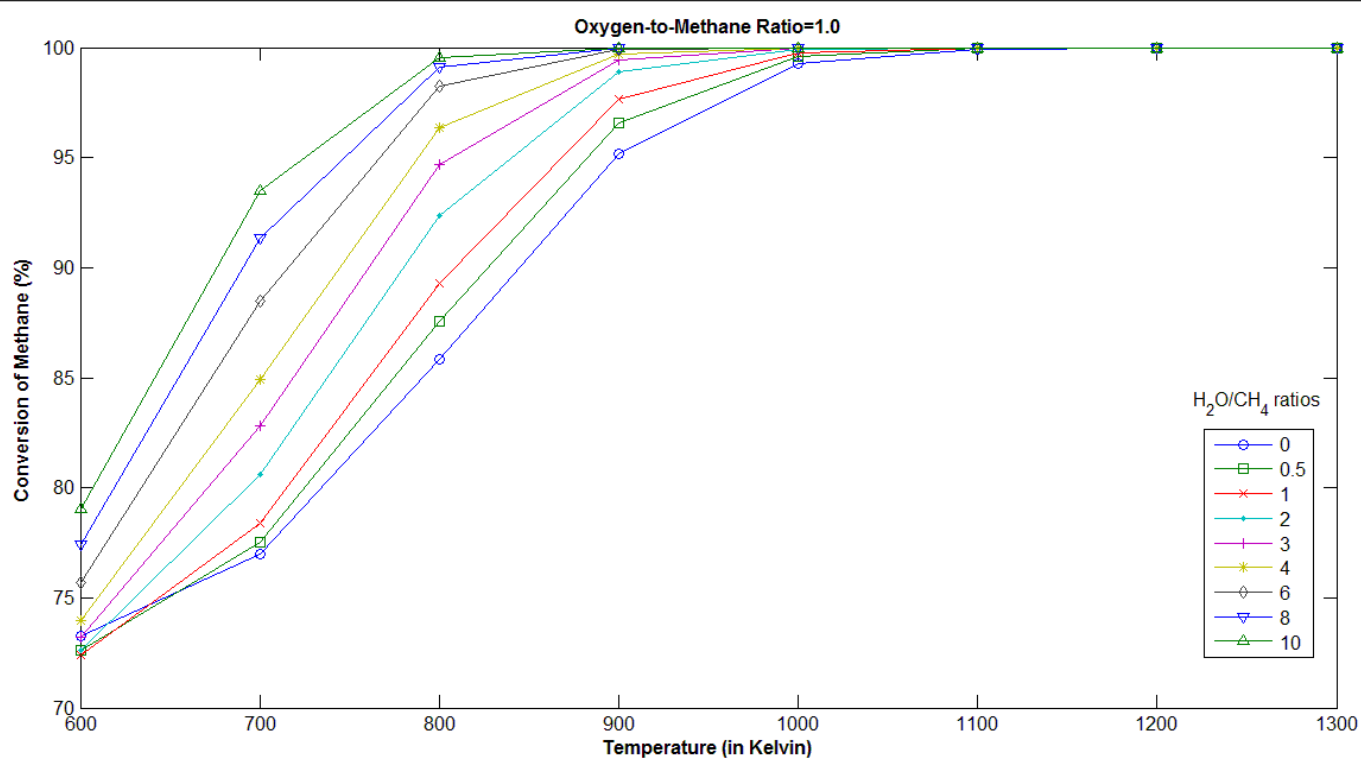


Figure 5.20: Conversion of methane at different steam/methane ratios with oxygen/methane=1.0

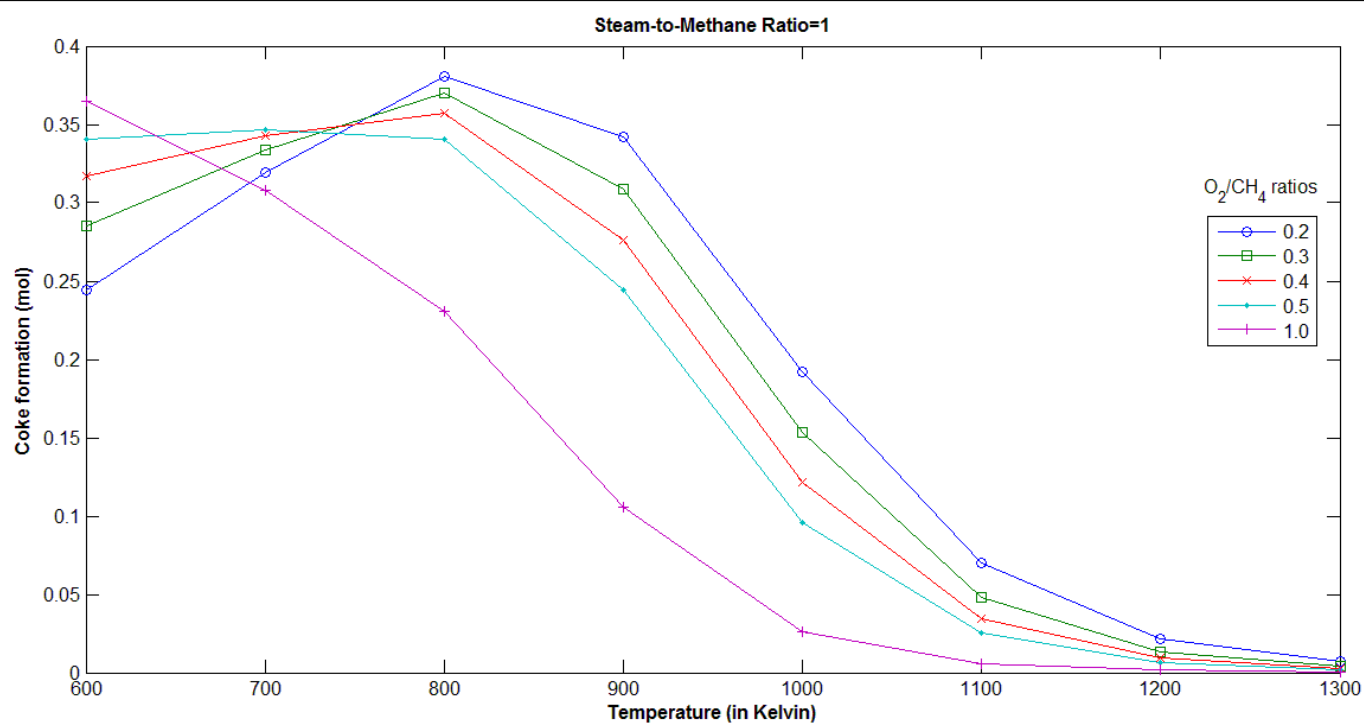


Figure 5.21: Effect of changing oxygen/methane ratio on coke formation at steam/methane=1.0

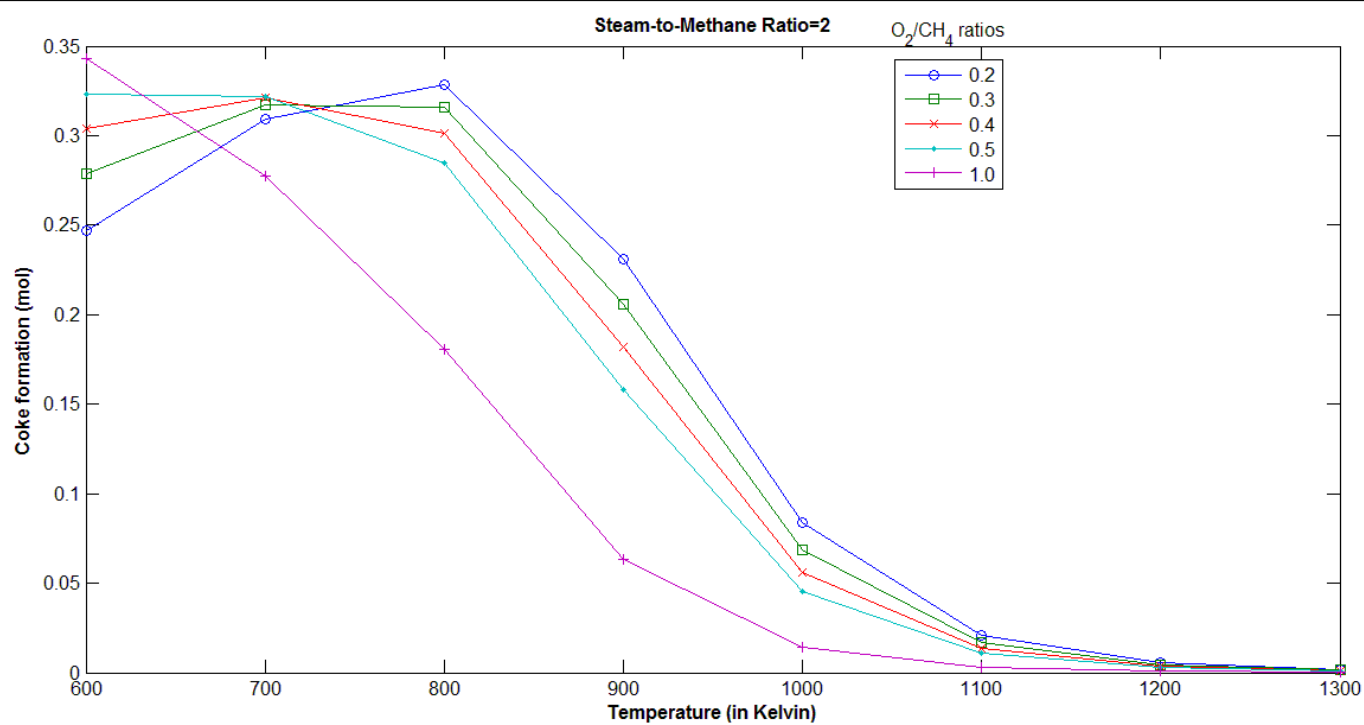


Figure 5.22: Effect of changing oxygen/methane ratio on coke formation at steam/methane=2.0

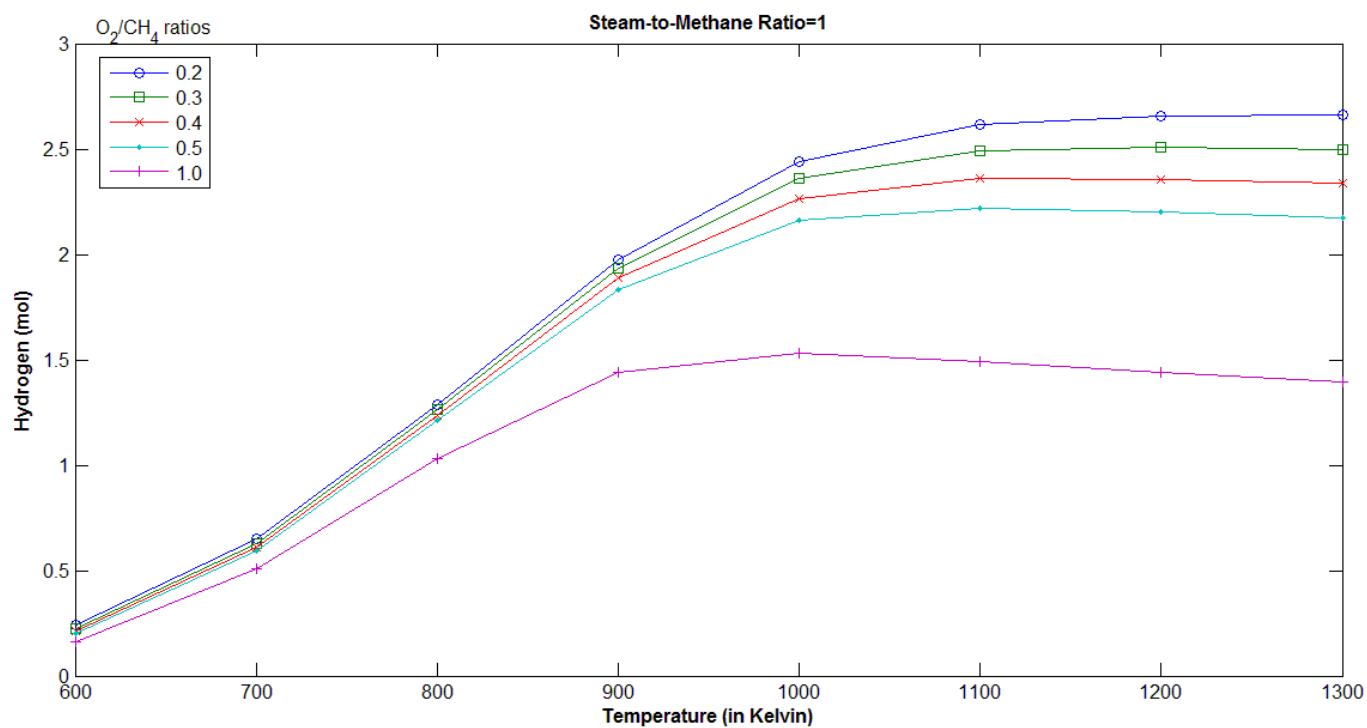


Figure 5.23: Effect of changing oxygen/methane ratio on hydrogen moles at steam/methane=1.0

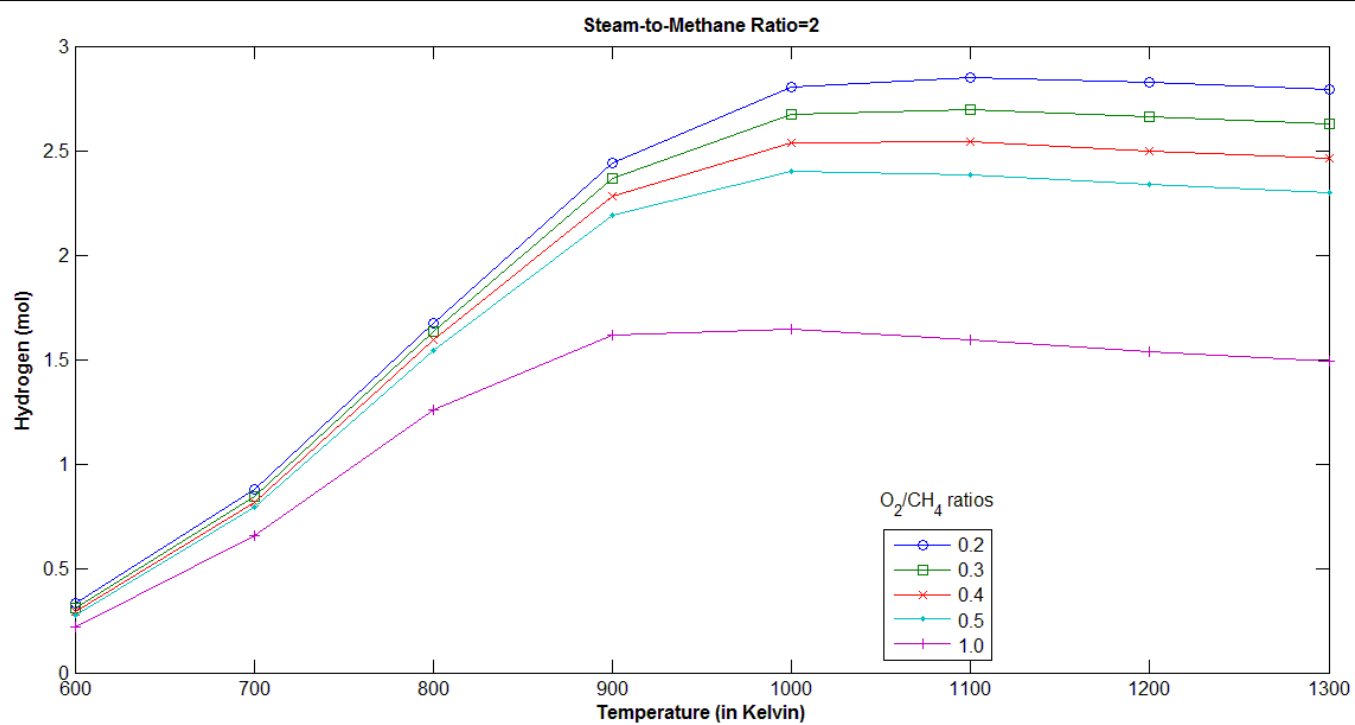


Figure 5.24: Effect of changing oxygen/methane ratio on hydrogen moles at steam/methane=2.0

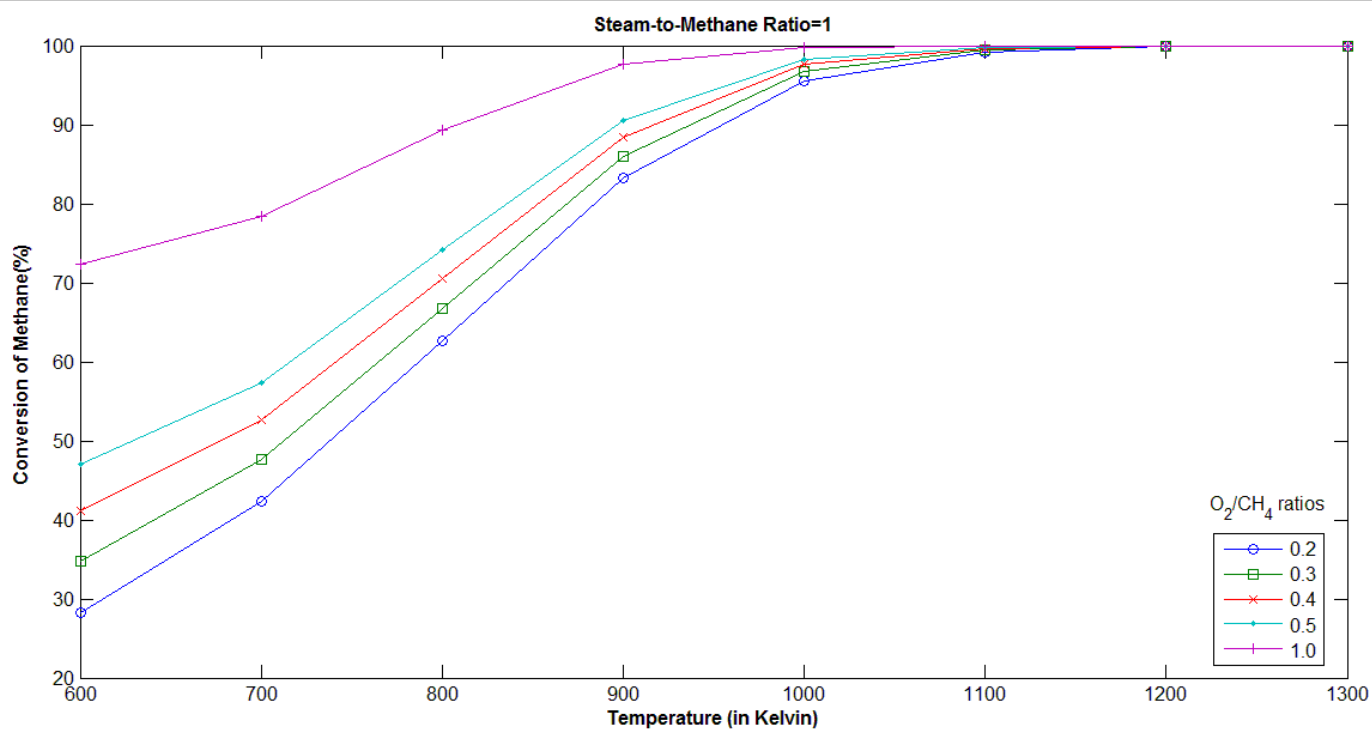


Figure 5.25: Effect of changing oxygen/methane ratio on methane conversion at steam/methane=1.0

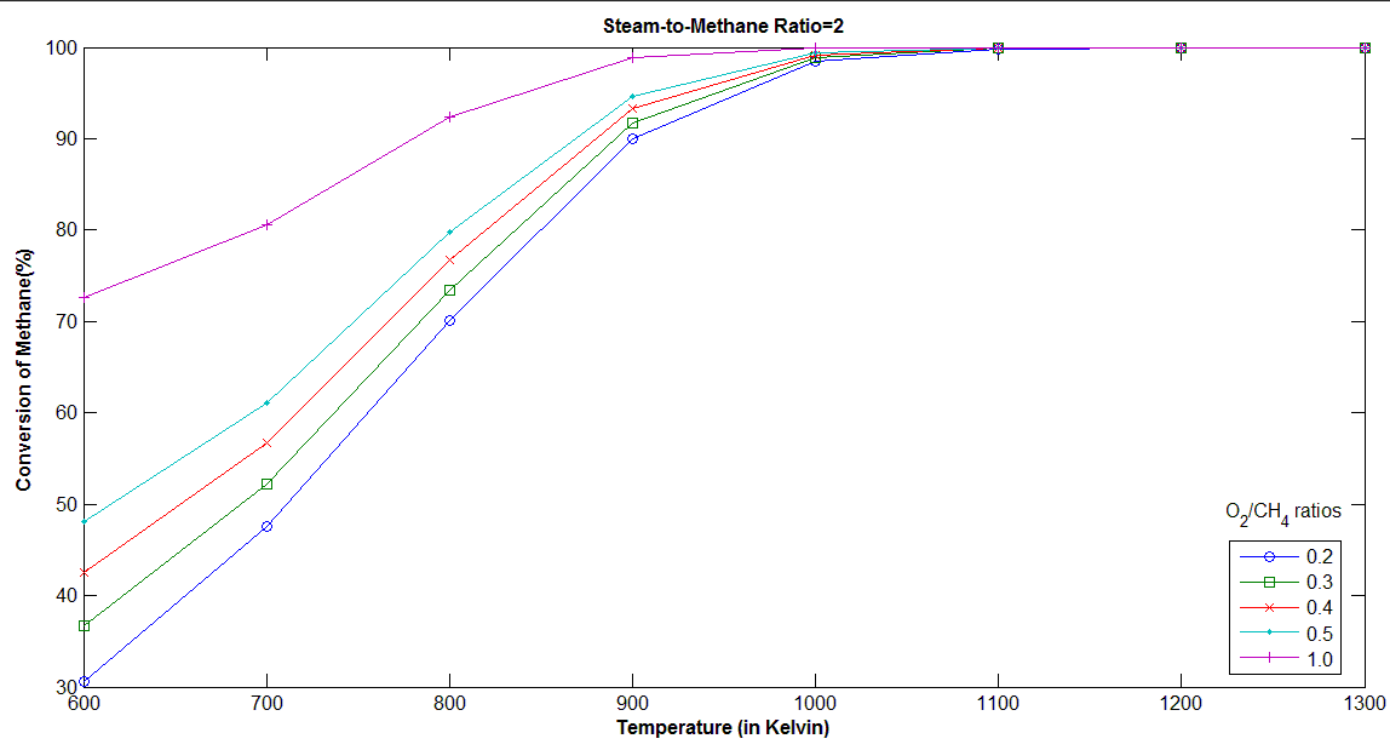


Figure 5.26: Effect of changing oxygen/methane ratio on methane conversion at steam/methane=2.0

5.2 MODEL SIMULATION

The simulation for the study of the reactor has been done by using the reactor specifications used by Kumar et al. [27] who have utilized the specifications of Ji et al. [25] The specifications are tabulated below:

Table 5.3: Initial flow rates for simulation of model ^[27]

Parameter	Value	Unit
Initial methane flow rate	2.50×10^{-3}	mol s^{-1}
Initial CO flow rate	0.00	mol s^{-1}
Initial CO ₂ flow rate	0.00	mol s^{-1}
Initial H ₂ flow rate	10^{-10}	mol s^{-1}

The hydrogen flow rate is taken tending to zero because there is no hydrogen in feed. However, the Xu and Froment kinetics used for reforming reaction will be mathematically NaN (Not a Number, mathematically speaking) if the hydrogen partial pressure is zero. Thus, to avoid indeterminate flow rates at the start, this assumption has to be taken. Mathematically, this value is trivial to cause any change of result to the simulation. For the reactor and catalyst specifications once again values from Kumar et al. have been used to know a feasible range. These values have been used in an experimental setup by Ji et al.

Table 5.4: Reactor specifications for simulation of model

Parameter	Value	Unit
Reactor diameter	24	mm
Catalyst density	2100	kg m^{-3}
Void fraction of packing	0.43	-
Length	1	metre

Table 5.5: Operating conditions for simulation of model

Parameter	Value	Unit
Pressure	1	bar
Temperature	900	Kelvin
Steam-to-methane ratio	1.5	-
Oxygen-to-methane ratio	0.6	-

Steam content and oxygen content for the purpose of the study is kept variable within the range determined by the thermodynamic analysis. The operating parameters i.e. temperature is also variable in view of the thermodynamic study. The effectiveness factors reported by De Groote and Froment are used for the simulation. The results of simulation are given in graphical form in figures 5.27 to 5.42.

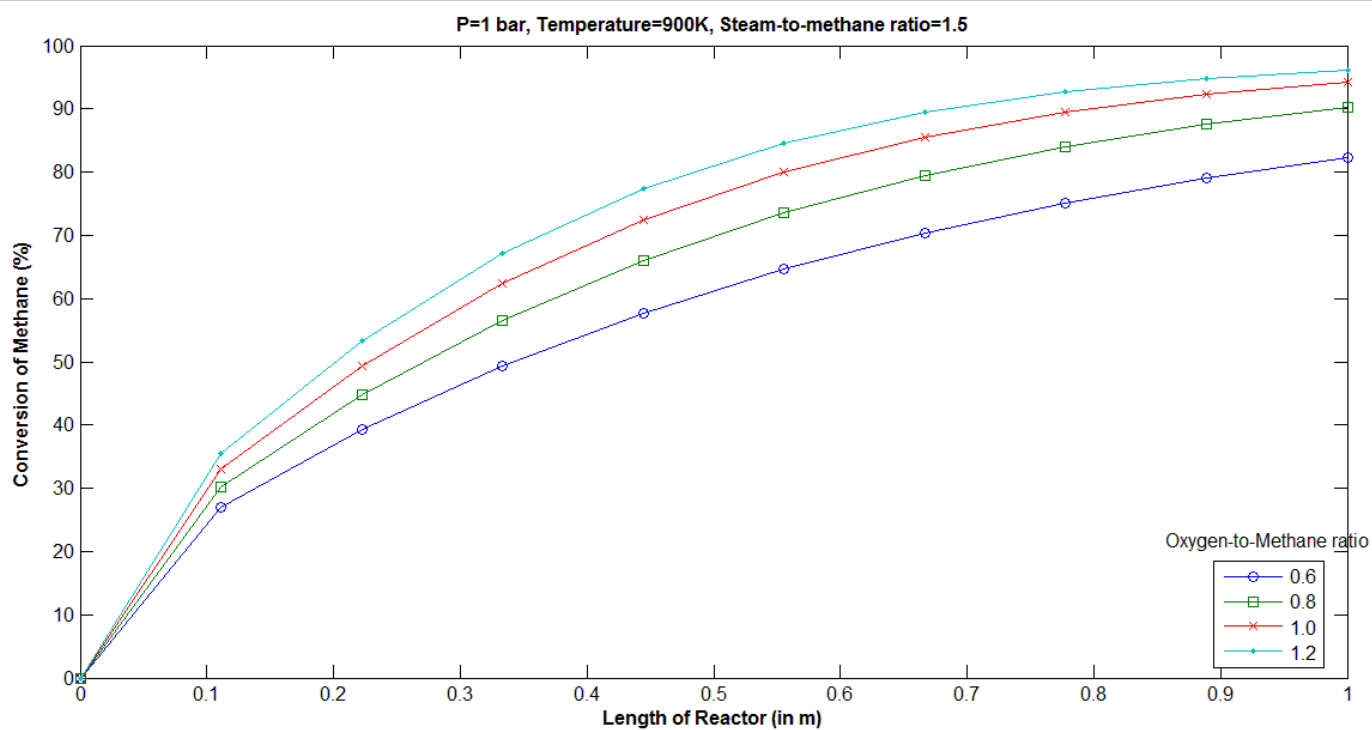


Figure 5.27: Conversion at different positions with varying oxygen content

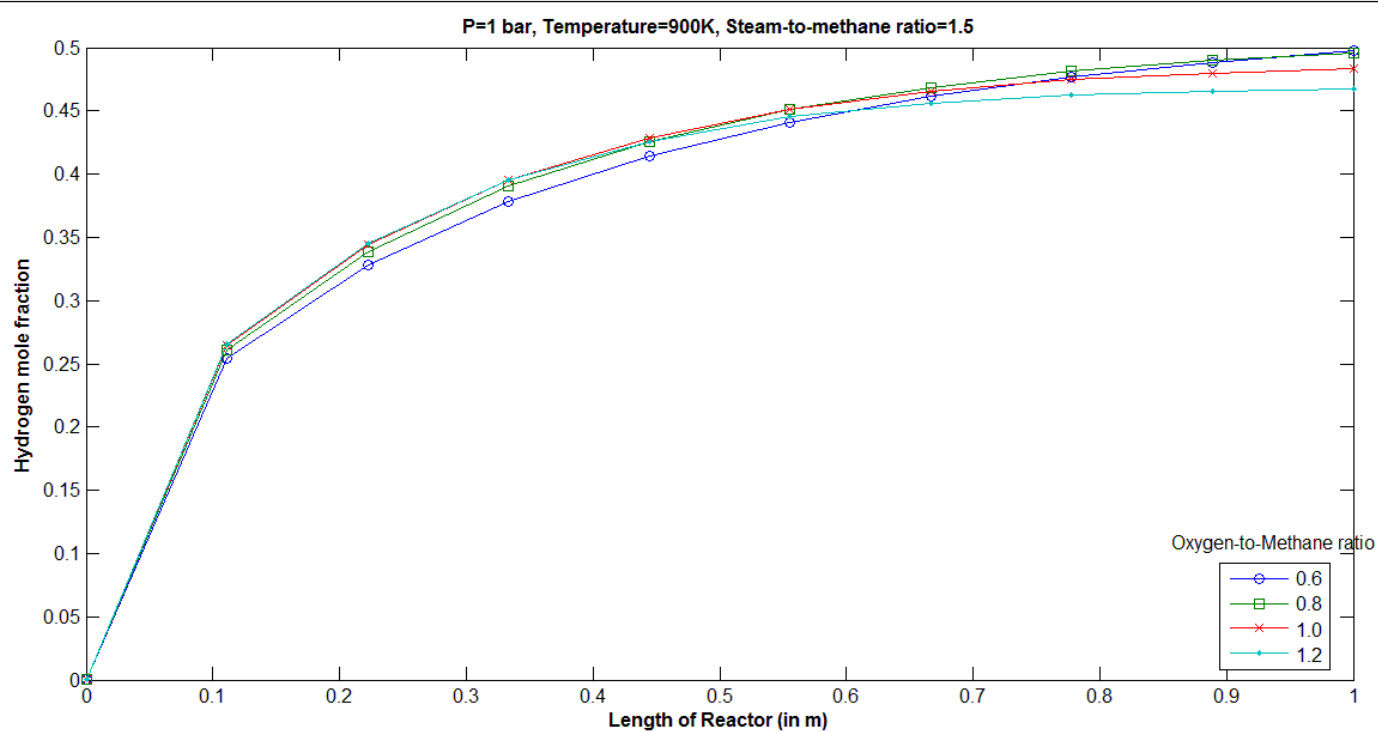


Figure 5.28: Hydrogen mole fraction at different positions with varying oxygen content

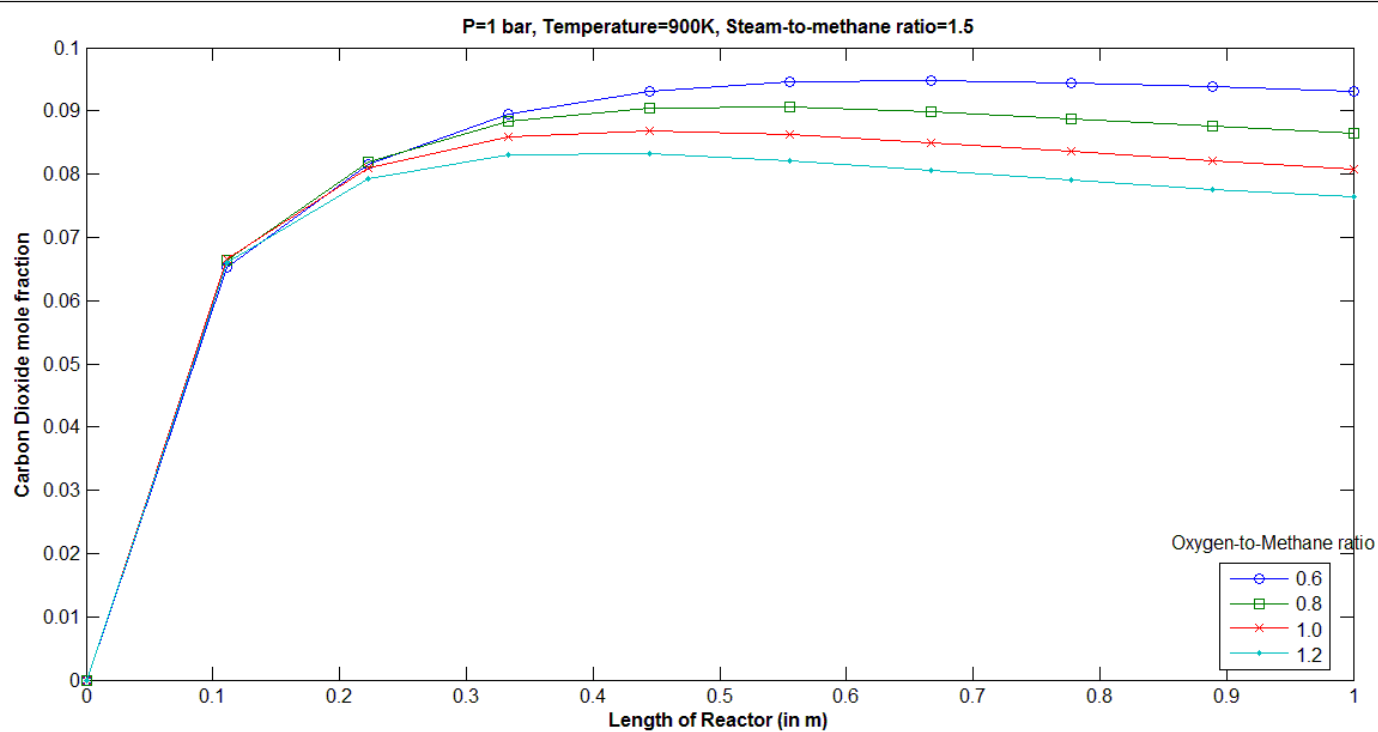


Figure 5.29: CO₂ mole fraction at different positions with varying oxygen content

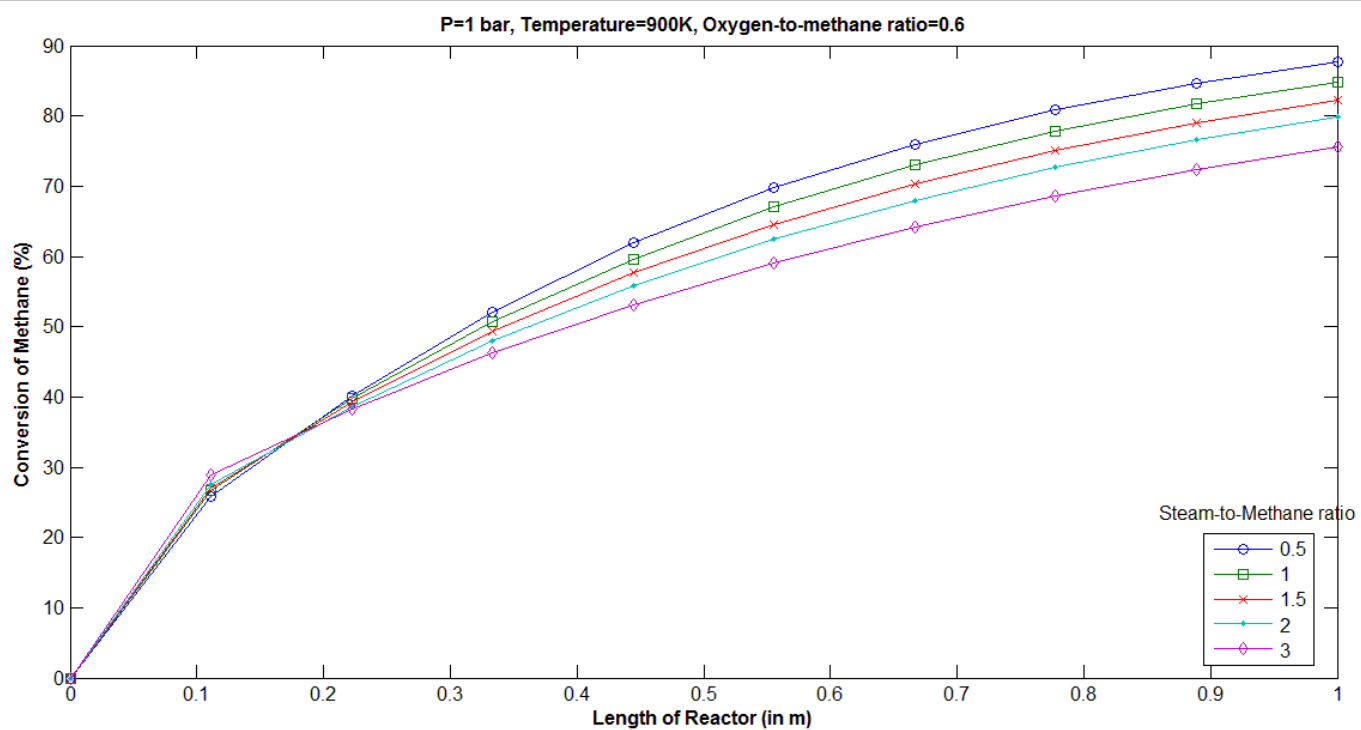


Figure 5.30: CO mole fraction at different positions with varying oxygen content

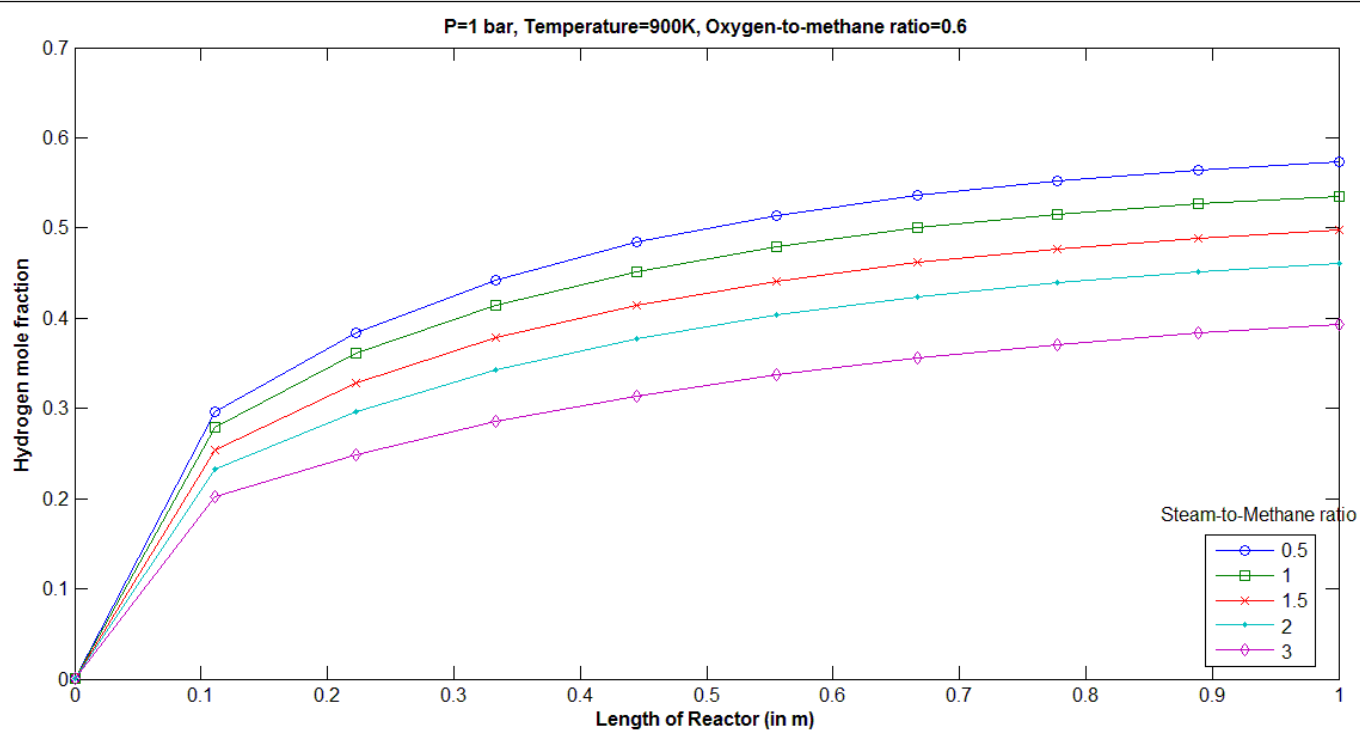


Figure 5.31: Hydrogen mole fraction at different positions with varying steam content

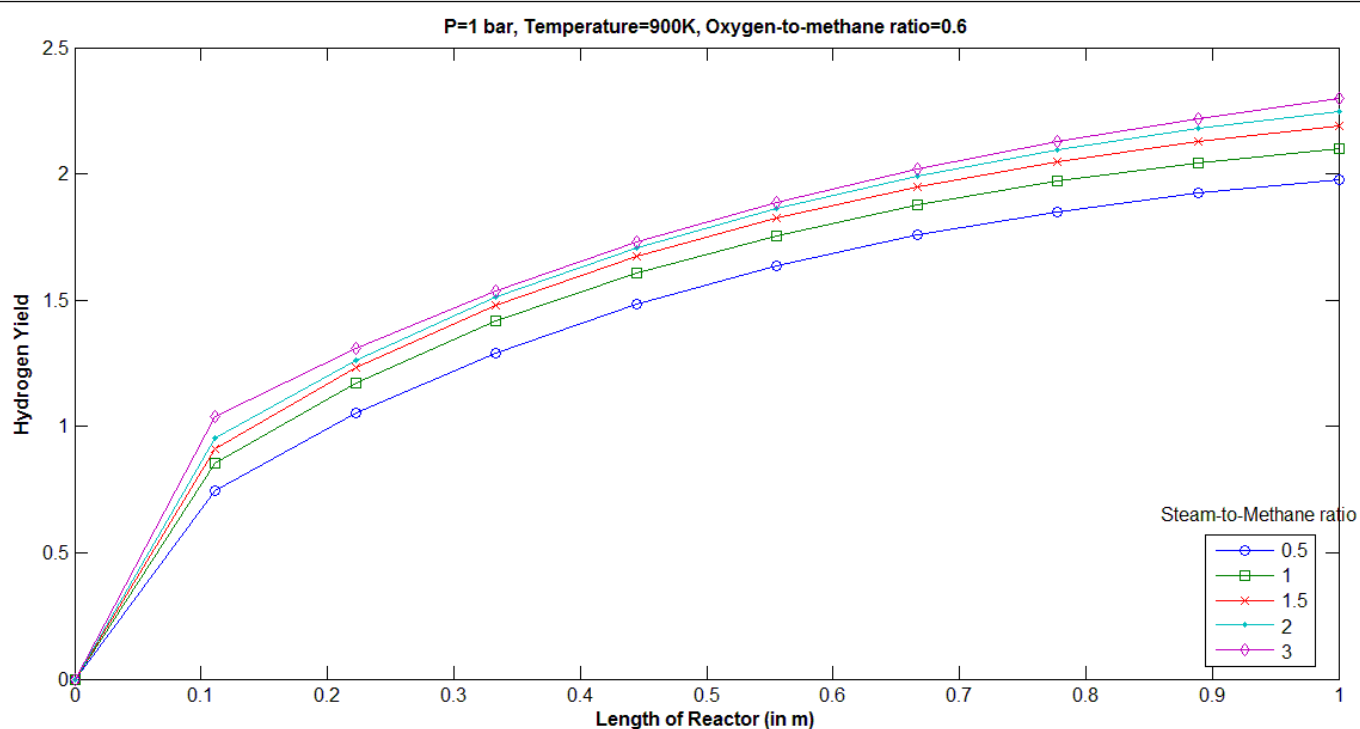


Figure 5.32: Hydrogen yield at different positions with varying steam content

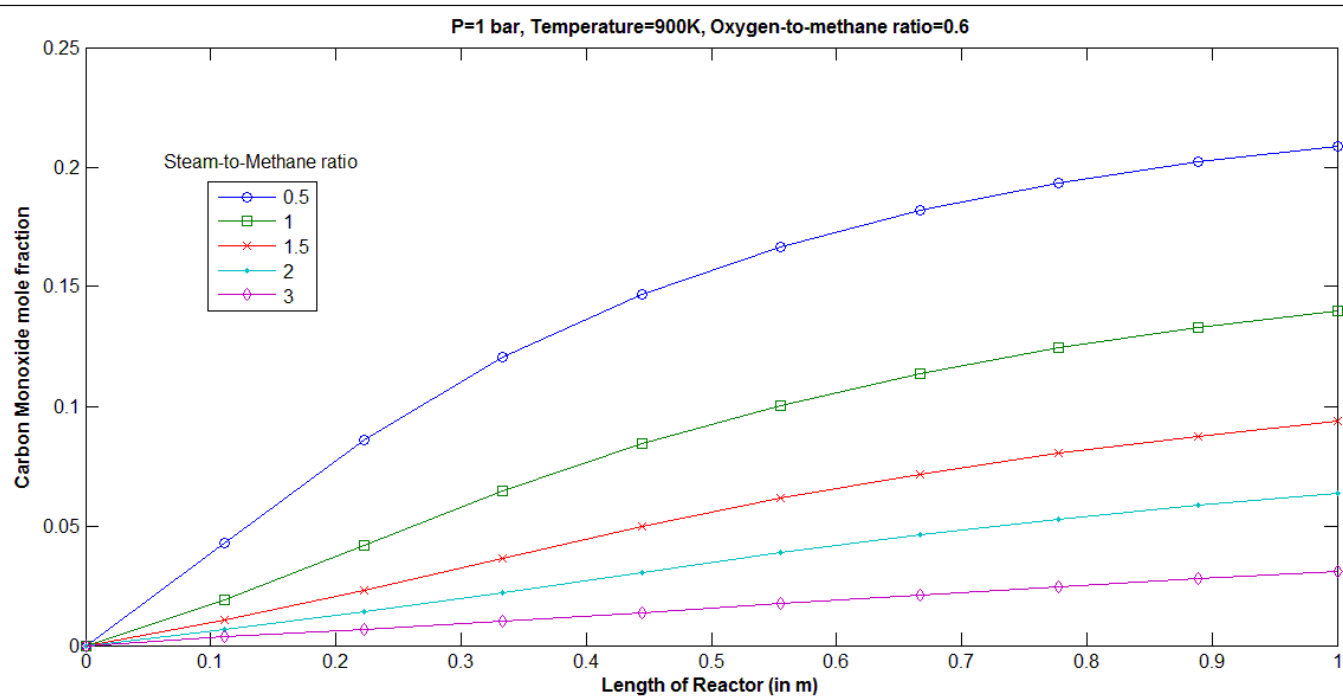


Figure 5.33: CO mole fraction at different positions with varying steam content

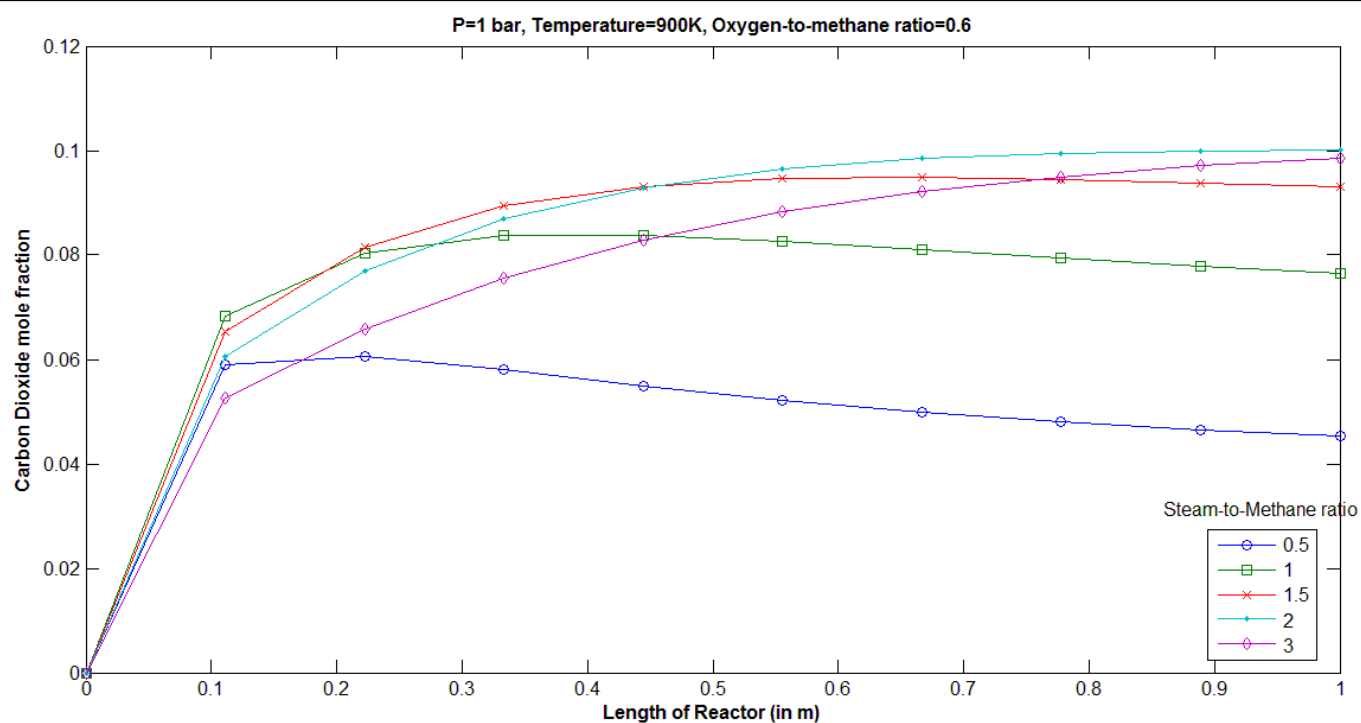


Figure 5.34: CO₂ mole fraction at different positions with varying steam content

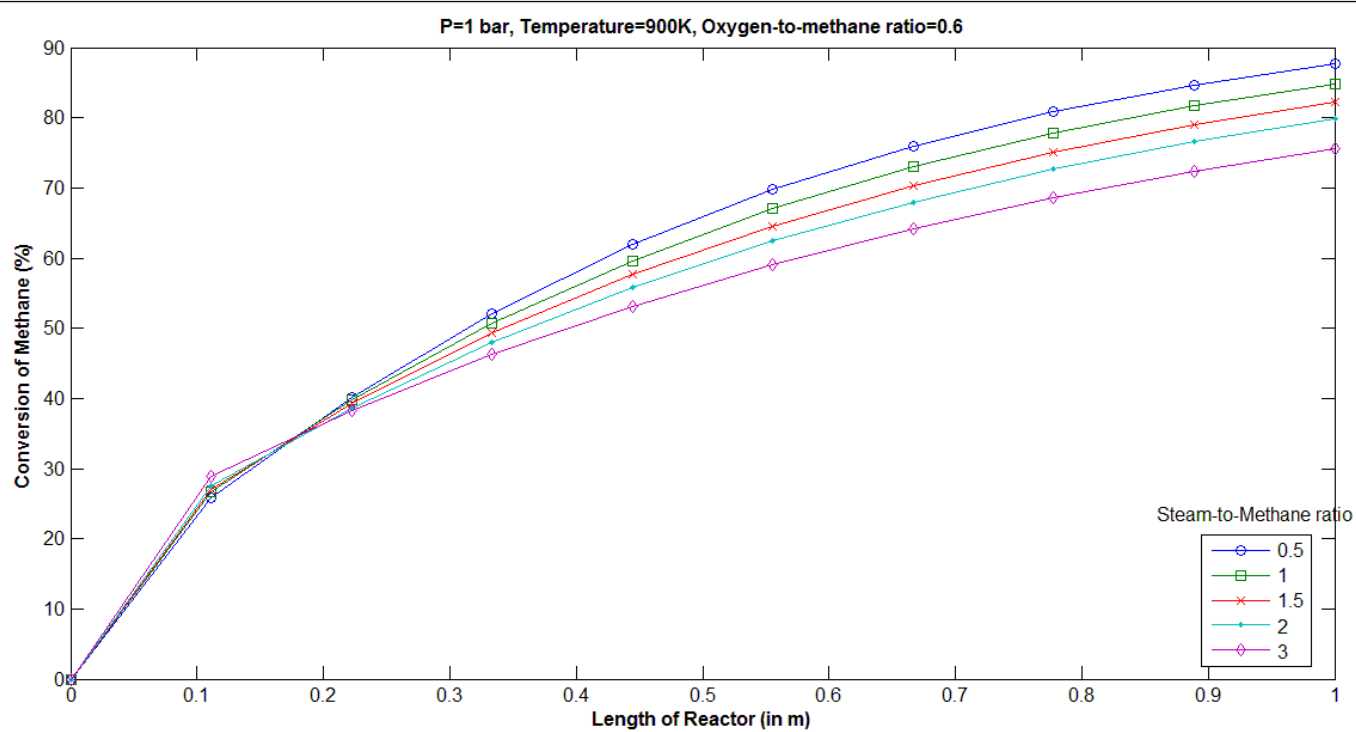


Figure 5.35: Conversion at different positions with varying steam content

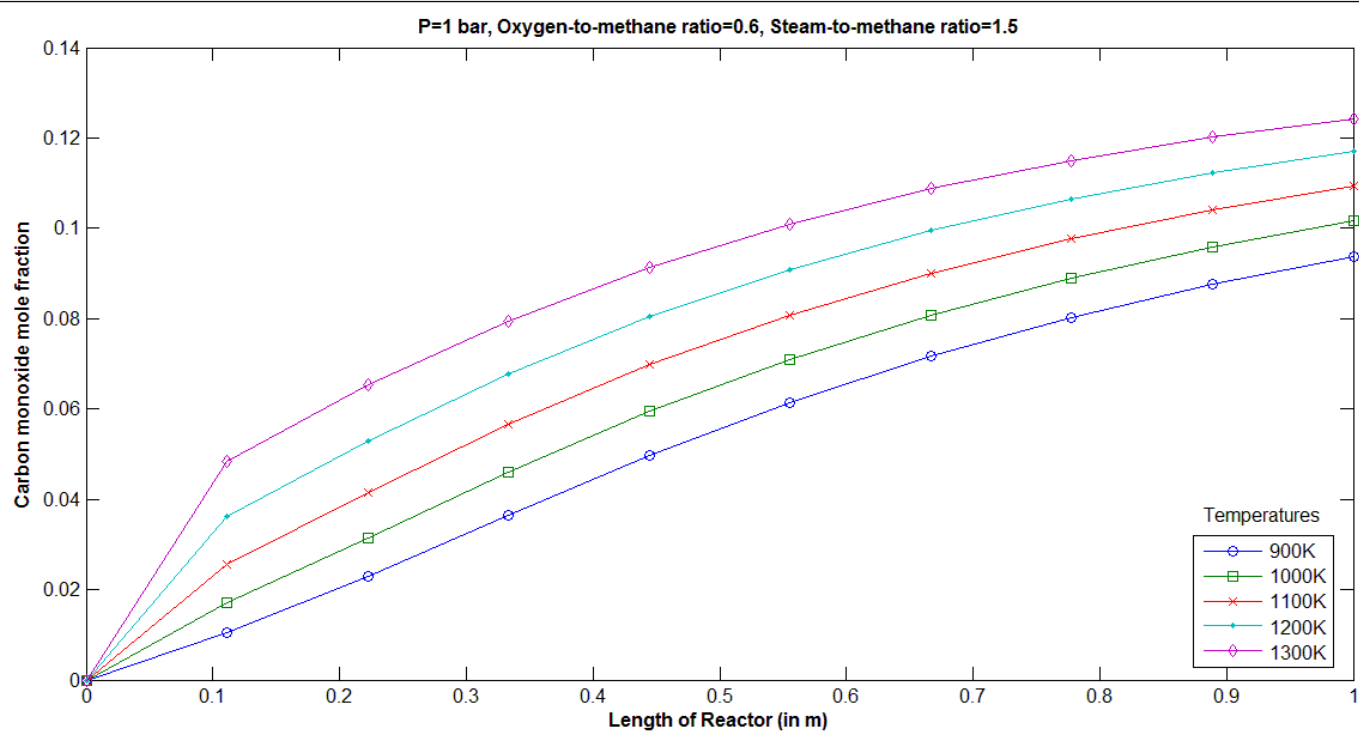


Figure 5.36: CO mole fraction at different positions with varying temperatures

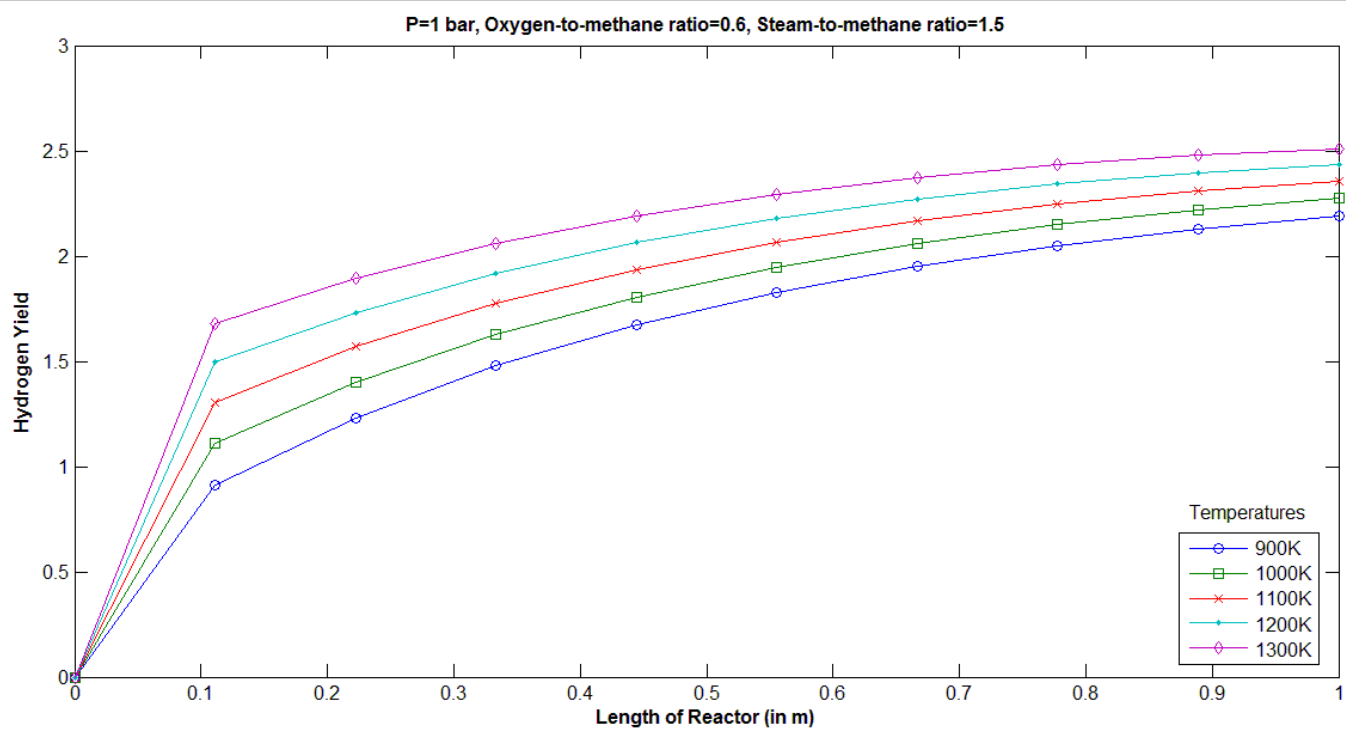


Figure 5.37: Hydrogen yield at different positions with varying temperatures

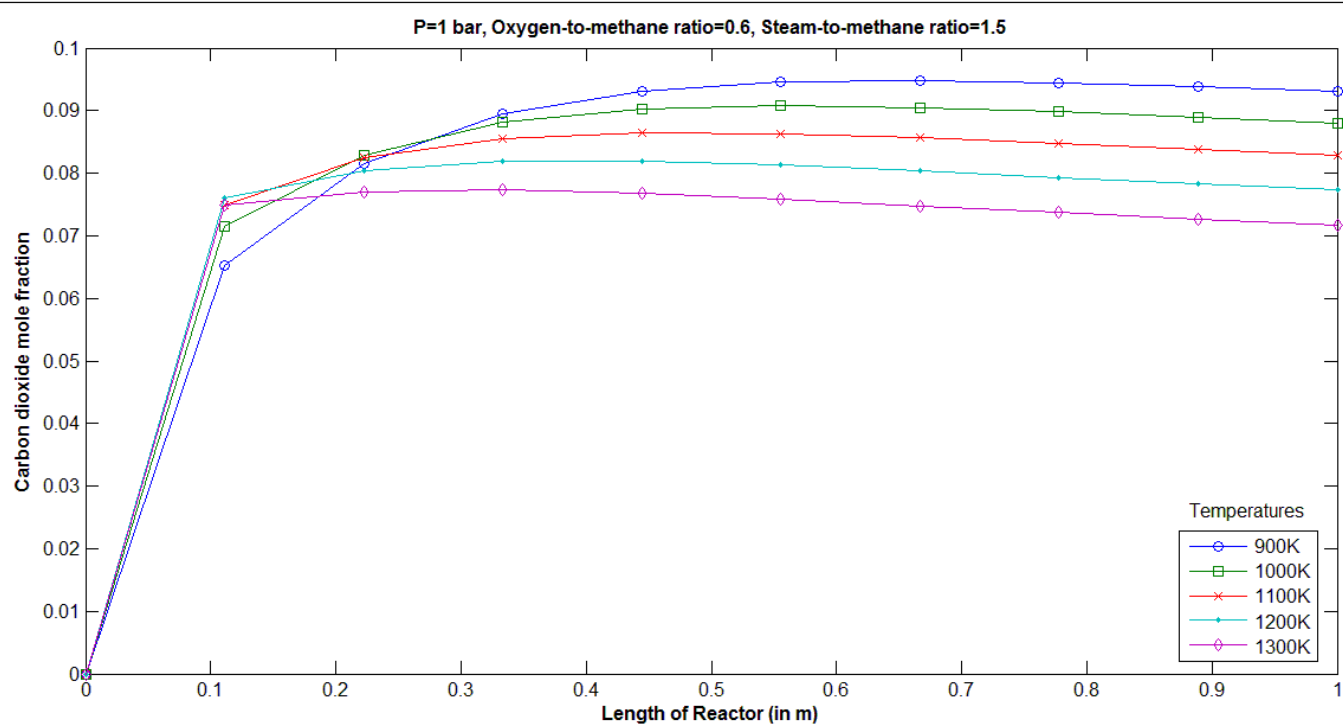


Figure 5.38: CO₂ mole fraction at different positions with varying temperatures

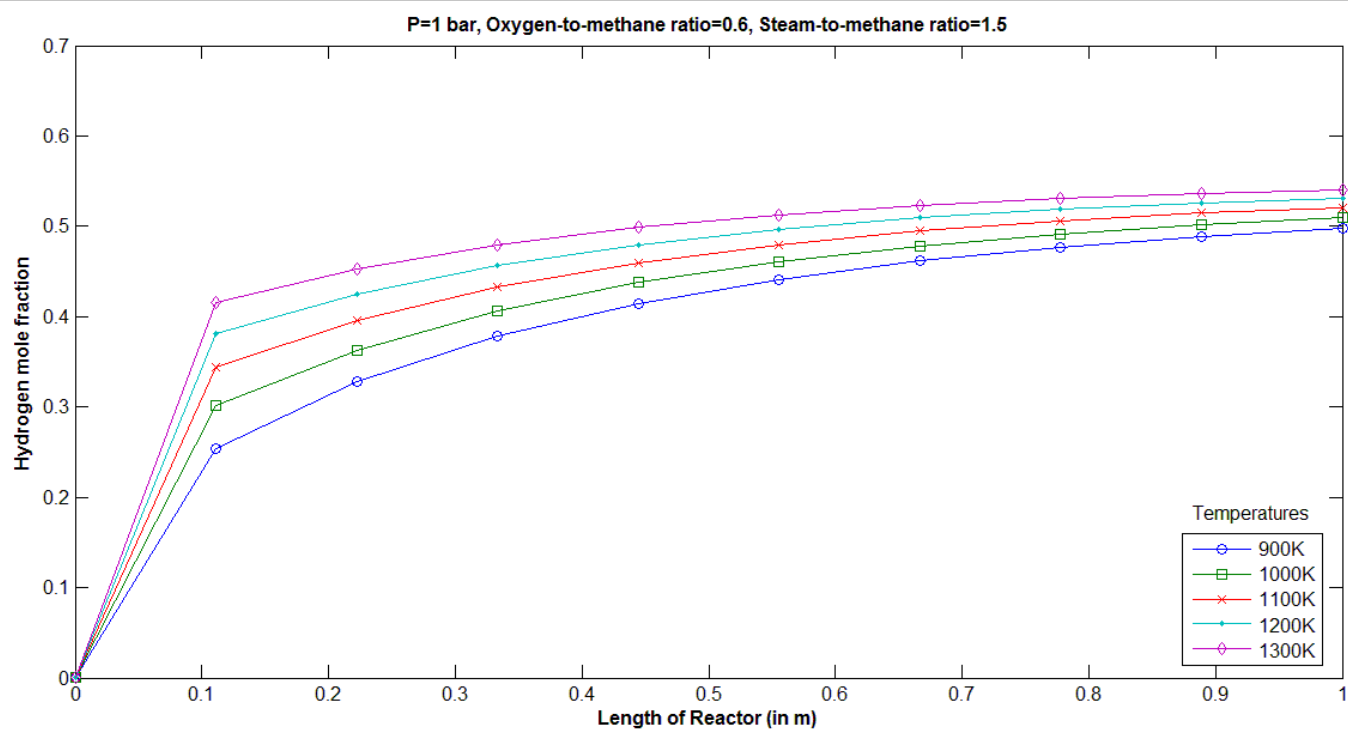


Figure 5.39: Hydrogen mole fraction at different positions with varying temperatures

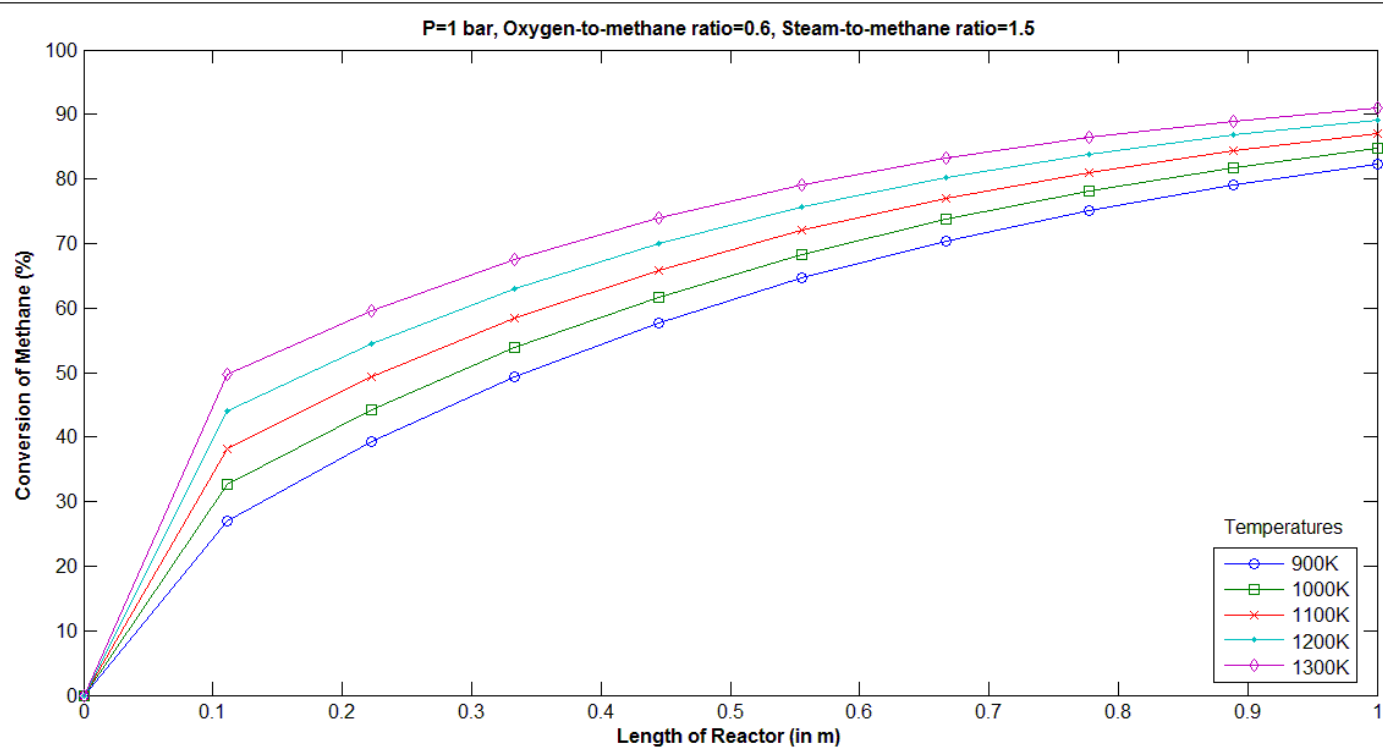


Figure 5.40: Conversion at different positions with varying temperatures

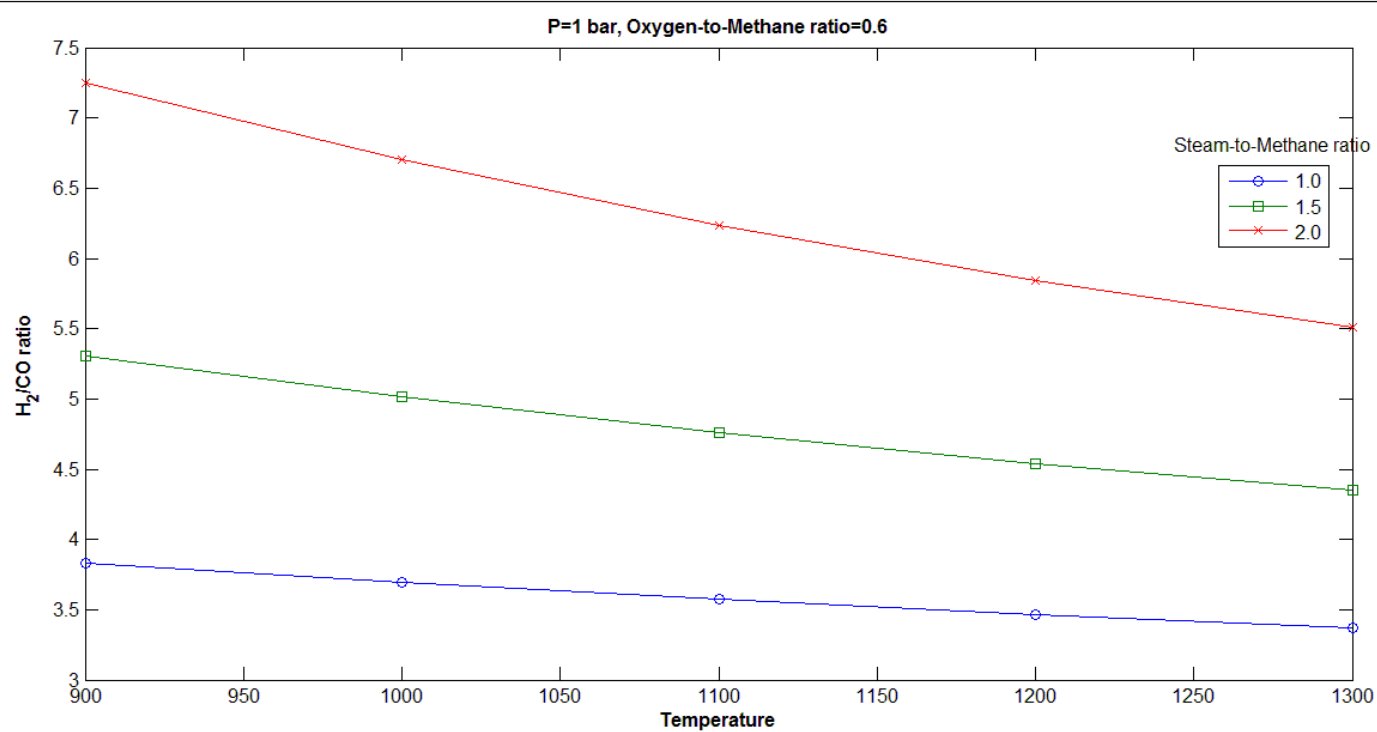


Figure 5.41: H₂/CO ratios at different temperatures with varying steam content

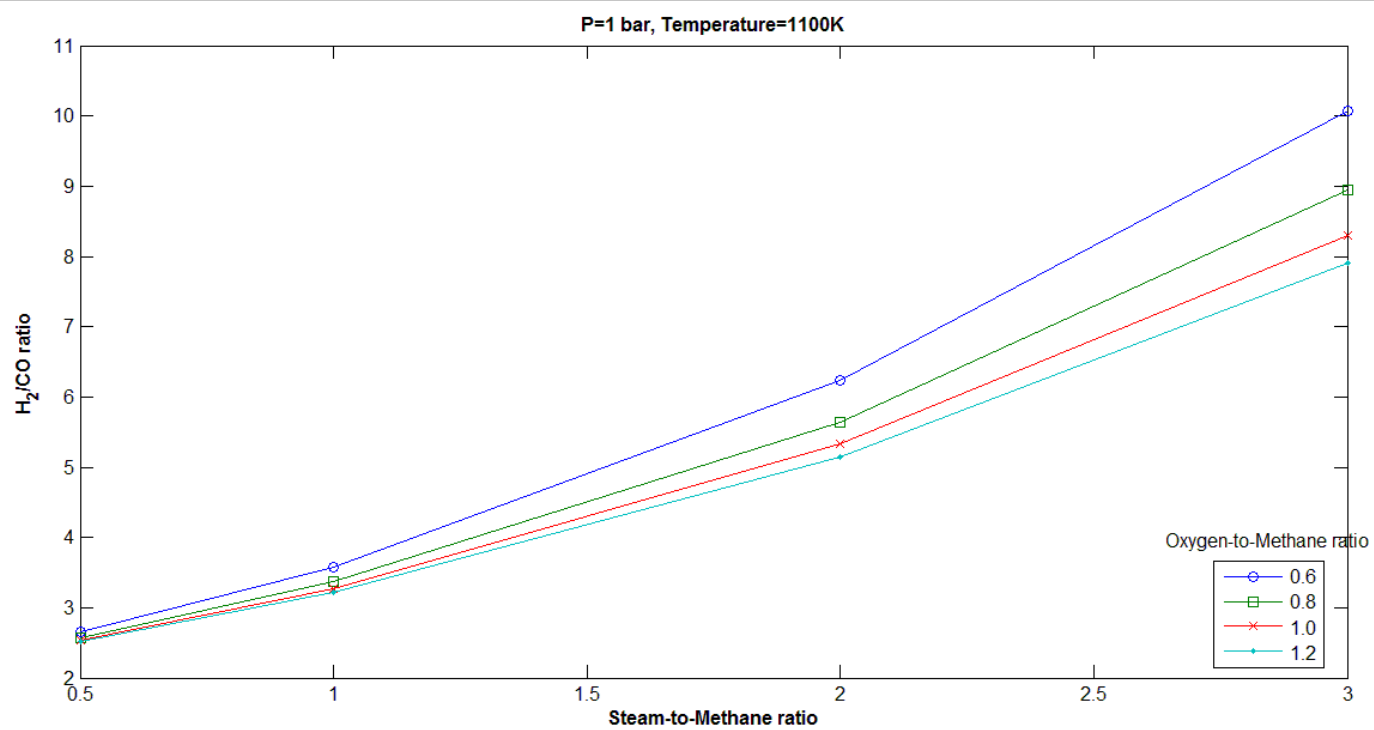


Figure 5.42: H_2/CO ratios at different steam content with varying oxygen content

The simulations can be divided into three major portions for the sake of ease of classification and understanding. The first part evaluates changes in the output parameters by varying oxygen to methane ratio. For this part the steam ratio is fixed at 0.6 while the temperature was taken to be 900K for the sake of maximum applicability of Trimm and Lam kinetics which were derived in the temperature range of 800K. The evaluated parameters are defined as follows:

$$Conversion = X_{CH_4} = \frac{F_{CH_4 @ z=0} - F_{CH_4 @ z=L}}{F_{CH_4 @ z=0}} \times 100\% \quad (5.1)$$

$$Yield = Y_{H_2} = \frac{F_{H_2 @ z=L} - F_{H_2 @ z=0}}{F_{CH_4 @ z=0}} \quad (5.2)$$

The mole fraction of any of the six species is defined as:

$$x_i = \frac{F_i}{\sum_{i=1}^6 F_i} \quad (5.3)$$

It was found that the conversion of methane increases with increasing oxygen ratio (see Figure 5.27). This is expected because the methane combustion reaction is an irreversible reaction with a large equilibrium constant. The oxygen supplied is consumed in that reaction, and hence increases the percentage of methane consumed overall. The hydrogen mole fractions for a lower oxygen ratio was initially lower (see Figure 5.28); however at the outlet of the reactor it increases above the mole fractions obtained with higher oxygen content. Increasing oxygen to methane ratio also increases the yield of carbon monoxide produced (see Figure 5.30). This increase reduces visibly as the oxygen content is increased. The higher moles of carbon monoxide (see Figure 5.29) can be explained by the higher moles of produced carbon dioxide during combustion reaction which then contributes to the reverse water gas shift reaction leading to higher carbon monoxide at the outlet. The trend of higher oxygen to methane ratio leading to lower mole fraction of carbon dioxide at the outlet also supports this explanation.

The second part of this simulation is done to analyse the effect of changing steam to methane ratios on output parameters. As the results suggest, increasing the amount of steam supplied reduces the conversion of methane at the same constant oxygen to methane ratio and

keeping the temperature constant, although this difference is not large and within a ten percent band for the simulated conditions (see Figure 5.35). This difference is further reduced on increasing the temperature. The hydrogen yield obtained is improved marginally on increasing the steam supplied (see Figure 5.32). The hydrogen mole fraction obtained at the outlet brings out the fact even more clearly that reducing the steam supplied produces a better hydrogen production (see Figure 5.31). The carbon monoxide mole fraction is reduced on increasing the supply of steam (see Figure 5.33). There is a very clear trend in falling carbon monoxide moles throughout the reactor on increasing steam supplied. For carbon dioxide, the trend is not that clear throughout the length of the reactor (see Figure 5.34), however, at the outlet it is clear that increasing the supplied steam to methane ratio causes more moles of carbon dioxide to be formed.

The third part of this simulation evaluates the effect of increasing temperatures on various outlet parameters, keeping the oxygen to methane ratio at 0.6 and steam to methane ratio at 1.5 . In this case the trends are very uniform throughout the reactor. For the conversion of methane the outlet conversion is higher at higher temperatures, as was indicated by thermodynamic study as well (see Figure 5.40). The hydrogen yield is better at higher temperatures owing to a better conversion of methane (see Figure 5.37). The outlet hydrogen mole fraction is also higher for higher temperatures, however the difference is not significant (see Figure 5.39). The carbon monoxide clearly shows an increasing trend with temperature (see Figure 5.36). The trend for carbon dioxide is not uniform throughout the length of the reactor, but at the outlet position, it is clearly visible that carbon dioxide production tapers off at higher temperatures (see Figure 5.38). It is clearly indicated that a higher temperature is useful to us.

The study would be incomplete without studying the effect of changing the different parameters on hydrogen to carbon monoxide ratio which is a crucial property for synthesis gas. The simulation study on the hydrogen to carbon monoxide ratio points to the fact that a higher temperature coupled with a low steam to methane ratio would bring the outlet gas composition within the desired range for syngas for Fischer Tropsch synthesis. A second analysis on the effect of oxygen input to this ratio shows that higher oxygen supply reduces the outlet hydrogen to carbon monoxide ratio. However, this effect is less pronounced at lower steam to methane

ratios and becomes significantly clear at higher steam supply at input conditions (see Figures 5.41 and 5.42).

CHAPTER 6

CONCLUSIONS AND RECOMMENDATIONS

The conclusions are enumerated under two heads, the first drawn from results of thermodynamic analysis and the second from the modeling and simulation of oxidative reforming of methane.

Thermodynamic Analysis

On the basis of $\Delta G < 0$, the temperature feasibility of reactions was determined in Section 3.2 to be 900K-1100K. This range was extended to 600-1300K for thermodynamic analysis based upon Gibb's free energy minimization, which was conducted by optimization tool *fmincon* in MATLAB. From this thermodynamic analysis it has been found that an increasing temperature enhances the conversion and decreases the coke formation. Theoretically, at temperatures around 1000K the conversion is quite high of the order of 95%. Thus, for simulation runs a temperature range of 900K -1200K was chosen.

Thermodynamically it has been shown that increasing the steam content also increases the conversion and reduces the coke formation. However, the hydrogen to carbon monoxide ratio increases as well. Thus, a limit of 5 was set on hydrogen to carbon monoxide ratio and hence steam ratio for simulation was limited to 0.5-3.0.

The oxygen content for autothermal operation was determined as a function of temperature in Section 3.1. This serves as defining the lower bound on the oxygen content for purposes of thermodynamic analysis. Increasing oxygen-to-methane ratio improves conversion, lowers coke deposition and brings the hydrogen to carbon monoxide ratio to lower values. Consequently, increasing it also causes a reduction in the number of moles of hydrogen produced. Thus, there is a tradeoff and for this reason the oxygen to methane ratio was kept between 0.5-1.2 for simulation studies to study its effect on output parameters.

The low pressure operation (1 bar) was determined on the basis of literature survey which pointed out theoretical benefits of enhanced conversion when operating at lower pressure. This is

also supported by Le Chateliers principle which dictates that lowering pressure would enhance the forward reaction because of increase in number of moles due to forward reaction of methane.

Modeling and Simulation

A steady state one-dimensional, non-isothermal, mathematical model for oxidative reforming of methane in a fixed bed reactor has been developed. This model utilizes the Xu and Froment kinetics for steam reforming and water gas shift reactions, and that of Trimm and Lam for methane combustion. In the reactor Ni based alumina catalyst is used. Variation of physical properties with temperature has also been accounted for. Variables' values at the inlet to the reactor have been taken as the input to the model, which constitute an initial value problem. Therefore this has been solved using *ode23s* solver in MATLAB. Model has been validated with the experimental data of De Groote and Froment. Using the output from the solver, methane conversion, hydrogen yield, mole fractions of hydrogen, carbon monoxide and carbon dioxide, and hydrogen to carbon monoxide ratio beside others have been computed.

The simulation results show that a higher oxygen supply leads to better conversion of methane (although the difference is not too large), lower carbon dioxide mole fraction and higher carbon monoxide mole fraction. The hydrogen mole fraction is also lowered to a limited extent at the outlet of the reactor. Thus, operating with higher oxygen to methane ratio lowers the hydrogen to carbon monoxide ratio, enhancing the applicability of outlet gas for gas to liquid (GTL) technologies. However, it is important to keep in mind the fact that a higher oxygen supply adds to the cost, and lowers the number of moles of hydrogen produced (as ascertained by thermodynamic analysis). Thus, based on these facts, it can be postulated that oxygen to methane ratio should be kept at reasonably high levels (say >0.5) to aid in conversion and better hydrogen/carbon monoxide ratio, but at the same time, an upper limit is required. Based on this logic the optimum oxygen to methane ratio for operation of reactor should be 0.8.

A higher temperature of operation implies higher carbon monoxide moles in outlet gas, marginally better hydrogen yield, and lower carbon dioxide mole fraction. The dependence of conversion and outlet hydrogen mole fraction on temperature is less significant. A higher temperature also reduces the hydrogen to carbon monoxide ratio in the outlet gas. Hence for a sufficiently high conversion, a temperature range of 1000-1100K is adequate.

The increasing steam supply lowers the outlet conversion slightly, as well as lowers the mole fraction of carbon monoxide. The mole fraction of carbon dioxide is increased and hydrogen yield is marginally improved. The hydrogen mole fraction also drops off. Once again the hydrogen to carbon monoxide ratio becomes an important parameter and it is found that a lower steam supply lowers the outlet hydrogen-to-carbon monoxide ratio. Based on model simulation ratio at the chosen temperature range (1000-1100K) and the oxygen to methane ratio (0.8) the hydrogen to carbon monoxide ratio varies from 2.7 to 9 when the steam to methane ratio is varied from 0.5 to 3.0. Hence, the steam content can be seen as a controlling parameter for hydrogen/carbon monoxide ratio, depending on the usage. GTL applications require this ratio to be around 2-2.5.

In summary, thermodynamic analysis predicted the theoretical ranges for the operating conditions, which were then utilized to simulate the developed mathematical model. On the basis of results obtained it can be summarized that the reaction operation at 1 bar pressure at temperature 1000-1100K and oxygen to methane ratio of 0.8 is versatile and satisfactory. At this configuration, the minimum hydrogen to carbon monoxide ratio in the outlet was found to be 2.7 at steam to methane ratio of 0.5. This ratio can be further altered as desired by using another separation unit. It is further stated that this operation requires low P and reasonable temperature. Thus, it is preferable to be used in practice.

REFERENCES

- [1]. *BP Statistical Review fo World Energy June 2012*. s.l. : BP, 2012.
- [2]. Global Warming FAQ's. **Easterling, David and Karl, Tom**. *National Oceanic and Atmospheric Administration, National Climatic Data Center*. [Online]
<http://www.ncdc.noaa.gov/cmb-faq/globalwarming.html>.
- [3]. *New and improved catalytic priocesses for clean fuel*. **Maxwell, I. E. and Naber, J. E.** 1992, Caltalyst Letters, Vol. 12, pp. 105-116.
- [4]. *Perry's chemical engineers' handbook*. **Perry, Robert H.; Green, Don W. and Maloney, James O'**. 7th. s.l. : McGraw-Hill, 1997. 0-07-049841-5.
- [5]. *Syngas production for gas-to-liquids applications:technologies, issues and outlook*. **Wilhelm, D. J.; Simbeck, D. R.; Karp, A. D. and Dickenson, R. L.** 2001, Fuel Processing Technology, Vol. 71, pp. 139-148.
- [6]. *New catalytic routes for syngas and hydrogen production*. **Pena, M. A.; Gomez, J. P. and Fierro, J. L.G.** 1996, Applied Catalyts A: Gen., Vol. 144, pp. 7-57.
- [7]. *Gas to liquids: A technology for natural gas industrialization in Bolivia*. **Velasco, J. A.; Lopez, L.; Velasquez, M.; Boutonnet, M.; Cabrera, S. and Jaras, S.** 2011, Journal of Natural Gas Science and Engineering, Vol. 3, pp. 423-459.
- [8]. Preliminary screeneing- technical and economic assessment of synthesis gas to fuels and chemicals with emphaissis on biomass derived syngas. **Spath, P. L. and Dayton, D. C.** *National Renewable Energy Labaratory*. December 2003. NREL/TP-510-34929.
- [9]. *Catalytic partial oxidation of natural gas to syngas*. **Bhardwaj, S. S. and Schmidt, L. D.** 1995, Fuel Porcessing Technology, Vol. 42, pp. 109-127.
- [10]. *Modelling of packed bed membrane reactors for autothermal production of ultrapure hydroge*. **Tiemersma, T. P.; Patil, C. S.; Annaland, M. van Sint and Kuipers, J. A.M.** 2006, Chemical Engineering Science, Vol. 61, pp. 1602-1616.

- [11]. *New aspects of syngas production and use*. **Rostrup-Nielsen, Jens R.** 2000, Catalysis Today, Vol. 63, pp. 159-164.
- [12]. *Technologies for large scale gas conversion*. **Aasberg-Petersen, K.; Bak Hansen, J. H.; Christensen, T. S.; Dybkjaer, I.; Seier Christensen, P.; Stub Nielsen, C.; Winter Madsen, S. E. L. and Rostrup-Nielsen, J.R.** 2001, Applied Catalysis A: General, Vol. 221, pp. 379-387.
- [13]. *Hydrogen production from methane through catalytic partial oxidation reactions*. **Freni, S.; Calogero, G. and Cavallaro, S.,** 2000, Journal of Power Sources, Vol. 87, pp. 28-38.
- [14]. *Thermodynamic analysis of hydrogen production by partial oxidation reforming*. **Lutz, Andrew E.; Bradshaw, Robert W.; Bromberg, Leslie and Rabinovich, Alex** 2004, International Journal of Hydrogen Energy, Vol. 29, pp. 809-816.
- [15]. *Thermodynamic equilibrium analysis of combined carbon dioxide reforming with partial oxidation of methane to syngas*. **Amin, Nor Aishah and Yaw, Tung Chun** 2007, International Journal of Hydrogen Energy, Vol. 32, pp. 1789–1798.
- [16]. *Thermodynamic analysis of autothermal steam and CO₂ reforming of methane*. **Li, Yunhua; Wang, Yaquan; Zhang, Xiangwen and Mi, Zhentao** 2008, International Journal of Hydrogen Energy, Vol. 33, pp. 2507-2514.
- [17]. *Thermodynamic analysis of hydrogen production from methane via autothermal reforming and partial oxidation followed by water gas shift reaction*. **Chen, Wei-Hsen; Lin, Mu-Rong; Lu, Jau-Jang; Chao, Yu and Leu, Tzong-Shyng** 2010, International Journal of Hydrogen Energy, Vol. 35, pp. 11787-11797.
- [18]. *Oxidative reforming of methane for hydrogen and synthesis gas production: Thermodynamic equilibrium analysis*. **Freitas, Antonio C. D. and Guirardello, Reginaldo.** 2012, Journal of Natural Gas Chemistry, Vol. 21, pp. 571-580.
- [19]. *Thermodynamic analysis of combined reforming process using Gibbs energy minimization method: In view of solid carbon formation*. **Nematollahi, Behzad; Rezaei, Mehran; Nemati, Ebrahim Lay and Khajenoori, Majid** 2012, Journal of Natural Gas Chemistry, Vol. 21, pp. 694–702.

- [20]. *Simulation of the catalytic partial oxidation of methane to synthesis gas*. **De Groote, Ann M. and Froment, Gilbert F.** 1996, Applied Catalysis A: General, Vol. 138, pp. 245-264.
- [21]. *Comparative study of the catalytic partial oxidation of methane to synthesis gas in fixed-bed and fluidized-bed membrane reactors Part I: A modeling approach*. **Ostrowski, T.; Giroir-Fendler, A.; Mirodatos, C. and Mleczko, L.** 1998, Catalysis Today, Vol. 40, pp. 181-190.
- [22]. *Design of adiabatic fixed-bed reactors for the partial oxidation of methane to synthesis gas. Application to production of methanol and hydrogen-for-fuel-cells*. **de Smet, C. R.H.; de Croon, M. H.J.M.; Berger, R. J.; Marin, G. B. and Schouten, J. C.** 2001, Chemical Engineering Science, Vol. 56, pp. 4849-4861.
- [23]. *Methane Steam Reforming, Methanation and Water-Gas Shift: 1. Intrinsic Kinetics*. **Xu, Jianguo and Froment, Gilbert F.** 1989, A.I.Ch.E Journal, Vol. 35, pp. 88-96.
- [24]. *Heterogeneous reactor modeling for simulation of catalytic oxidation and steam reforming of methane*. **Avci, A. K.; Trimm, D. L. and Onsan, Z.** 2001, Chemical Engineering Science, Vol. 56, pp. 641-649.
- [25]. *Simulation and thermodynamic analysis of conventional and oxygen permeable CPO reactors*. **Ji, Peijun; Kooi, H. J. van der and Arons, J. de Swaan.** 2003, Chemical Engineering Science, Vol. 58, pp. 2921-2930.
- [26]. *Modeling and analysis of autothermal reforming of methane to hydrogen in a fixed bed reformer*. **Halabi, M. H.; de Croon, M. H.J.M.; Schaff, J. van der; Cobden, P. D. and Schouten, J. C.** 2008, Chemical Engineering Journal, Vol. 137, pp. 568-578.
- [27]. *Hydrogen production by partial oxidation of methane: Modeling and Simulation*. **Kumar, Shashi; Kumar, Surendra and Prajapati, Jitendra K.** 2009, International Journal of Hydrogen Energy, Vol. 34, pp. 6655-6668.
- [28]. *Autothermal reforming of methane to synthesis gas: Modeling and simulation*. **Zahedi nezhad, M.; Rowshanzamir, S. and Eikani, M.** 2009, International Journal of Hydrogen Energy, Vol. 34, pp. 1292-1300.

- [29]. *Kinetic modeling of high pressure autothermal reforming*. **Reese, Mark A.; Turn, Scott Q. and Cui, Hong** 2010, Journal of Power Sources, Vol. 195, pp. 553-558.
- [30]. *Modelling and simulation of a catalytic autothermal methane reformer with Rh catalyst*. **Scognamiglio, Diego; Russo, L.; Maffetonne, P. L.; Salemm, L.; Simeone, M. and Crescitelli, S.** 2012, International journal of Hydrogen Energy, Vol. 37, pp. 263-175.
- [31]. *Combustion of methane on platinum-alumina fibre catalysts-I: Kinetics and mechanism*. **Trimm, D. L. and Lam, C. W.** 1980, Chemical Engineering Science, Vol. 35, pp. 1405-1413.
- [32]. *Catalytic partial oxidation of methane to synthesis gas*. **Heitnes, K.; Lindberg, S.; Rokstad, O. A. and Holmen, A.** 1995, Catalysis Today, Vol. 24, pp. 211-216.
- [33]. *CO₂ reforming of methane combined with steam reforming or partial oxidation of methane to syngas over NdCoO₃ perovskite-type mixed metal-oxide catalyst*. **Choudhary, Vasant R. and Mondal, Kartick C.** 2006, Applied Energy, Vol. 83, pp. 1024–1032.
- [34]. *Hydrogen production by catalytic partial oxidation of methane and propane on Ni and Pt catalysts*. **Corbo, Pasquale and Migliardini, Fortunato.** 2007, International Journal of Hydrogen Energy, Vol. 32, pp. 55-66.
- [35]. *Combined oxidation and reforming of methane to produce pure H₂ in a membrane reactor*. **Munera, J. F.; Carrara, C.; Cornaglia, L. M. and Lombardo, E. A.** 2010, Chemical Engineering Journal, Vol. 161, pp. 204-211.
- [36]. *Hydrogen production from oxidative reforming of methane on supported nickel catalysts: An experimental and modeling study*. **Dantas, S. C.; Resende, K. A.; Rossi, R. L.; Assis, A. J. and Hori, C. E.** 2012, Chemical Engineering Journal, Vol. 197, pp. 407–413.
- [37]. *Hydrogen from hydrocarbon fuels for fuel cells*. **Ahmed, S. and Krumpelt, M.** 2001, International Journal of Hydrogen Energy, Vol. 26, pp. 291-301.
- [38]. NIST Chemistry Webbook-NIST Standard Reference Database Number 69. *NIST: National Institute of Standards and Technology, US Department of Commerce*. [Online] National Institute of Standards and Technology. <http://webbook.nist.gov/chemistry/> .

- [39]. *NIST-JANAF Thermochemical Tables*. **Chase, M.W. Jr.** 1998, J. Phys. Chem. Ref. Data, Monograph 9, Vol. Fourth Ed., pp. 1-1951. Data compilation copyright by the U.S. Secretary of Commerce on behalf of the U.S.A.
- [40]. **Cox, J. D., Wagman, D. D., and Medvedev, V. A.** *CODATA Key Values for Thermodynamics*. New York : Hemisphere Publishing Corp., 1984. Data compilation copyright by the U.S. Secretary of Commerce on behalf of the U.S.A.
- [41]. *Comparative thermodynamic analysis of adsorption, membrane and adsorption-membrane hybrid reactor systems for methanol steam reforming*. **Katiyar, Nisha; Kumar, Shashi; and Kumar, Surendra** 2013, International Journal of Hydrogen Energy, Vol. 38, pp. 1363-1375.
- [42]. *Partial oxidation of methane to carbon monoxide and hydrogen over a Ni-Al₂O₃ catalyst*. **Dissanayake, Dhammike; Rosynek, Michael P.; Kharas, Karl C.C. and Lunsford, Jack H.** 1991, Journal of Catalysis, Vol. 132, pp. 117-127.
- [43]. *Catalytic and thermodynamic approach of the oxyreforming reaction of methane*. **Vermeiren, W.J.M.; Blomsma, E. and Jacobs, P.A.** 1992, Catal.Today, Vol. 13, pp. 427-436.
- [44]. *A simulation study of the steam reforming of methane in a dense tubular membrane reactor*. **Gallucci, Fausto; Paturzo, Luca and Basile, Angelo** 2004, International Journal of Hydrogen Energy, Vol. 29, pp. 611-617.
- [45]. *Methane steam reforming modeling in a palladium membrane reactor*. **Fernandes, Fabiano A.N. and Soares Jr., Aldo B.** 2006, Fuel, Vol. 85, pp. 569-573.
- [46]. *Modeling of a Fluidized Bed Membrane Reactor for the Steam Reforming of Methane: Advantages of Oxygen Addition for Favorable Hydrogen Production*. **Rakib, M. A. and Alhumaizi, K.** 2005, Energy & Fuels, Vol. 19, pp. 2129-2139.
- [47]. *Effect of intraparticle transport limitations on temperature profiles and catalytic performance of the reverse-flow reactor for the partial oxidation of methane to synthesis gas*. **Gosiewski, K., Bartmann, Ulrich; Moszczynski, Marek and Mleczko, Leslaw** 1999, Chemical Engineering Science, Vol. 54, pp. 4589-4602.